



HAL
open science

Friction Reduction and Reliability Improvement of Plain Bearing Lubrication with Lubricating Automotive Engine Oil

Moritsugu Kasai

► **To cite this version:**

Moritsugu Kasai. Friction Reduction and Reliability Improvement of Plain Bearing Lubrication with Lubricating Automotive Engine Oil. Engineering Sciences [physics]. Université de Poitiers, 2010. English. NNT: . tel-00477348

HAL Id: tel-00477348

<https://theses.hal.science/tel-00477348>

Submitted on 28 Apr 2010

HAL is a multi-disciplinary open access archive for the deposit and dissemination of scientific research documents, whether they are published or not. The documents may come from teaching and research institutions in France or abroad, or from public or private research centers.

L'archive ouverte pluridisciplinaire **HAL**, est destinée au dépôt et à la diffusion de documents scientifiques de niveau recherche, publiés ou non, émanant des établissements d'enseignement et de recherche français ou étrangers, des laboratoires publics ou privés.

THESE

pour l'obtention du grade de

DOCTEUR DE L'UNIVERSITE DE POITIERS

Faculté des Sciences Fondamentales et Appliquées
(Diplôme National – Arrêté du 7 août 2006)

Ecole Doctorale Sciences et Ingénierie en Matériaux, Mécanique, Energétique et Aéronautique

Spécialité : Génie Mécanique, Productique, Transport

Présentée par :

Moritsugu KASAI

Réduction du frottement et amélioration de la fiabilité de la lubrification des paliers avec des huiles de moteurs automobiles

Directeur de thèse : **Michel FILLON**

Codirecteur de thèse : **Jean BOUYER**

Soutenance prévue le lundi 12 avril 2010

JURY

Rapporteurs **Masato TANAKA**, Président université, Université Préfectorale de Toyama
Philippe VERGNE, Directeur de Recherche CNRS, LaMCoS, INSA de Lyon

Examineurs **Denis MAZUYER**, Professeur, LTDS, Ecole Centrale de Lyon
Dominique BONNEAU, Professeur Emérite, Institut P', Université de Poitiers
Hiroshi FUJITA, Chef de groupe, Dr., Idemitsu Kosan Co.
Michel FILLON, Directeur de Recherche CNRS, Institut P', Université de Poitiers
Jean BOUYER, Maître de Conférences, Institut P', Université de Poitiers
Sébastien JARNY, Maître de Conférences, Institut P', Université de Poitiers

Forward

I have been responsible for the development of engine oil formulation since 1999 at the lubricant research laboratory of Idemitsu Kosan Co., Ltd, which is a petroleum company in Japan. Improvement of fuel economy with engine oil has been required for many years. It is well known that lowering oil viscosity is effective but deteriorate the reliability of plain bearings used in engines. Therefore, we are currently focusing on the development of fuel economy engine oils that satisfy both of the performances, for the future.

A bearing test apparatus was introduced and some experiments were performed in our laboratory. Some of the results obtained were presented at international conferences and published in engineering journals. In fact, we found a difficulty in investigating the effect of additives (especially polymer) used in engine oil. In order to proceed with the investigation of polymer effect in plain bearing lubrication, we concluded to collaborate with a university which has strength in that field. The collaboration with the Poitiers University was started in October, 2008. (The collaboration among Poitiers University-CNRS-Idemitsu Kosan Co., Ltd.)

Professor Fillon, Directeur de recherche CNRS at LMS is the scientific manager of the collaboration research. The bearing tests were carried out under the supervision of Dr. Jean Bouyer, Maître de conférences at LMS. The rheological tests were carried out with the supervision of Dr. Sébastien Jarny, Maître de conférences at LEA.

Thus, from the above mentioned background, the first part of this thesis consists of the research activity that was performed at the Idemitsu lubricants research laboratory. The results from the collaboration research compose the chapter 7.

Contents

| | |
|--|----|
| Forward | 3 |
| Extended abstract in French (Résumé étendu) | 9 |
| Notations | 21 |
| Introduction | 23 |
| 1. Review concerning this work | 27 |
| 1-1 Research on friction reduction and reliability improvement with lubricants | 27 |
| 1-2 Research on friction reduction and reliability improvement with lead-free bearing materials | 37 |
| 1-3 Aim of this study | 39 |
| 1-4 Composition of this thesis | 42 |
| 2. A test apparatus for automotive engine bearings | 45 |
| 2-1 Plain bearing test apparatus | 46 |
| 2-2 Plain bearing test conditions | 51 |
| 2-3 Measuring items | 52 |
| 2-4 Plain bearing test procedure | 54 |
| 2-5 Measurement examples with the developed bearing test apparatus | 55 |
| 2-5-1 Friction coefficient and contact resistance (CR) ratio under static load condition | 55 |
| 2-5-2 Relative shaft displacement under static load condition | 58 |
| 2-5-3 Bearing torque and contact resistance (CR) ratio under dynamic load condition | 59 |

| | |
|--|-----|
| 3. Effect of base oils on plain bearing performance | 61 |
| 3-1 Plain bearings used | 62 |
| 3-2 Base oil samples tested | 63 |
| 3-3 Test results under static load condition and discussion | 64 |
| 3-4 Test results under dynamic load condition and discussion | 75 |
| 3-5 Conclusions | 78 |
| 4. Effect of bearing materials on plain bearing performance | 81 |
| 4-1 Plain bearings used | 81 |
| 4-2 Base oil samples tested | 83 |
| 4-3 Test results with the Al-Si plain bearing and the Cu-Pb plain bearing under static load condition and discussion | 83 |
| 4-4 Test results with the Al-Si plain bearing and the Cu-Pb plain bearing under dynamic load condition and discussion | 93 |
| 4-5 Conclusions | 94 |
| 5. Effect of friction modifiers(FMs) on plain bearing performance | 95 |
| 5-1 Plain bearing used | 95 |
| 5-2 Plain bearing test conditions | 96 |
| 5-3 Lubricant samples tested | 97 |
| 5-4 Bearing test results with a base oil containing no additives | 98 |
| 5-5 Bearing test results with an oil containing FM without sulfur | 100 |
| 5-6 Bearing test results with an oil containing FM with sulfur | 101 |
| 5-7 Difference of the results between the base oils with no additives and FMs | 103 |
| 5-8 Friction characteristics of oils in the boundary lubrication region with a reciprocating type friction tester | 106 |
| 5-9 Discussion | 108 |

| | |
|--|-----|
| 5-10 Conclusions | 112 |
| 6. Effect of polymers on plain bearing performance | 113 |
| 6-1 Plain bearings used | 113 |
| 6-2 Lubricant samples tested | 114 |
| 6-3 Test results with the Cu-Pb plain bearings under static load condition | 116 |
| 6-4 Test results with the Al-Si plain bearings under static load condition | 118 |
| 6-5 Discussion of the effect of polymer-containing oils under static load condition | 120 |
| 6-6 Test results with the Cu-Pb plain bearing and the Al-Si plain bearing under dynamic load condition | 124 |
| 6-7 Conclusions | 125 |
| 7. Experiments and numerical analysis of bearing lubrication with polymer- containing oils, investigation of the mechanisms of their action | 127 |
| 7-1 Plain bearing test | 130 |
| 7-1-1 Plain bearing test apparatus | 130 |
| 7-1-2 Measurement items of plain bearing performance and test conditions | 132 |
| 7-1-3 Plain bearing test procedure | 134 |
| 7-1-4 Typical property of lubricants used in the bearing tests | 135 |
| 7-2 Measurement of rheological property for the polymer-containing oils | 137 |
| 7-2-1 Rheometer for measurement in a low shear rate range | 137 |
| 7-2-2 Rheometer for measurement in a high shear rate range | 138 |
| 7-2-3 Lubricants tested | 142 |
| 7-2-4 Rheological property of the lubricants tested | 142 |
| 7-3 Plain bearing performance of the Babbitted bearing in comparison with the bronze bearing | 145 |
| 7-3-1 Friction coefficient | 145 |

| | |
|---|-----|
| 7-3-2 Relative shaft displacement | 148 |
| 7-3-3 Bearing pressure distribution | 156 |
| 7-3-4 Bearing temperature distribution | 159 |
| 7-4 Analysis of the effect of the temporary viscosity loss and the normal stress at high shear rates in the bearing performance with the Babbitted bearing and the bronze bearing | 160 |
| 7-4-1 Approximation equations for the temporary viscosity loss and the first normal stress difference | 161 |
| 7-4-2 Simulation condition | 163 |
| 7-4-3 Effect of the temporary viscosity loss and the first normal stress difference in the bearing performance | 163 |
| 7-4 Conclusions | 168 |
| 8. Conclusions | 169 |
| Appendix I | 175 |
| References | 179 |
| List of figures | 185 |
| List of tables | 192 |
| Acknowledgment | 193 |

Résumé étendu

1. Introduction

Du point de vue de la prévention du réchauffement climatique, notamment de la réduction des émissions de CO₂, il est devenu nécessaire d'améliorer la consommation des moteurs thermiques grâce à l'utilisation de lubrifiants plus performants. L'un des moyens les plus efficaces pour réduire les pertes par frottement est de réduire le diamètre des paliers et diminuer la viscosité de l'huile lubrifiante. Cependant, ces modifications mettent en exergue l'importance de la fiabilité des paliers, d'autant plus que les moteurs sont de plus en plus puissants. Bien que l'efficacité de réduire la viscosité du lubrifiant soit supérieure, peu d'études ont été menées sur ce sujet en raison de l'influence importante de cette solution sur les performances des paliers. De plus, une réglementation sur l'utilisation du plomb dans les matériaux de paliers a été mise en place afin de limiter la pollution par les métaux lourds lors de la destruction des véhicules usagés. Cette nouvelle réglementation a conduit les fabricants de paliers de moteurs automobiles à développer de nouveaux matériaux ne contenant pas de plomb. Ainsi, il est apparu nécessaire de réaliser cette étude, qui porte sur la diminution du frottement et l'amélioration de la fiabilité des paliers grâce à l'utilisation de lubrifiants adaptés aux matériaux qui les constituent. Les principaux objectifs de cette étude sont donc les suivants :

- (1) Analyser l'effet des huiles de base dans la réduction coefficient de frottement en lubrification hydrodynamique ainsi que l'amélioration de la fiabilité en lubrification mixte,
- (2) Analyser l'influence des matériaux constituant le palier dans la réduction du frottement en lubrification hydrodynamique ainsi que l'amélioration de la fiabilité en lubrification mixte,
- (3) Analyser l'effet des modificateurs de frottement dans l'amélioration de la fiabilité en lubrification mixte,
- (4) Analyser l'effet des polymères dans la réduction du frottement en lubrification hydrodynamique,
- (5) Etudier expérimentalement et numériquement la lubrification de paliers avec des huiles contenant des polymères et comprendre les mécanismes de leur action.

2. 2. Banc d'essais de paliers de moteurs automobiles

La figure 2.1 montre une vue générale du dispositif d'essais développé afin de tester les paliers de moteurs automobiles. La charge est appliquée par l'intermédiaire d'un vérin hydraulique et le palier est alimenté par un trou d'alimentation créé dans l'arbre.

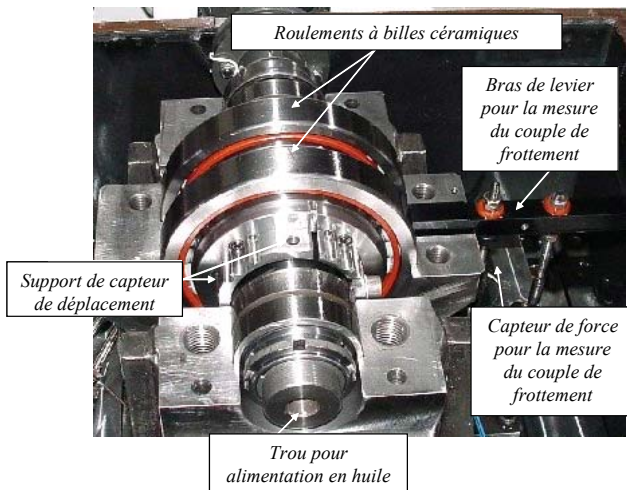


Figure 2-1 Vue générale du banc d'essais.

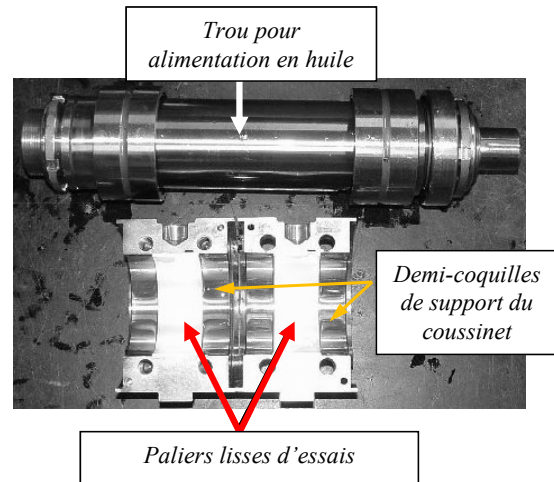


Figure 2-2 Vue du dispositif démonté

La figure 2.2 ci-dessous montre l'ensemble démonté. Les supports de coussinets, en deux parties, sont guidés par des roulements à billes céramiques. Les coussinets à tester sont installés dans ces supports de façon à reproduire le plus fidèlement les conditions de montage réelles dans un moteur thermique. L'arbre est quant à lui guidé par deux roulement à billes, montés à l'extérieur des roulements céramique et lubrifiés par le fluide d'alimentation des paliers à travers les supports de coussinets. Les paliers d'essais ont un diamètre intérieur de 53 mm et une longueur de 26 ou 14,85 mm.

Le chargement statique ou dynamique est appliqué verticalement sur la partie supérieure du palier grâce au vérin hydraulique. Le coefficient de frottement dans le palier est mesuré par l'intermédiaire d'un bras attaché au coussinet, qui transmet l'effort à un capteur de force placé sur le côté du dispositif (fig. 2.1). La résistance de contact (CR ratio), exprimée en pourcentage de sa valeur maximale, sert à surveiller un éventuel contact entre l'arbre et le coussinet (100% lorsque les surfaces sont éloignées et 0% lorsqu'il y a contact). Quatre capteurs de proximité (2 suivant la direction de la charge et 2 suivant la normale à cette même direction) sont également installés de part et d'autre du coussinet afin de mesurer la distance relative séparant l'arbre et le coussinet.

3. Effet de l'huile de base sur les performances des paliers

Afin d'évaluer l'effet de l'huile de base, les performances du palier ont été mesurées sur le dispositif d'essais avec un palier en alliage Cu-Pb. Des huiles de base de faible viscosité 150N (neutre) ainsi que de forte viscosité 500N (neutre) avec différentes catégories API (différents niveaux de raffinage) ont été testées. Les figures 3.1 et 3.2 ci-dessous montrent les résultats obtenus pour le coefficient de frottement et le ratio de contact en fonction du nombre de Hersey avec :

$$Hs = \eta N / P_{spec}$$

où η est la viscosité absolue de l'huile testée, N la vitesse de rotation et P_{spec} la pression spécifique.

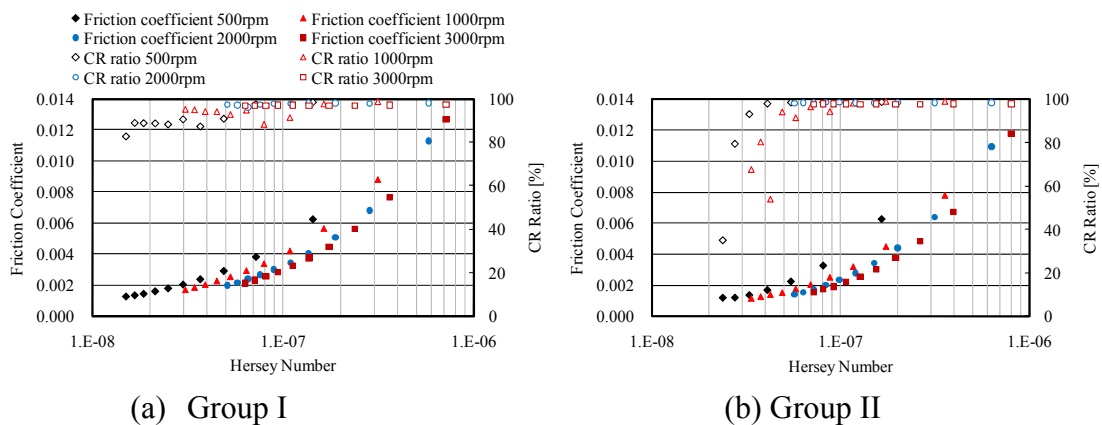


Figure 3-1 Coefficient de frottement et ratio de contact pour les huiles à faible viscosité.

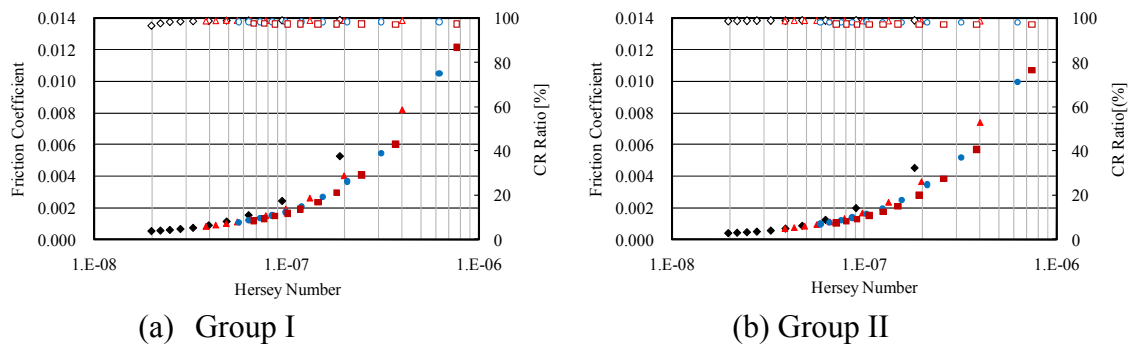


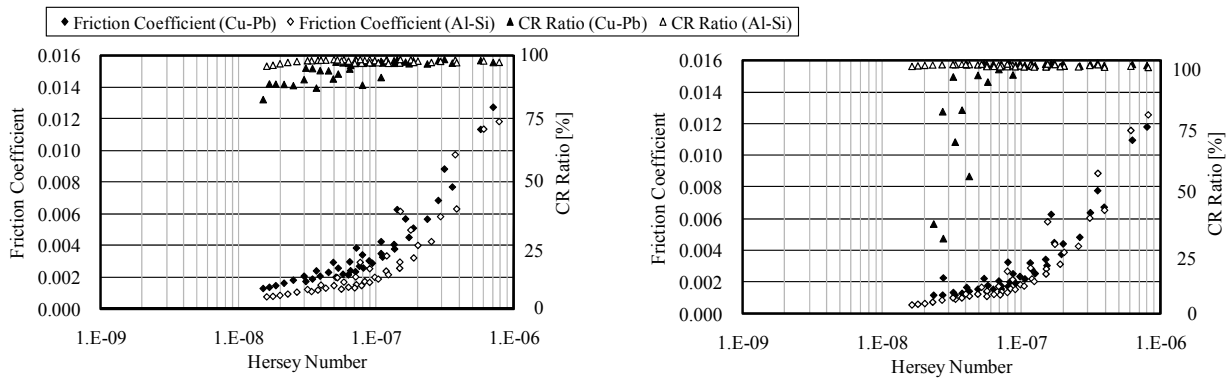
Figure 3-2 Coefficient de frottement et ratio de contact pour les huiles à forte viscosité.

Le contact entre l'arbre et le coussinet apparaît plus rapidement lorsque l'on utilise des huiles à faible viscosité plutôt que des huiles à viscosité forte. De plus, le contact semble apparaître plus tôt avec les huiles hautement raffinées qu'avec les huiles de base moins raffinées (c'est-à-dire les huiles de base du groupe I), même si elles ont une viscosité comparable à celle des huiles très raffinées. Cette observation nous permet de conclure que le contact entre l'arbre et le coussinet a été évité grâce à la réaction entre le matériau du coussinet et le soufre contenu dans les huiles de base du groupe I. Les pertes par frottement pour les huiles de base à forte

viscosité sont inférieures à celles observées pour les huiles de base à faible viscosité pour un même nombre de Hersey. Ces résultats montrent que les performances du palier sont fortement dépendantes de la masse moléculaire et des éléments de l'huile de base.

4. Effet des matériaux sur les performances des paliers

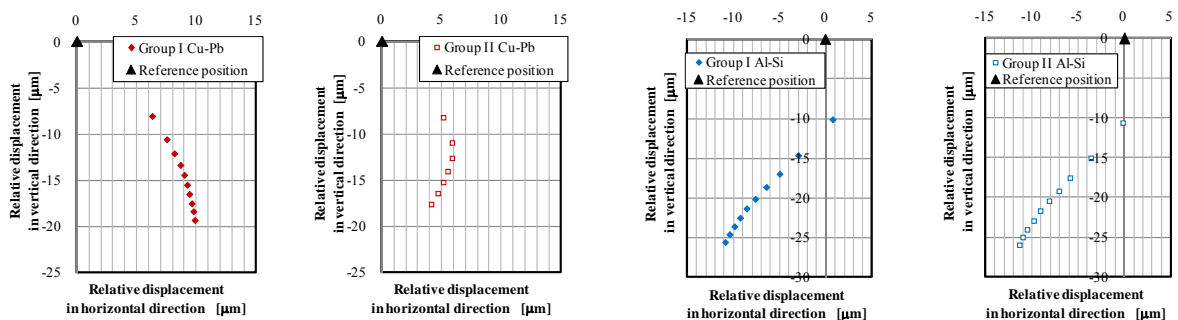
L'effet des matériaux sur les performances des paliers a été analysé pour deux types de paliers (alliage Cu-Pb et alliage Al-Si) avec plusieurs huiles de base à faible viscosité 150N. Ces deux types de paliers conventionnels contiennent du plomb mais ils ont été tout de même utilisés afin de connaître leur effet en termes de performances du palier. La figure 4.1 présente les coefficients de frottement ainsi que les ratios de contact pour les deux types de paliers. On peut remarquer que le palier en alliage Al-Si présente un coefficient de frottement inférieur à celui obtenu pour le palier en alliage Cu-Pb. La figure 4.2, qui représente le déplacement relatif de l'arbre pour les paliers en alliage Cu-Pb et Al-Si, montre que l'épaisseur du film pour le palier en alliage Al-Si est supérieure à celle obtenue pour le palier en alliage Cu-Pb avec les mêmes huiles de base.



(a) Huile de base du groupe I

(b) Huile de base du groupe II

Figure 4-1 Coefficient de frottement et ratio de contact en fonction du nombre de Hersey pour les paliers en alliage Cu-Pb et Al-Si.



(a) Groupe I, Cu-Pb

(b) Groupe II, Cu-Pb

(c) Groupe I, Al-Si

(d) Groupe II, Al-Si

Figure 4-2 Déplacement relatif de l'arbre pour les paliers en alliage Cu-Pb et Al-Si.

Il est donc nécessaire, afin de développer un moteur qui économise le carburant tout en assurant à la fois une réduction du coefficient de frottement et une bonne fiabilité, d'assurer une corrélation entre la composition du lubrifiant et les matériaux utilisés pour la fabrication du palier.

5. Effet des modificateurs de frottement sur les performances des paliers

Afin de définir un procédé permettant l'amélioration des performances de paliers grâce aux modificateurs de frottement (FMs), leur effet lorsqu'ils sont mélangés à l'huile de base a été examiné. Compte tenu du fait que l'influence des matériaux sur les performances des paliers a été montrée dans les chapitres précédents, le tout dernier matériau de palier ne contenant pas de plomb a été sélectionné pour réaliser cette partie de l'étude. La figure 5.1 montre les ratios de contact de paliers en alliage à base de cuivre (PB-A) et en alliage à base d'aluminium (PB-C), revêtus d'une couche de Bismuth (Bi). Trois échantillons de lubrifiants différents ont été utilisés pour évaluer les performances des paliers. Le premier est une huile de base de type polyalphaoléfine (PAO) dont la viscosité est approximativement de 6 mm²/s à 100°C. Les deux autres échantillons ont été préparés à partir de cette huile en y intégrant 1% en masse de modificateurs de frottement de type ester contenant du soufre ou sans soufre. Ces lubrifiants contenant des modificateurs de frottement seront nommés FM-A et FM-B, respectivement.

Nous avons pu montrer que l'alliage des paliers et l'expression des performances des modificateurs de frottement étaient liés. Les modificateurs de frottement sans soufre et avec soufre ont respectivement permis d'améliorer la fiabilité de paliers en alliage à base de cuivre et à base d'aluminium.

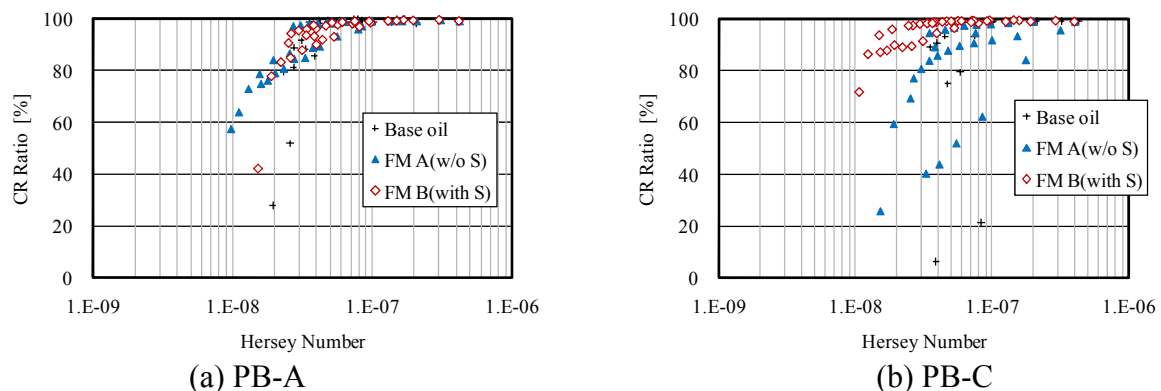


Figure 5-1 Ratio de contact en fonction du nombre de Hersey pour les échantillons PB-A et PB-C

6. Effet des polymères sur les performances des paliers

Afin de mettre en évidence l'influence des polymères sur les performances des paliers, des expérimentations supplémentaires ont été réalisées avec des polymères de masses moléculaires différentes (polymère A : $M_w=25000$ et polymère B : $M_w=370000$). Les figures 6.1 et 6.2 ci-dessous montrent les coefficients de frottement ainsi que les ratios de contact obtenus lors de ces essais. Les échantillons de lubrifiant utilisés étaient une huile de base de type polyalphaoléfine (PAO) dont la viscosité à 100°C est de $7 \text{ mm}^2/\text{s}$ et deux huiles contenant des polymères préparées à partir d'une huile de base de viscosité $4 \text{ mm}^2/\text{s}$ à 100°C .

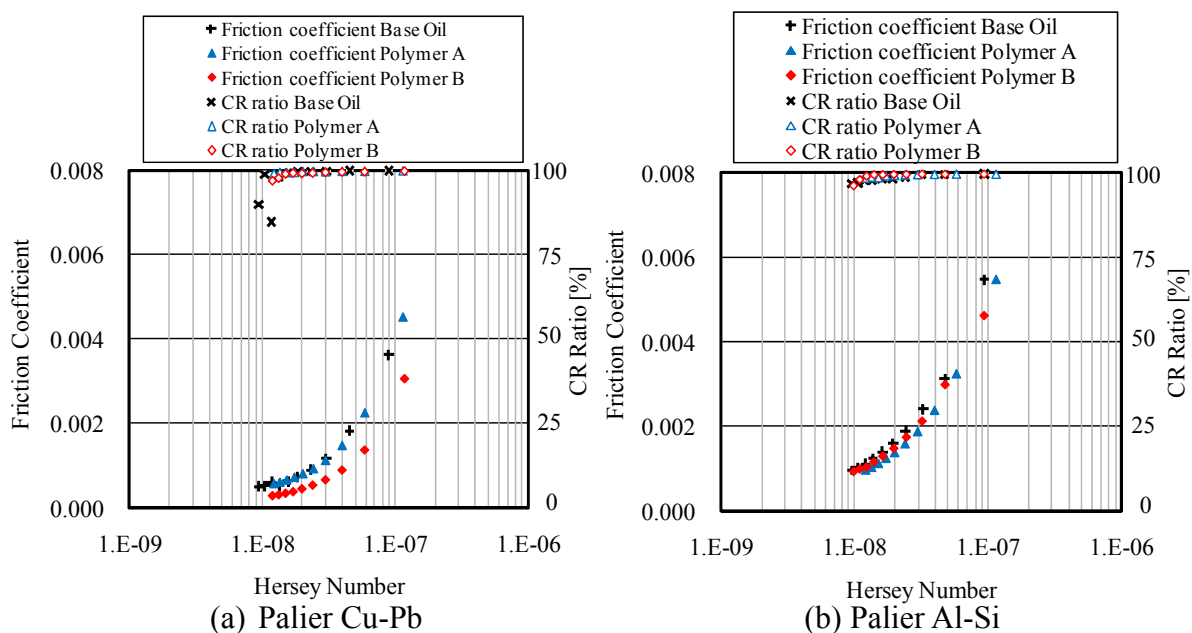


Figure 6-1 Coefficient de frottement et ratio de contact en fonction du nombre de Hersey pour les paliers en alliage Cu-Pb et Al-Si.

L'huile contenant le polymère de forte masse moléculaire (polymère B) a permis d'obtenir des coefficients de frottement inférieurs à ceux de l'huile de base pour le palier en alliage Cu-Pb. En revanche, cet effet n'a pas été observé avec le palier en alliage Al-Si. Du fait que le déplacement horizontal de l'arbre dans le coussinet est positif pour le palier en alliage Cu-Pb, l'épaisseur du film peut être considérée comme inférieure à celle obtenue pour le palier en alliage Al-Si dans les mêmes conditions. Ce phénomène peut affecter la réduction temporaire de viscosité dans les lubrifiants contenant des polymères. Par conséquent, il a été montré que le coefficient de frottement obtenu avec des lubrifiants contenant des polymères est dépendant du type de matériaux utilisé pour fabriquer les coussinets de paliers.

7. Analyses expérimentale et numérique de la lubrification de paliers avec des huiles contenant des polymères, recherche de leur mode d'action

Des essais expérimentaux supplémentaires ont été réalisés grâce à un dispositif d'essais qui permet de mesurer les champs de pression et de température dans le palier, ainsi que le coefficient de frottement et les déplacements relatifs de l'arbre par rapport au coussinet. Le comportement non newtonien des lubrifiants (huiles contenant des polymères) a été analysé à la fois expérimentalement et numériquement. De plus, du fait que les huiles contenant des polymères devraient présenter une diminution de viscosité et des contraintes normales à un fort taux de cisaillement, donc avoir un comportement non newtonien, leurs propriétés rhéologiques ont été examinées en fonction des conditions de fonctionnement des paliers afin d'enrichir nos recherches.

7-1 Dispositif expérimental

La figure 7.1 présente une vue schématique du dispositif expérimental et une vue du palier monté et équipé. Les paliers utilisés pour cette étude sont des paliers en acier régulé et en bronze comportant une seule rainure d'alimentation. Le diamètre et la longueur des paliers sont respectivement de 100 mm et 80 mm. Les paliers utilisés ne sont pas des paliers de moteur automobile mais le but principal de notre étude est de déterminer de manière précise l'influence des polymères sur les performances des paliers. Le couple de frottement est mesuré grâce à un couplemètre par l'intermédiaire d'un bras rigide relié au coussinet. La position relative du coussinet par rapport à l'arbre est déterminée à partir de quatre capteurs de proximité situés à plus ou moins 45° par rapport à la direction de la charge (fig. 7.2).

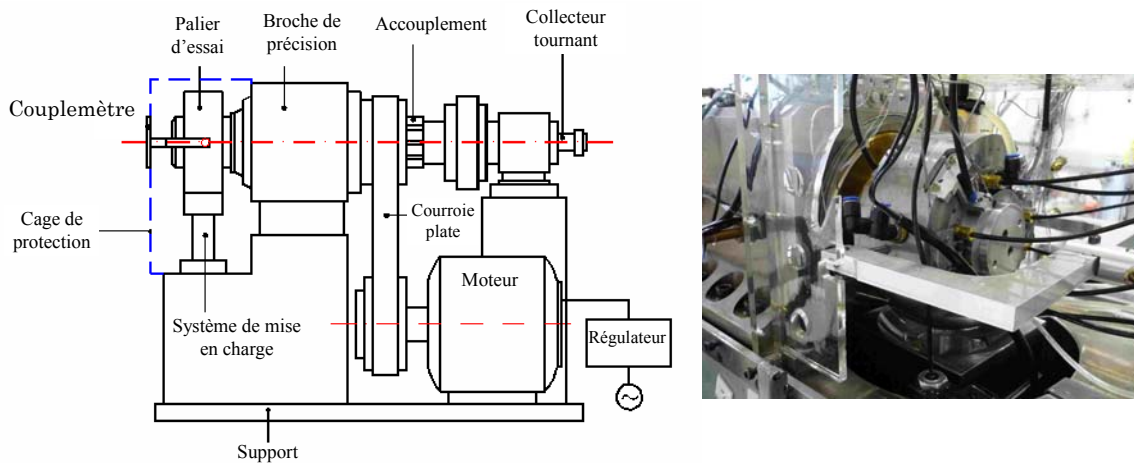


Figure 7-1 Schéma du dispositif expérimental et vue du palier équipé

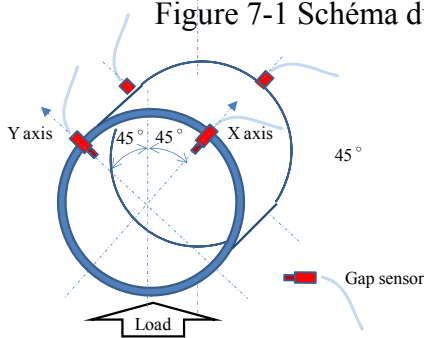


Figure 7-2 Position des capteurs de proximité

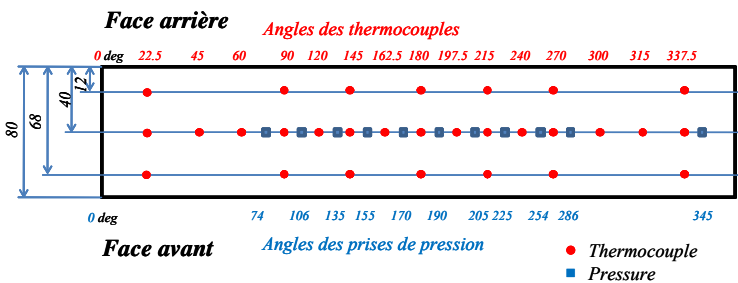


Figure 7-3 Position des thermocouples et des prises de pression

La figure 7.3 détaille le positionnement des capteurs de pression et de température dans le palier. 29 thermocouples sont placés à l’interface film/oussinet dont 15 dans le plan médian et 14 suivant la direction axiale pour 7 valeurs angulaires (22,5°, 90°, 145°, 180°, 215°, 270° et 337,5°). La pression hydrodynamique est mesurée à l’aide de capteurs de pression connectés aux 15 trous réalisés dans le plan médian du palier.

7-2 Résultats expérimentaux et discussion

Les essais expérimentaux ont été réalisés avec une huile de base et trois huiles additivées contenant des polymères de type polyméthacrylate. Les polymères proviennent tous des mêmes monomères mais leurs masses moléculaires diffèrent : $M_w=25000$ pour le PMA1, $M_w=190000$ pour le PMA2 et $M_w=370000$ pour le PMA3. Des mesures de contrainte normale et de viscosité ont été effectuées sur chacune des huiles contenant des polymères. Comme observé sur la figure 7.4 ci-dessous, nous avons pu noter à la fois l’apparition des contraintes normales (sur la première différence de contraintes normales) et la perte temporaire de viscosité.

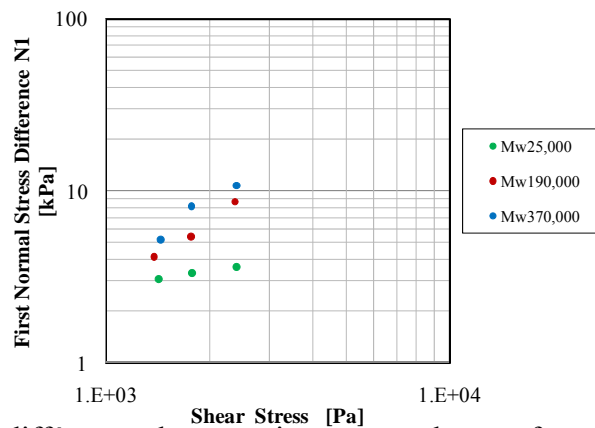


Figure 7-4 Première différence de contraintes normales en fonction de la contrainte de cisaillement.

La figure 7.5 montre les coefficients de frottement en fonction du nombre de Hersey pour une température d'alimentation de 60°C, deux vitesses de 500 et 1000 tr/min et pour des charges statiques allant de 0,8 à 9 kN. On peut remarquer que toutes les huiles contenant des polymères permettent de diminuer les coefficients de frottement pour le palier en bronze, mais pas pour le palier en acier régulé. De plus, alors que la différence de coefficient de frottement entre 1000 et 500 tr/min est significative pour l'huile de base, la réduction de la vitesse de rotation de 1000 à 500 tr/min a une très forte influence sur la réduction des coefficients de frottement pour les huiles contenant des polymères. Ceci nous suggère que la viscosité apparente a diminué avec l'augmentation du cisaillement pour les huiles contenant des polymères, du à la diminution de l'épaisseur du film à plus faible vitesse.

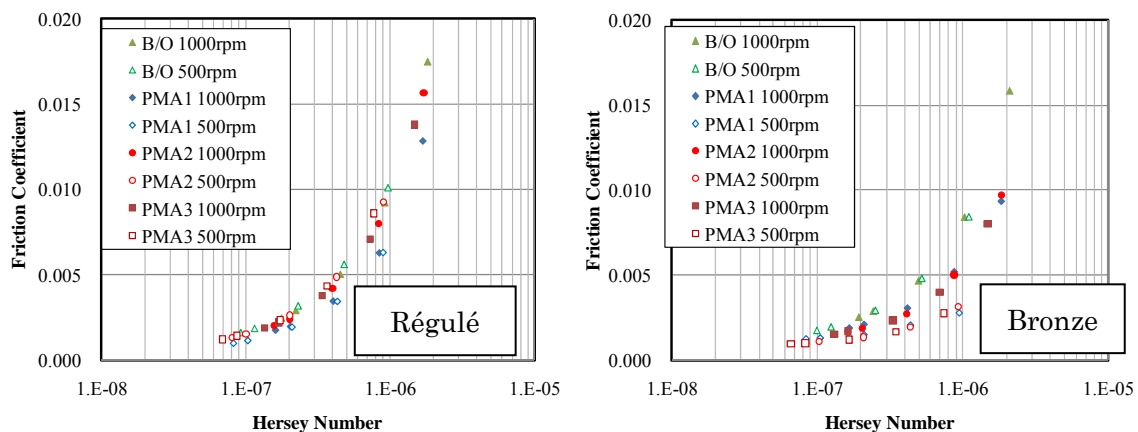
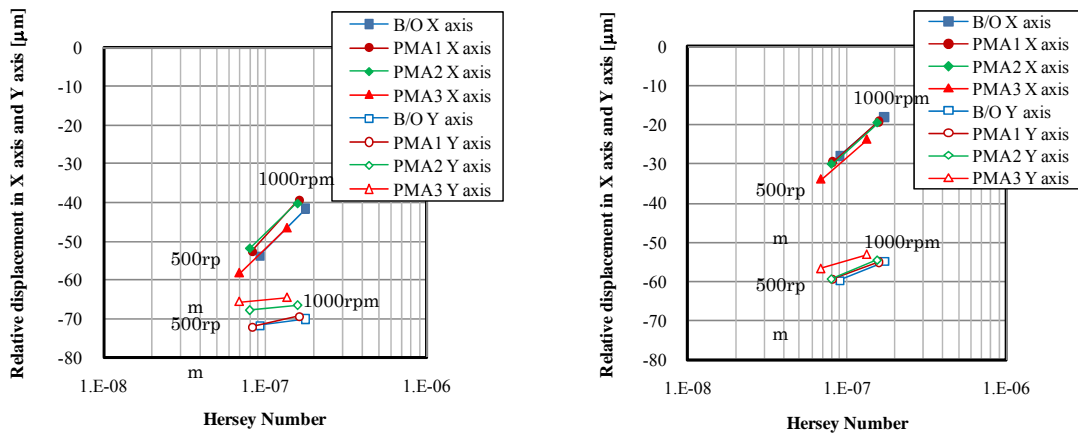


Figure 7-5 Coefficient de frottement pour les paliers bronze et régulé.

Le déplacement relatif de l'arbre par rapport au coussinet en fonction du nombre de Hersey est présenté dans les figures 7.6 et 7.7 pour une température d'alimentation de 60°C, deux vitesses de 500 et 1000 tr/min et pour une charge statique de 1,72 et 9 kN. Le modèle

thermohydrodynamique (THD) développé à l'Université de Poitiers a été utilisé pour les simulations en considérant les lubrifiants comme des fluides newtoniens.

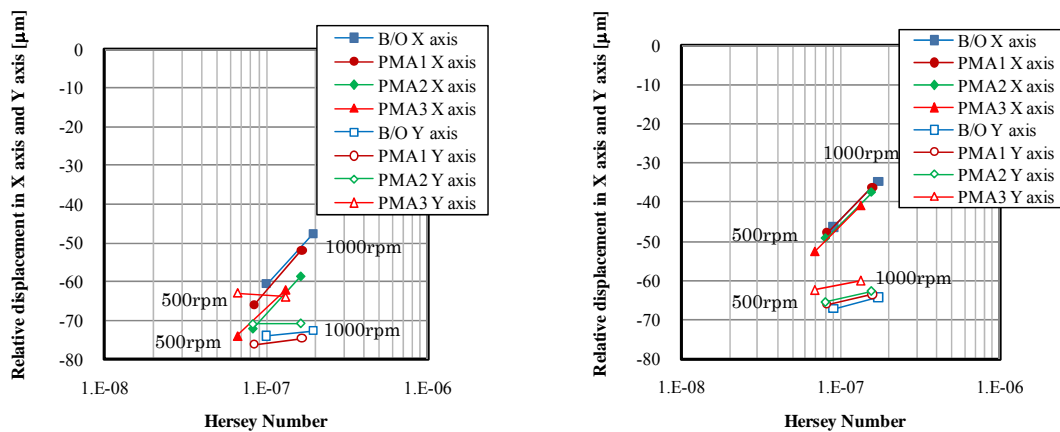


(a) Résultats expérimentaux

(b) Simulation

Figure 7-6 Déplacement relatif de l'arbre en fonction du nombre de Hersey pour le palier en acier régulé.

Les résultats numériques montrent que le déplacement relatif suivant l'axe X, pour tous les lubrifiants, peut être regroupé suivant une même ligne pour les deux types de paliers (figures 7.6(b) et 7.7(b)). Sur la figure 7.6(a), nous pouvons observer que le déplacement relatif de l'arbre suivant l'axe X avec les huiles contenant des polymères est toujours supérieur ou égal à celui obtenu avec l'huile de base pour le palier en acier régulé. L'amplitude du déplacement relatif pour les huiles contenant des polymères peut être inférieure à celle à laquelle on pourrait s'attendre pour des fluides newtoniens. Ceci nous permet de penser que l'apparition de l'effet de la contrainte normale avec les huiles contenant des polymères est anticipée avec les paliers en acier régulé mais pas avec les paliers en bronze. L'effet de la diminution temporaire de viscosité est supérieur à celui de la contrainte normale pour le palier en bronze.



(a) Résultats expérimentaux

(b) Simulation

Figure 7-7 Déplacement relatif de l'arbre en fonction du nombre de Hersey pour le palier en bronze.

8. Conclusions

Les conclusions que nous pouvons tirer de cette étude sont les suivantes :

- (1) Cette étude a permis de confirmer que la fiabilité du palier fonctionnant en régime de lubrification mixte dépend à la fois de l'huile de base, des modificateurs de frottement ainsi que des matériaux constituant le palier.
- (2) L'huile de base, tout comme les polymères, affecte les propriétés du frottement en lubrification hydrodynamique. Leur efficacité dépend également des paliers considérés.

Notations

| | |
|------------|---------------------------------------|
| B | bearing length |
| C | radial clearance |
| C_p | lubricant specific heat |
| D | bearing diameter |
| D_s | shaft diameter |
| e | eccentricity of the shaft centre |
| g | switch function |
| h | film thickness |
| H | heat transfer coefficient |
| H_r | slit height of rheometer |
| K | thermal conductivity |
| L_r | slit length of rheometer |
| N | rotational speed |
| p | fluid pressure |
| p_c | cavitation pressure |
| P_{spec} | specific load = W/BD |
| Q | flow rate |
| R | bearing radius |
| T | temperature |
| u, v, w | velocity components in the fluid film |
| W | applied load |
| W_r | slit width of rheometer |
| x, y, z | Cartesian coordinates |

| | |
|----------------------|--|
| γ | bulk modulus in Elrod's model |
| θ, r, z | cylindrical coordinates for plain bearing |
| θ, ϕ, r | cylindrical coordinates for rheometer |
| θ_1, θ_2 | angular coordinates that indicate the beginning and the end respectively of the axial groove |
| Θ | density ratio in the full-film region and mass fraction in the rupture zone |
| μ, η | fluid dynamic viscosity |
| μ_0 | fluid dynamic viscosity at the supply temperature T_{sup} |
| σ | shear stress |
| $\dot{\gamma}$ | shear rate |
| ρ | fluid density |
| ω | angular velocity of the shaft |
| ω_0 | angular velocity of the cone geometry of rheometer |

Subscripts

| | |
|-----|------------------------------|
| a | apparent |
| b | bush (plain journal bearing) |
| L | liquid |
| g | groove |
| G | gas |
| r | rheometer |
| sup | supply |
| w | wall |
| x | exit |

Introduction

From the viewpoint of the prevention from global warming (reduction of CO₂), it has been necessary to improve fuel economy in automotive engines. It is very important, in improving fuel economy, to decrease the friction loss even in engine oil. Recently, the ratio of hydrodynamic lubrication region in engines has been increasing because improvement of machine elements which are in boundary lubrication has been advancing.

Thus, the ratio of plain bearing lubrication is increased, and the friction reduction of bearing lubrication is required. Figure 1 shows motoring engine friction torques with a commercially available 1.8 liters, linear four cylinders DOHC engine using engine oils with and without MoDTC (molybdenum dithiocarbamate) which is a friction modifier widely used for fuel economy engine oils in Japan [1].

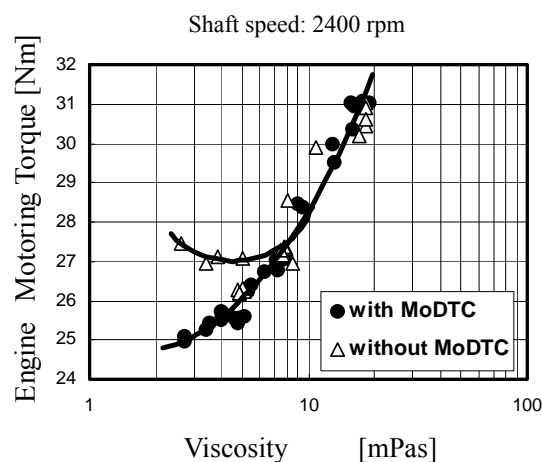


Figure 1 Effect of oil viscosity in engine motoring torque (fuel economy)

The horizontal axis shows viscosity which is high shear viscosity at the tested temperatures calculated from HTHS viscosity (high temperature high shear viscosity, American Society of Testing and Materials D4683) at 100 and 150 °C. The vertical axis shows the engine motoring torque which means friction loss. Basically the lower the oil viscosity, the lower the motoring torque. The point of the minimum friction torque is existed. In order to reduce the friction, reducing the bearing diameter [2] is also effective as well as lowering lubricating oil viscosity [3-8]. However, these raise the importance of securing the reliability of the plain bearings especially in the circumstance that the engine output has been increasing [9].

Although the effectiveness of lowering oil viscosity is greater, sufficient amounts of research have not been carried out in this area because of concerns about the influence in engine plain-bearing lubrication and the subjects were mainly concerning improvement of securing the reliability of the plain bearing in hydrodynamic lubrication. Thus, the analysis of plain bearing performance is limited to considering only physical properties of lubricating oil. In order to improve the fuel efficiency with lubricants, polymers have been widely used for decreasing apparent viscosity at a low temperature keeping a high temperature viscosity at a certain limit for most of engine oil. It is known that the viscosity of oil containing polymer is decreased at a high shear rate. While such viscosity loss contributes to decrease friction loss, it can cause metal contact and deteriorate the reliability of plain bearings [1, 10].

In a part of our study, it was observed that friction losses in high-viscosity base oils were lower than those in low-viscosity base oils under an equal bearing constant [11]. The contact between the shaft and the plain bearing occurred more readily when low-viscosity base oils were used. Also, this contact is more likely to occur with highly refined base oils than with low-refined base oils containing sulfur as impurities. Furthermore, outstanding evaluation methods to optimize lubricant formulation have not been established.

In addition, non-ferrous metal is used for plain bearings in automotive engines. Copper-lead plain bearings have been used from the past, but lead is well-known as environmentally hazardous material. The regulation of lead in bearing materials has begun with the goal of preventing heavy metal pollution when automobiles are scrapped [12], necessitating the development of lead-free bearing materials [13, 14]. This has greatly changed automotive bearing systems. Many of bearing manufacturers have been investigating alternative materials for lead. The influence of bearing materials on plain bearing lubrication is normally

investigated for boundary lubrication but not for hydrodynamic lubrication. However, it was observed that bearing performance greatly varied with different kinds of plain bearing materials in mixed and hydrodynamic lubrication in our previous study. Thus, the authors considered that the plain bearing performance would depend on bearing materials and kinds of lubricants used, and their compatibility will be important.

Therefore, further study for friction reduction and reliability improvement in engine plain bearing with lubricants considering bearing materials is required. (When a load is increased in experiments, the contact resistance (CR) ratio between a shaft and a bearing becomes close to 0 % and the friction coefficient starts to fluctuate. "Reliability" in this study was defined as the maximum load before the fluctuation of the friction coefficients starts.)

Chapter 1

Review concerning this work

1-1 Research on friction reduction and reliability improvement with lubricants

There are publications on the friction reduction and reliability improvement with lubricants. They are mainly concerning lubricants containing polymers and there are a few publications concerning base oils and friction modifiers.

In 1961, Okrent investigated the effect of lubricant viscosity and composition on engine friction and bearing wear [15]. Two sets of engine tests were carried out to determine engine friction and measure the connecting-rod bearing wear rates. Paraffinic mineral oils (which mainly contain alkane hydrocarbons of straight chain) and naphthenic mineral oils (which mainly contains types of alkanes with one or more rings of carbon atoms in the chemical structure) oils were evaluated in addition to polymer-containing oils with polyisobutylene. The addition of polymers to mineral base oils resulted in reduced engine friction and lower bearing wear. The amount of friction and wear reduction observed was dependent on polymer type and concentration. They continued this work, and evaluated other polymer-containing oils [16]. Two polyisobutylenes and three polymethacrylates were used as polymers. For those polymers, there was no difference in chemical structure, and the differences were only molecular weight. They were blended with mineral base oils. It was found that polymer-containing oils gave less friction and less bearing wear than straight mineral oils of the same viscosity. They also studied the effect of detergents, which is mainly used to clean engine pistons. The addition of 4.0% of the detergent increased friction. Studies with polar detergents suggested that the surface properties of polymers were playing a part. In 1964, they also studied the role of elasticity of lubricants in plain bearing performance [17]. Fourteen kinds of oils containing different

polymers were evaluated. Each oil was blended in the same base oil and contained polymer to bring the viscosity to $12.5 \text{ mm}^2 \cdot \text{s}^{-1}$ @ 210 °F. Polymers used were five polyisobutylenes, four polymethacrylates and three multi-functional copolymer system. For those polymers, there was no difference in chemical structure, and the differences were only molecular weight as well as the previous study. The load-carrying ability of the oil was evaluated by measuring the wear rate of the connecting-rod bearing of a V-8 engine. Also, the viscosity and elasticity of the polymer-containing oils were measured in a Mason ultrasonic viscometer. Studies with polymer solutions of the same viscosity and same base oil containing different polymers of various molecular weights and concentrations showed that bearing wear rate correlated with the recoverable elastic strain (recoverable shear). Overall, they studied the effect of polymer-containing oils on friction reduction and plain bearing wear. However, it seems that the analysis on the behavior of lubricants considering chemical structure of the polymers may not be sufficient.

Tao et al. studied the hydrodynamic effect of viscoelasticity in plain bearing performance by measuring the pressure distribution of viscoelastic liquids with polymers (polyisobutylenes of low and high molecular weight) and Newtonian liquids in 1967 [18]. The experimental data were compared with a theoretical pressure field. The load-carrying capacity was calculated by integration of the pressure distribution. It was about 15% above the calculated value compared with the experiment. Friction at journal was also measured but the data obtained were not sufficient to estimate the superior polymer for engine oil development.

Waddey et al. conducted a field test with a taxicab to determine the effect of engine oil composition on engine bearing wear using 10W-40 oil compared with #40 of a single grade in 1969 [19]. The 10W-40 engine oil showed lower wear than the #40 oil with the same low-shear viscosity. Schardel also performed a field test with a number of wear tests with European gasoline and diesel engines in 1970 [20]. It was confirmed that polymethacrylate viscosity index improvers could lower wear below that predicted on the basis of oil viscosity. They could observe the significant effect in anti-wear performance with polymer-containing oils but analysis of the behavior of the lubricants in bearing lubrication was not included.

Wada et al. studied hydrodynamic lubrication of journal bearings with pseudo-plastic lubricant which is a low viscosity base oil containing of polyisobutylene of 2 wt% compared with the base oil in 1970 [21, 22]. They theoretically and experimentally evaluated bearing performance. Also, viscosity loss of the lubricants used was measured at high shear rates using a rheometer. As a result, the oil with polyisobutylene showed viscosity loss which is behavior

as pseudo-plastic lubricants. It was confirmed that bearing pressure distribution for the oil with polyisobutylene was lower than with the base oil in the journal bearing tests. That is, the bearing load-carrying capacity with the oil containing polyisobutylene was lower than with base oil. In this case, the polymer-containing oil evaluated was only one kind and the data were not sufficient for finding the tendency of lubricant characteristics.

Rosenberg developed an experimental technique to measure the minimum oil film thickness and friction coefficient of dynamically loaded journal bearings in 1973 [23]. The plain bearing used for this apparatus consisted of a lead-based Babbitt cast into and on a porous copper-nickel matrix which in turn was bonded to a steel backing. Measurement was conducted with base oil and multigrade oils of 10W-30 and 10W-40 containing polymethacrylate or polyisobutylene. The measured film thickness correlated with analytically predicted values for the base oil. However, those for a few oils containing polymers could not be predicted from the ASTM low shear rate viscosity. They suggested that other viscosity measurements should be developed. In addition, all the oils containing polymers showed lower friction coefficient than expected by their low viscometer values. He continued this work further, and examined the ability of oils containing polymers to lubricate crankshaft journal bearings in 1975 [24]. Thirteen kinds of oils containing polymers such as polymethacrylates, styrene polyesters, polyacrylates, polyisobutylenes and olefin-copolymers were evaluated with the developed apparatus. Polymer additives which increase the minimum oil film thickness also increased friction by a proportional amount. No one kind of polymers was shown to be superior. There is information about the bearing material used in their literature and the tests were carried out with various kinds of polymer-containing oils. However, the effect of the bearing material on the bearing performance was not mentioned.

Harnoy analyzed the effect of elasto-viscous lubricants in bearing performance using a constitutive equation which takes into account normal stress and relaxation time of the lubricants [25]. It was confirmed with the calculation that the bearing performance was improved with increasing eccentricity and relaxation time.

Bell et al. investigated some relationships between the viscometric properties of motor oils and performance in actual engines in 1977 [26]. Fuel consumption and engine wear were evaluated with typical European gasoline engines. Six kinds of oils containing commercially available polymers were tested and the results were compared with those tested with a base oil. As a result, it was shown that fuel consumption during moderate steady state engine operation correlated with dynamic viscosity at a shear rate of 10^6 s^{-1} at $100 \text{ }^\circ\text{C}$. Also, it was found that

bearing wear during severe steady state engine operation correlated with dynamic viscosity at a shear rate of 10^6 s^{-1} at $150 \text{ }^\circ\text{C}$.

McMillan et al. evaluated anti-wear performance of multigrade oils for plain bearings in severe field tests of 80,000 km in 1978 [27]. They tested engine oils containing polymer of which the chemical composition and the molecular weight were known. Also, there were descriptions of the plain bearing materials used. They found that the bearing wear with high molecular weight polymer was greater than with low molecular weight polymer, but did not investigate the effect of the bearing materials.

Dancy et al. developed a motored-engine test with a single-cylinder and air-cooled engine in 1980 [28]. They evaluated friction characteristics of engine oils by engine friction using the developed motored-engine and viscosity measurements using high shear rate viscosity tests. Several kinds of single-grade oils and multigrade engine oils of 10W-40 and 20W50 containing the same dispersant-inhibitor additive package with no friction modifiers were prepared. The multigrade engine oils contained the same type of polymer which is a viscosity index improver. It was found that kinematic viscosities did not represent viscosity conditions experienced during engine operation. Better relationship between friction with the motored-engine test and viscosities measured at a shear rate of $1 \cdot 10^6 \text{ s}^{-1}$ was observed. They also developed an engine oil test method to evaluate the load carrying capacity with an electrical contact method in 1981 [29]. It was found that the load carrying capacity of non-Newtonian oils in plain bearings was related to the viscosities measured at a shear rate of $1 \cdot 10^6 \text{ s}^{-1}$.

DeHart et al. evaluated the plain bearing load-carrying capacity of polymer-containing oils in comparison with base oils using a plain bearing test apparatus developed in 1980 [30]. A radiometric method was used to determine the load-carrying capacity. Polymethacrylates were selected as polymers. A correlation between the relative load-carrying capacity and the effective oil viscosity at $110 \text{ }^\circ\text{C}$ and a shear rate of $1 \cdot 10^5 \text{ s}^{-1}$ was observed.

Phan-Thien et al. analyzed the plane isothermal flow in a journal bearing using the most general viscometric constitutive model at low eccentricity model in 1981 [31]. They suggested a method to measure the first normal stress difference at high shear rates.

Van Os et al. investigated the relationship between high-temperature, high shear-rate viscosity and plain bearing wear of an engine under boundary lubrication conditions with multi-grade engine oils which contained polymers in 1981 [32]. Experiments to evaluate wear were carried out with a plain bearing tester. Commercially available plain bearings made of copper-lead-tin alloy were used for the tests. It was found that wear was not influenced by the

high-shear rate viscosity at least in the region between 2.1 and 4.9 mPa.s. They also studied the effect under static load. It was confirmed that the minimum oil film thickness and the total friction were the same for polymer-containing oils compared with polymer-free oils if the Sommerfeld number was provided with the high-shear rate viscosity. They also investigated the effect of lubricant elasticity on plain bearing performance in 1983 [33]. An experimental measurement apparatus of oil film thickness for a statically loaded plain bearing (Babbitted bearing) was developed. They measured the minimum oil film thickness, the friction coefficient and the bearing attitude angle using two single grade engine oils and seven multigrade engine oils. The multigrade engine oils tested were formulated with different polymers as viscosity index improver. (There was no indication about the chemical composition of those polymers.) The relationship between the minimum oil film thickness and the Sommerfeld number was the same for oils with and without polymers. However, a significant decrease in the bearing attitude angle was observed for the polymer containing oils compared with oils containing no polymers at the same Sommerfeld number.

Rhodes et al. developed two procedures to evaluate single-grade and multigrade oils using Rebeco L-38 engine with the standard test bearing of SAE 480 sintered copper-lead with no overlay and studied the effects of engine oil viscosity and chemical composition on plain bearing wear in 1981 [34]. Several single-grade oils and multigrade oils containing polymers such as styrene/diene copolymer, olefin copolymer and polymethacrylate were evaluated. Chemical composition such as over-based detergent was found to have a dominant effect on plain bearing wear. For the eleven multigrade oils compounded with the same dispersant-inhibitor, there was no correlation between bearing distress and dynamic viscosity measured at shear rate of $1 \cdot 10^6 \text{ s}^{-1}$ and 150 °C. They pointed out that the lack of correlation was attributed to the viscoelastic characteristics of the non-Newtonian fluids. Even if there was the description of the bearing material, the effect of the bearing material was not discussed.

Filowitz et al. developed a plain bearing test apparatus to measure relative oil film thickness with a single cylinder engine in 1982 [35]. The main bearing was electrically insulated from the block and a small voltage impressed between the bearing and crankshaft. The relative film thickness was determined by the extent of the electrical discharge. They evaluated three kinds of base oil of different viscosities and five polymer-containing oils. As a result, polymer-containing oils showed thinner oil film thickness than the Newtonian oils of the same low-shear viscosity. It was noted that further investigation would be needed to find out viscoelasticity and concentration effects for polymers. Craig et al., co-workers of Filowitz

developed another plain bearing test apparatus to calculate oil film thickness from the measurement of the bearing's capacitance in 1982 [36]. Single grade engine oils of which low-shear viscosity range was from about 6 to 29 $\text{mm}^2 \cdot \text{s}^{-1}$ at 100 °C were evaluated. The effect of viscosity in the minimum film thickness was investigated. It was noted that the minimum oil film thickness in low viscosity range was significantly reduced compared with that in high viscosity range. Since the data were arranged with the oil viscosity measured at 100 °C with a viscometer, measurements of temperature at the bearing was considered to be preferable to evaluate the effect of viscosity.

Schneider et al. evaluated plain bearing performance with a centrifugal bearing test machine which applied a rotating load to the bearing in 1982 [37]. Thirteen commercial polymers such as polymethacrylates, polyisobutylenes and olefin copolymers were blended with base oil. The oil film thickness and friction of the oil samples were evaluated using the plain bearing test apparatus developed. The tendency of superior polymer class was not found. They also studied the effect of fuel-saving engine oils containing friction modifiers on plain bearing load capacity with the bearing test machine. The use of an insoluble friction modifier (graphite additive) resulted in a higher bearing load capacity than expected.

Hutton et al. measured viscosity of 10W-40 engine oils containing different viscosity index improvers such as polymethacrylate and styrene/diene copolymer at high pressures up to 200 MPa over a wide temperature and shear rate range in 1983 [38]. A plain bearing wear was also measured using a bearing test to investigate the effect of oil viscosity. It was found that bearing weight loss of multigrade oils containing different viscosity improvers showed a better relationship with high shear viscosities at high pressure than with high shear viscosities at atmospheric pressure.

Bates et al. investigated a correlation between engine oil rheology and oil film thickness in engine plain bearings in 1986 [39]. They measured the oil film thickness in the bearing by using the electrical measurement technique with a 3.8 liters, V-6 engine. Measurements of viscosity and elasticity were also made using kinematic and tapered bearing simulator viscometer and Weissenberg rheogoniometer and Lodge stress meter. Twenty two of oils including single grade and multi grade engine oils were evaluated. The use of a viscous and an elastic parameter improved the correlations of bearing oil film thickness with oil rheological properties. They continued this work and developed a cyclic durability test to evaluate bearing wear with a 2.8 liter, V-6 engine in 1989 [40]. The anti-wear performance for three multigrade oils of SAE 5W-30 and four single grade oils was evaluated. The SAE 5W-30 oils were

formulated with different kinds of polymers such as styrene/isoprene of a high molecular weight, styrene/isoprene of a low molecular weight and styrene/butadiene. It was found that there was a critical minimum level for the load bearing capacity, and it corresponded to a HTHS (high temperature high shear) viscosity at least equal to 2.5 mPa·s for the engine used. A minimum value for HTHS viscosity measured at $1 \cdot 10^6 \text{ s}^{-1}$ of a shear rate was deficient as a correlation of bearing oil film thickness.

Olson investigated a relationship between engine bearing wear and oil rheology. This study was an attempt to extend the work of T.W. Bates et al. in 1987 [41]. He conducted engine bearing wear tests using two different engines (2.3 liter and 3.8 liter engines). Oils used were two multigrade oils of SAE5W-30 containing styrene/diene polymer or olefin copolymer and two single grade oils of SAE20 and SAE30. Viscosity and normal stress of the oils were measured, and relaxation times were also calculated. The elastic properties of the multigrade oils were represented by a relaxation time in an empirical model of bearing wear and oil rheology.

Rastogi et al. developed a theoretical analysis for lubricant flow in a dynamically loaded short journal bearing 1990 [42]. Their numerical calculation showed that the pressure distribution, the minimum oil film thickness, the attitude angle, and the shaft orbit were affected by the presence of fluid elasticity for time varying loads.

Davies et al. numerically investigated the temperature and pressure effects in two-dimensional viscoelastic flow between eccentrically rotating cylinders for high eccentricities in 1994 [43]. They suggested that pressure-thickening dominates the viscosity behavior rather than shear-thinning or temperature-thinning at high eccentricities.

Berker et al. experimentally investigated the flow of single grade and multigrade oils between eccentric cylinders to evaluate the effect of polymers in 1995 [44]. They measured an oil film thickness in a dynamically loaded plain bearing. Three single grade oils and four multigrade oils were tested. It was found that viscoelasticity associated with polymers did not influence minimum oil film thickness or attitude angle under loading characteristic of an engine cycle.

Williamson et al. applied a measurement technique of lubricant viscoelasticity using a slit die rheometer to measure the viscoelasticity of conventional multigrade engine oils at temperatures and shear rates in 1995 [45]. They evaluated nine multigrade oils. Multigrade oils with the same shear viscometric properties showed significant differences in their viscoelastic behavior. No comparison between the results of the viscoelasticity evaluation and plain bearing

performance was indicated. Also, there was not any information about polymers in the multigrade engine oils. They also evaluated the effect of polymer-containing oils on plain bearing load carrying capacity by using the plain bearing simulator developed in 1997 [46]. Four single grade engine oils and twelve multigrade engine oils were evaluated. A significant enhancement of load carrying capacity in the multigrade oils was discovered under operation at a high eccentricity ratio but no enhancement was observed at lower eccentricity ratios. They measured the viscoelastic properties of multigrade engine oils (10W-40) and investigated their effect on plain bearing performance in 1997 [47]. Four multigrade engine oils of 10W-40 were evaluated. It was found that viscoelasticity produced a measurable and beneficial effect on lubrication characteristics at the higher eccentricity ratios in plain bearing lubrication, and longer relaxation time would be needed. Li et al. also investigated the effect of lubricant rheology on the dynamically loaded plain bearing performance by taking a computational study with B.P. Williamson. It was found that a piezoviscous lubricant stabilized the motion of a journal [48].

Bair developed a high pressure rheogoniometer which can measure shear stress, and normal stress difference in torsional flow to pressures of 240 MPa and shear rates of more than $1 \cdot 10^4 \text{ s}^{-1}$ in 1996 [49]. The instrument was constructed by replacing the concentric cylinder pair, torque transducer and closure in the pressure vessel of the Couette device by a rheogoniometer cartridge. Four kinds of lubricants were evaluated. Three of them were base oils, which are mineral oil and polyphenyl ether. The other oil is a polymer blend with polybutene of which number average molecular weight of 25,000. Simple low molecular weight liquids generated measurable and significant normal stress differences when the shear rate is high. The relationship between the normal stress difference and the shear stress was a weak function of pressure. Bair et al. also measured elasticity in multigrade engine oils at elevated pressure using the rheogoniometer developed in 2007 [50]. Eight kinds of oils with different polymers were blended with an API group II mineral oil to meet 10W-40 viscosity specification. The polymers used were the following: styrene, olefin copolymer polyisobutylene, star and polymethacrylate. The effect of pressure is to increase the normal stress for a fixed shear rate, but the normal stress difference when plotted versus the shear stress is relatively independent of the temperature and the pressure. There was not any data of plain bearing performance compared with the normal stress obtained.

Sorab et al. investigated friction reducing potential of low viscosity engine oils in plain bearings in 1996 [51]. They developed a plain bearing test apparatus using an engine

connecting rod to measure friction and wear in plain bearings under various speed, load and temperature conditions. Eight kinds of oils were evaluated. The baseline oil was a synthetic base oil, and multigrade engine oils of various SAE viscosity grades (5W-20, 5W-30 and 20W-50) were used. In 5W-30, ILSAC GF-2 type (fuel economy type) oils with and without friction modifiers were included. Significant friction reduction was observed with the use of low viscosity oils under hydrodynamic lubrication conditions. The oils with friction modifiers showed lower friction than those without such additives in mixed lubrication conditions.

Ono et al. investigated plain bearing performance with low HTHS (high temperature high shear) viscosity oil by means of an engine test (JASO M333-93 specification) which is a high temperature oxidation test procedure for gasoline engine oils and a bearing rig test in 1998 [52]. Three kinds of plain bearing materials were used. Two of them were Cu-Pb bearings with different overlays. The overlay was plated on the inner surface of the bearings with a thickness of 20 μm . The other type was an Al-Sn-Si bearing with no overlay. Seven kinds of engine oils having API SG performance were prepared. Their HTHS viscosity range was from 1.8 to 3.0 mPa·s at 150 °C. Five engine oils contained polymethacrylates and one engine oil olefin copolymer. An engine oil was a single grade with no polymer. It was found in both the engine tests and the rig tests that wear of the Cu-Pb bearing with lead-tin-copper overlay increased for low HTHS viscosity engine oil. The Cu-Pb bearing with lead-tin-indium overlay showed the highest applicability of the three materials. The Al-Sn-Si bearing showed the least wear in the rig test. Also, it was confirmed that the bearing wear correlated with HTHS viscosity. In fact, they investigated the effect of the bearing material in anti-wear and anti-seizure performances, but there was no explanation about bearing friction in the tests performed.

Tamoto et al. examined the possibility of ultra-low-viscosity fuel saving gasoline engine oil in 2004 [1]. An ultra-low-viscosity engine oil was formulated with a special synthetic base oil of which volatility is low in order to solve problems such as viscosity increase and oil consumption increase in JASO engine test for a mineral oil based ultra-low-viscosity engine oil. It showed better performance than the mineral oil based oil but poor wear resistance on plain bearings in JASO engine oil oxidation test. Further study is considered to be needed in order to achieve both the fuel economy and the improvement of the plain bearing reliability.

<Critical review>

(1) Investigation of the effect of base oils

There are a few publications investigating the effect of base oils or singlegrade engine oils on bearing performance. They state only the relationship between the dynamic viscosity of oils and the bearing performance [26, 46]. Also, it is considered that there is no publication concerning the investigation of highly refined base oils which have been widely used in the world in these years.

(2) Investigation of the effect of polymer-containing oils

Most of the research activities for the effect of lubricants are concerning the investigation of polymer-containing oils (multigrade engine oils). The relationship with either the friction reduction or the reliability in bearing lubrication has been mainly investigated. The information such as the chemical structure and the molecular of polymers is hardly described although general chemical names are described in some of the publications [15, 18, 21, 24, 30, 37, 38]. Also, commercially available engine oils are normally used in the experiments [19, 23, 26, 28, 32, 34, 36, 40, 44, 51]. Therefore, it is difficult to select appropriate polymer types for the development of lubricant formulation. Some of the research activities are taking into account and state the effect of viscoelastic properties of polymers [18, 25, 31, 39, 40, 41, 42, 45, 49]. However, they focused on only the research about anti-wear performance or improvement of load-carrying capacity which mean the reliability improvement of plain bearings even if the viscoelastic properties are also considered to affect the friction reduction (the friction coefficients have not been evaluated).

(3) Investigation of the effect of friction modifiers

Friction modifiers are often used for lubricants to reduce the friction in mixed and boundary lubrication. One publication which was investigating the load carrying capacity in plain bearing lubrication was found [37]. However, only a graphite additive which is not normally used for engine oils was evaluated. Since friction modifiers are effective when the lubricating condition shifts from hydrodynamic to mixed and boundary lubrication, further investigation is considered to be needed.

In addition, common to the above all research, is that they do not give consideration to the effect of bearing materials on both of the friction reduction and reliability improvement using lubricants.

1-2 Research on friction reduction and reliability improvement with lead-free bearing materials

In recent years, papers on the friction reduction and reliability improvement with new bearing materials which are lead-free have been published.

Kawagoe et al. investigated new conceptual lead-free overlay of engine plain bearings. In the first place, they performed in 2003 a basic sliding test using Bowden type stick-slip tester to evaluate sliding property with a steel ball for solid lubricants such as molybdenum disulfide (MoS_2), graphite and hexagonal boron nitride (h-BN) [53]. Those materials were mixed with resin, and coated on copper alloy plates with back steel as test specimens. An engine oil of SAE 10W-30 which has API CD performance was used as a lubricant. The MoS_2 showed the smallest roughness on the steel ball. They also examined types of binding resin using a rotating load tester with plain bearings and SAE 5W-30 engine oil of API SJ, and found that the overlay with polyamideimide (PAI) resin had good seizure resistance. As a result, they developed two types of lead-free overlay with MoS_2 and PAI resin for binding. Both of the overlays indicated good corrosion resistance, wear resistance and fatigue resistance compared with the conventional bearings.

Sakai et al. investigated lead-free copper based alloy for three layer bearings under higher load engines in 2004 [13]. They studied the effects of bismuth and molybdenum carbide particle addition into copper based bearing alloy to maintain the anti-seizure performance without lead. The anti-seizure performance for the new materials was evaluated by using a plain bearing test machine. SAE 20 was used as a lubricant. The new copper-tin-bismuth alloy with molybdenum carbide particles showed similar anti-seizure performance to the conventional copper-tin-lead alloy. It was also confirmed that the fatigue strength of the copper-tin-bismuth alloys with molybdenum carbide particle increased compared with that of the copper-tin-bismuth alloy without molybdenum carbide particles. Kawachi et al. continued this work in 2005 [14], and developed a lead-free overlay for three layer bearings of highly loaded engines. A dual-layer of bismuth and silver overlay was chosen and found to be equal or superior to lead/nickel overlays in the reliability in preventing seizure against wear, and demonstrating high potential for applications in bearings under higher specific load engines. In addition, it was found that adjustment of crystal orientation in bismuth plating into microscopic pyramid shapes enhanced the oil wettability of the overlay, leading to improved anti-seizure property.

Hunter et al. introduced two new lead-free aluminum materials, which were AlSn10Si3 and AlSn6Si4 in 2005 [54]. Anti-seizure performance for those materials was evaluated using a journal seizure test machine with 10W-30 engine oil. The new lead-free alloy of AlSn10Si3 showed slightly higher seizure resistance than the existing leaded alloy of AlSn8Si3Pb2 and a slight decrease in fatigue resistance evaluated with a fatigue test machine. However, this material was applicable for lower loaded application. Anti-seizure performance and fatigue resistance for another new material of AlSn6Si4 were equal to the existing leaded alloy in the experiments with 5W-20.

Asakura et al. studied lead-free aluminum alloy bearings with overlay for recent automotive engines in 2008 [55]. A seizure test carried out using a rig test machine to evaluate anti-seizure performance of the developed bearing (Al-Sn-Si alloy bearing with overlay of Bi/Ag) compared with a conventional bearing (Al-Sn-Si alloy bearing without overlay). Also, a fatigue resistance was evaluated. The developed bearing showed superior both anti-seizure performance and fatigue strength to the conventional Al-Sn-Si alloy without overlay under normal conditions. It was confirmed that the developed bearing had comparable performances due to possible enhancement of running-in property by the overlay through particular rig tests under purposeful abnormal conditions. Necessary influences to the bearing were simulated by avoidable foreign particles in lubricating oil and by larger dynamic deformation of the housing with lower stiffness in an engine.

<Critical review>

As mentioned above, research activities regarding lead-free plain bearing materials have been proceeding because of the reduction of lead from the perspective of reducing environmental pollutants. However, most of them are focusing on improvement of seizure resistance, wear resistance and corrosion resistance. Experiments in the research activities of bearing materials were carried out with a few kinds of lubricants.

The author considers that the effect of various lubricants on bearing performance in hydrodynamic and mixed lubrication needs to be investigated using different kinds of bearing materials.

1-3 Aim of this study

From the above mentioned circumstances of the plain bearing research, the aims of this study are the following:

- (1) To investigate the effect of base oils on the friction reduction in hydrodynamic lubrication and the reliability improvement in mixed lubrication,
- (2) To investigate the influence of bearing materials on the friction reduction in hydrodynamic lubrication and the reliability improvement in mixed lubrication,
- (3) To investigate the effect of friction modifiers on the reliability improvement in mixed lubrication,
- (4) To investigate the effect of polymers on the friction reduction in hydrodynamic lubrication,
- (5) To experimentally and numerically analyze the bearing lubrication with polymer-containing oils and investigate the mechanism of their action

A general formulation of engine oil for automotive four cycle engines is shown in Figure 1-1. Engine oil consists of base oils and additives such as anti-wear additives, detergents, dispersants (which acts to disperse sludge in engine oils), viscosity index improvers (polymers) and friction modifiers. In recent years, highly-refined low-viscosity base oils with high viscosity index have been widely used to enhance viscometric property for improving fuel economy and reduce volatility of engine oils. Polymers such as polymethacrylates and olefin copolymers are normally used in combination with highly refined low-viscosity base oils to achieve much higher viscosity index which means superior viscometric property against temperature as shown in Figure 1-2.

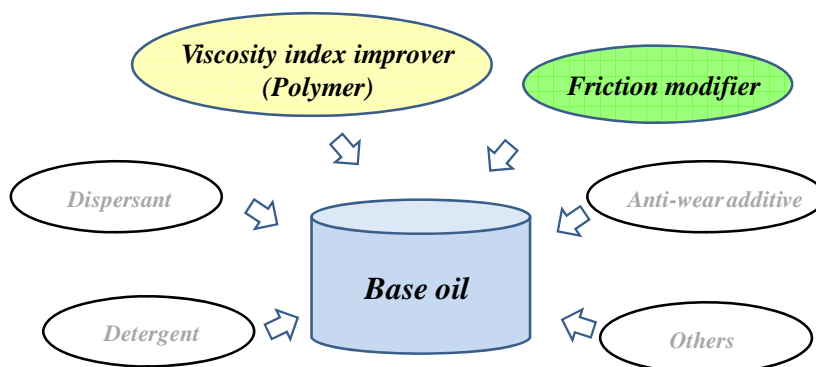


Figure 1-1 General formulation of engine oil

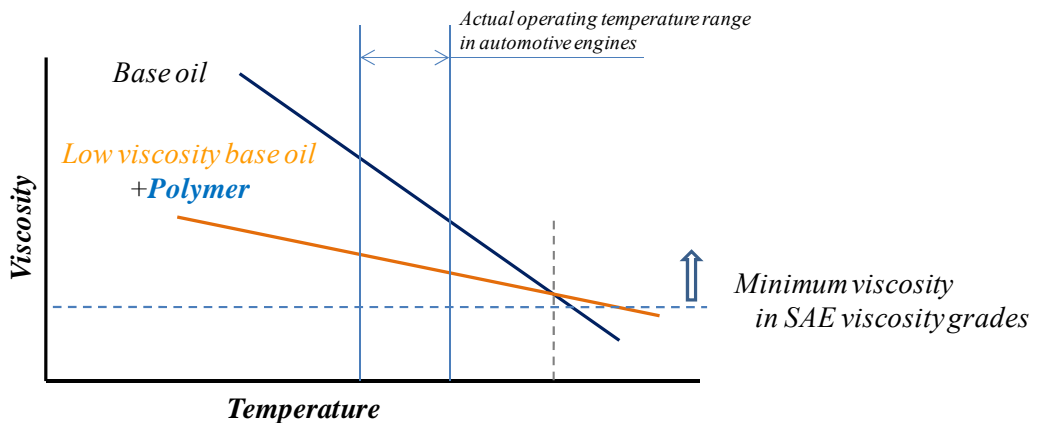


Figure 1-2 Viscometric property for base oil with and without polymer

Also, a common approach to reduce friction and improve reliability in automotive plain bearing lubrication with lubricants is summarized in Figure 1-3.

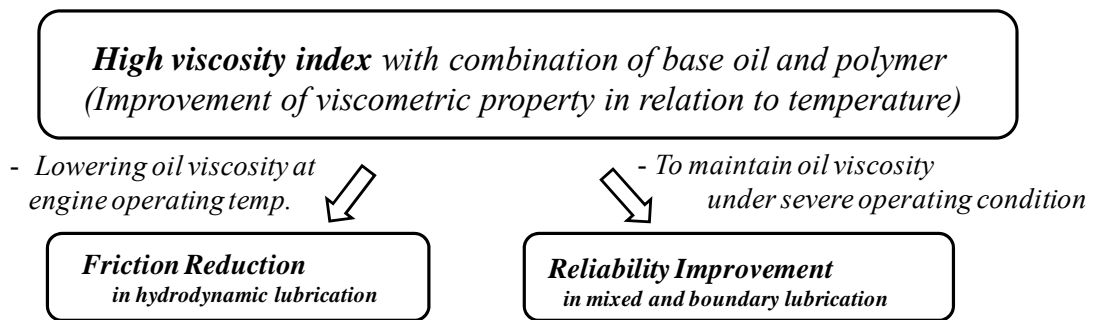


Figure 1-3 Common approach to reduce friction and improve reliability in plain bearing lubrication with lubricants

Basically, the lower the viscosity, the better the fuel economy. However, viscosity at a high temperature needs to be maintained at values that have been standardized in the SAE (Society of Automotive Engineers) viscosity grades for engine oils in order to avoid damage of plain bearings under severe operating conditions. Such an approach for fuel economy engine oils has been common for many years. Many of lubricant and additive manufactures have been making efforts at achieving higher viscosity index even in recent years [61-63] On the other hand, temporary viscosity loss and normal force for polymer-containing oils at high shear rates can be expected to improve fuel economy and reliability in plain bearing performance. Thus, there is a possibility to enhance the both performances with polymer-containing oils. As mentioned

above, although there are the previous research activities on the investigation of the lubricant rheology, they are not considered to be sufficient in order to estimate the optimum lubricant formulation. It is therefore necessary to resume this research with evaluation of various kinds of lubricants and bearings of which materials are known in detail.

Friction modifiers are frequently added to fuel economy engine oils in order to reduce friction in boundary lubrication region. Besides, the bearing performance can be influenced even in the region from hydrodynamic lubrication region to boundary lubrication region with such additives as mentioned in our previous study [11].

Therefore, for components of lubricants used we focused on base oils, polymers and friction modifiers that can improve frictional property and reliability in plain bearings. It is conceivable that the findings in this study can enhance both of the bearing performance (the friction reduction in hydrodynamic lubrication and the reliability in mixed lubrication) in addition to the contribution due to the viscosity index improvement.

For the first step of this study, an automotive plain bearing apparatus was manufactured. The second step was the investigation of the effect of lubricant components and bearing materials in the contribution to the frictional property and the reliability which are not originated from the viscometric property.

1.4 Composition of this thesis

This thesis consists of eight chapters. In the chapter 1, the background for this study and the research activities on plain bearing performance are described, and the necessity and aim of this study are also pointed out.

In the chapter 2, a test apparatus manufactured for automotive plain bearings is indicated. The bearing test apparatus enables to evaluate the plain bearing performance under static and dynamic load conditions and its features are explained in detail. The bearing friction torque, the contact resistance (CR) ratio between a shaft and a plain bearing and the shaft displacement are actually measured with the apparatus in order to evaluate the frictional property and the reliability. Their measurement systems are also indicated.

In the chapter 3, the bearing performance data (friction coefficient and CR ratio) using a Cu-Pb plain bearing for various base oils of different API (American Petroleum Institute) categories with various viscosity grades under static and dynamic load conditions is presented. Then, the effect of the kinds of the base oils is explained and discussed.

In the chapter 4, the bearing performance data for an Al-Si plain bearing and low-viscosity base oils is introduced in comparison with the Cu-Pb plain bearing performance data which was shown in the chapter 3. The effect of refinement level of base oils on bearing performance for two kinds of bearing materials is investigated and discussed.

In the chapter 5, the bearing performance is evaluated using several lead-free bearing materials (Cu alloy and Al alloy with a bismuth/silver overlay) which were newly developed. The effect of friction modifiers and bearing materials is explained with the data of the friction coefficient, the CR ratio and the relative shaft displacement. Also, a difference in the bearing performance between two friction modifiers is further discussed with some surface analysis results of the plain bearings tested.

In the chapter 6, the effect of polymers is introduced with the friction coefficient, the CR ratio and the relative shaft displacement obtained from bearing tests for two kinds of polymer-containing oils compared with those for a base oil. The different behavior of the polymer-containing oils with the two different bearing materials is presented.

In the chapter 7, the behavior of lubricating oil with polymers uniting experiment with a bearing test apparatus at the Poitiers University and simulation (numerical analysis) of plain bearing performance is analyzed. Also, rheological properties of the polymer-containing oils are measured with rheometers. The plain bearing performance will be discussed compared with

their rheological properties (viscosity and normal stress at high shear rates).

In the chapter 8, the conclusions in this study are described. Furthermore, an approach of fuel saving engine oil for the future by coping with both the friction reduction in hydrodynamic lubrication and the reliability improvement in mixed lubrication will be explained.

Chapter 2

A test apparatus for automotive engine bearings

Fuel efficiency of automotive engine oils is often evaluated using actual engines. One of the ways to evaluate fuel efficiency is a motored-engine test in which a crank shaft is rotated by an electric motor measuring friction torque of the shaft [1, 28]. Fuel consumption can be also measured with a fired engine bench test for fuel efficiency evaluation [15, 26, 39-41]. A field test with actual passenger cars is another method that enables to evaluate the fuel efficiency of engine oil [19, 20, 27, 34]. However, the fuel efficiency measured with such methods is originated from many parts such as a valvetrain system, piston rings and plain bearings. It is therefore very difficult to distinguish only the friction of plain bearings from other engine elements while damage of the plain bearings can be evaluated after testing. Also, accurate measurements are required especially in the fired engine bench tests and field tests.

Many of researchers developed their original test apparatuses in order to evaluate frictional properties and/or reliability of lubricants for automotive plain bearings in the past. Rosenberg et al. developed a dynamically loaded plain bearing test apparatus which was equipped with inductive transducers to measure a relative oil film thickness [23]. The measurements were repeatable and appeared to correlate with the values of oil film thickness which was analytically calculated. DeHart et al. used a radiometric method to determine plain bearing load-carrying capacity of polymer-containing oils in comparison with base oils [30, 37]. Van Os et al. developed a statically loaded plain test apparatus [32]. In order to determine a minimum oil film thickness, a shaft position was monitored using eight proximity probes. Filowitz et al. measured a relative oil film thickness by measuring the contact resistance between a shaft and a plain bearing [35]. Craig et al. and co-workers of Filowitz also developed another plain bearing test apparatus to calculate oil film thickness from bearing's capacitance in

1982 [36]. Berker et al. measured an oil film thickness with a dynamically loaded plain bearing test apparatus which was equipped with proximity probes [44]. Williamson et al. evaluated the effect of polymer-containing oils on plain bearing load carrying capacity by using a plain bearing simulator that they had developed [46]. The load-carrying capacity was measured by the load on a stator with piezoelectric force transducers. Sorab et al. developed a plain bearing test apparatus using an engine connecting rod to measure friction and wear in plain bearings under various speed, load and temperature conditions [51]. Loads on the test bearing were applied with an electro servo-hydraulic actuator and friction torque was measured under static load conditions. Ono et al. used a bearing test apparatus with an unbalanced weight, which is assembled on the test shaft [52]. When anti-seizure property of plain bearings is evaluated at bearing manufactures, test apparatuses which are used are often equipped with a hydraulic system to apply a static load to the test bearing [53-55]. The load is increased until seizure occurs to determine the anti-seizure property.

As mentioned above, there are many techniques to evaluate plain bearing performance. Each of them has advantages and disadvantages. Since this study is concerned with automotive engine oil and plain bearings, a test apparatus that enables to evaluate plain bearing performance in boundary lubrication and hydrodynamic lubrication conditions under both static and dynamic load conditions was manufactured. The detail of measurement technique of plain bearing performance is described in addition to the structure of the apparatus in this chapter.

2-1 Plain bearing test apparatus

Automotive bearings differ from ordinary industrial bearings. A fluctuating load corresponding to the crank shaft rotation that synchronizes with the combustion cycles is applied to automotive bearings. Another important characteristic of automotive plain bearings is that the oil is supplied to the bearing through an oil supply port created in the shaft. Thus, a bearing test apparatus in which a load is applied to the bearing by hydraulic pressure supplying oil through the port created in the shaft was manufactured.

Figure 2-1 shows the main portion of the apparatus. Figure 2-2 shows the disassembled apparatus which are a shaft and two half plain bearings installed in split bearing housings.

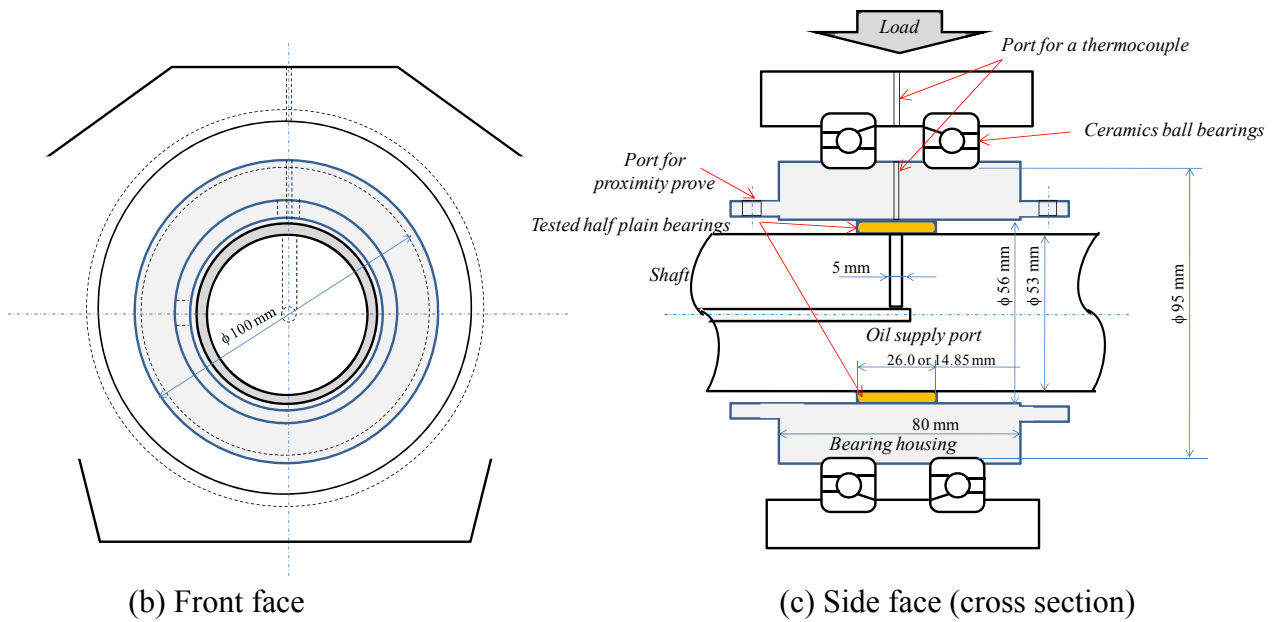
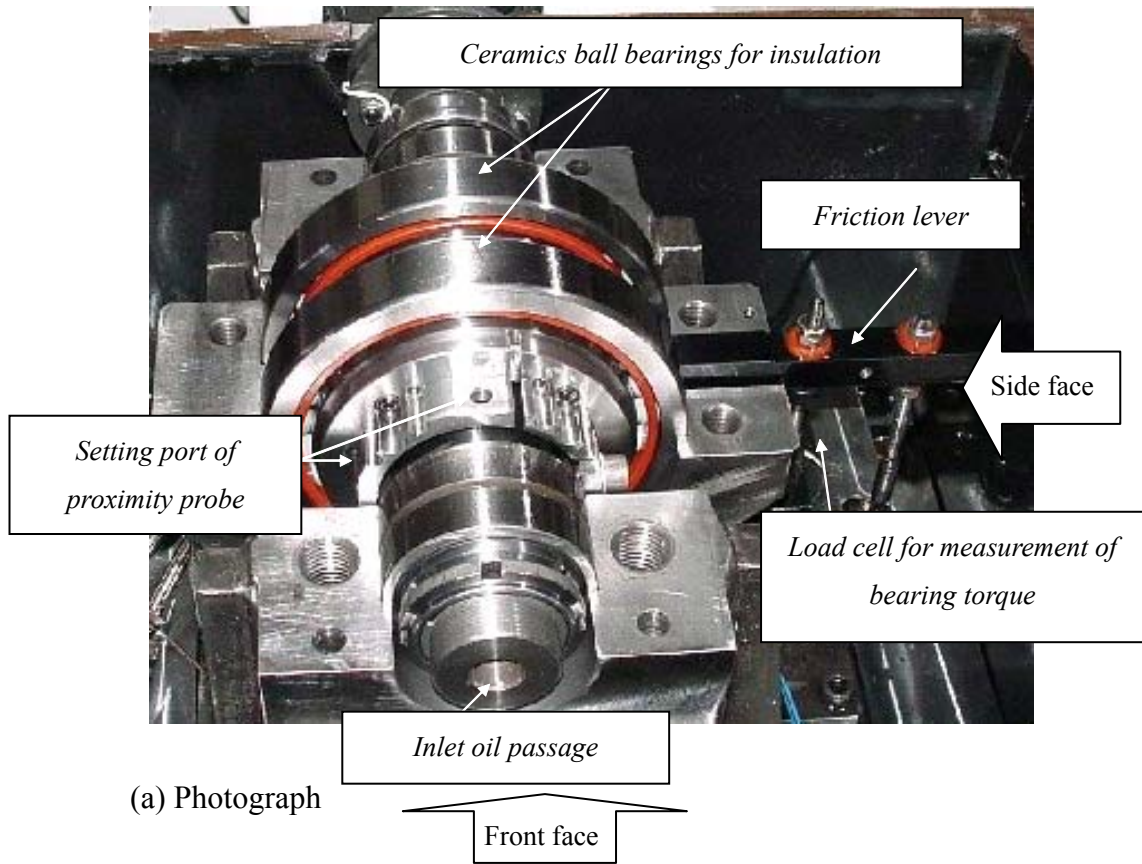


Figure 2-1 Main portion of the developed apparatus

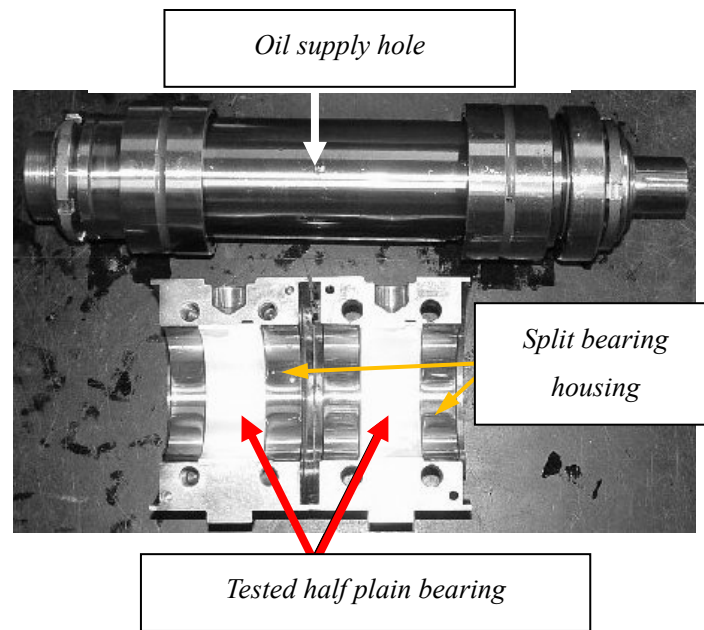


Figure 2-2 Disassembled apparatus

Both the top and bottom bearings are half plain bearings with no oil grooves. The bearings can be installed in the same way as automotive main bearings for engines in this apparatus, as shown in Figure 2-2, the split bearing housings were supported by ceramic ball bearings. The shaft is also supported with two roller bearings which are installed at the outer side of the bearing housing. A lever which is set on the bearing housing is connected with a load cell and prevents the rotation of the tested half bearings. They are also lubricated with the tested oil which is supplied from the outside of the bearings. The following are the main specifications of the shaft and the half plain bearing tested:

- (1) Shaft diameter: $\text{Ø}53$ mm
- (2) Shaft material: JIS (Japanese Industrial Standards) S55C
 --- Carbon steel with induction hardening
- (3) Diameter of oil supply port : $\text{Ø}5$ mm (CC 0.5)
- (4) Inside diameter of half plain bearing (D): $\text{Ø}53$ mm
- (5) Thickness of half plain bearing: 1.5 mm
- (6) Width of half plain bearing (B): 26 mm or 14.85 mm
- (7) Half plain bearing material: Various kinds ¹
- (8) Oil clearance between the shaft and the plain bearing ¹

End note: ¹ Detailed information will be described in the later chapters

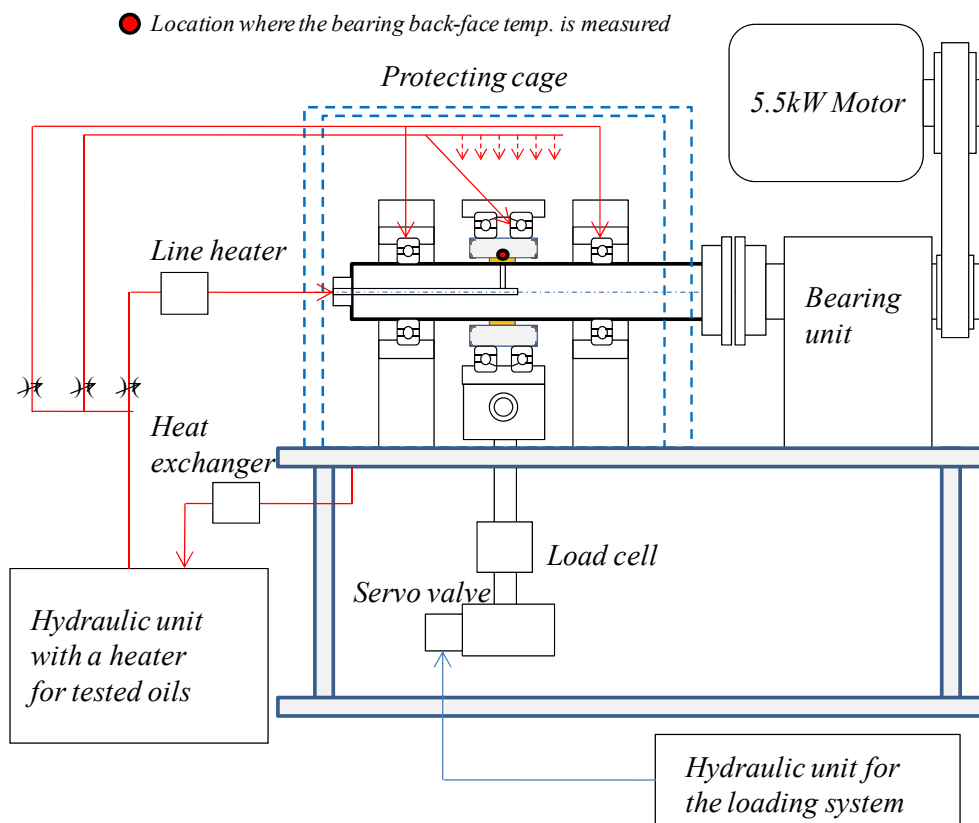


Figure 2-3 Schematic representation of the bearing test apparatus

Figure 2-3 shows the schematic representation of the plain bearing test apparatus. The main portion of the test apparatus was set in a cage made of steel. The cage has an observation window on the top so that the operation of the test apparatus can be visually checked. The oil which comes out of the plain bearing tested and the support roller bearings is flowing out from the bottom of the cage and pumped out to the oil tank.

The shaft is connected to an AC electric motor (AC 200V) of 5.5 kW through the belt and driven by an electronic controller. The maximum shaft speed is 6,000 rpm controlled with an accuracy of ± 2 rpm.

The feeding oil is supplied by an oil supply unit with a hydraulic pump controlling the oil temperature and pressure. The temperature of the oil tested is controlled using a heat exchanger and electric heaters in the oil supply line and the oil tank. The feeding oil temperature is maintained at tested temperatures of 60, 80 and 100 °C. The feeding oil pressure is maintained at 0.5 MPa. The oil is also sprinkled from the upper part to the main portion of the test apparatus in order to maintain the apparatus at a constant temperature.

The load is applied from the top of the half plain bearing downward along the vertical direction with a hydraulic actuator which was installed under the main portion of the test

apparatus. The hydraulic actuator and the half plain bearings which were set in the bearing housing were linked with a rod which flexibly moves to avoid any misalignment. The applied load was detected using a load cell with uncertainty of $\pm 0.5\%$. The maximum specific load applied for this study in this test apparatus is actually small compared with that in actual engines. It becomes approximately only 13 MPa at most in case of a plain bearing with width of 14.85 mm under 10 kN which is the maximum load. Also, since the dynamic load is sinusoidal, it is different from actual operation of engines. However, the purpose of this study is to investigate the behavior of lubricants and rank their bearing performance. The metal contact between the shaft and the plain bearing was observed with one lubricant but not with others using the test apparatus in this study. Therefore, the author considered that the lubricants tested in this study were evaluated under very severe conditions and the apparatus was sufficient to rank the bearing performance for different kinds of lubricants. The data obtained should lead to guidelines to develop fuel saving engine oils with the reliability in plain bearing lubrication even for actual engine operation.

The hydraulic actuator is controlled using another hydraulic system with an electric servo valve. A commercially available hydraulic fluid is used for the hydraulic system.

The rotation phase of the shaft corresponds to the location of the oil supply port. When a dynamic load is applied to the plain bearing with cyclic operation of a sine wave, the maximum load is controlled so that the oil supply port is not blocked, regardless of the shaft rotation in bearing tests under dynamic load condition.

Friction torque of the plain bearing was measured with a load cell attached at a distance of 120 mm from the bearing center through the lever that was set on the bearing housing. The friction coefficients were then deduced from the torque measured using the bearing inside radius and the applied load. The uncertainty of the load cell is $\pm 0.5\%$.

The tested plain bearing was supported with ceramic ball bearings in order to electrically insulate it from the test apparatus itself so that the contact resistant ratio, that is, the contact status between the shaft and the plain bearing, could be measured.

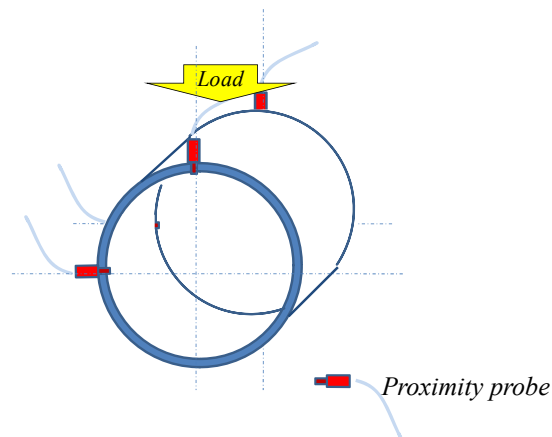


Figure 2-4 Location of proximity probes

As shown in Figure 2-4, four proximity probes of induction type were also attached to the bearing test apparatus on both side of the plain bearings in the direction of the applied load and the normal direction of the applied load. Thus, the relative distance between the shaft and the plain bearing could be measured. Two of them were attached on the one side while the other two were attached on the other side. The measurement range of the proximity probes was up to 10 mm. Since they were attached in a position of 0.25 mm from the shaft surface, the actual measurement range was from 0.25 mm to approximately below 0.50 mm and the uncertainties which are mainly affected by a change of electrical voltage are $\pm 6 \mu\text{m}$. A type K thermocouple with uncertainty of $\pm 0.7 \text{ }^\circ\text{C}$ was attached on the top half bearing in order to measure the temperature of its back face.

2-2 Plain bearing test conditions

The tests were conducted under the following conditions:

<Test condition 1: Static load condition>

(1) Load: The static load is increased from 1 kN to 10 kN by increments of 1 kN.

Variable load $\pm 0 \text{ kN}$

(2) Shaft speed: 1,000 \rightarrow 2,000 \rightarrow 3,000 \rightarrow 500 rpm

(3) Oil feed pressure: 0.5 MPa constant

(4) Feeding oil temp.: 60, 80, 100 $^\circ\text{C}$

<Test condition 2: Dynamic load condition>

(1) Load: Static load 8 kN, Variable load $\pm 3 \text{ kN}$

(2) The other conditions are the same as Test condition 1.

2-3 Measuring items

(1) Friction coefficient (Bearing friction torque)

The torque (Torque) of the bearing is measured with a load cell through the lever that was set on the bearing as shown in Figure 2-1 and the load (W) applied to the bearing by hydraulic pressure is also measured with a load cell. Then, the friction coefficients (F.C.) are calculated with the following formula:

$$\text{F.C.} = \text{Torque} / (\text{R} \times \text{W})$$

The term R is the radius of the plain bearing.

(2) Temperature

The plain bearing temperature and the feeding oil temperature are measured with thermocouples which are attached on the back face of the plain bearing and in the oil supply line.

(3) Contact resistance (CR) ratio

The split bearing housings in which half plain bearings are installed are supported with two ceramic ball bearings in order to electrically insulate it from the test apparatus itself so that the contact resistance ratio, that is, the contact status between the shaft and the plain bearing, can be measured.

Damage of plain bearings that decreases their reliability is due to the contact between the shaft and the plain bearings. To investigate this contact, the insulation ratio (contact resistance ratio: CR ratio) is measured by means of a method which is often used in researching mixed and boundary lubrication. The evaluation of the contact status between two metal surfaces is very common for mixed and boundary lubrication but not for plain bearing lubrication. In order to rapidly detect the contact status when the lubricating condition changes from hydrodynamic to mixed lubrication with increase of a load, it was selected as a superior method. Since it is difficult to insulate the plain bearings from the test apparatus, it was determined that the plain bearings are supported with two ceramic ball bearings, which acted as an electrical insulator. Since the surface resistance of the plain bearings is below $1 \Omega / \text{cm}^2$ which is a good electric conductivity, the metal contact between the shaft and the steel bearing can be measured as electric resistance. Figure 2-5 shows the circuit diagram for the CR ratio measurement.

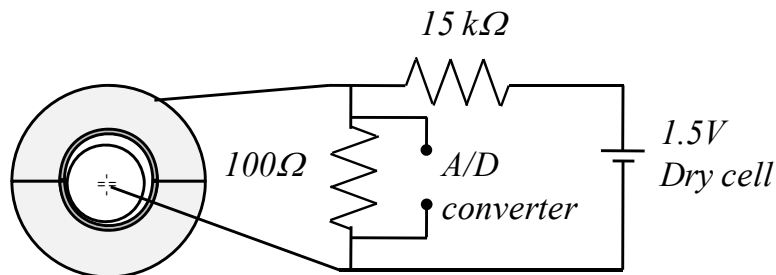


Figure 2-5 Circuit diagram to measure the CR (contact resistance) ratio

It is necessary to eliminate the electrical influence. Therefore, 100 Ω resistance was carefully selected and inserted in parallel between the shaft and the plain bearing so that a large applied voltage could be avoided when there was no contact between the shaft and the plain bearing. The CR ratio was calculated with the following formula:

$$\text{CR ratio [\%]} = (V_{\text{obs}} - V_{\text{sc}}) / (V_{\text{oc}} - V_{\text{sc}}) \times 100$$

V_{obs} : Measured voltage

V_{oc} : Voltage at open circuit condition

V_{sc} : Voltage at short circuit condition

If there is contact between the shaft and the plain bearing, the electric resistance between the shaft and the plain bearing becomes small, and the voltage becomes 0 mV. If there is no contact, the electric resistance between the shaft and the plain bearing becomes large, and the voltage becomes 10 mV. The potential difference between the shaft and the plain bearing in the states with and without metal contacts is assumed to be 0 % and 100 % of the contact resistance (CR) ratio, respectively. When a load is increased in experiments, the CR ratio becomes close to 0 % and the friction coefficient start to fluctuate. “Reliability” in this study was defined as the maximum load before the fluctuation of the friction coefficients starts.

(4) Displacement of shaft

Proximity probes were attached to the bearing test apparatus so that the relative distance between the shaft and the plain bearing could be measured as previously shown in Figure 2-4. Figure 2-6 shows that the gap between the shaft and the plain bearing was measured and provides the definition of the displacement direction. The relative shaft displacement was calculated by subtracting the gap in a reference case from that under an operating condition for both of the directions.

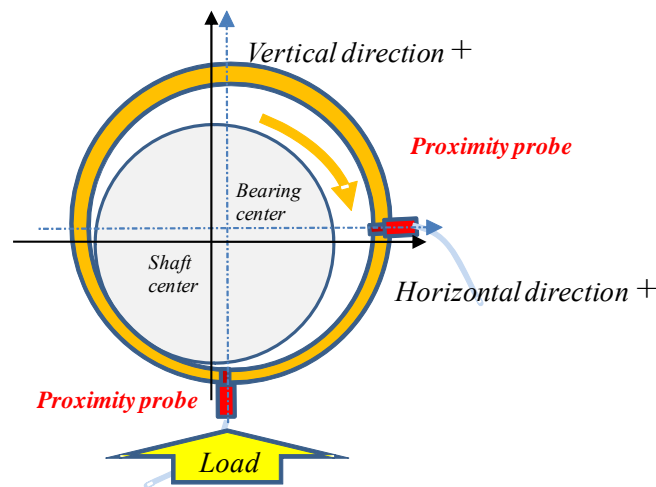


Figure 2-6 Positions for measuring the gap between the shaft and the plain bearing and the definition of the displacement direction

Since the main purpose of the measurements is to investigate the balanced status, electrical output of data are converted from analogue to digital data with a $\Delta\Sigma$ type A/D converter once a second for 200 times for experiments under static load condition. All of the converted data for three minutes are then averaged. The friction torque and the CR ratio are also measured under dynamic load conditions, but the data are sampled every 0.2 ms using a high speed A/D converter without the averaging process.

2-4 Plain bearing test procedure

Figure 2-7 shows the bearing test patterns for the feeding oil temperature, the shaft speed and the load. The oil circulation is started and the oil temperature is increased until sufficient fluidity was obtained without the shaft rotation. Rotation of the shaft is started and maintained at 1,000 rpm under a low static load of 0.6 kN for more than three hours in order to increase the feeding oil temperature to a tested temperature and homogenize the test apparatus. After it is stopped, the zero position of the load cell for the torque measurement is adjusted and the shaft rotation of 1,000 rpm is resumed.

Measurement of the friction torque, the applied load, the feeding oil temperature, the temperature of the plain bearing back face, the contact resistance ratio and the gap between the shaft and the plain bearing are taken at 1,000 rpm under 1 kN of a load. Subsequently, the static load was increased from 1 kN to 10 kN by increments of 1 kN. After completion of the

measurement under static load conditions, the load is changed to 8 kN in order to perform measurement under dynamic load conditions with a variable load of ± 3 kN.

Then, the load is decreased to 0.6 kN, and the shaft speed is also changed to 2,000 rpm. The shaft rotation is maintained for more than 20 minutes to homogenize the test apparatus. The measurements under static and dynamic load conditions are taken with the same conditions as the above mentioned. Measurement is subsequently continued for 3,000 rpm and 500 rpm with the same procedure.

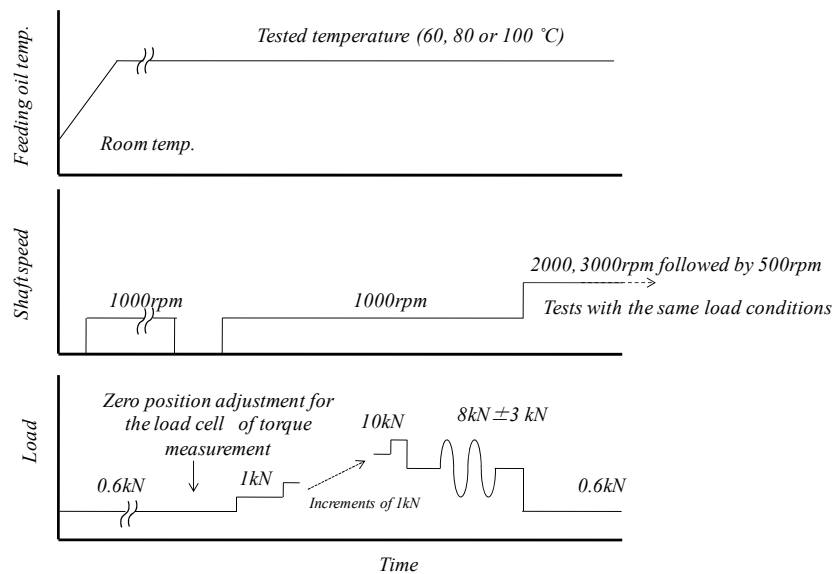


Figure 2-7 Bearing test patterns

2-5 Measurement examples with the developed bearing test apparatus

2-5-1 Friction coefficient and contact resistance (CR) ratio under static load condition

Since the data obtained are slightly fluctuating during the high-speed acquisition for three minutes, the minimum and maximum friction coefficients exist. Therefore, in Figure 2-8 those data were plotted in addition to the average friction coefficients and CR ratios versus the applied load at a feeding oil temperature of 60 °C and a shaft speed of 500 rpm with an API group III 150 N base oil, such that an oil film is unlikely to be formed. As the load is increased, the CR ratio is decreased. When the CR ratio reaches 0%, a drastic increase of the maximum friction coefficient is observed. On the other hand, even if the CR ratio reaches 0 %, the minimum friction coefficient continuously tends to decrease. A slight increase of the average friction coefficient is observed when the CR ratio reaches 0 %. The reason why the average friction coefficient is hardly changed is that the maximum friction coefficient is detected only

for a short period of time during the overall measuring time. Since the purpose of this study is the measurement of the friction loss in plain bearings, figures are arranged using average friction coefficient.

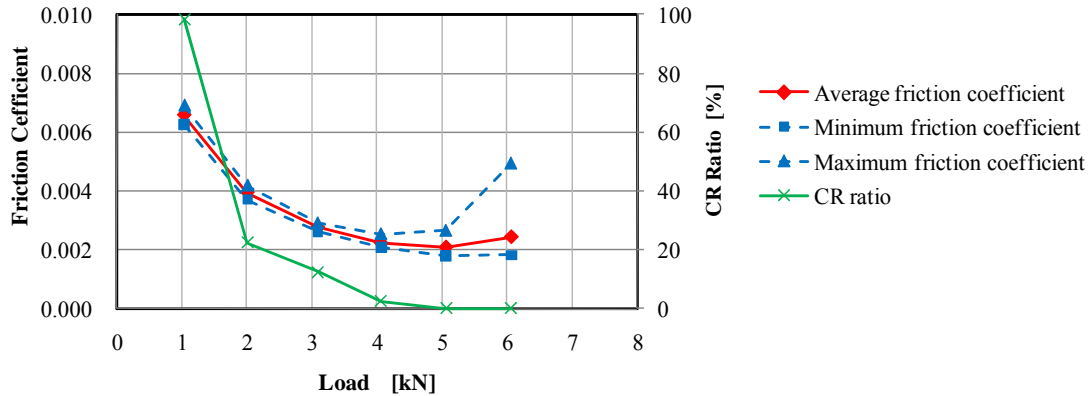


Figure 2-8 Friction coefficient and CR ratio vs. applied load for base oil of API Group III 150N at an oil temperature of 60 °C and a shaft speed of 500 rpm (Cu-Pb plain bearing)

In order to compare the obtained results by the same yardstick, the friction coefficients and the CR ratios are arranged with a non-dimensional Hersey number ($\eta N/P_{\text{spec}}$, η : absolute viscosity of tested oil, N : revolutions per second, P_{spec} : specific bearing load) [59]. η was calculated either with the supplied oil temperature or the temperature of the back face of the plain bearing. Figure 2-9 shows the friction coefficients and the CR ratios versus the Hersey number calculated at a feeding oil temperature of 100 °C for a base oil of API Group IV 500N and a Cu-Pb plain bearing. The friction coefficients decrease with the increase of the applied load from 1 to 10 kN. It has to be noted that the decrease of the Hersey number corresponds to an increase of applied load.

Figure 2-10 also shows the friction coefficients and the Hersey number calculated at the temperature of the back face of the plain bearing. As seen in these figures, it was found that the relationship between the Hersey number and the friction coefficient varies at each rotational speed of the shaft if the data are arranged with the feeding oil temperature. In contrast, the influence of the rotational speed on the friction coefficient becomes small with the back face temperature of the bearing. The data are relatively well-arranged on one line. As a result, it is conceivable that the lubricating condition in the severe bearing tests is in the thermal hydrodynamic region because the back face temperature of the bearing well-characterizes the bearing performance compared with the feeding oil temperature.

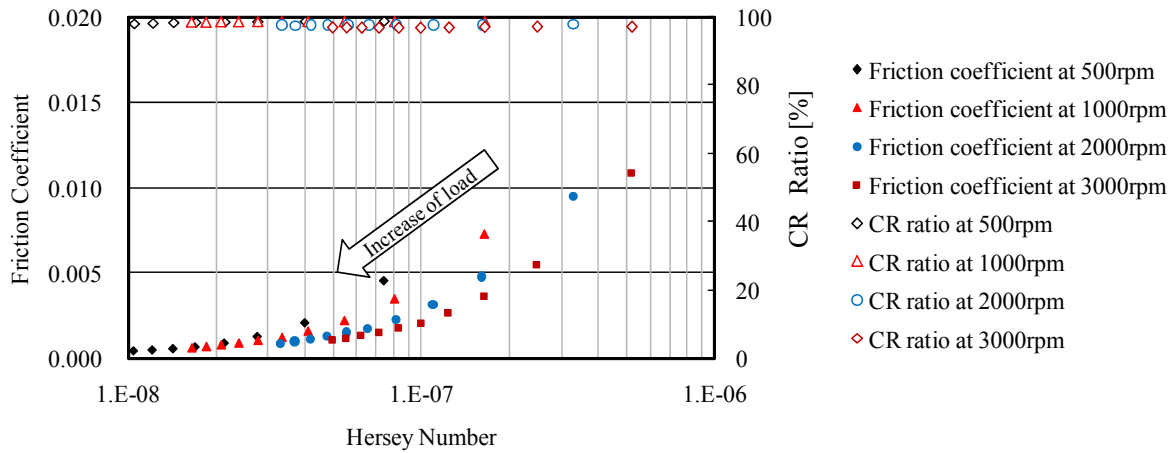


Figure 2-9 Friction coefficient and CR ratio vs. Hersey number for API Group IV 500N at 100 °C with Cu-Pb bearing (η was calculated with the feeding oil temp.)

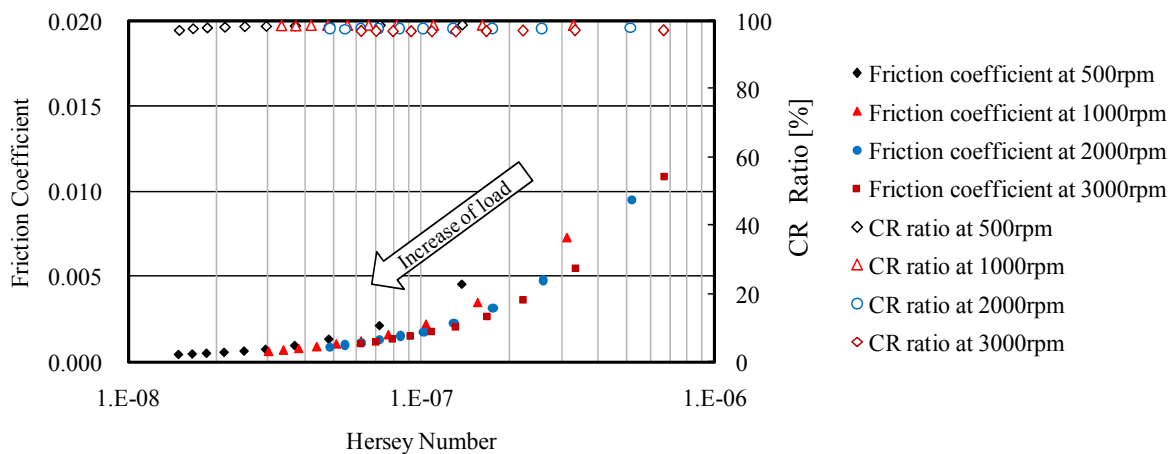


Figure 2-10 Friction coefficient and CR ratio vs. Hersey number for API Group IV 500N at 100 °C with Cu-Pb bearing (η was calculated with temperature at the bearing back-face)

At high shaft speeds such as 2,000 and 3,000 rpm, the fluid film temperature can be higher than the bearing back face temperature. If the fluid film temperature was used to calculate the viscosity, the Hersey number can be lower, and then the friction coefficients for high shaft speeds could approach those for lower shaft speeds and be more well-arranged. However, it is very difficult to measure the fluid film temperature in automotive plain bearings because of difficulty in thermocouple installation to the bearing surface. Therefore, the data are arranged by calculating the viscosity of oils with the back face temperature of the plain bearing in this study.

The bearing test with the Group IV of 500N was carried out twice under the same test

condition. Figure 2-11 shows the friction coefficients and the CR ratios from the first and second experiments at 500 and 2,000 rpm of shaft speeds. Both of them for the first and second tests are almost placed on the same line. Those data in the second tests are positioned slightly to the right side compared with the first results. This is because a slight difference in the stabilized bearing temperature was observed. It was however concluded that good repeatability was ensured.

In fact, the plain bearing used for the second test in Figure 2-11 was manufactured as a different lot from the one for the first test. However, in this study plain bearings manufactured in the same lot were used for the same bearing materials in order to avoid inconsistency of data due to inequalities in the manufacturing process.

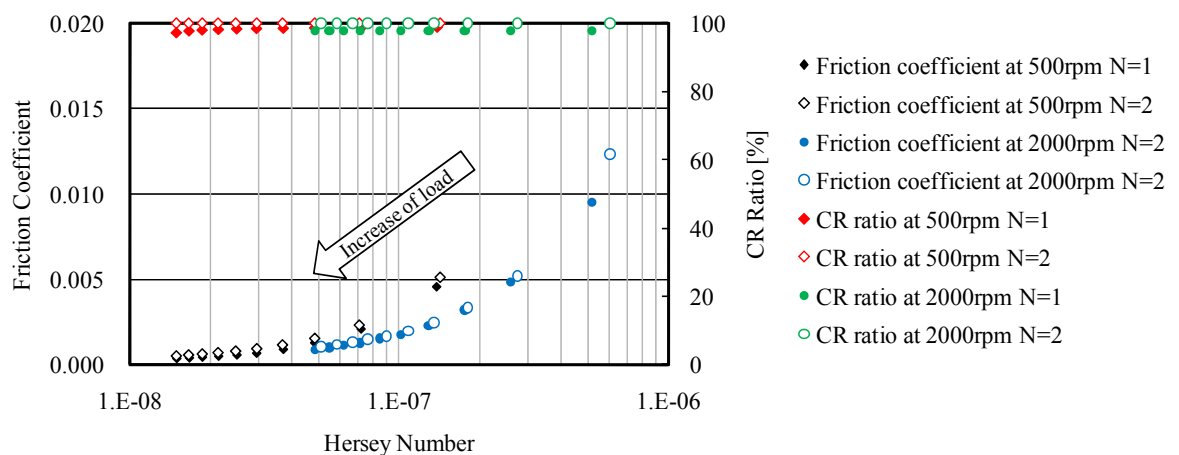


Figure 2-11 Repeatability for friction coefficient and CR ratio vs. Hersey number for API Group IV 500N at 100 °C with Cu-Pb bearing (η was calculated with the temperature of the bearing back-face)

2-5-2 Relative shaft displacement under static load condition

Figure 2-12 shows the results of a test with a base oil of API Group IV 500N and a Cu-Pb plain bearing at a feeding oil temperature of 100 °C and a shaft speed of 1,000 rpm. The horizontal and vertical axis show the relative displacement between the shaft and the plain bearing at a reference point under a load of 1 kN and a shaft speed of 3,000 rpm in the horizontal and vertical direction, respectively. The reference point at 1 kN and 3,000 rpm was plotted at the coordinates of the point of (0, 0) with the triangle symbol in the Figure 2-12. The diamond symbols show the actual relative displacement measured. When the load was increased from 1 to 10 kN with increments of 1 kN, the relative shaft displacement moved to the negative direction for the horizontal and vertical axes.

In this study, the reference positions were measured for each oil sample. Therefore, if two different oil samples are evaluated, their reference positions (absolute positions) are different each other.

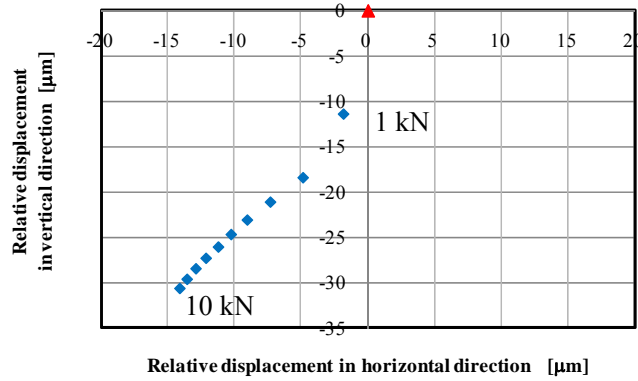


Figure 2-12 Relative shaft displacement for Group III 500N at 100 °C with Cu-Pb bearing

2-5-3 Bearing torque and contact resistance (CR) ratio under dynamic load condition

Figure 2-13 shows the relationship between the applied load and the rotation phase of the shaft with a bearing test under dynamic load condition. The actual load was measured at various shaft speeds by controlling the applied static load at 8 kN and the applied variable load at ± 3 kN to confirm the control condition for the experiment.

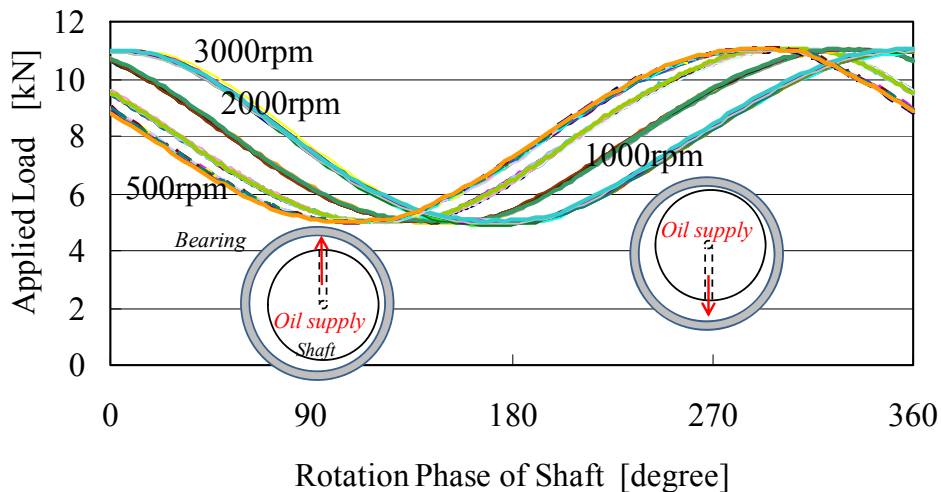


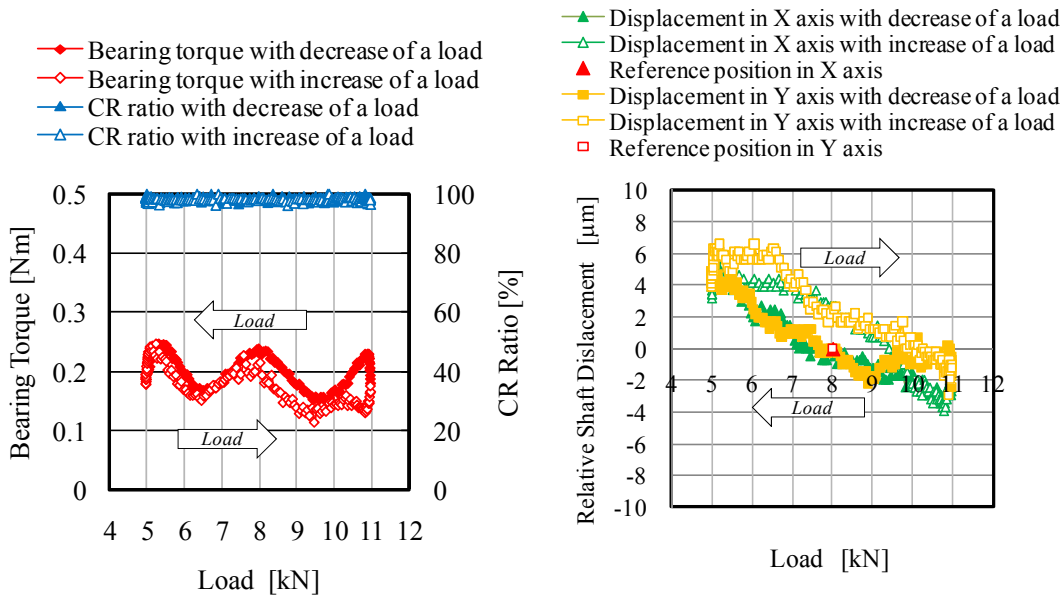
Figure 2-13 Relationship between applied dynamic load and rotation phase of the shaft

As mentioned above, the rotation phase of the shaft corresponds to the location of the oil supply port. The load is applied to the upper part, and the maximum load is controlled so that

the oil supply port is not blocked, regardless of the shaft rotation. The oil supply ports are located in the upper part at 90 degrees and in the lower part at 270 degrees.

Figure 2-14(a) shows the test results with a base oil of API Group IV 500N and a Cu-Pb plain bearing at a feeding oil temperature of 100 °C and a shaft speed of 1,000 rpm. The red and blue symbols indicate the bearing torques and the CR ratios when the dynamic load was decreased. The outline red and blue symbols indicate the data when the dynamic load was increased. In the bearing torques, the hysteresis was observed.

The relative shaft displacement in the horizontal (X) and vertical (Y) axes was arranged in Figure 2-14(b) in comparison with the applied load in order to discuss the bearing torque obtained. It was calculated by subtracting the shaft displacement at 8 kN with decrease of a load from that at each applied load. The relative shaft displacement in both of the X and Y axes becomes lower with decrease of a load than with increase of a load. That is, the oil film thickness can be thinner when the load is decreased after it reaches the maximum load, and it can be a reason why the bearing torque is higher when decreasing a load.



(a) Bearing torque and CR ratio vs. load (b) Relative shaft displacement vs. load
 Figure 2-14 Bearing torque, CR ratio and relative shaft displacement vs. load
 under dynamic load for Group IV 500N at 100 °C with Cu-Pb bearing

Chapter 3

Effect of base oil on plain bearing performance

As mentioned in the background, lowering lubricating oil viscosity is effective to improve fuel economy in engines. The market of low-viscosity grade engine oils which contain low-viscosity base oils has been expanded. Also, kinds of base oils used for engine oils tend to change from solvent refined base oils to highly refined base oils. Such highly refined low-viscosity base oils are nowadays widely used for the main purpose of reducing volatility and increasing viscosity index in combination with polymers. However, the investigation for the effect of base oil on plain bearing performance has not been advanced.

There are a few publications which describe the research activity on it. E.H. Okrent et al. evaluated engine friction and bearing wear using four kinds of paraffinic mineral oils and a naphthenic mineral oil [15]. They evaluated frictional property with those oils using only a motored engine testing. No difference was observed between the two base oils. It is considered that the friction is originated from not only the plain bearing of a crank shaft but also other engine parts, and the actual effect could not be detected.

Bell et al. investigated some relationships between the viscometric properties of engine oils and performance in actual engines [26]. Fuel consumption and bearing wear were evaluated with two single-grade engine oils of different viscosity grades. They just found that the engine test results could be correlated with dynamic viscosity at high shear rates. Williamson et al. also evaluated plain bearing load carrying capacity by using the plain bearing simulator [46]. Single grade engine oils were evaluated in addition to polymer-containing oils. A correlation was found between the load-carrying capacity and the dynamic viscosity of the oils. Unfortunately, in those studies [26, 46], detail of the base oil composition was not indicated.

Filowitz calculated oil film thickness in plain bearings using the measurement of the

bearing's capacitance [36]. A correlation between the oil film thickness and the oil viscosity measured at 100 °C was observed, but discussion taking into account the oil film temperature is considered to be needed.

Thus, we concluded that a necessity to investigate the effect of base oil has arisen.

Kinds of base oils are classified in API (American Petroleum Institute) standard [60] as shown in Table 3-1. Base oils are divided into five categories. Groups I to III are mineral base oils and groups IV and V are synthetic base oils. Since group I base oils are manufactured with a solvent refined process, they normally include sulfur and aromatic molecules. Groups II and III are manufactured with a hydro-treating process. Group IV is polyalphaolefin, which is a synthetic base oil. While viscosity index of group II is similar to that of group I, group III has similar viscosity index to group IV and higher viscosity index than the other mineral base oils.

In recent years, groups II and III have been widely used for engine oils all over the world because of the above mentioned low volatility and high viscosity index. Group IV is generally used for special engine oil applications which require heat resistance in addition to superior fuel economy performance and volatility to groups II and III because of its higher cost than the other oils. The effect of those base oils on the plain bearing performance in hydrodynamic and mixed lubrication is described in this chapter.

Table 3-1 API base oil category

| Category | Sulfur | Saturation | Viscosity Index |
|-----------|--------------------------------|------------|-----------------|
| Group I | > 0.03 and/or < 90 | | 80-120 |
| Group II | ≤ 0.03 | ≥ 90 | 80-120 |
| Group III | ≤ 0.03 | ≥ 90 | ≥ 120 |
| Group IV | polyalphaolefin | | |
| Group V | Exception of I, II, III and IV | | |

3-1 Plain bearings used

Cu-Pb plain bearings of which outside diameter, width and thickness are respectively 56 mm, 26 mm and 1.5 mm were used. The bearing material was L23P9N (overlay ingredient(%)/alloy ingredient(%)=(Pb:Rem,Sn:9,In:9)/(Cu:Rem,Pb:23,Sn:3.5) on a steel plate). The plain bearings used were supplied from Daido Metal Co., Ltd. The plain bearing clearance which was calculated using the measured shaft diameter and the plain bearing inside diameter at room temperature was 40 μm. The same shaft was used for all of bearing tests performed.

3-2 Base oil samples tested

Table 3-2 shows the typical properties of the base oils tested. The kinematic viscosity at 40 and 100 °C was measured and that at 60 and 80 °C was calculated with the Mac Coull and Walther formula. Figure 3-1 shows the dynamic viscosity of the samples. The dynamic viscosity was calculated using the kinematic viscosity and the density. All of the samples were paraffinic base oils. The samples from A to D and AA to CC are low-viscosity base oils of 150N (neutral) and high-viscosity base oils of 500N (neutral), respectively. Base oils of various API categories were evaluated.

Table 3-2 Typical properties of the base oils tested

| | | Low-Viscosity Base Oils | | | | High-Viscosity Base Oils | | |
|--|--------|-------------------------|--------|--------|--------|--------------------------|--------|--------|
| Sample Name | | A | B | C | D | AA | BB | CC |
| API Categories | | Gr.I | Gr.II | Gr.III | Gr.IV | Gr.I | Gr.II | Gr.IV |
| Density (g/cm ³) | @15°C | 0.8700 | 0.8630 | 0.8452 | 0.8260 | 0.8838 | 0.8650 | 0.8350 |
| Kinematic Viscosity (mm ² ·s ⁻¹) | @40°C | 29.90 | 30.98 | 34.52 | 28.80 | 88.77 | 90.51 | 63.00 |
| | @60°C | 14.46 | 14.85 | 16.69 | 14.62 | 36.12 | 36.61 | 29.20 |
| | @80°C | 8.232 | 8.406 | 9.472 | 8.589 | 18.05 | 18.22 | 15.94 |
| | @100°C | 5.258 | 5.346 | 6.025 | 5.600 | 10.43 | 10.50 | 9.800 |
| Viscosity Index | - | 107 | 105 | 121 | 136 | 99 | 101 | 139 |
| Sulfur Content | wt% | 0.48 | 0.00 | 0.00 | 0.00 | 0.10 | 0.01> | 0.01> |

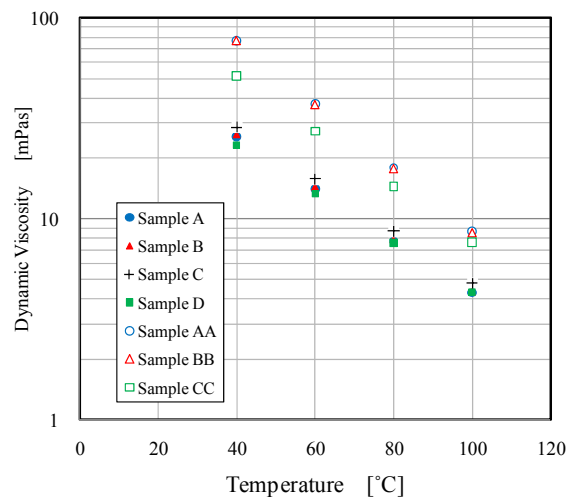


Figure 3-1 Dynamic viscosity vs. temperature for the base oil samples

Samples A and AA of Group I are solvent refined base oils which contain a small amount of sulfur as impurity from crude oil. Samples B, C and BB of Group II or Group III are highly refined base oils which hardly contain sulfur. Sample C has higher viscosity index than

Samples B and BB. Samples D and CC are synthetic base oils of polyalphaolefins which hardly contain sulfur and have the highest viscosity index in the tested oils. The influence of viscosity and composition on the plain bearing performance was investigated. In fact, bearing tests were performed using the apparatus indicated in the chapter 2 with the same test conditions and operating procedure.

3-3 Test results under static load condition and discussion

<Test results>

Figures 3-2, 3-3, 3-4 and 3-5 show the friction coefficients and the contact resistance (CR) ratios between the shaft and the plain bearing with samples A, B, C and D for a feeding temperature of 60 °C. The Hersey number was calculated by using the absolute viscosity at the back-face temperature of the uppermost part of the bearing as the representative value. The results obtained using samples AA, BB and CC for a feeding oil temperature of 100 °C are shown in Figures 3-6, 3-7 and 3-8, respectively. They were arranged at a higher temperature of 100 °C with the high-viscosity oils because the viscosity is close to that for 60 °C with the low-viscosity oils.

A drastic increase of the maximum friction coefficient was observed for samples B, C and D in the low-viscosity base oils if the CR ratio reached 0 % when increasing a load. Therefore, the operation of the test apparatus was not allowed under more severe test conditions although the tests with samples A, AA, BB and CC could be performed successfully even at higher feeding oil temperatures of 80 and 100 °C. The number of data obtained for samples B, C and D was limited compared with the other samples (for those samples, the experiments were conducted only for a feeding temperature of 60 °C and limited load conditions).

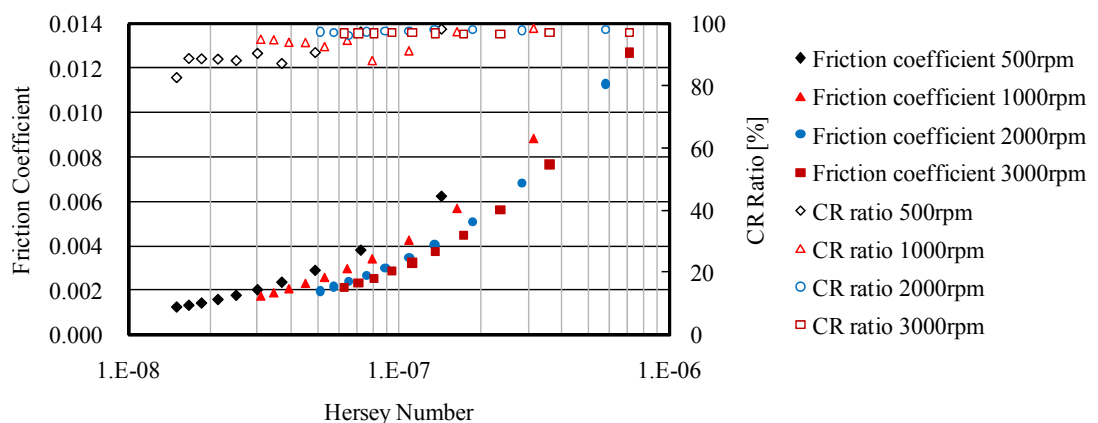


Figure 3-2 Friction coefficient and CR ratio vs. Hersey number for sample A at 60 °C

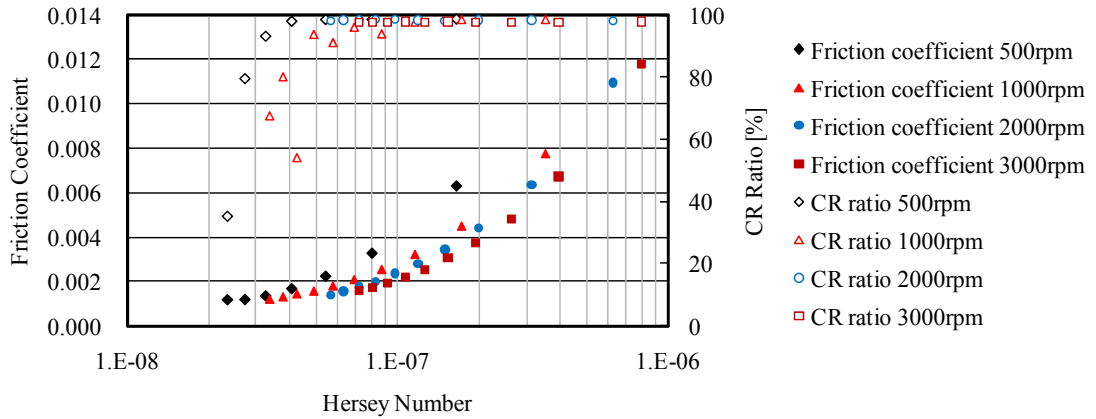


Figure 3-3 Friction coefficient and CR ratio vs. Hersey number for sample B at 60 °C

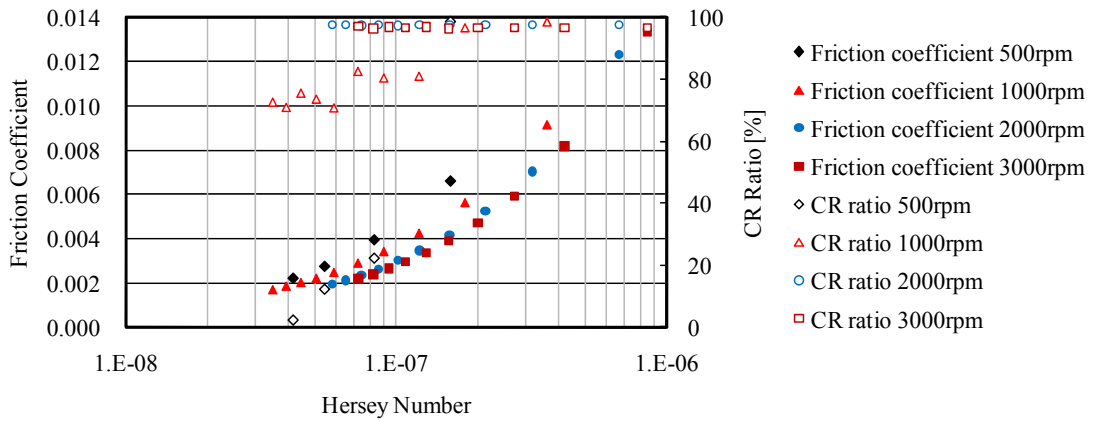


Figure 3-4 Friction coefficient and CR ratio vs. Hersey number for sample C at 60 °C

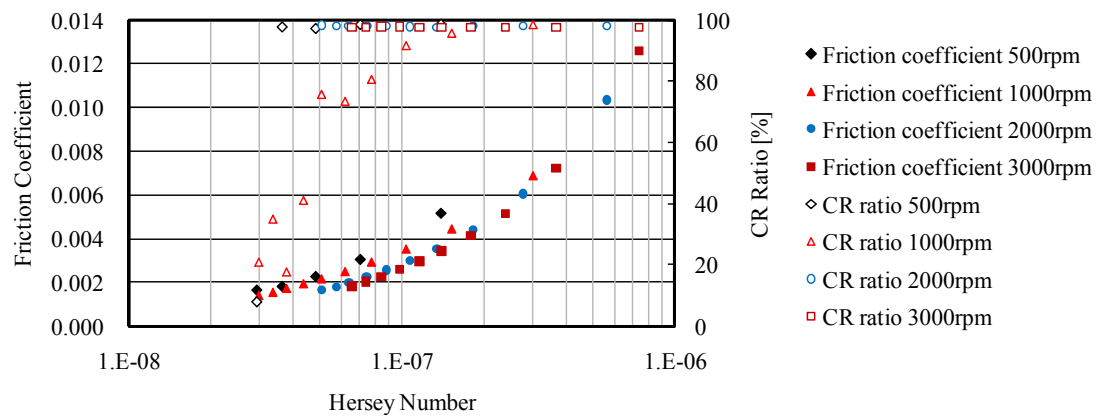


Figure 3-5 Friction coefficient and CR ratio vs. Hersey number for sample D at 60 °C

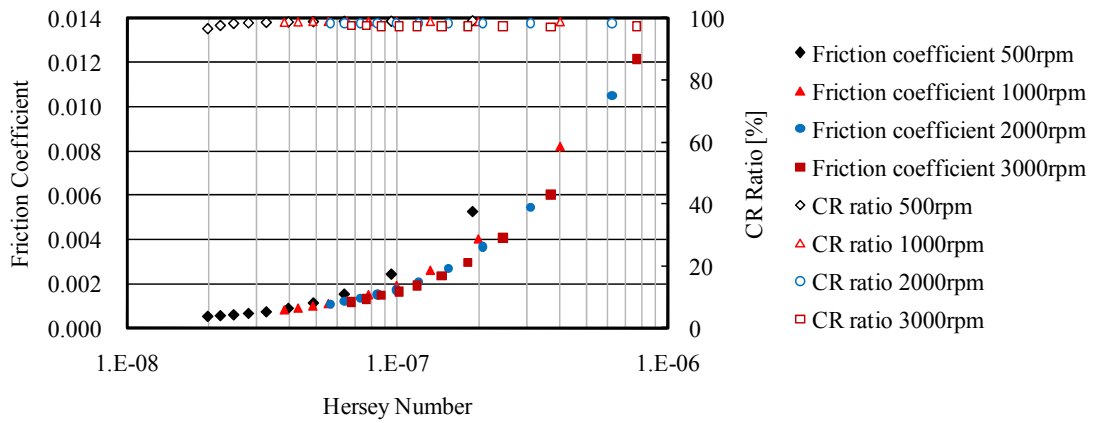


Figure 3-6 Friction coefficient and CR ratio vs. Hersey number for sample AA at 100 °C

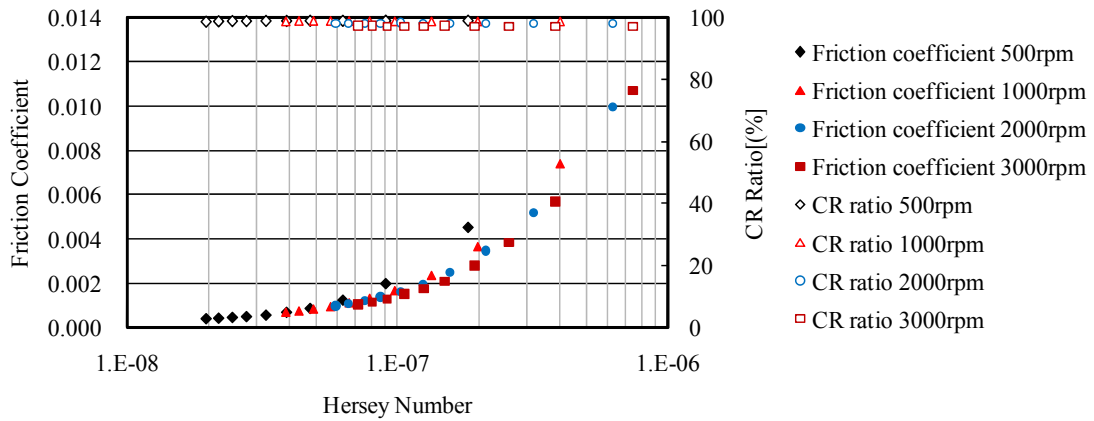


Figure 3-7 Friction coefficient and CR ratio vs. Hersey number for sample BB at 100 °C

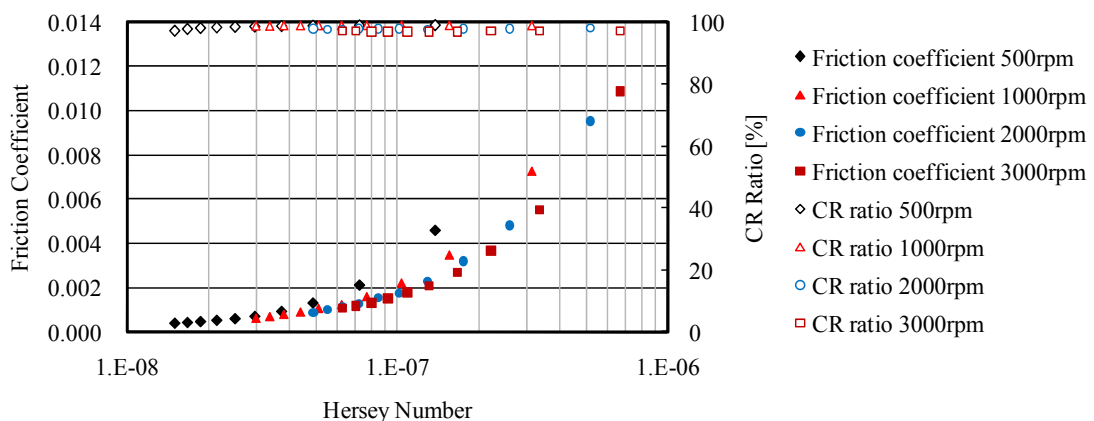


Figure 3-8 Friction coefficient and CR ratio vs. Hersey number for sample CC at 100 °C

Serious damage on the surface of the plain bearings was also observed if the CR ratio reached 0 % and the friction coefficient was increased. From such phenomena, it was

determined that avoiding the decrease of the CR ratio between the shaft and the plain bearing during operation of the test apparatus was important.

If the high-viscosity base oils were used as test oils, no decrease in the CR ratio occurred, even in the low-viscosity range at high oil temperatures. Comparing the tendency of the CR ratio reduction, it was found that the CR ratios between the shaft and the plain bearing for the low-viscosity base oils were lower than those for the high-viscosity base oils. The CR ratios were the lowest for sample C, and those for samples D and B were the next lowest. The CR ratios obtained for the low-viscosity base oils can be listed in the following order:

(High) Gr.I base oil > Gr.II base oil ~ Gr.IV base oil > Gr.III base oil (Low)

In the comprehensive judgment from the results with samples B, C and D, the influence of viscosity index was not observed with the low-viscosity base oil. It is conceivable that the Hersey number changes according to the oil viscosity in the plain bearing, and the influence of the Hersey number did not appear in the relationship among the Hersey number, friction coefficient and CR ratio.

<Discussion>

In order to readily compare superiority or inferiority in the results of the low-viscosity base oils, the data of the friction coefficients, the CR ratios and the relative shaft displacement (only for a shaft speed of 500 rpm and a feeding oil temperature of 60 °C which are a very severe condition) were arranged in the same figures. As mentioned above, the number of data obtained for samples B, C and D of the low-viscosity base oils was limited compared with sample A (since the friction coefficients fluctuated widely in the low CR ratio when the load was increased, the tests were terminated before the load was increased to 10 kN, and that load was defined as the limitation). In addition, the relative shaft displacement was arranged in graphs to estimate oil film formation.

Figures 3-9 to 3-11 respectively show the friction coefficients and the CR ratios versus the Hersey number and the relative shaft displacement for samples A to D. In Figure 3-9, the friction coefficients are the lowest for sample B and D, and those for sample C are the next lowest. Sample A shows the highest friction coefficients. The uncertainty for the measurements of the bearing torque, the applied load and the bearing back-face temperature was respectively $\pm 0.5\%$, $\pm 0.5\%$ and $\pm 0.7\%$ as mentioned above. Also, the error of the shaft rotation was ± 2 rpm. Since the difference of the friction coefficients between sample A and sample B is

approximately 50 % at the Hersey number of $3 \cdot 10^{-8}$, it is considered to be significant even if the uncertainty of measurements is taken into account.

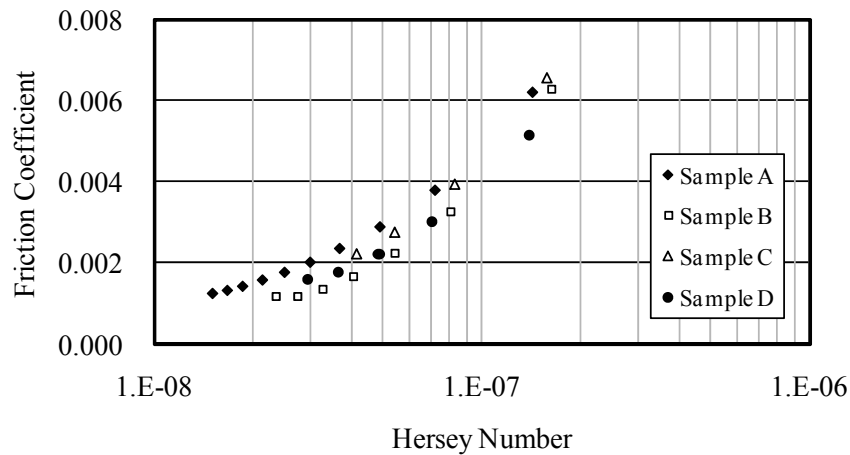


Figure 3-9 Friction coefficient vs. Hersey number for the low-viscosity base oils at 500 rpm and 60 °C

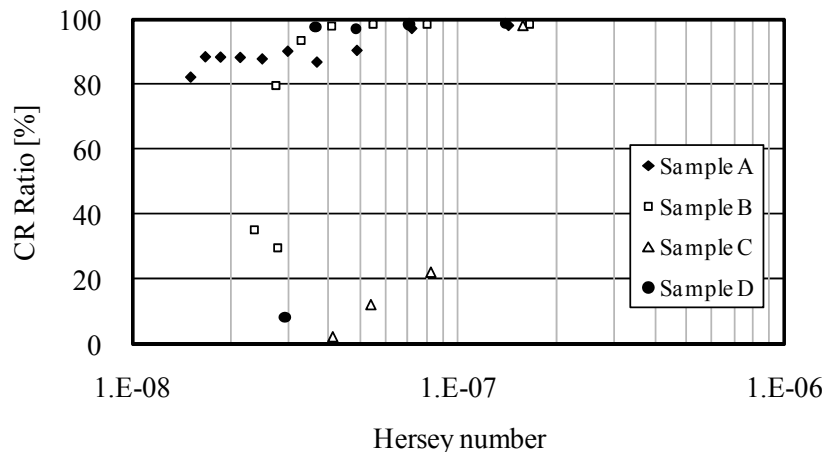
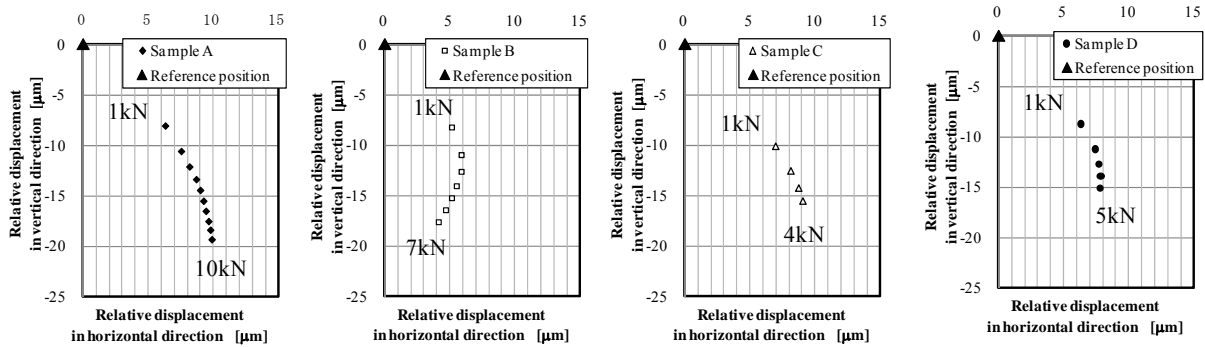


Figure 3-10 CR ratio vs. Hersey number for the low-viscosity base oils at 500 rpm and 60 °C

Although the low-viscosity group I base oil of sample A can prevent contact between the shaft and the plain bearing, use of this oil has the disadvantage of showing high friction coefficients. A difference between sample A and the other base oils is not only the saturation level but also the content of sulfur. Since Cu and Pb are transition elements, it can be expected that those materials react with sulfur. It is conceivable that the increase in friction with sample A is due to the formation of a tribological film induced by the reaction of the plain bearing with the sulfur in the base oil.

In Figure 3-11(a), the horizontal axis represents the relative displacement in the horizontal

direction between the shaft and the plain bearing at a reference position under a load of 1 kN and a shaft speed of 3,000 rpm for each oil sample. The load was increased with increments of 1 kN. The vertical axis shows the relative displacement in the direction of the applied load. It seems that oil film formation varies among the low-viscosity base oils.



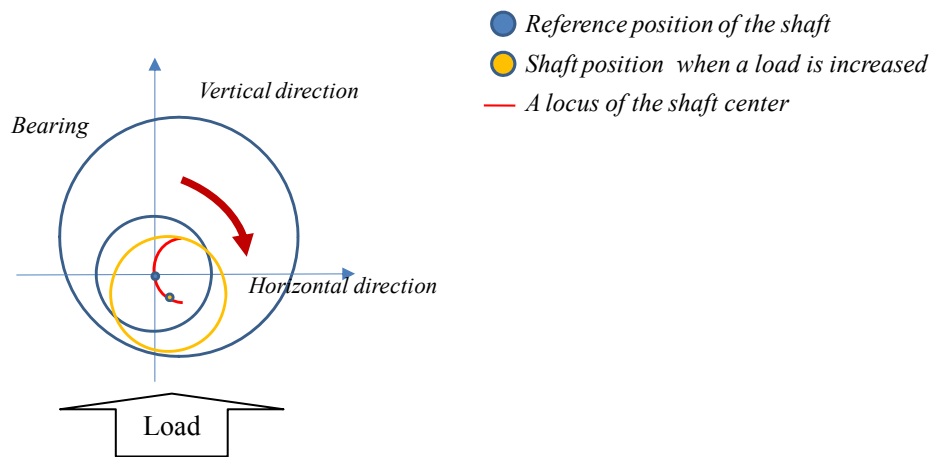
(a)-1 Sample A

(a)-2 Sample B

(a)-3 Sample C

(a)-4 Sample D

(a) Relative shaft displacement



(b) Illustration for estimated shaft displacement for sample A

Figure 3-11 Relative shaft displacement and estimated shaft displacement for the low-viscosity base oils at 500 rpm and 60°C

It is likely for the relative shaft displacement in the horizontal direction that the higher the limitation of the load-carrying capacity, the smaller the relative shaft displacement compared to the applied load, except for sample A. In case of sample A, the bearing test was successfully carried out up to 10 kN with the small decrease of the CR ratio although the relative shaft displacement was almost the same as sample C until the load reached 4 kN. This may also suggest that not only the viscosity but also other factors such as sulfur in the oil play an important role in preventing contact between the shaft and the plain bearing.

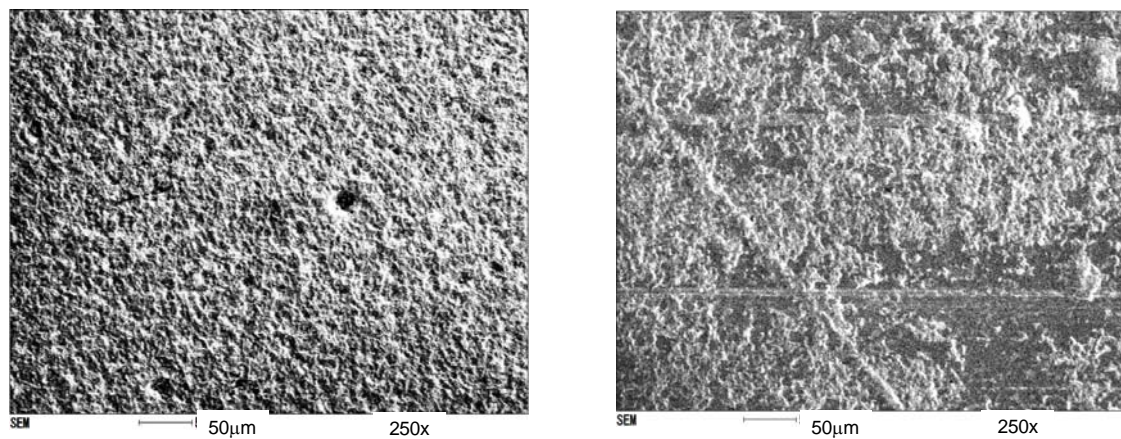
Figure 3-11(b) shows an illustration of estimated shaft displacement only for sample A of

the low-viscosity base oil. This figure was additionally drawn to estimate and explain the direction of the shaft movement for sample A. The blue circle shows the reference position of the shaft at 3,000 rpm and 1 kN. The orange circle shows the shaft position when a load was increased at 500 rpm.

The relative shaft displacement in the horizontal direction was positive for sample A in Figure 3-11(a). Therefore, as shown in Figure 3-11(b), comparing the reference position (blue circle) at 3,000 rpm and 1 kN with the shaft position (orange circle) with increasing a load, the shaft position (orange circle) is considered to be placed in the right side of the reference position (the shaft is considered to move to the positive direction). It suggests that the eccentricity ratio of the shaft was large. It is not an apparent evidence to explain the oil film thickness of the low-viscosity base oils tested because the absolute position of the reference case was not confirmed. Thus, measurement of the oil film thickness should be necessary to ensure the ability of oil film formation for various base oils.

In order to confirm the reason why the metal contact was prevented and the friction coefficients were high for sample A, the surface of the Cu-Pb plain bearing after the bearing test was analyzed by using a scanning electron microscopy-energy dispersive spectrometer (SEM-EDS). In fact, sulfur was not detected on the surface of the Cu-Pb bearing. Figure 3-12 shows the photographs of a new Cu-Pb bearing and the Cu-Pb bearing (loaded side) after the test. It is observed that there are some smooth areas on the surface of the tested Cu-Pb bearing. This occurred because a small part of the overlay on the top surface was removed due to the conformability between the rotational shaft and the bearing material of Pb, which is very soft. It is conceivable that sulfur was also removed as well as the overlay since all of the bearing tests were carried out even under very severe test conditions for the Cu-Pb bearing with group I base oil.

The existence of sulfur was not confirmed but the phenomenon of increasing the friction and preventing the metal contact which appeared in the experiment was apparent. As shown in Figure 3-10, the CR ratio for sample A begins to decrease from a low load as well as the other base oils. This is probably due to the change in the lubricating condition which is shifting from hydrodynamic lubrication region to mixed lubrication region even for sample A as well as the other base oils. Only sample A containing sulfur showed a different behavior. Therefore, the effect of the tribological film formed with the sulfur on the Cu-Pb bearing surface should be a reasonable explanation.



(a) New Cu-Pb bearing (b) Cu-Pb bearing after the test (loaded side)
Figure 3-12 Photograph of the Cu-Pb bearing surface

For the high-viscosity base oils, the data obtained at 500 rpm of a shaft speed and a feeding oil temperature of 100 °C (which were the most severe test conditions) were arranged. Figures 3-13 to 3-15 respectively show the friction coefficients, the CR ratios versus the Hersey number and the relative shaft displacement for samples AA to CC.

In Figure 3-13, the friction coefficients of samples AA to CC are well-arranged and almost equal in the small Hersey number unlike the results with the low-viscosity oils. Although the friction coefficients for sample A containing sulfur were higher than the other low-viscosity base oils, the same tendency was not observed for sample AA in the high-viscosity base oils. In addition, the friction coefficients in the high-viscosity base oils are less than those in the low-viscosity base oils under an equal Hersey number. The difference in the friction coefficients between the high-viscosity base oils and the low-viscosity base oils was considered to be more than uncertainty of the various measurements.

Although the bearing back-face temperature was used to calculate the dynamic viscosity of the oil samples and induce the Hersey number, it is actually necessary to take into account the oil film temperature. If there is a difference in the temperature between the bearing back-face and the oil film, it should affect the derived Hersey number. The author measured temperatures in fluid film and bearing outer surface using a bronze bearing with inner diameter of 100 mm, outer diameter of 200 mm (if the bearing is set in a bearing housing) and width of 80 mm. The temperatures were measured on the inner bearing surface and also at the position of the outer surface of the bearing housing. Even if the thickness of the bearing including the bearing housing is 50 mm, the temperature difference was between 1 to 2 °C which is relatively considered to be small. The thickness of the automotive bearings used in this study is 1.5 mm

which is much thinner than the one used for measuring the temperature difference between the fluid film and the bearing outer surface. Therefore, the fluid film temperature is considered to be very close to the bearing outer surface temperature (the Hersey numbers are not needed to be corrected).

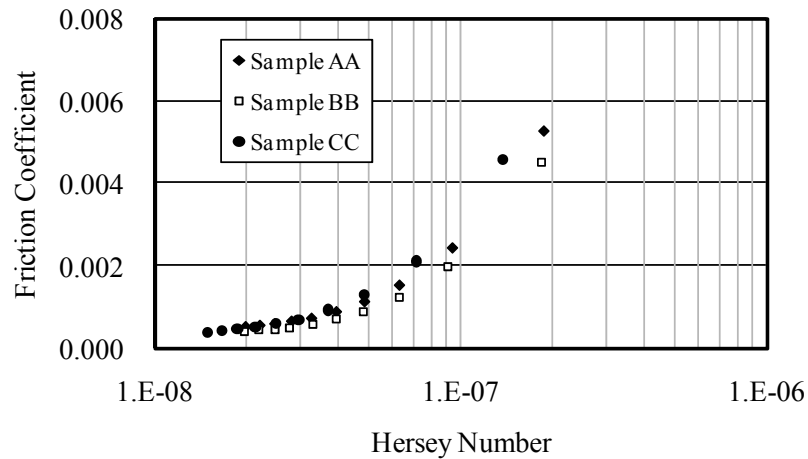


Figure 3-13 Friction coefficient vs. Hersey number for the high-viscosity base oils at 500 rpm and 100 °C

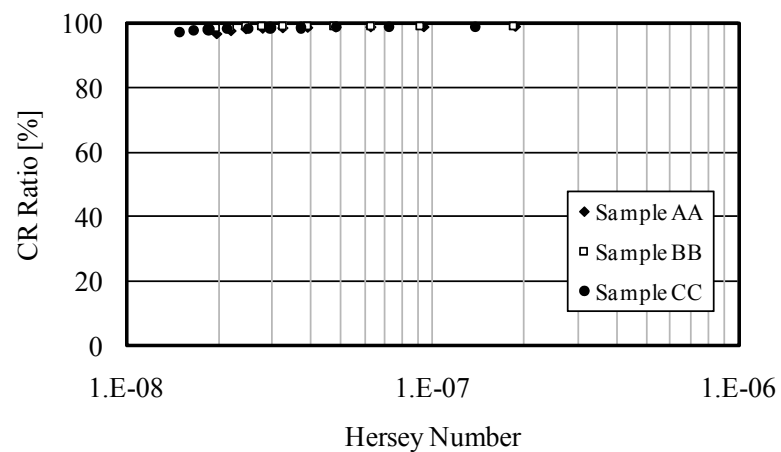


Figure 3-14 CR ratio vs. Hersey number for the high-viscosity base oils at 500 rpm and 100 °C

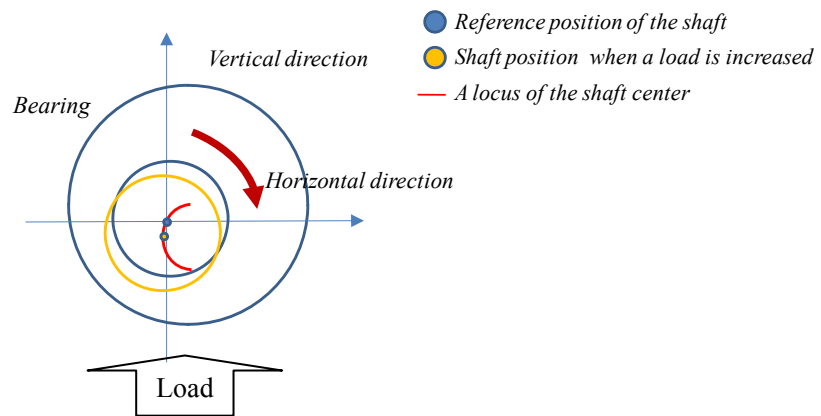
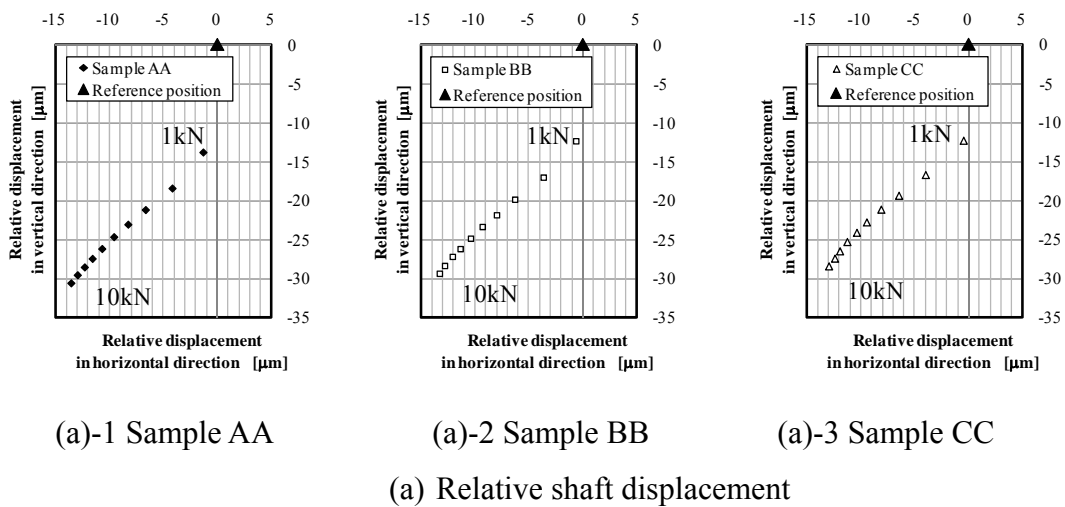


Figure 3-15 Relative shaft displacement and estimated shaft displacement for the high-viscosity base oils at 500 rpm and 100 °C

As mentioned above, no decrease of the CR ratios was observed for all of the high-viscosity base oils as shown in Figure 3-14. Therefore, the oil film thickness with the high-viscosity base oils could be considered to be thicker than with the low-viscosity base oils under an equal Hersey number. The relative shaft displacement showed the similar tendency for all of the high-viscosity base oils as shown in Figure 3-15(a). Although the values of the relative shaft displacement in the horizontal direction for the high-viscosity base oils were negative, those for the low-viscosity base oils were positive. This may suggest that the eccentricity ratio for the high-viscosity base oils could be smaller than that for the low-viscosity base oils even if the viscosity at 100 °C for samples AA to CC is lower than that at 60 °C for Samples A to D as shown in Table 3-2. It is not however an apparent evidence to explain the difference in the oil film thickness between the low-viscosity base oils and the high-viscosity base oils.

In this study, the friction coefficients were calculated using the data accumulated for three minutes. Thus, if the shaft contacts with the bearing for a short period during the experiments of the low-viscosity oils, they are calculated as average values under hydrodynamic and mixed lubrication. (Therefore, it may be a reason that the friction coefficients with the low-viscosity oils were higher than with the high-viscosity oils in the small Hersey number range even if they are decreased with decreasing a Hersey number such as a phenomenon under hydrodynamic lubrication.)

Figure 3-16 shows the friction coefficients from the experiments and the simulation with samples A and AA for 60 °C and 500 rpm. The THD (Thermohydrodynamic) analysis developed at the Poitiers University was used for the simulation of the bearing performance and its detailed explanation is indicated in Appendix I [61-65]. The oil was supplied through the hole in the shaft in the experiment but the friction coefficients were calculated with the oil supply from the opposite bearing side of the load. The thermal characteristics of only the bearing alloy were taken into account for the simulation. While the friction coefficients from the experiment were plotted for 1 kN to 10 kN loads, those from the simulation were presented only for 1 kN and 10 kN in Figure 3-16. Although the friction coefficients for sample AA in the experiments are almost arranged on the same line as in the simulation, those for sample A in the experiments are higher than in the simulation. From these results, it can be also said that the sulfur in sample A affected and increased the friction coefficients in the mixed regions of hydrodynamic and mixed lubrication, and sample AA of the high-viscosity base oil maintain hydrodynamic lubrication.

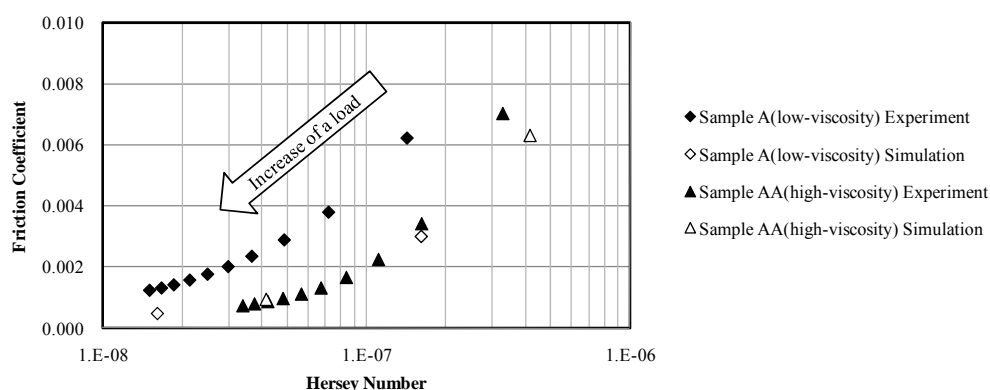


Figure 3-16 Friction coefficient vs. Hersey number in the experiment and simulation (60 °C, 500 rpm)

It is well-known that viscosity versus pressure is presented with the Barus formula of

$\eta(p)=\eta_0\exp(\alpha p)$ (η_0 : viscosity at atmospheric pressure, α : pressure viscosity coefficient, p : pressure). As shown in Figure 3-17, the calculated maximum pressure for sample AA at 60 °C, 500 rpm and 10 kN load becomes approximately 40 MPa which is a very large value and may be high enough to affect the viscosity. However, a difference in the friction coefficients between the experiment and the simulation was hardly observed. It is conceivable that the pressure in the bearing drastically increased only in the narrow area of the bearing and it did not affect the bearing torque.

It is a fact for the high-viscosity base oils that no decrease in the CR ratio occurred and lower friction coefficients were shown. Also, it is apparent that they contain higher molecules than the low-viscosity base oil, and not only the viscosity but also the molecular weight plays an important role in preventing contact between the shaft and the plain bearing. The molecular weight of base oils will be one of the essential factors to take into account the careful selection of the base oils used for the development of prospective engine oils. The use of low-viscosity with the performance of high-viscosity index and low volatility will certainly be necessary because it is a very effective method to achieve the fuel economy and a global trend. In addition, we need to examine kinds of base oils to be used and combination of different base oils, of course with various additives.

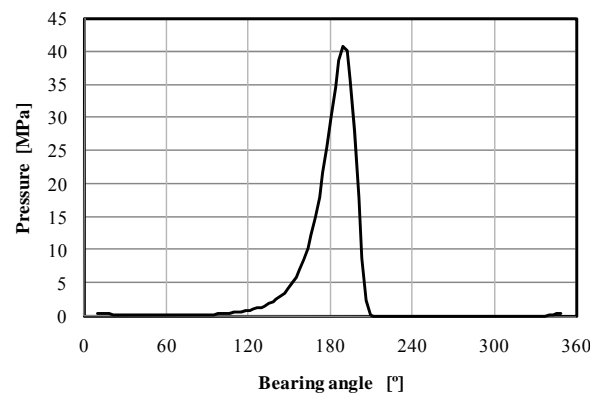
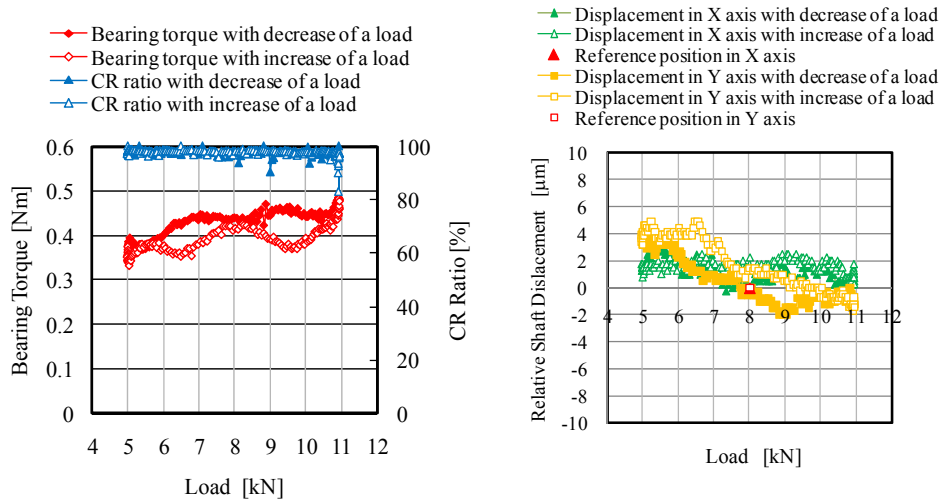


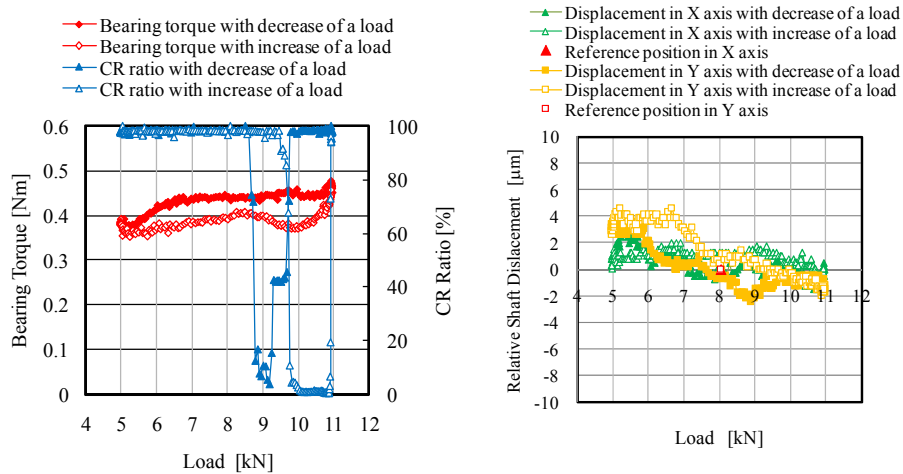
Figure 3-17 Bearing pressure distribution vs. bearing angle in the simulation for sample AA (60 °C, 500 rpm and 10 kN, Angle 0°: The opposite side of the loading.)

3-4 Test results under dynamic load condition and discussion

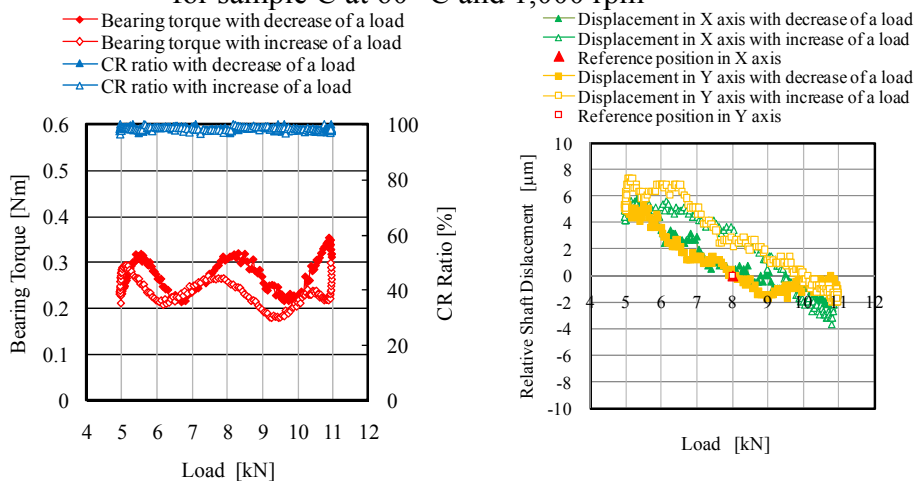
Figures 3-18 and 3-19 show the results under dynamic load conditions with samples A and C (Low-viscosity group I and III base oils) at a feeding oil temperature of 60 °C and a shaft speed of 1,000 rpm, which were the most severe conditions in the low-viscosity base oil tests.



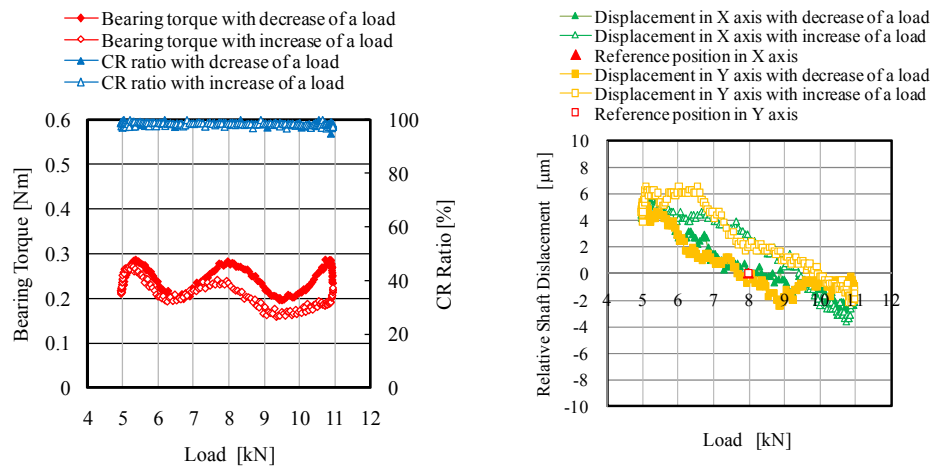
(a) Bearing torque and CR ratio vs. load (b) Relative shaft displacement vs. load
 Figure 3-18 Bearing torque, CR ratio and relative shaft displacement vs. load for sample A at 60 °C and 1,000 rpm



(a) Bearing torque and CR ratio vs. load (b) Relative shaft displacement vs. load
 Figure 3-19 Bearing torque, CR ratio and relative shaft displacement vs. load for sample C at 60 °C and 1,000 rpm



(a) Bearing torque and CR ratio vs. load (b) Relative shaft displacement vs. load
 Figure 3-20 Bearing torque, CR ratio and relative shaft displacement vs. load for sample AA at 80 °C and 1,000 rpm



(a) Bearing torque and CR ratio vs. load (b) Relative shaft displacement vs. load
 Figure 3-21 Bearing torque, CR ratio and relative shaft displacement vs. load
 for sample CC at 80 °C and 1,000 rpm

It has to be noted that since the bearing tests were terminated before the load reached 10 kN for sample C, the data under dynamic load condition could not be obtained for 500 rpm and 60 °C.

The results for samples AA and CC, which were the high-viscosity base oils of Group I and IV, at 80 °C and 1,000 rpm are shown in Figure 3-20. (Although the tests were conducted at 60, 80 and 100 °C, the figures were created using only the data obtained at 80 °C because the viscosity of samples AA and CC was relatively close to and slightly higher than that of samples A and C.)

The CR ratio, which is used to investigate the contact state between the shaft and the plain bearing, was decreased in the high-load range for Samples C of the low-viscosity base oil. Although there was a range of loads for which the CR ratio was 0 % in Sample C, no influence of the 0 % CR ratio on the friction coefficient was observed. It is conceivable that the friction coefficient was not influenced if bearing materials of low shear resistance such as lead used in a lead-based overlay of the Cu-Pb bearing were used and the CR ratio of 0 % was not held for an extended period of time. These results of the CR ratios obtained with the low-viscosity base oils indicate the same tendency as those under the static load condition. On the other hand, no decrease was observed in the CR ratio with the change of the load in the high-viscosity base oil (samples AA and CC).

A slight increase in the bearing torque was observed with increasing a load for samples A

and C of the low-viscosity base oils but not for sample AA of the high-viscosity oil. It is noticed that the locus of the bearing torque curves versus the loads correlates with the relative shaft displacement of the horizontal axis (it is likely that, the lower the relative shaft displacement in the horizontal axis, the higher the bearing torque).

The high-viscosity base oils showed a lower bearing torque than did the low-viscosity base oils. This is also the same tendency as the test results under static load conditions. If the oil film is sufficiently thick in the plain bearing at a low feeding oil temperature, the higher the viscosity index of base oils, the lower the oil viscosity. It is the reason why the base oils of high viscosity index showed low friction coefficient for the high-viscosity base oils.

The group I base oil (sample A) showed a higher bearing torque under static and dynamic load condition. According to these results, although the low-viscosity group I base oil can prevent contact between the shaft and the plain bearing, use of this oil has the disadvantage of creating a large bearing torque.

3-5 Conclusions

The influence of base oil viscosity and composition was investigated to evaluate the performance of lubricants in plain bearings used in automotive engines. The following results were obtained:

- (1) Contact between the shaft and the plain bearing occurred more readily when low-viscosity base oils were used in comparison with high-viscosity base oils under an equal Hersey number in mixed lubrication region. Thus, even if the viscosity was the same in the test operating conditions, the high-viscosity base oils presented superior reliability in bearing lubrication.

In addition, frictional losses in the high-viscosity base oils were less than in the low-viscosity base oils under an equal Hersey number in hydrodynamic lubrication. The friction difference between the high-viscosity base oils and low-viscosity was larger than the uncertainty of the measurements such as the temperature and the bearing friction torque. Since the bearing back-face temperature was also considered to be the same as the oil film temperature, it is conceivable that the bearing friction was affected by the molecular weight of the base oil.

- (2) The contact between the shaft and the bearing was more likely to occur with

highly refined base oils than with low refined base oil (group I base oil) among base oils with the same low viscosity in mixed lubrication region. Higher friction coefficients were also observed with the group I base oil of low-viscosity.

(3) From these results, it was found that the selection of base oils could affect the friction reduction and the reliability improvement in mixed and hydrodynamic lubrication.

Chapter 4

Effect of bearing materials on plain bearing performance

The reduction of lead (Pb), which has often been used for plain bearings, is necessary from the perspective of reducing environmental pollutants [12]. Many of bearing manufacturers have been investigating alternative materials for lead [13, 14, 53-55]. Therefore, the effect of plain bearing materials in bearing performance was investigated using two kinds of bearings with several low-viscosity base oils.

4-1 Plain bearings used

Plain bearings of which outside diameter, width and thickness are respectively 56 mm, 26 mm and 1.5 mm were used. In order to clarify the influence of the bearing materials, two kinds of plain bearings made by the Daido Metal Co., Ltd. were selected as the representatives of automobile plain bearings. One of the plain bearings was a Cu-Pb alloy bearing with an overlay (the data shown for the “Effect of base oil in plain bearing performance” in the chapter 3 are used in comparison with the other plain bearing data). The other plain bearing used was an Al-Si alloy bearing with no overlay. Tables 4-1 and 4-2 respectively show the ingredients of the plain bearings used. In fact, the Al-Si plain bearing was not fully a lead-free material. However, the main alloy used for the two materials were completely different. Also, the amount of lead in the Al-Si bearing material is 1.7 % which is a very small quantity. Therefore, the Al-Si plain bearing which is currently on the market was selected in order to evaluate and estimate the effect of bearing materials and lubricants in comparison with the Cu-Pb plain bearing.

Table 4-1 Ingredients of the Cu-Pb plain bearing

| Ingredients of inner layer (%) | | | Ingredients of overlay (%) | | |
|--------------------------------|----|-----|----------------------------|----|----|
| Cu | Pb | Sn | Pb | Sn | In |
| Rem | 23 | 3.5 | Rem | 9 | 9 |

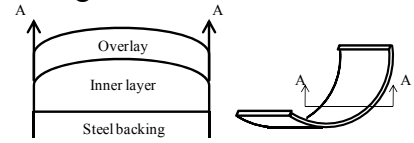
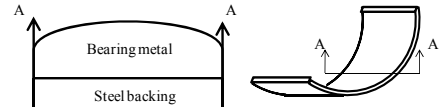


Table 4-2 Ingredients of the Al-Si plain bearing

| Ingredients of bearing metal (%) | | | | |
|----------------------------------|----|-----|-----|-----|
| Al | Sn | Si | Cu | Pb |
| Rem | 12 | 2.5 | 0.7 | 1.7 |

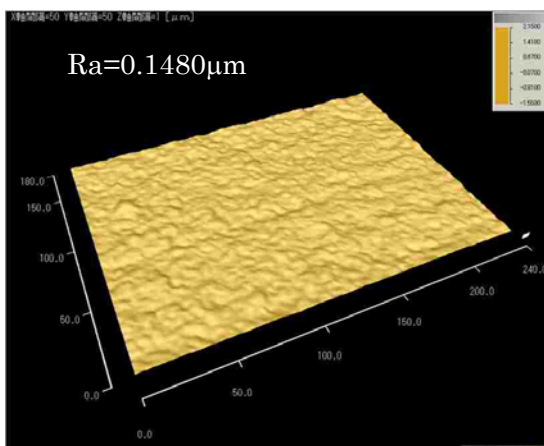


The plain bearing clearances which were calculated using the measured shaft diameter and the plain bearing inside diameter at room temperature are the following:

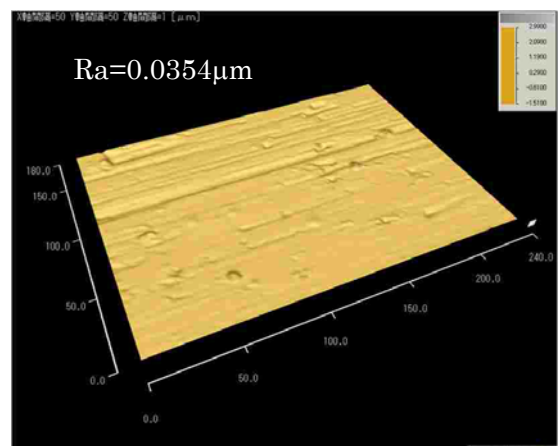
- (1) Cu-Pb plain bearing: 40 μm
- (2) Al-Si plain bearing : 37μm

Also, the surfaces of the new plain bearings were analyzed by using a scanning electron microscopy-energy dispersive spectrometer (SEM-EDS). Figure 4-1 shows three-dimensional images of the bearing surfaces. The roughness (Ra: arithmetic average roughness) of the bearings was also measured. Although the roughness of the two bearings is very small (less than 1 μm), the Cu-Pb bearing is slightly rougher than the Al-Si bearing. However, there is a fact that the Pb of the overlay on the Cu-Pb bearing can become smoother in an actual bearing test operation because of its softness and conformability.

The same shaft was used for all of bearing tests performed.



(a) Cu-Pb plain bearing



(b) Al-Si plain bearing

Figure 4-1 Three-dimensional images and surface roughness of the new plain bearings

4-2 Base oil samples tested

Most of fuel-saving engine oils are multi-grade oils in which polymers are mixed into low-viscosity base oils. Since the oil viscosity in such engine oils is decreased at a high shear rate, low-viscosity base oils were selected to investigate their influence.

Four kinds of low-viscosity base oils with a different API (American Petroleum Institute) base oil category were used in the tests to investigate the influence of the base oil refinement level. They are the same base oils as used in the study of “Effect of base oil in plain bearing performance” in the chapter 3. Samples A of group I is a solvent refined base oil which contain small amount of sulfur. Samples B and C of Group II or Group III are highly refined base oils with no sulfur. (Sample C has higher viscosity index than samples B). Sample D is a synthetic base oil of polyalphaolefin with no sulfur and have the highest viscosity index in the tested oils. The influence of viscosity and composition in the plain bearing performance was investigated with the Al-Si plain bearing as well as the Cu-Pb plain bearing.

Typical properties of the base oils tested are shown in Table 4-3. Bearing tests were performed using the apparatus indicated in the chapter 2 with the same test conditions and operating procedure.

Table 4-3 Typical properties of the base oils tested

| | | Low-Viscosity Base Oils | | | |
|--|-------------------|-------------------------|--------|--------|--------|
| Sample Name | | A | B | C | D |
| API Categories | | Gr.I | Gr.II | Gr.III | Gr.IV |
| Density | g/cm ³ | 0.8700 | 0.8630 | 0.8452 | 0.8260 |
| Kinematic Viscosity (mm ² ·s ⁻¹) | @40°C | 29.90 | 30.98 | 34.52 | 28.80 |
| | @60°C | 14.46 | 14.85 | 16.69 | 14.62 |
| | @80°C | 8.232 | 8.406 | 9.472 | 8.589 |
| | @100°C | 5.258 | 5.346 | 6.025 | 5.600 |
| Viscosity Index | - | 107 | 105 | 121 | 136 |
| Sulfur Content | wt% | 0.48 | 0.00 | 0.00 | 0.00 |

4-3 Test results with the Al-Si plain bearing and the Cu-Pb plain bearing under static load condition and discussion

Figure 4-2 shows the friction coefficients and the contact resistance (CR) ratios versus the Hersey number between the shaft and the plain bearing with sample A. The data for both of the Al-Si plain bearing and the Cu-Pb plain bearing were plotted in the same figure for comparison.

As mentioned above, the Hersey number was calculated by using the back-face temperature of the uppermost part of the bearing as the representative value. Figures 4-3 to 4-5 show the results obtained using samples B, C and D, respectively.

Although all of the bearing tests at 60, 80 and 100 °C of feeding temperatures with the Al-Si plain bearings were successfully carried out with samples A to D unlike the tests with the Cu-Pb plain bearings, only the data at 60 °C for loads of 1 to 10 kN and shaft speeds of 500, 1,000, 2,000 and 3,000 rpm were arranged in Figures 4-2 to 4-5 because those with the Cu-Pb bearing were limited for that feeding oil temperature (60 °C). In Figure 4-2, a reduction in the CR ratio was observed in the vicinity of $1 \cdot 10^{-8}$ of the Hersey number for the Al-Si plain bearing with sample A, with the reduction in the CR ratio being smaller for the Cu-Pb bearing than with the other base oils. No reduction in the CR ratio occurred with samples B, C and D (Figures 4-3 to 4-5), even in the small Hersey number. Since the reduction in the CR ratio was small and there was no metal contact between the shaft and the plain bearing, the friction coefficients were not increased in all of the test conditions with decreasing the Hersey number for the Al-Si plain bearing.

The friction coefficients are apparently higher for sample A with the Cu-Pb plain bearing than with the Al-Si plain bearing, as shown in Figure 4-2. While the difference in the friction coefficient due to the difference in bearing material in base oils B, C, and D is smaller than that in sample A, the friction coefficients with the Cu-Pb plain bearing is positioned in a slightly higher location than those with the Al-Si plain bearing. The reason for this small difference in the friction coefficient between the two bearing materials is that the value of the load, which is a denominator to calculate the friction coefficients, is exceedingly high. However, the bearing friction torque itself between the two bearing materials apparently differs even in hydrodynamic lubrication region.

From the results of the CR ratio in Figures 4-2 to 4-5, it was found that the Al-Si plain bearing showed a higher CR ratio and had better ability to form an oil film that prevents metallic contact compared with the Cu-Pb plain bearing. Furthermore, sample A has better ability to prevent metallic contact between the rotational shaft and the Cu-Pb plain bearing, but conversely not with the Al-Si plain bearing compared to the other base oils.

It was confirmed that the Al-Si plain bearing has the ability to prevent metallic contact between the shaft and plain bearing in the region of a one digit smaller Hersey number compared with the Cu-Pb plain bearing.

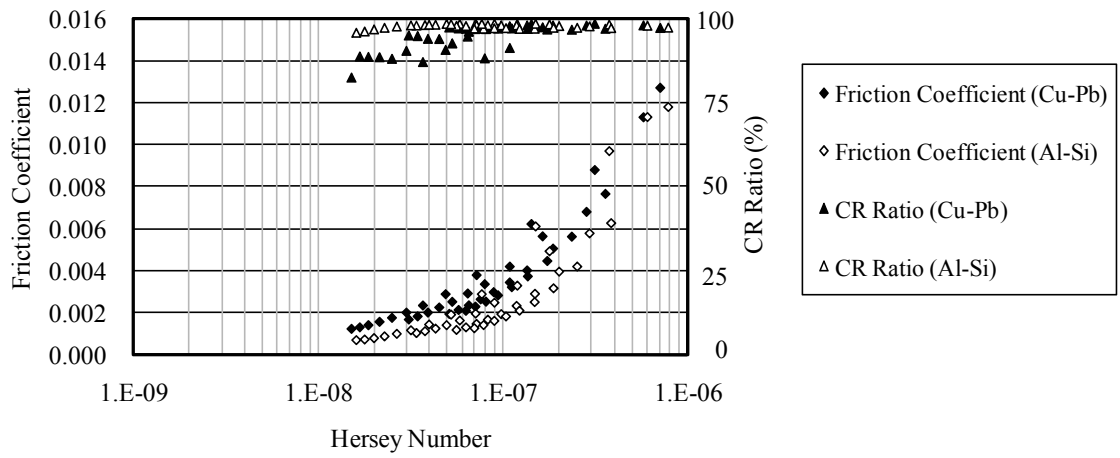


Figure 4-2 Friction coefficient and CR ratio vs. Hersey number for 60 °C and shaft speeds of 500, 1,000, 2,000 and 3,000 rpm with sample A

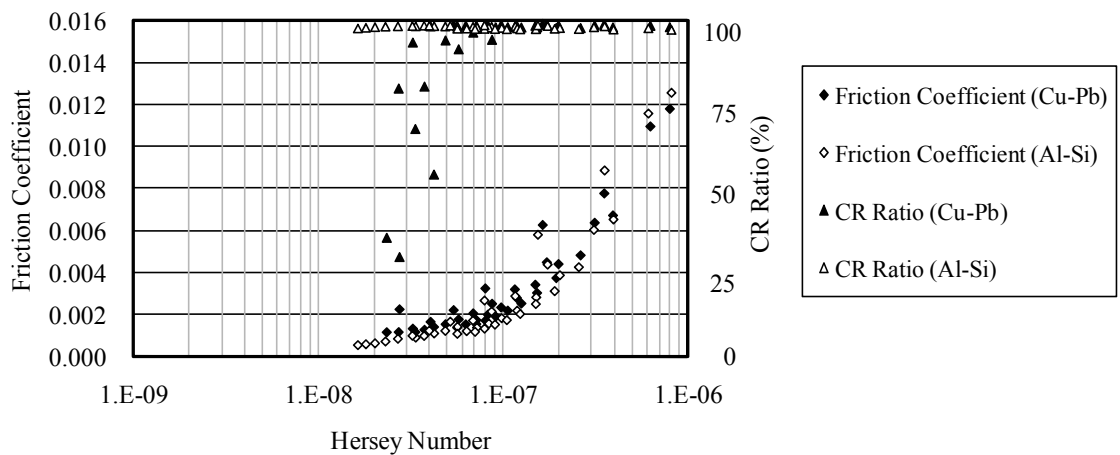


Figure 4-3 Friction coefficient and CR ratio vs. Hersey number for 60 °C and shaft speeds of 500, 1,000, 2,000 and 3,000 rpm with sample B

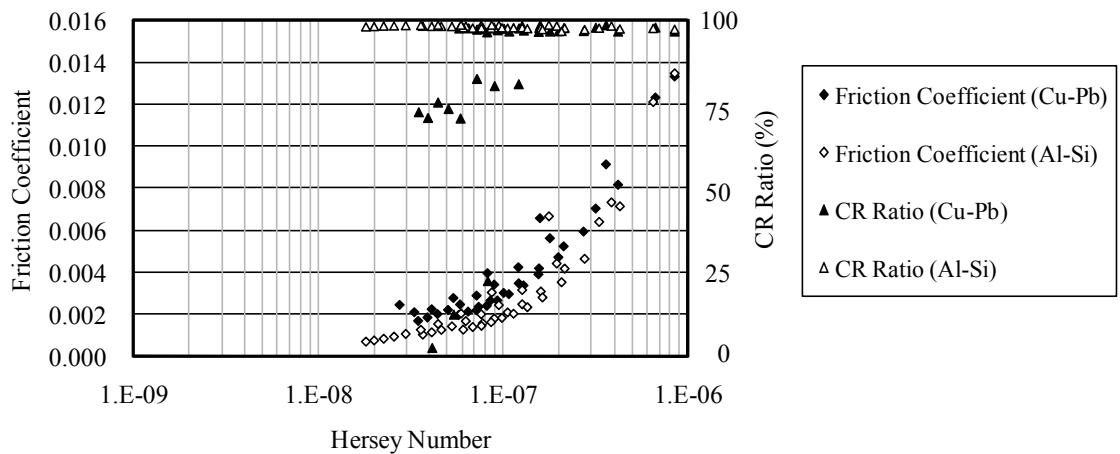


Figure 4-4 Friction coefficient and CR ratio vs. Hersey number for 60 °C and shaft speeds of 500, 1,000, 2,000 and 3,000 rpm with sample C

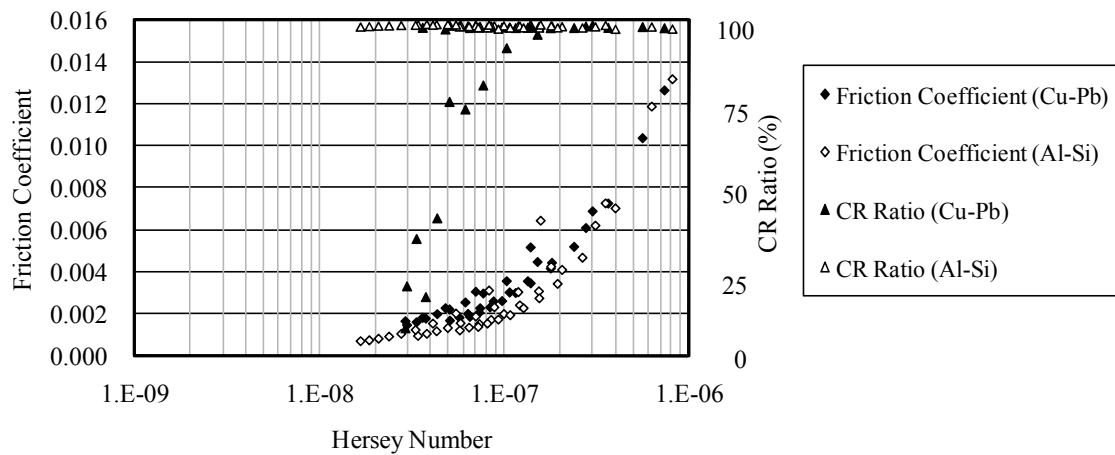


Figure 4-5 Friction coefficient and CR ratio vs. Hersey number for 60 °C and shaft speeds of 500, 1,000, 2,000 and 3,000 rpm with sample D

In order to readily compare superiority or inferiority in the results with both of the plain bearing materials, the data of the friction coefficients, the CR ratios and the relative shaft displacement only for 500 rpm of a shaft speed and 60 °C of a feeding oil temperature which are the most severe condition for the Cu-Pb plain bearing were arranged (the number of data obtained for samples B, C and D was limited compared with sample A for the Cu-Pb plain bearing because the lubricating condition is mixed lubrication and the tests were terminated before the load reached 10 kN). In addition, the relative shaft displacement was arranged in a graph to estimate oil film formation.

Figures 4-6 and 4-7 respectively show the friction coefficients and the CR ratio versus the Hersey number for samples A to D. In Figure 4-6, no friction increase in sample A was observed and the friction coefficients of samples A to D were almost equal in the small Hersey

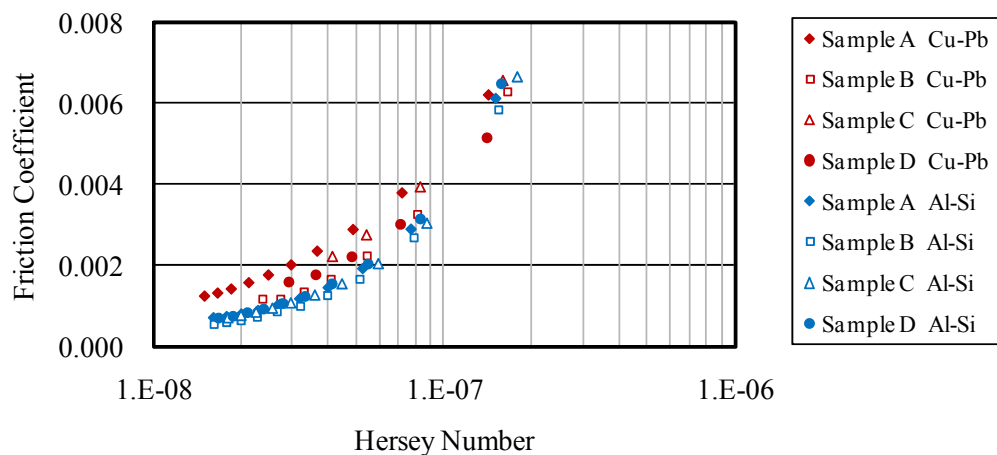


Figure 4-6 Friction coefficient vs. Hersey number at 500 rpm and 60 °C

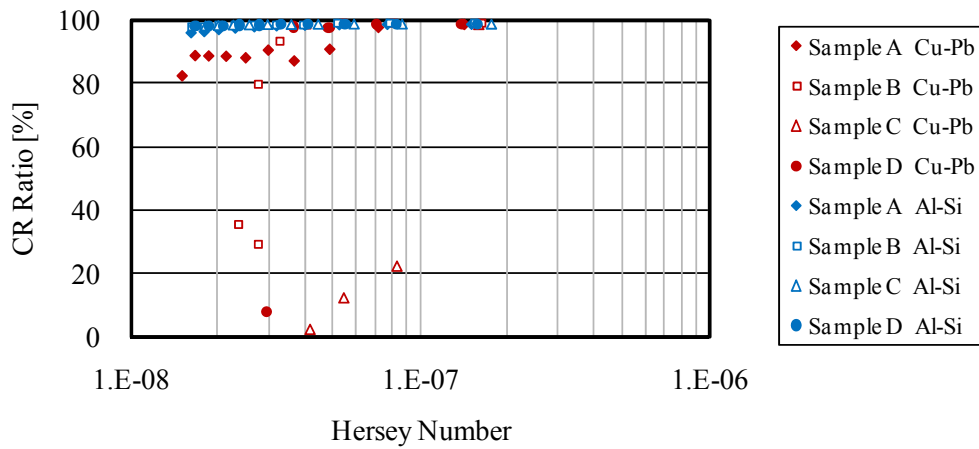


Figure 4-7 CR ratio vs. Hersey number at 500 rpm and 60 °C

number for the Al-Si plain bearing. These were the same tendency as the results with the Cu-Pb plain bearing for the high-viscosity base oils. As shown in Figure 4-7, no decrease in the CR ratio was also observed for the Al-Si plain bearing unlike for the Cu-Pb plain bearing.

In order to confirm the influence of the bearing materials, the measured back-face temperatures were also arranged in Figure 4-8. This figure shows the bearing back-face temperature versus the applied load only for sample A at a feeding oil temperature of 60 °C for 500 rpm and 1,000 rpm with the Cu-Pb bearing and the Al-Si bearing.

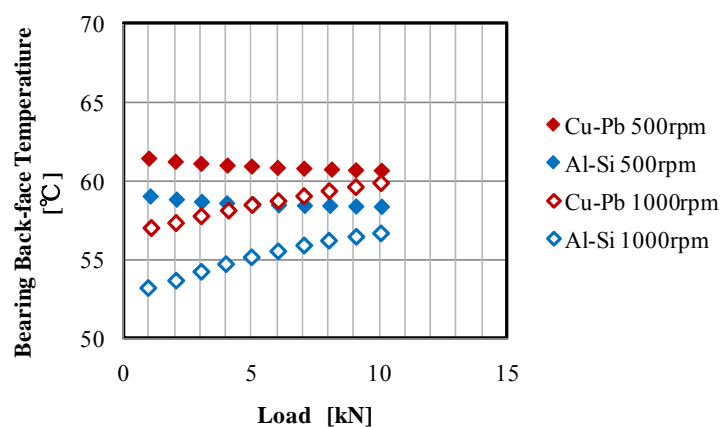


Figure 4-8 Bearing back-face temperature vs. load for sample A at a feeding oil temperature of 60 °C

The bearing back-face temperature with the Al-Si bearing is slightly lower than with the Cu-Pb bearing. There is a possibility that the actual oil film temperature with the Al-Si bearing

could be higher than the expected temperature and close to that with the Cu-Pb bearing. In that case, the line of the friction coefficients for the Al-Si bearing in Figure 4-6 can shift to the left side and approach to that for the Cu-Pb bearing.

Therefore, the author attempted to calculate the Hersey number using the back-face temperature of the Cu-Pb bearing for the Al-Si bearing and sample A in comparison with the Cu-Pb bearing test results. Figure 4-9 shows the results for a feeding oil temperature of 60 °C and shaft speeds of 500 rpm and 1,000 rpm. The friction coefficients for sample A with the Al-Si bearing slightly shifted to the left side, but a difference between the two bearings still exist. The friction coefficients in the Cu-Pb bearing are higher than in the Al-Si bearing.

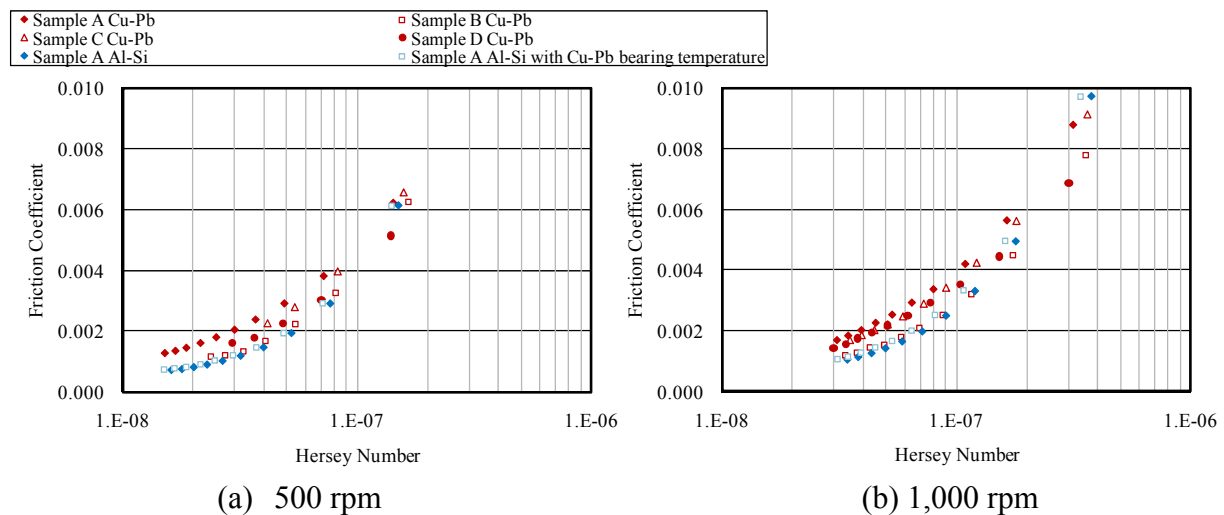


Figure 4-9 Friction coefficients vs. Hersey number calculated using the back-face temperature of the Cu-Pb bearing for the Al-Si bearing test with sample A

Figure 4-10 shows the relative shaft displacement. For the Al-Si plain bearing, the relative shaft displacement was well-arranged on one line with all of the base oils although it varied for Cu-Pb plain bearings as shown in Figure 3-11. Also, it is noticed that the relative shaft displacement in the horizontal direction is negative for the Al-Si plain bearings, but positive for the Cu-Pb plain bearing.

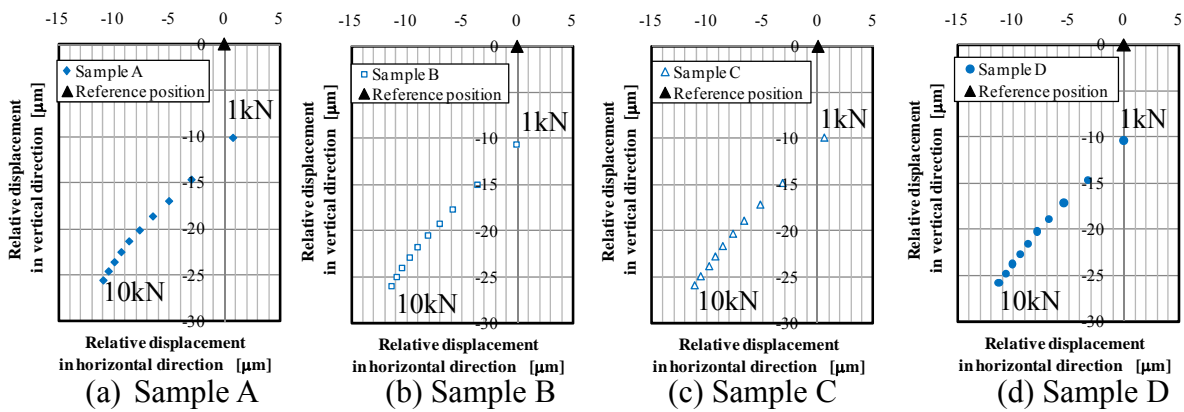


Figure 4-10 Relative shaft displacement at 500 rpm and 60 °C

Figure 4-11 shows illustrations of estimated shaft displacement (a locus of the shaft center) as examples for both of the Cu-Pb plain bearing and the Al-Si plain bearing with sample A. Since the values of the relative shaft displacement were positive for the Cu-Pb plain bearing, the eccentricity ratio of the shaft could be large while that for the Al-Si plain bearing seems to be small. That is, the oil film thickness for the Al-Si plain bearing could be thicker than that for the Cu-Pb plain bearing. It may have led to lower friction with the Al-Si plain bearing in an equal Hersey number compared with the Cu-Pb plain bearing. However, further study should be necessary to ensure the oil film thickness by directly measuring it.

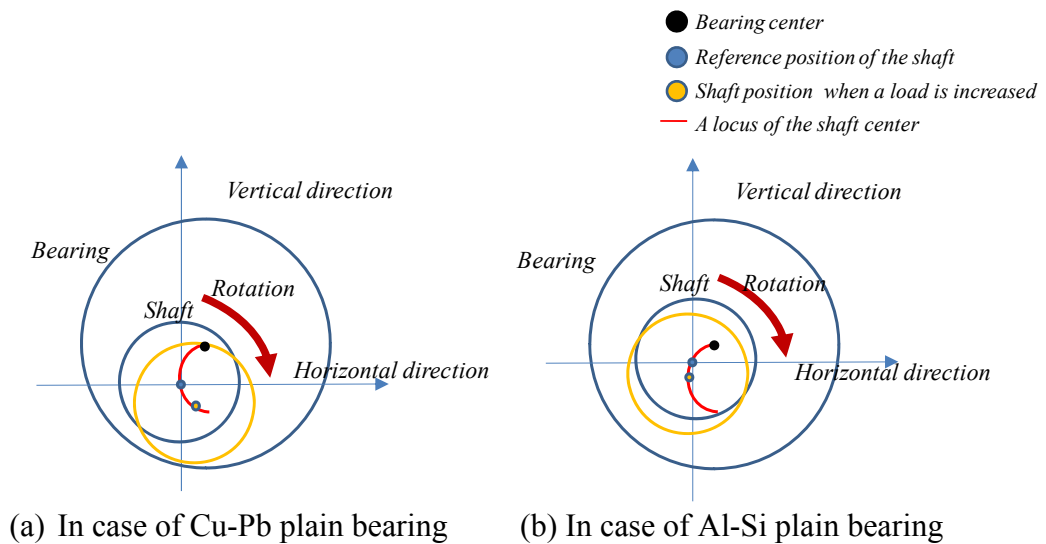


Figure 4-11 Estimated shaft displacement for sample A

Figure 4-12 shows the friction coefficients from the experiments and the simulation with samples A for 60 °C and 500 rpm. While the friction coefficients from the experiment were plotted for 1 kN to 10 kN of loads, those from the simulation were presented only for 1 kN and

10 kN in Figure 4-10. The THD (Thermohydrodynamic) analysis developed at the Poitiers University was used for the simulation and its detailed explanation is indicated in Appendix I (the oil was supplied through the hole in the shaft in the experiment but the friction coefficients were calculated with the oil supply from the opposite bearing side of the load). The thermal characteristics of only the bearing alloy were taken into account for the simulation. The lubricating condition for sample A with the Cu-Pb bearing is considered to be the mixture of hydrodynamic and mixed lubrication while that with the Al-Si bearing is hydrodynamic lubrication because the CR ratios with the Al-Si bearing maintained almost at 100 %.

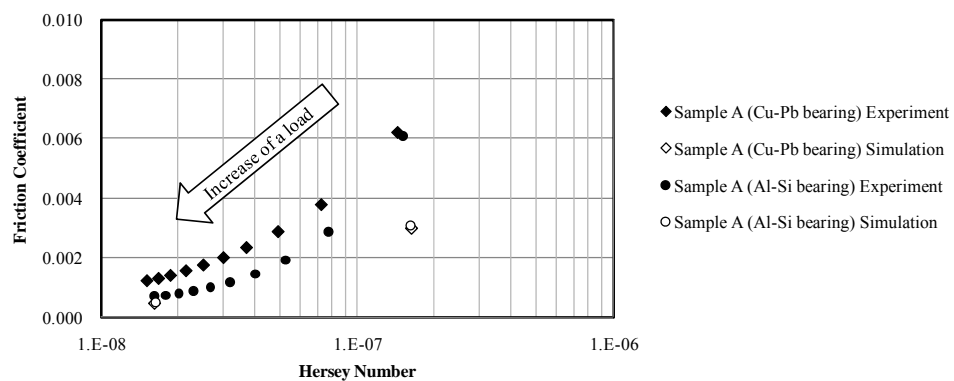


Figure 4-12 Friction coefficient vs. Hersey number in the experiment and simulation (60 °C, 500 rpm)

Although the bearing clearance of the Al-Si plain bearing is slightly smaller than that of the Cu-Pb plain bearing as mentioned previously, the friction coefficients of the two bearings were almost equal in the simulation. The effect of the clearance difference was very small. In fact, the initial bearing clearances were measured at room temperature, and they should be changed at a high operating temperature because of thermal expansion of the shaft and the plain bearing. The bearing clearances were therefore calculated using the bearing back face temperature. Since the increase of the bearing clearance was less than 1 μm for both of the plain bearings in the calculation, its effects should be very small. Although the thermal characteristics such as the heat conductivity of the bearing materials were different between the two bearings, they were, of course, taken into account in the simulation. Also, the difference in the friction coefficients between the two materials is larger than the uncertainty of the measurements.

As discussed previously, a lubrication film preventing metallic contact between the shaft and the plain bearing could be formed by the reaction of the Cu-Pb plain bearing with the sulfur in base oil A, but was not formed with the Al-Si plain bearing because that bearing does not

contain any ingredients that can react with sulfur. This is because Cu and Pb, which are constituent elements of the Cu-Pb bearing, are transition elements and are likely to react with sulfur. On the other hand, a lubrication film could not be formed because Al and Si in the Al-Si bearing are typical elements and are not likely to react with sulfur. It is also conceivable that the reaction film with the sulfur in sample A and the Cu-Pb plain bearing works conversely and increases the friction coefficient for the Cu-Pb plain bearing.

In addition, although the friction coefficients for sample A with the Al-Si plain bearing in the experiments are closer to those in the simulation than with the Cu-Pb plain bearing, a difference is still observed between the experiment and the simulation. In the Al-Si plain bearing lubrication with the low-viscosity base oils, it is supposed that the oil film formation is still not sufficient compared with the Cu-Pb plain bearing lubrication using the high-viscosity base oils presented in the chapter 3.

The experiments for the Cu-Pb bearing under the condition of 60 °C and 500 rpm are basically in mixed lubrication region. Therefore, the friction coefficients, the CR ratios and the relative shaft displacement at 60 °C and 3,000 rpm are also arranged in Figure 4-13 in order to discuss the bearing performance in hydrodynamic lubrication. Since no reduction in the CR ratio was observed under the condition of 60 °C and 3,000 rpm for both the Cu-Pb and Al-Si bearings, the lubricating condition should be hydrodynamic lubrication. The friction coefficients in sample A are almost equal to those in samples C and D for the Cu-Pb plain bearing. In addition, the relative shaft displacement for the Cu-Pb bearing came almost on the same line. In these results, the difference in the friction coefficients between the two bearings still exists in hydrodynamic lubrication region.

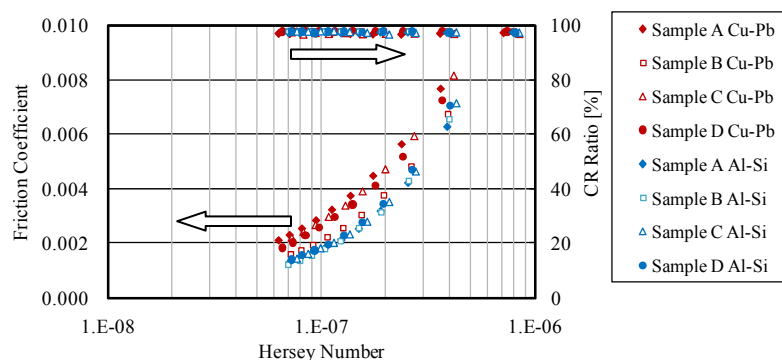


Figure 4-13 Friction coefficient and CR ratio vs. Hersey number at 60 °C and 3,000 rpm

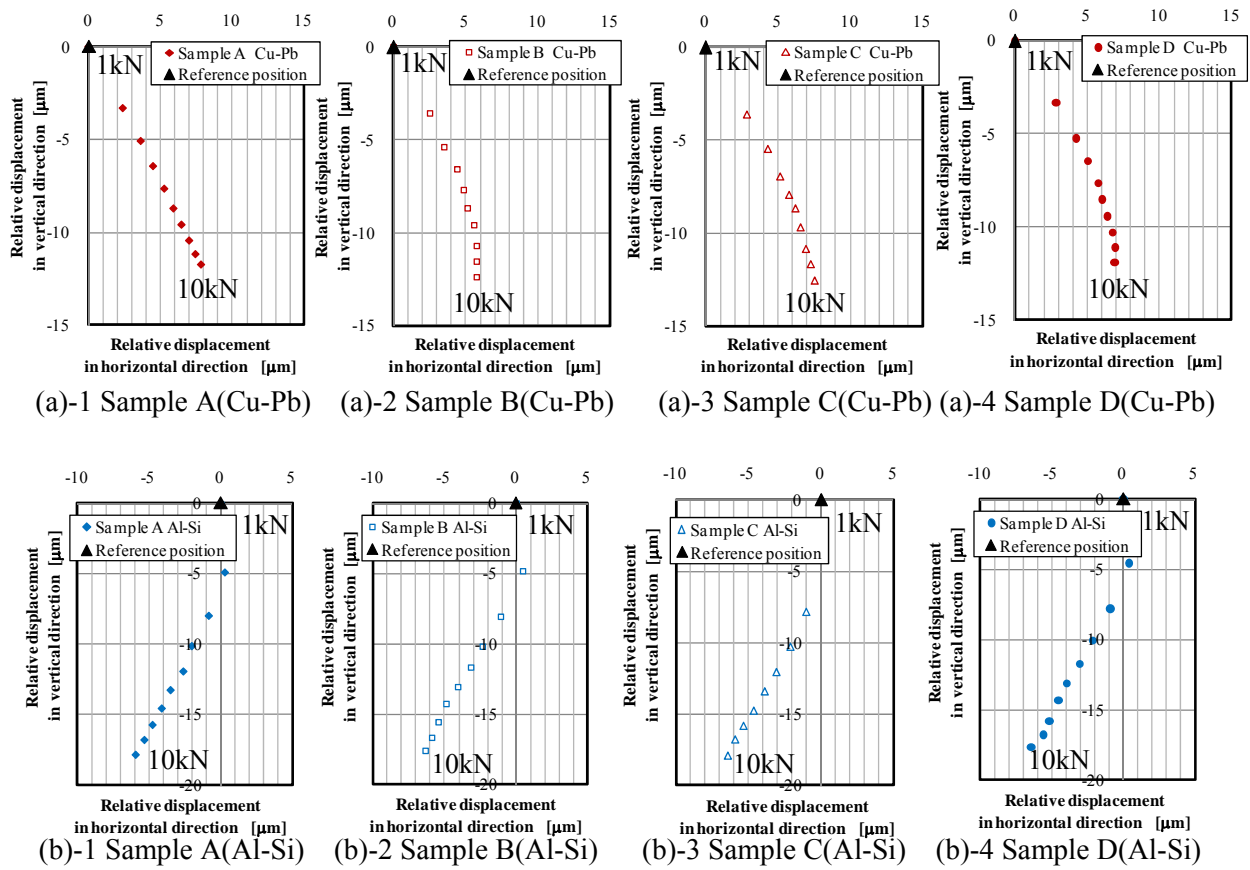


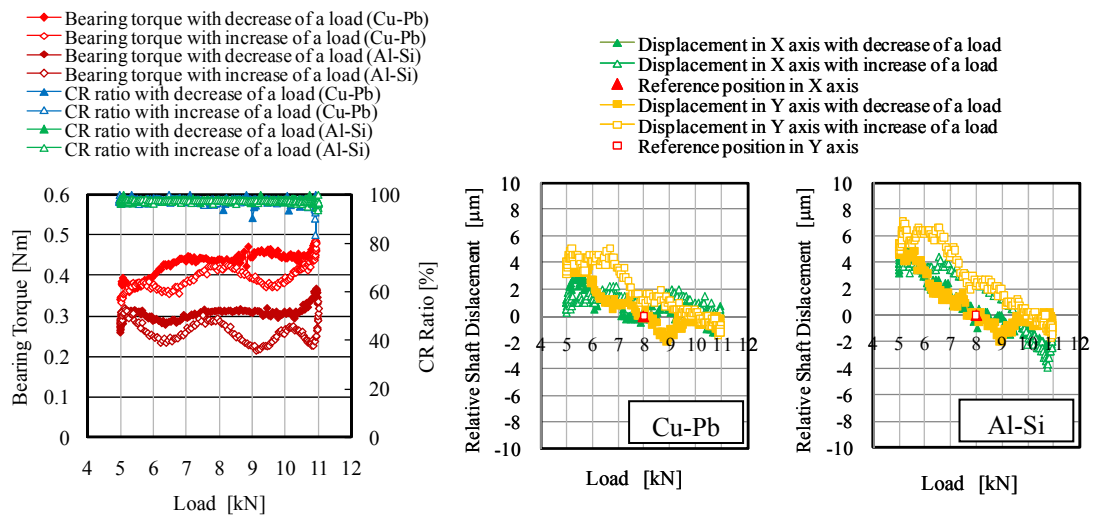
Figure 4-14 Relative shaft displacement at 60 °C and 3,000 rpm

Boedo et al. and some other researchers investigated the effect of bearing surface roughness or texture in plain bearing performance [66-68]. Boedo et al. calculated minimum oil film thickness using a developed computational model for big and connecting rod bearings with a smooth surface and roughness of 1 μm , and found that the effect of surface roughness was small. Since the surface roughness of the plain bearings used in this study was one digit smaller (nearly 0.1 μm), it is conceivable that its effect in the oil film thickness and the friction coefficients can be also small. However, the difference between the Cu-Pb bearing and the Al-Si bearing is apparent.

In this study, the temperature of the oil film was not directly measured although that of the bearing back-face was considered to be very close to it. The actual oil film thickness was not measured to confirm of its influence on the friction reduction. Those direct measurements might be important to ensure the effect of the bearing materials on the bearing performance in future. Moreover, other method to be examined should be measurement of the oil flow (velocity distribution) with various bearing materials.

4-4 Test results with the Al-Si plain bearing and the Cu-Pb plain bearing under dynamic load condition and discussion

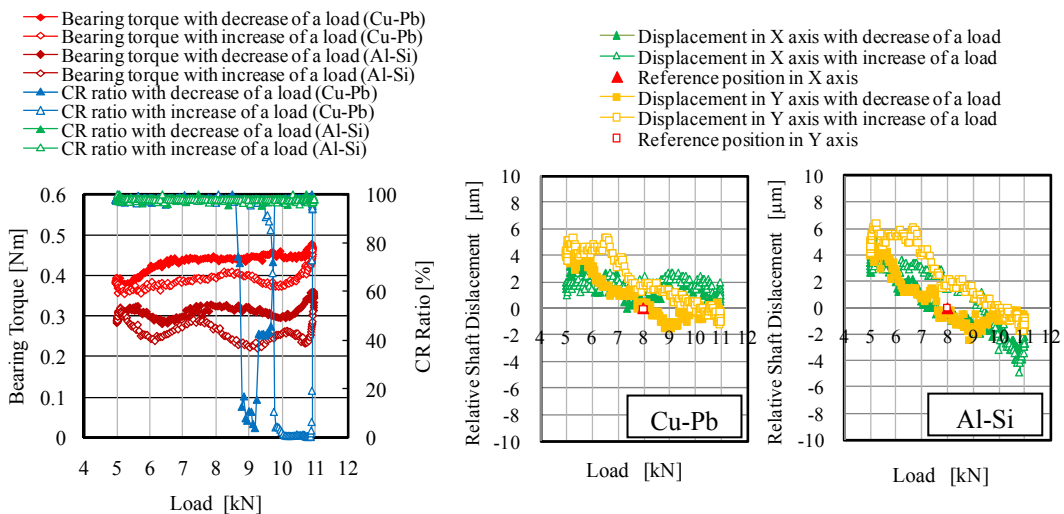
Figures 4-15 and 4-16 show the bearing torques, the CR ratios and the relative shaft displacement versus a load with samples A and C for the Al-Si plain bearing at a feeding oil temperature of 60 °C and a shaft speed of 1,000 rpm in comparison with the results for the Cu-Pb plain bearing (although the tests were conducted at 60, 80 and 100 °C for the Al-Si plain bearing, the figures were created using only the data obtained at 60 °C because the test with sample C for the Cu-Pb bearing was terminated at 500 rpm and 60 °C).



(a) Bearing torque, CR ratio

(b) Relative shaft displacement

Figure 4-15 Bearing torque, CR ratio and relative shaft displacement vs. load for sample A at 60 °C under dynamic load condition



(a) Bearing torque, CR ratio

(b) Relative shaft displacement

Figure 4-16 Bearing torque, CR ratio and relative shaft displacement vs. load for sample C at 60 °C under dynamic load condition

The bearing torques for the Al-Si plain bearing were lower than those for the Cu-Pb plain bearing. A reduction in the CR ratios for the Al-Si bearing was not observed but for the Cu-Pb bearing. These results are the same tendency as under static load conditions. As seen in Figures 4-15(b) and 4-16(b), the relative shaft displacement for the Al-Si bearing fluctuates in a wider range in the X and Y axes than for the Cu-Pb bearing. This suggests that the oil film thickness could be larger at the reference position for the Al-Si bearing, and it caused the lower bearing torques than for the Cu-Pb bearing and the wide fluctuation of the relative shaft displacement with changing the load.

4-5 Conclusions

In order to investigate the influence of lowering the viscosity of base oils in automotive plain bearings, the bearing performance in two kinds of typical automotive plain bearings was evaluated for four kinds of low-viscosity base oils with different refinement levels. The conclusions are the following:

- (1) The contact between the shaft and the bearing with the Cu-Pb bearing was likely to occur in a larger Hersey number than with the Al-Si bearing. Thus, the lubricating mode with the Cu-Pb bearing shifted from hydrodynamic to mixed lubrication under a smaller applied load than with the Al-Si bearing.
- (2) The Cu-Pb plain bearing showed a higher friction coefficient than the Al-Si plain bearing in hydrodynamic lubrication and in the region that the lubrication condition with the Cu-Pb was considered to be mixed lubrication. Since the difference in the relative shaft displacement between the two bearings appeared, the bearing materials were considered to affect the oil film formation and subsequently the friction coefficient. However, further study is required to ensure the theory for the effect of the bearing materials on the bearing performance.

Chapter 5

Effect of friction modifiers on plain bearing performance

Friction modifiers are normally used to reduce friction in mixed and boundary lubrication condition. The influence of lubricants with the Cu-Pb plain bearing material on bearing performance was investigated and determined that the bearing performance was greatly influenced by the molecular weight and refinement level of the base oil as shown in the previous chapters. The Cu-Pb plain bearing apparently showed a higher friction coefficient than the Al-Si plain bearing.

In order to obtain a guideline for improving the bearing performance with lubricants, the effect of friction modifiers added to base oils was examined. Since the influence for each bearing material is very important, the latest lead-free bearing materials were selected for the evaluation of bearing performance. The lead-free bearings used are plain bearings of Cu alloy and Al alloy with bismuth or bismuth/silver overlay. The effect of friction modifiers on bearing performance have not been investigated for those bearing materials in the past. Therefore, two kinds of friction modifiers were selected as representatives to confirm their influence mainly on reliability in mixed and boundary lubrication.

5-1 Plain bearings used

Four kinds of plain bearing materials were used as lead-free bearing materials. Two of those were plain bearings of Cu alloy in which hard particles were dispersed on a steel plate. The others were plain bearings of Al alloy on a steel plate. All of the plain bearings were made by Daido Metal Co., Ltd.

Figure 5-1 shows an illustration of the structure of the plain bearings used. Table 5-1 shows

the ingredients of the plain bearings. The plain bearings had no oil groove, and their width was 14.85 mm. Since it was conceivable that friction modifiers could affect the bearing performance in the vicinity of mixed or boundary lubrication region, the narrower plain bearings than 26 mm of width which were used for the investigation of the base oil and bearing material effects were selected in order to increase an applied specific load. The inside bearing diameter and the bearing thickness were respectively 53 mm and 1.5 mm. In fact, all of the plain bearings were manufactured with a bearing clearance of approximately 50 μm . They were steel plates of 1.2 mm on which a lining layer was applied with an overlay. The applied overlay was bismuth or bismuth/silver of which thickness was approximately 5 and 10 μm , respectively (in case of the bismuth/silver overlays, each thickness was approximately 5 μm).

Plain bearings manufactured in the same lot were used in order to avoid inconsistency of data due to inequalities in the manufacturing process.

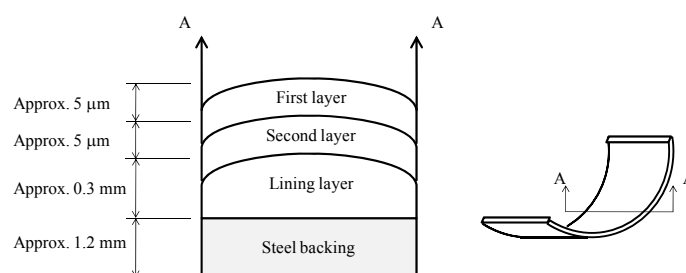


Figure 5-1 Structure of cross-section of the plain bearings

Table 5-1 Ingredients of lead-free plain bearings

| Abbreviations | Overlay | | Ingredients of bearing alloy |
|-----------------|-------------|--------------|------------------------------|
| | First layer | Second layer | Lining layer |
| PB-A (Bi/Ag-Cu) | Bi | Ag | Cu-10Sn-4Bi |
| PB-B (Bi-Cu) | Bi | - | Cu-6Sn |
| PB-C (Bi/Ag-Al) | Bi | Ag | Al-4Zn-6Si-1.2Cu |
| PB-D (Bi/Ag-Al) | Bi | Ag | Al-10Sn-2.5Si-1.5Cu |

5-2 Plain bearing test conditions

The tests were conducted under the following static load conditions:

- (1) Shaft speed: 1,000, 2,000, 3,000 rpm followed by 500 rpm
- (2) Feeding oil temperature: 60 °C
- (3) Feeding oil pressure: 0.5 MPa constant

The static load was increased from 1 kN to 10 kN by increments of 1 kN until the fluctuation of the friction coefficients became large. The tests were carried out only at 60 °C of a low feeding oil temperature because the narrower plain bearings were used and the fluctuation of the friction coefficient was observed at 500 rpm of a shaft speed under high load condition. The test procedure was the same as mentioned in the chapter 2. Plain bearing tests under dynamic load condition were not performed.

5-3 Lubricant samples tested

Three oil samples were prepared for the evaluation of the plain bearing performance. One is a base oil of polyalphaolefin (PAO), which is one of the API group IV base oils multiused as low-viscosity base oils for engine oil and has viscosity of approximately $6 \text{ mm}^2\cdot\text{s}^{-1}$ at 100 °C. The other two oil samples were prepared by adding 1 wt% of ester type friction modifiers (FMs) without or with sulfur [69] into polyalphaolefin (the difference between the two friction modifiers is not only the existence of sulfur in the molecule but also the chemical structure). Those oil samples are abbreviated as FM-A (w/o S) and FM-B (with S) in later descriptions. Table 5-2 shows the typical properties of the oil samples. The kinematic viscosity at 40 and 100 °C was measured and that at 60 and 80 °C was calculated with the Mac Coull and Walther formula. Dynamic viscosity calculated from the kinematic viscosity and the density is also shown in Figure 5-2. Since the addition of the friction modifiers were very small quantity, the viscometric properties were almost equal in the three oils.

Table 5-2 Typical properties of the oils tested

| | | Base Oil + FM(1wt%) | | |
|---------------------|------------------------|---------------------|----------------|--------------|
| | | Base Oil no FM | FM-A (with S) | FM-B (w/o S) |
| | | | without sulfur | with sulfur |
| Density | g/cm^3 | 0.8274 | 0.8282 | 0.8285 |
| Kinematic Viscosity | @15 °C | | | |
| | @40 °C | 31.28 | 31.13 | 30.50 |
| | @60 °C | 15.71 | 15.63 | 15.38 |
| | @80 °C | 9.151 | 9.107 | 8.987 |
| | @100 °C | 5.927 | 5.899 | 5.835 |
| Viscosity Index | - | 137 | 137 | 138 |

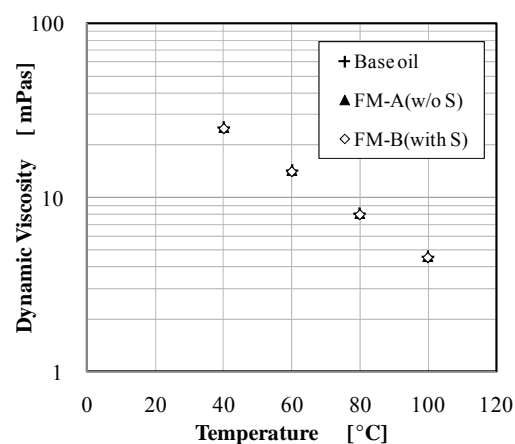


Figure 5-2 Dynamic vis. of the oils tested

5-4 Bearing test results with a base oil containing no additives

The test results obtained with the base oil containing no additives versus the Hersey number ($\eta N/P_{\text{spec}}$, η : absolute viscosity of tested oil, N : revolutions per second of shaft, P_{spec} : specific bearing load) were arranged. η was calculated with the temperature of the back face of the plain bearing.

Figure 5-3 shows the results when PB-A (Bi/Ag-Cu) was used as the plain bearing. The results with PB-B (Bi-Cu), PB-C (Bi/Ag-Al) and PB-D (Bi/Ag-Al) are shown in Figures 5-4, 5-5 and 5-6, respectively. The horizontal axis shows the Hersey number, and the vertical axis shows the friction coefficients and CR ratios.

Although a significant difference in the friction coefficients among the plain bearing materials was not observed, it was noted that the Hersey number at which the CR ratio begins to decrease varies. We were able to conduct the test with PB-D (Bi/Ag-Al) until the smallest CR ratio was reached. The CR ratio with PB-A (Bi/Ag-Cu) and PB-B (Bi-Cu) began to decrease in the next smallest Hersey number and with PB-C (Bi/Ag-Al) in the highest Hersey number. It was found that the contact condition between the shaft and the plain bearing depends on the plain bearing materials. Based on these results, the load carrying capacity of the plain bearing materials with the base oil can be listed in the following order:

<High> PB-D (Bi/Ag-Al) > PB-A (Bi/Ag-Cu), PB-B (Bi-Cu) > PB-C (Bi/Ag-Al) <Low>

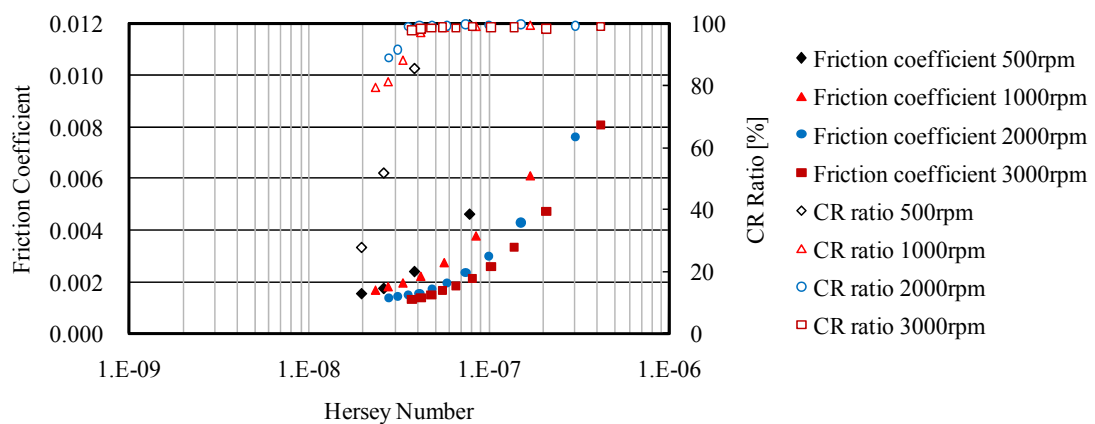


Figure 5-3 Friction coefficient and CR ratio vs. Hersey number with the base oil in PB-A (Bi/Ag-Cu)

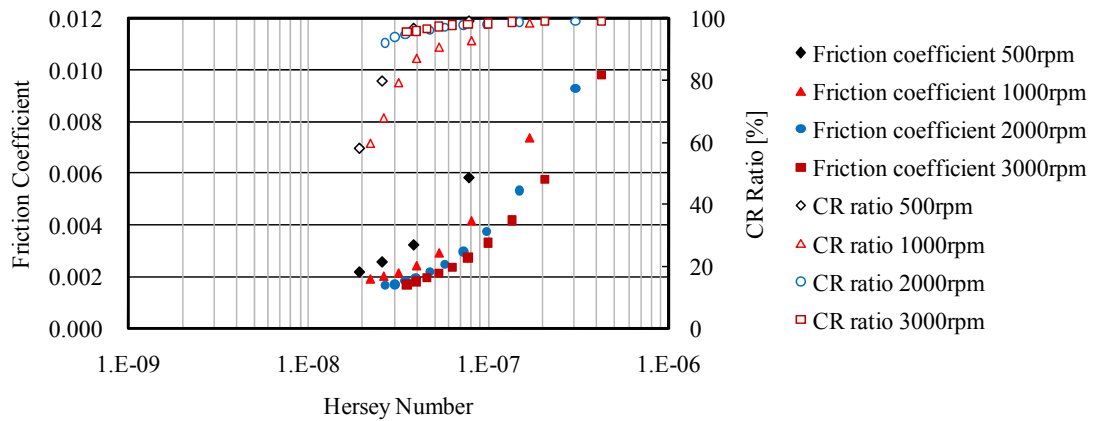


Figure 5-4 Friction coefficient and CR ratio vs. Hersey number with the base oil in PB-B (Bi-Cu)

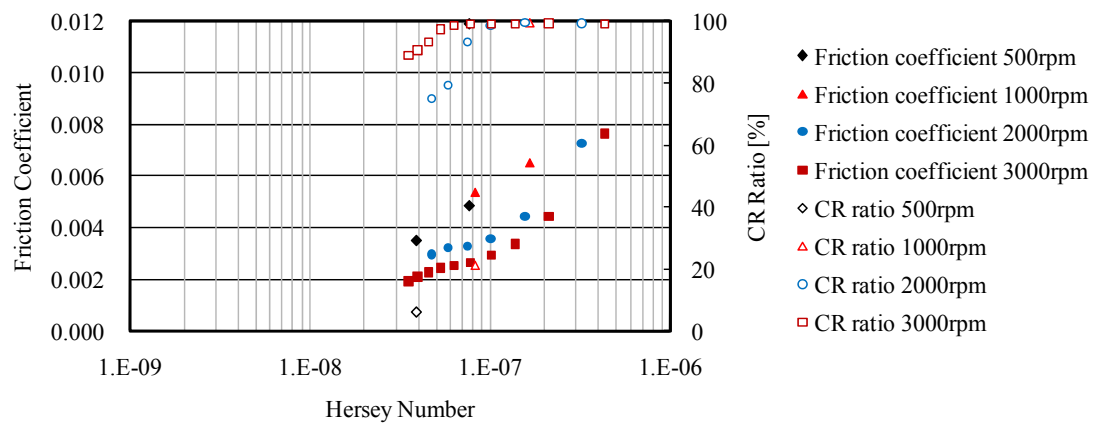


Figure 5-5 Friction coefficient and CR ratio vs. Hersey number with the base oil in PB-C (Bi/Ag-Al)

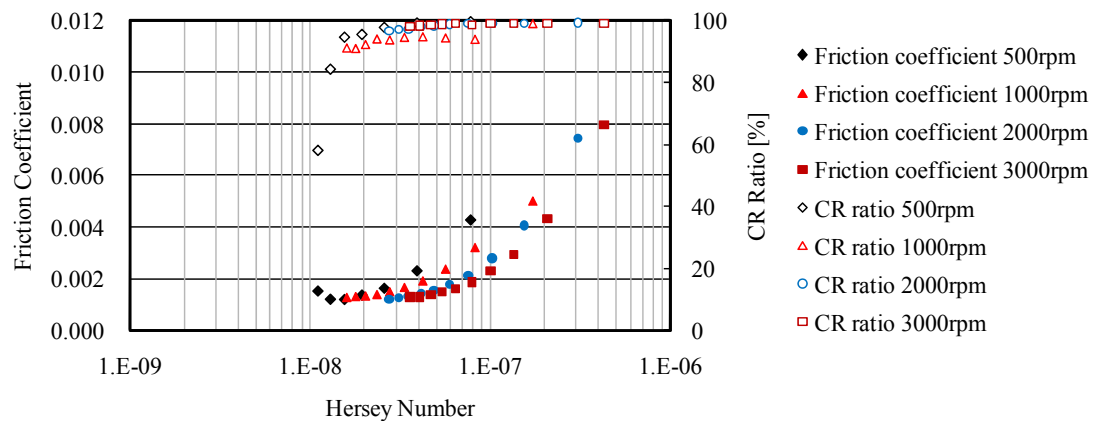


Figure 5-6 Friction coefficient and CR ratio vs. Hersey number with the base oil in PB-D (Bi/Ag-Al)

5-5 Bearing test results with an oil containing FM without sulfur

The test results obtained with the oil containing FM without sulfur (FM-A (w/o S)) versus the Hersey number was arranged. Figure 5-7 shows the test results when PB-A (Bi/Ag-Cu) was used as the plain bearing. The results for PB-B (Bi-Cu), PB-C (Bi/Ag-Al) and PB-D (Bi/Ag-Al) are shown in Figures 5-8, 5-9 and 5-10, respectively. The friction coefficients with FM-A (w/o S) are lower than those with only the base oil in the same Hersey number. It was also observed that the CR ratio tended to be decreased with PB-A (Bi/Ag-Cu) and PB-B (Bi-Cu) in the vicinity of the same smallest Hersey number.

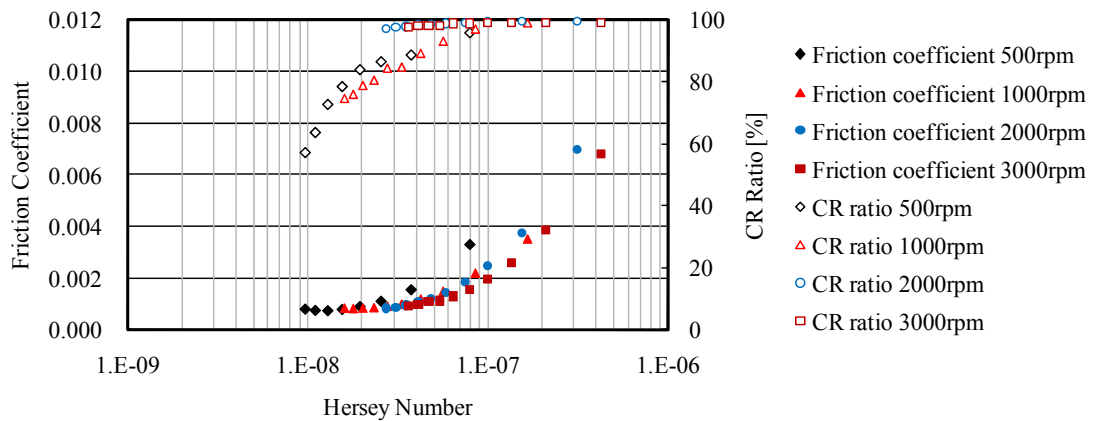


Figure 5-7 Friction coefficient and CR ratio vs. Hersey number with FM-A (w/o S) in PB-A (Bi-Ag-Cu)

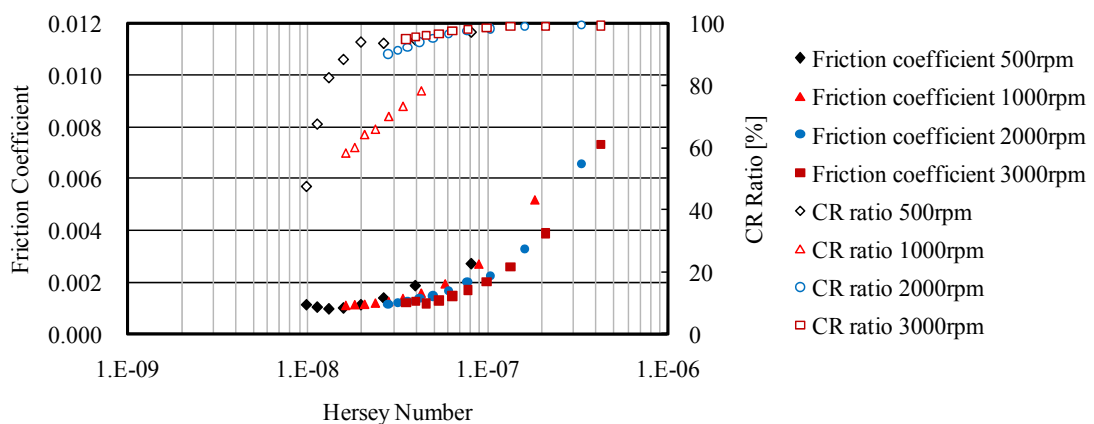


Figure 5-8 Friction coefficient and CR ratio vs. Hersey number with FM-A (w/o S) in PB-B (Bi-Cu)

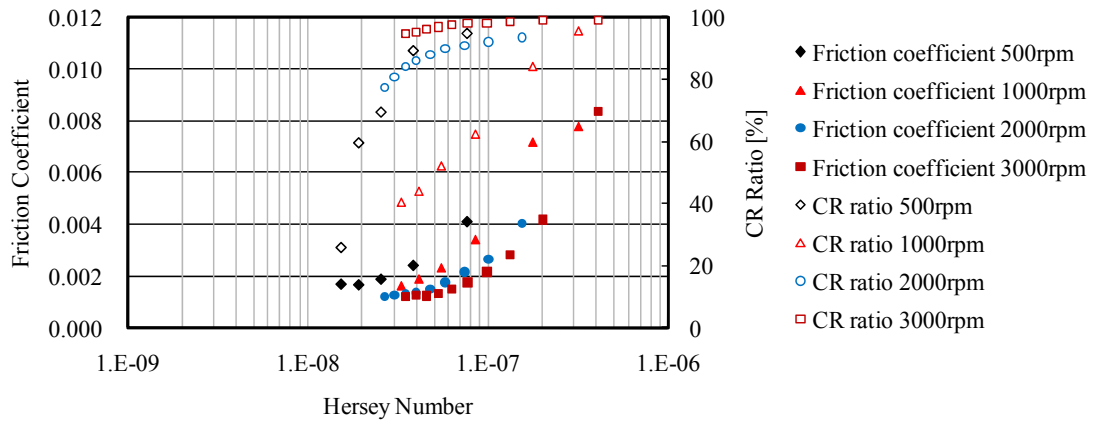


Figure 5-9 Friction coefficient and CR ratio vs. Hersey number with FM-A (w/o S) in PB-C (Bi/Ag-Al)

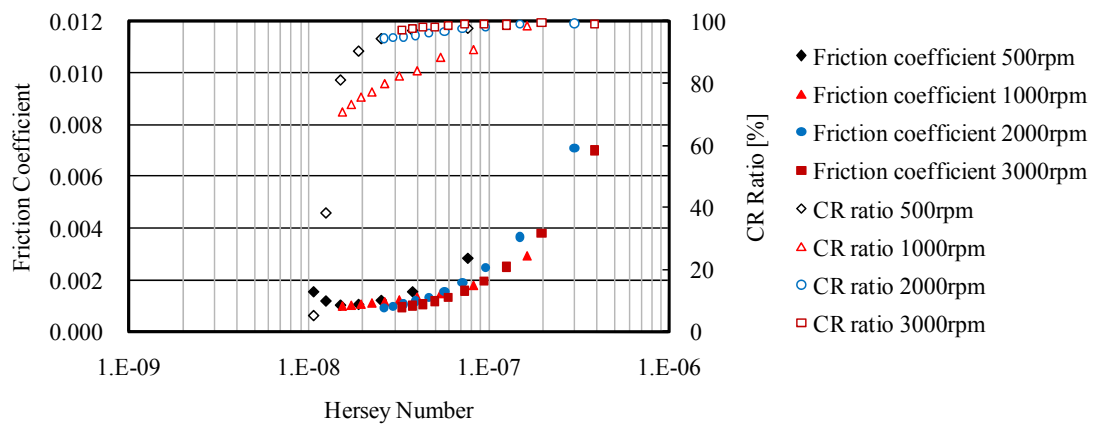


Figure 5-10 Friction coefficient and CR ratio vs. Hersey number with FM-A (w/o S) in PB-D (Bi/Ag-Al)

The CR ratio with PB-D (Bi/Ag-Al) began to decrease in the next smallest Hersey number and with PB-C (Bi/Ag-Al) in the highest Hersey number. Based on these results, the load carrying capacity of the plain bearing materials with FM-A (w/o S) can be listed in the following order:

<High> PB-A (Bi/Ag-Cu) > PB-B (Bi-Cu) > PB-D (Bi/Ag-Al) > PB-C (Bi/Ag-Al) <Low>

5-6 Bearing test results with an oil containing FM with sulfur

The test results obtained with the base oil containing FM (FM-B (with S)) versus the Hersey number were arranged. Figure 5-11, 5-12, 5-13 and 5-14 show the test results for PB-A

(Bi/Ag-Cu), PB-B (Bi-Cu), PB-C (Bi/Ag-Al) and PB-D(Bi/Ag-Al), respectively.

A reduction of the CR ratio for FM-B (with S) with PB-D (Bi/Ag-Al) until the smallest Hersey number was not observed. The CR ratio with PB-C (Bi/Ag-Al) began to decrease in the next smallest Hersey number, and with PB-A (Bi/Ag-Cu) and PB-B (Bi-Cu) in almost the same highest Hersey number. From these results, it was found that the tendency of the CR ratio to be reduced with FM-B (with S) was apparently different from the tendency with the base oil or FM-A (w/o S). Although the friction coefficients for FM-B (with S) are lower than those for only the base oil in the same Hersey number, they are close to those for FM-A (w/o S). Based on these results, the load carrying capacity of the plain bearing materials with FM-B (with S) can be listed in the following order:

<High> PB-D (Bi/Ag-Al) > PB-C (Bi/Ag-Al) > PB-A (Bi/Ag-Cu), PB-B (Bi-Cu) <Low>

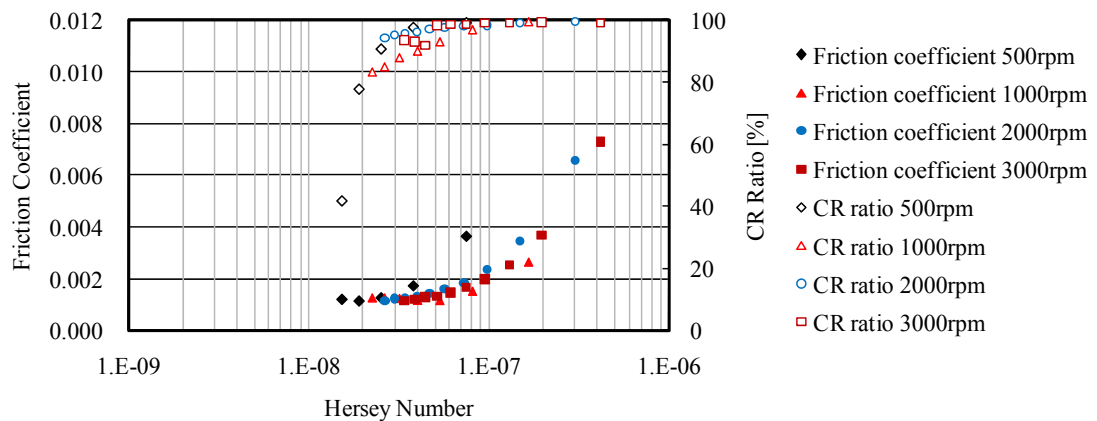


Figure 5-11 Friction coefficient and CR ratio vs. Hersey number with FM-B (with S) in PB-A (Bi/Ag-Cu)

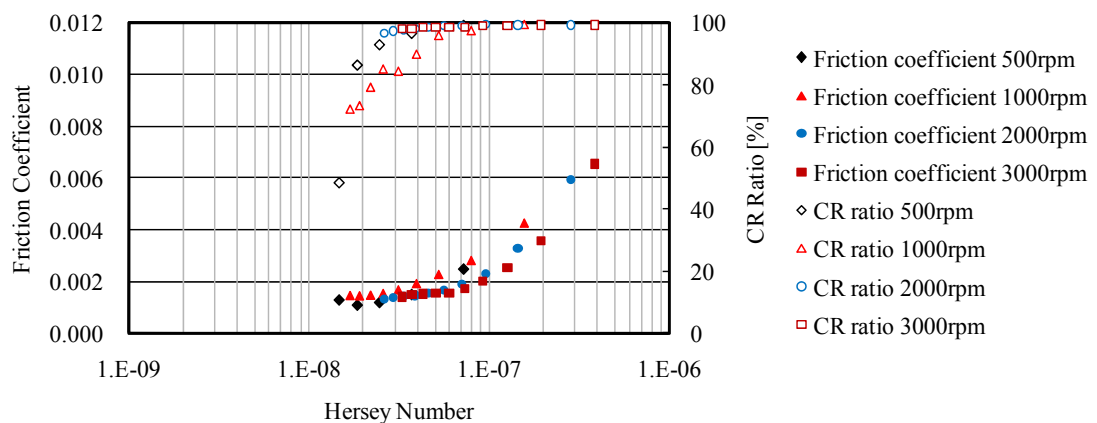


Figure 5-12 Friction coefficient and CR ratio vs. Hersey number with FM-B (with S) in PB-B (Bi-Cu)

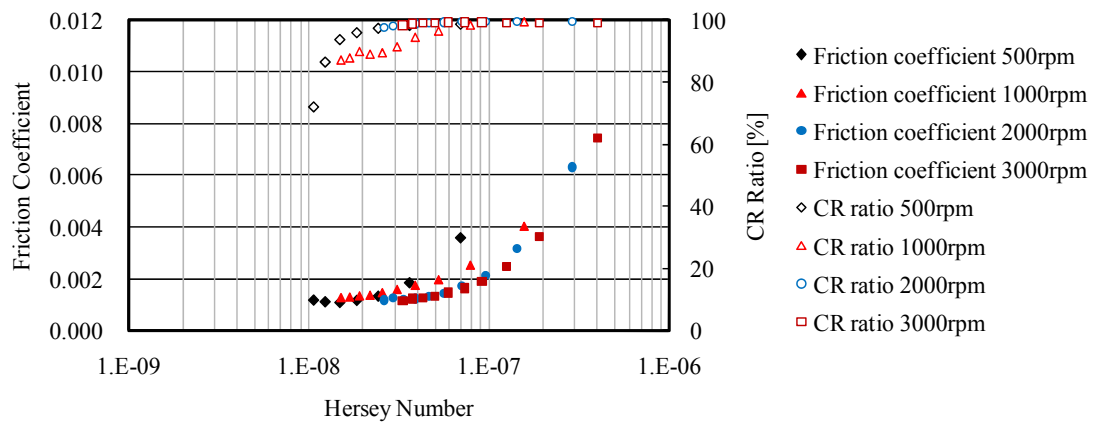


Figure 5-13 Friction coefficient and CR ratio vs. Hersey number with FM-B (with S) in PB-C (Bi/Ag-Al)

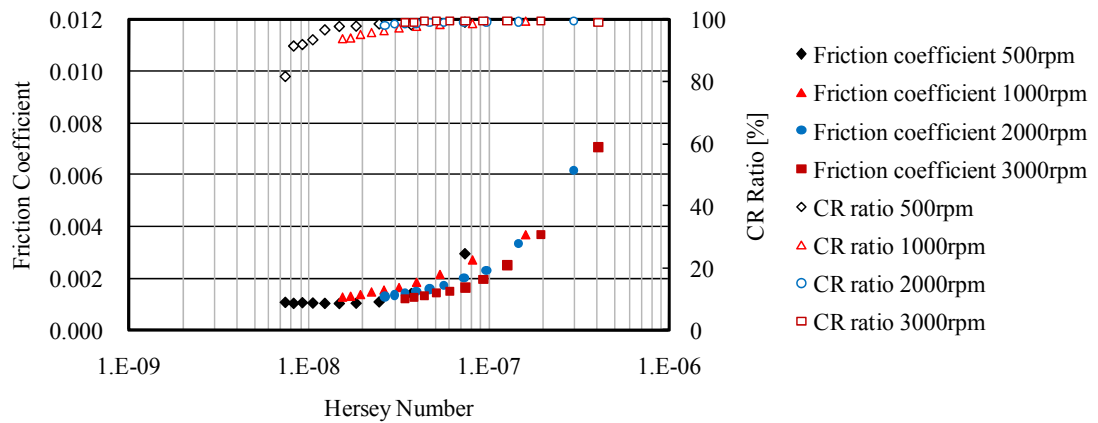


Figure 5-14 Friction coefficient and CR ratio vs. Hersey number with FM-B (with S) in PB-D (Bi/Ag-Al)

5-7 Difference of the results between the base oils with no additives and with FMs

Since it was found that the superiority or inferiority of load carrying capacity for the plain bearings varied when the friction modifiers (FMs) were added into the base oil, the bearing test results for each plain bearing were also arranged in order to clarify the influence of the FMs. Figure 5-15 shows the friction coefficients for PB-A (Bi/Ag-Cu). Figures 5-16, 5-17 and 5-18 show the friction coefficients for PB-B (Bi-Cu), PB-C (Bi/Ag-Al) and PB-D (Bi/Ag-Al), respectively. The horizontal axis shows the Hersey number, and the vertical axis shows the friction coefficients.

In case of PB-A (Bi/Ag-Cu) using Cu alloy as a bearing alloy, the friction coefficients for FM-A (w/o S) are the lowest. The friction coefficients for FM-B (with S) are the next lowest, and for the base oil with no additives they are the highest. The same tendency was observed

with PB-B (Bi-Cu), which also used the Cu alloy bearing. Therefore, the friction coefficients with the plain bearings of Cu alloy for the small Hersey number are in the following order:

$$\langle \text{Low} \rangle \text{ FM-A (w/o S)} < \text{FM-B (with S)} < \text{Base oil} \langle \text{High} \rangle$$

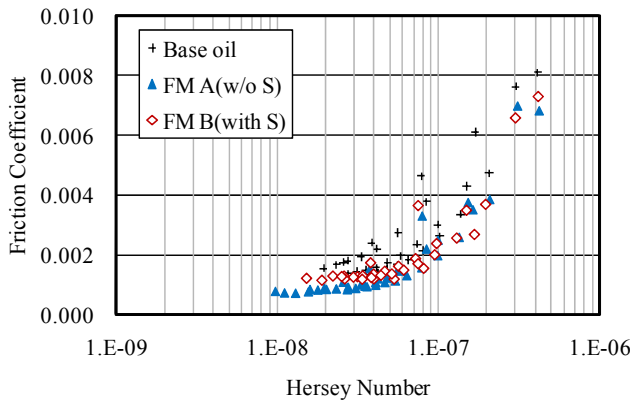


Figure 5-15 Friction coefficient with PB-A (Bi/Ag-Cu)

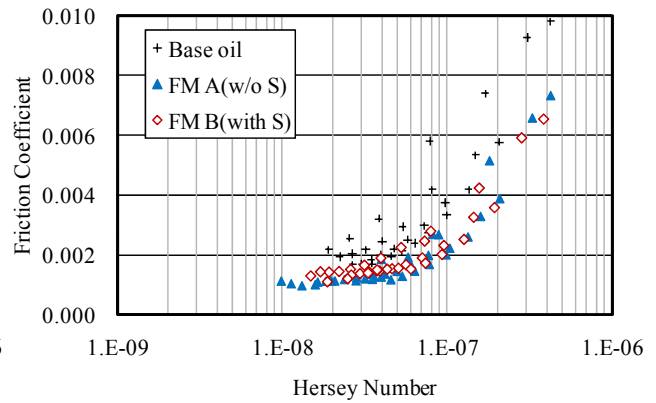


Figure 5-16 Friction coefficient with PB-B (Bi-Cu)

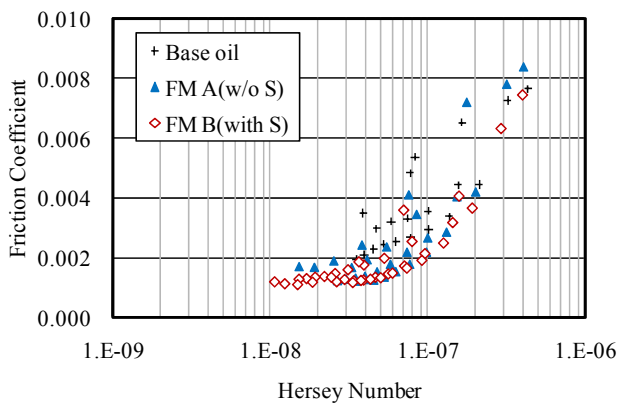


Figure 5-17 Friction coefficient with PB-C (Bi/Ag-Al)

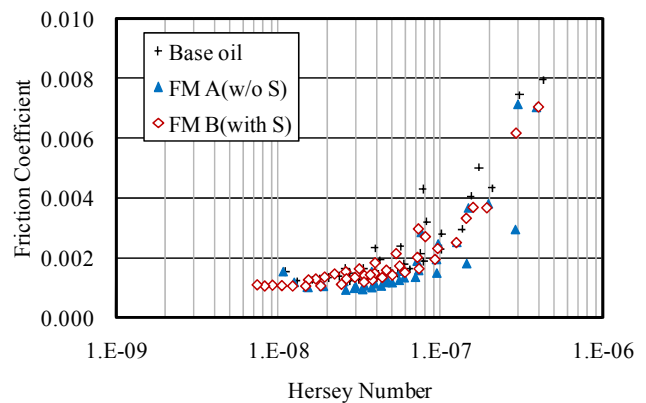


Figure 5-18 Friction coefficient with PB-D (Bi/Ag-Al)

On the other hand, in case of PB-C (Bi/Ag-Al) using Al alloy as a bearing alloy, the friction coefficients for FM-B (with S) are the lowest. The friction coefficients for FM-A (w/o S) are the next lowest. Although the friction coefficients for PB-D (Bi/Ag-Al) using Al alloy are the lowest with FM-A (w/o S) at the large Hersey number, they become larger than for FM-B (with S) at the small Hersey number. This is the same tendency as for PB-C (Bi/Ag-Al). Thus, the friction coefficients with the plain bearings using Al alloy at the small Hersey number can be listed in the following order:

$$\langle \text{Low} \rangle \text{ FM-B (with S)} < \text{FM-A (w/o S)} < \text{Base oil} \langle \text{High} \rangle$$

Indeed, the effect of FM-A (w/o S) in the small Hersey number range differed from that in

the large Hersey number range. The bearing performance can depend on the bearing material especially in the small Hersey number in which the lubricating condition is considered to be mixed lubrication.

The CR ratios for PB-A (Bi/Ag-Cu), PB-B (Bi-Cu), PB-C (Bi/Ag-Al) and PB-D (Bi/Ag-Al) are shown in Figures 5-19, 5-20, 5-21 and 5-22, respectively. The horizontal axis shows the Hersey number, and the vertical axis shows the CR ratio. In case of PB-A (Bi/Ag-Cu) using Cu alloy as a bearing alloy, the CR ratio for FM-A (w/o S) is decreased in the smallest Hersey number range. The CR ratio for FM-B (with S) is decreased at the next lowest Hersey number, and for the base oil with no additives it is decreased at the highest Hersey number. The same tendency was observed with PB-B (Bi-Cu), which also used the Cu alloy bearing as well as PB-A (Bi/Ag-Cu). The CR ratios with the Cu alloy bearings can be listed in the following order:

$$\langle \text{Low} \rangle \quad \text{Base oil} < \text{FM-B (with S)} < \text{FM-A (w/o S)} \quad \langle \text{High} \rangle$$

On the other hand, in case of PB-C (Bi/Ag-Al) and PB-D (Bi/Ag-Al) using Al alloy as a bearing alloy, the CR ratio for FM-B (with S) is decreased at the smallest Hersey number. The CR ratios with the Al alloy bearings can be listed in the following order:

$$\langle \text{Low} \rangle \quad \text{Base oil} , \text{FM-A (w/o S)} < \text{FM-B (with S)} \quad \langle \text{High} \rangle$$

Based on these results, it was found that the effect of FM-A (w/o S) was greater with the Cu alloy bearings than that of FM-B (with S), but, in contrast, the effect of FM-B (with S) with the Al alloy bearings was greater in mixed lubrication. It is conceivable that the friction coefficients were inversed as shown in Figures 5-17 and 5-18 because the reduction of the CR ratio was small with the Al alloy bearing and FM-B (with S) due to mutual interaction between the friction modifier and the plain bearing.

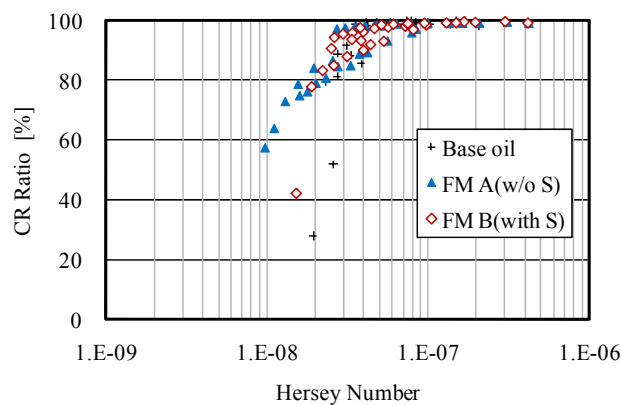


Figure 5-19 CR ratio with PB-A (Bi/Ag-Cu)

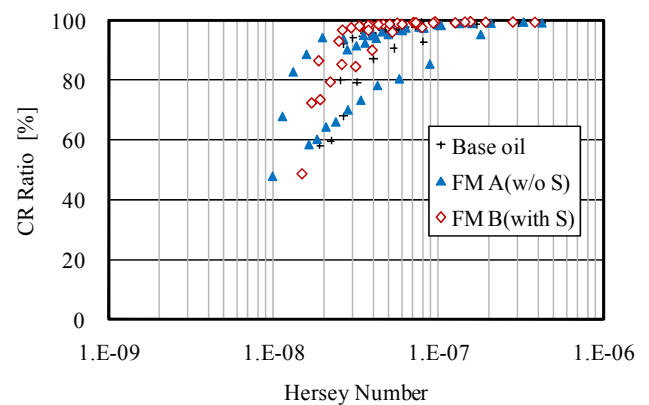


Figure 5-20 CR ratio with PB-B (Bi-Cu)

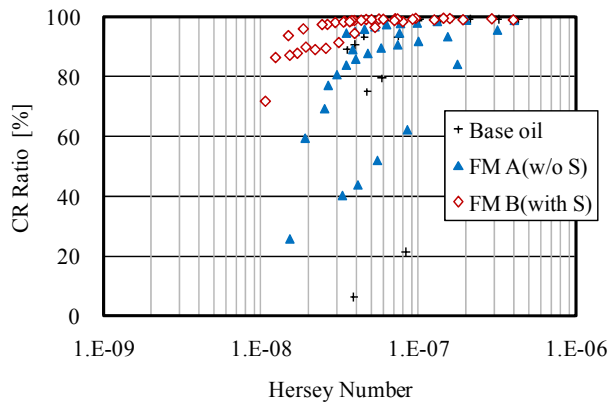


Figure 5-21 CR ratio with PB-C (Bi/Ag-Al)

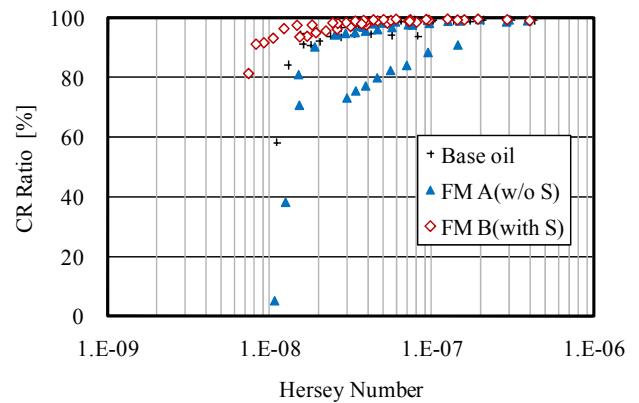


Figure 5-22 CR ratio with PB-D (Bi/Ag-Al)

5-8 Friction characteristics of oils in the boundary lubrication region with a reciprocating type friction tester

In order to simplify the evaluation of friction modifier and readily analyze the friction characteristics of the plain bearings, tribological tests with each oil sample using a reciprocating type friction tester was attempted. Figure 5-23 shows an illustration of the friction tester used. Plates made with the same materials as the plain bearings were used as test pieces. A drop of the oil sample was applied onto the plate, and the friction coefficients as well as the contact resistance (CR) ratio between the plate and a three quarter inch steel ball were measured. The test conditions are the following:

- (1) Load: 0.98 N, 1.96 N, 2.94 N
- (2) Sliding velocity: 10 mm·s⁻¹
- (3) Number of cycles: 20 times under each load condition
- (4) Amplitude: 10 mm
- (4) Temperature of plate: 60 °C

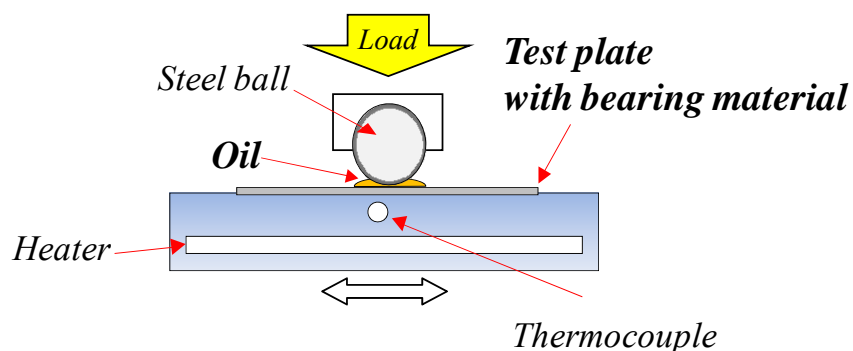


Figure 5-23 Reciprocating type friction tester

In addition, to investigate the effect of the overlay of Bi/Ag, tests were also carried out with PB-D plain bearings with no overlay.

Since the tendency of friction characteristics of each oil were almost the same under various load conditions in the reciprocating type friction test, only the results with PB-A (Bi/Ag-Cu), PB-B (Bi-Cu), PB-C (Bi/Ag-Al), PB-D (Bi/Ag-Al) and PB-D (no overlay) of plain bearings for a load of 1.96 N are shown in Figure 5-24. The horizontal axis shows the number of cycles of the reciprocating motion, and the vertical axis shows the friction coefficients.

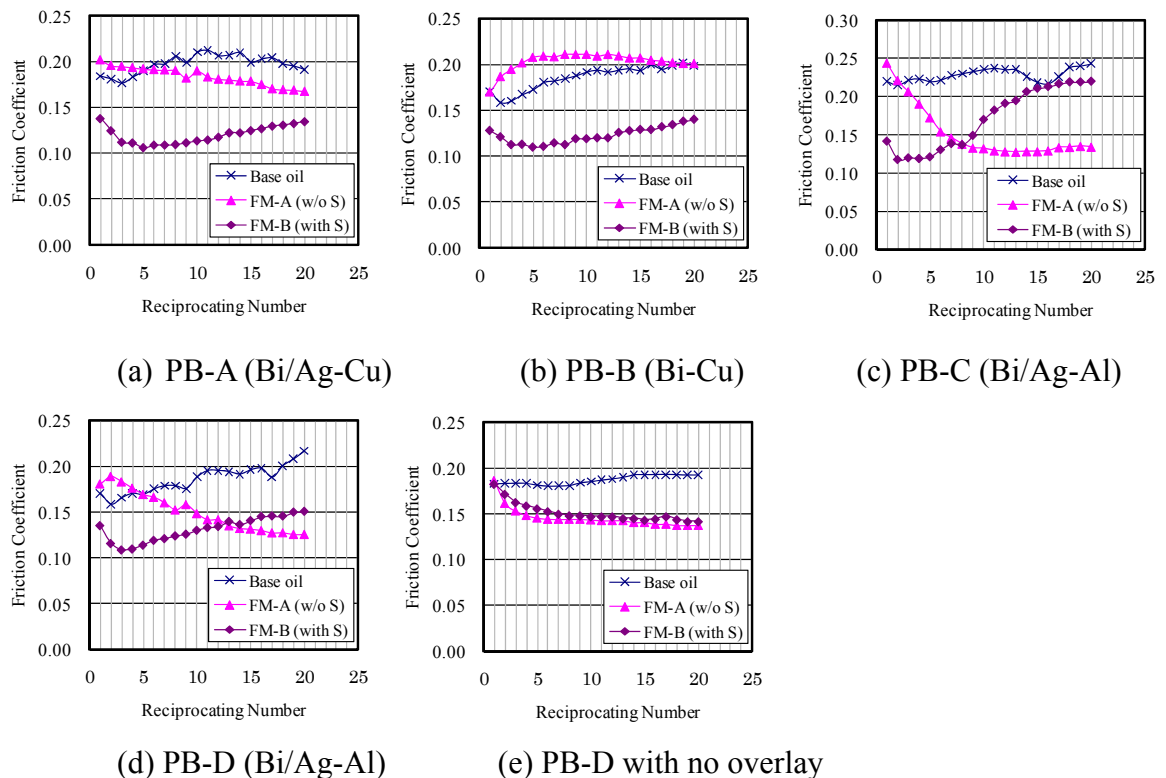


Figure 5-24 Friction coefficients vs. reciprocating number with the reciprocating friction tester

FM-B (with S) showed the lowest friction coefficients for PB-A (Bi/Ag-Cu) and PB-B (Bi-Cu) of Cu alloy bearings at the large reciprocating number, but FM-A (w/o S) does for PB-C (Bi/Ag-Al) and PB-D (Bi/Ag-Al). This is the quite different tendency from the results at the small Hersey number with the plain bearing tests.

In the initial stage of the reciprocating friction test, the friction coefficients for PB-D with no overlay are almost the same for the three oils. Then, according to repetition of sliding, they do, however, tend to be decreased with the oils containing FMs, while they are increased with the base oil. This is a different tendency from the results with PB-D

(Bi/Ag-Al).

From these results, it was found that the overlay strongly affected the friction coefficients in boundary lubrication because they depended on the existence of the overlay, but that the tendency of the friction coefficients in the bearing test was very different from that in the reciprocating friction test. Thus, it was concluded that the estimation of the plain bearing test results by using the reciprocating friction test in boundary lubrication was difficult.

5-9 Discussion

It was clarified that the ingredients of the plain bearing material were strongly related to the bearing performance, but this could not be estimated by the reciprocating friction test in boundary lubrication.

In order to discuss the reliability with the oils containing friction modifiers, the relationships between the CR ratio and the shaft displacement were arranged. The relative displacement and the CR ratio between the shaft and the plain bearing of PB-A (Bi/Ag-Cu) at a shaft speed of 500 rpm are shown in Figure 5-25. The horizontal axis shows the relative displacement in the horizontal direction between the shaft and the plain bearing at a reference point under the load of 1 kN and 500 rpm for each oil sample. The load was increased with increments of 1 kN. The vertical axis shows both the relative displacement in the vertical direction and the CR ratio. The relative shaft displacement and the CR ratio for PB-B (Bi-Cu), PB-C (Bi/Ag-Al) and PB-D (Bi/Ag-Al) of the plain bearings are shown in Figures 5-26, 5-27 and 5-28, respectively. Since the friction coefficients fluctuated widely in the low CR ratio when the load was increased, the tests were terminated before the load reached 10 kN, and that load was defined as the limitation.

It is likely in the bearing tests that the lower the limitation of the load, the smaller the relative shaft displacement with the applied load. When the applied load is increased, the inclination of the relative displacement in the vertical direction versus that in the direction of the applied load is likely to be small.

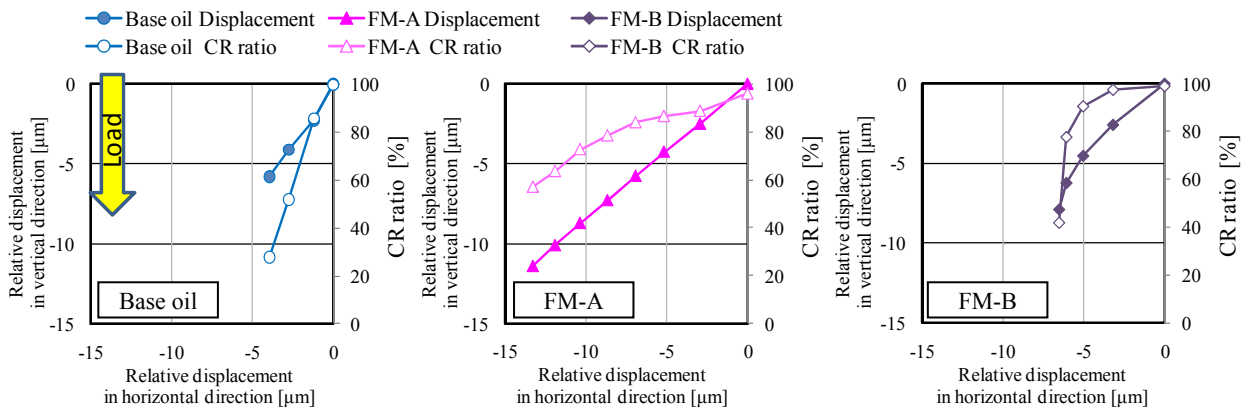


Figure 5-25 Relative shaft displacement in vertical direction and CR ratio vs. relative shaft displacement in horizontal direction with PB-A (Bi/Ag-Cu)

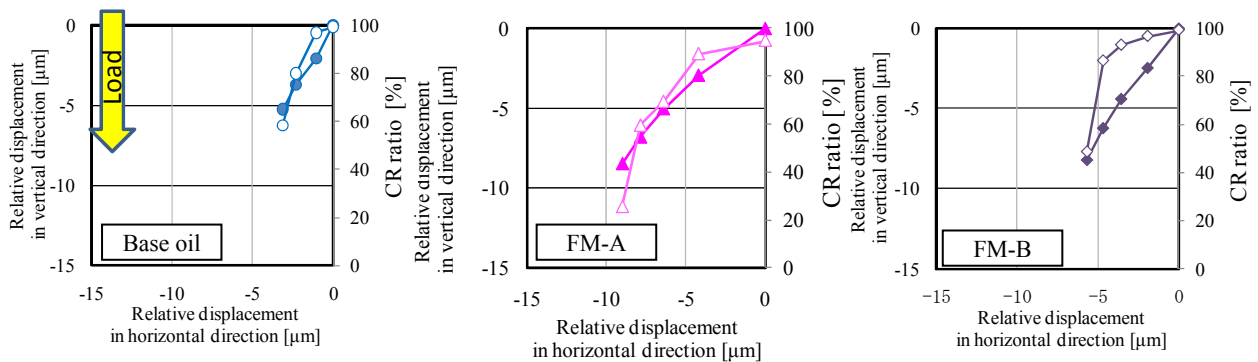


Figure 5-26 Relative shaft displacement in vertical direction and CR ratio vs. relative shaft displacement in horizontal direction with PB-B (Bi-Cu)

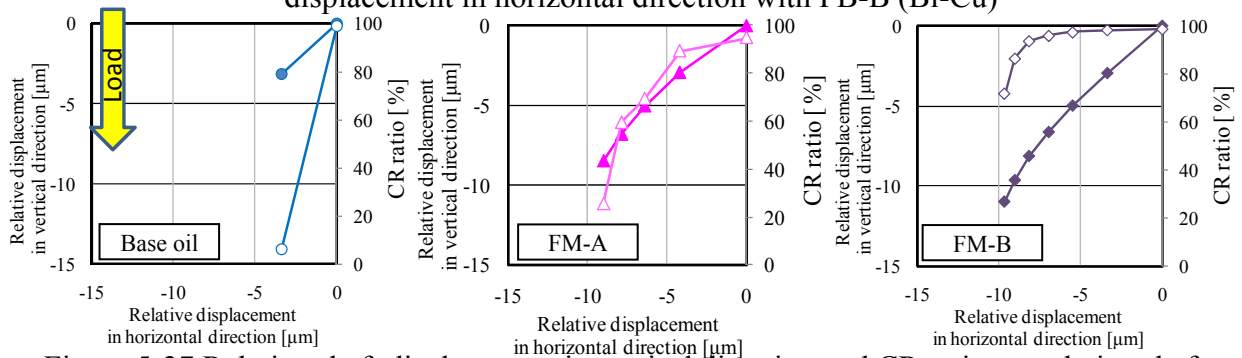


Figure 5-27 Relative shaft displacement in vertical direction and CR ratio vs. relative shaft displacement in horizontal direction with PB-C (Bi/Ag-Al)

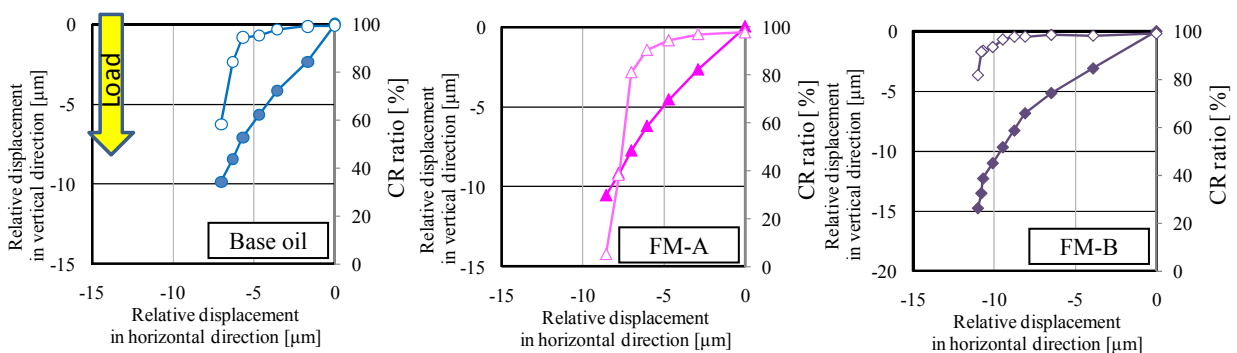


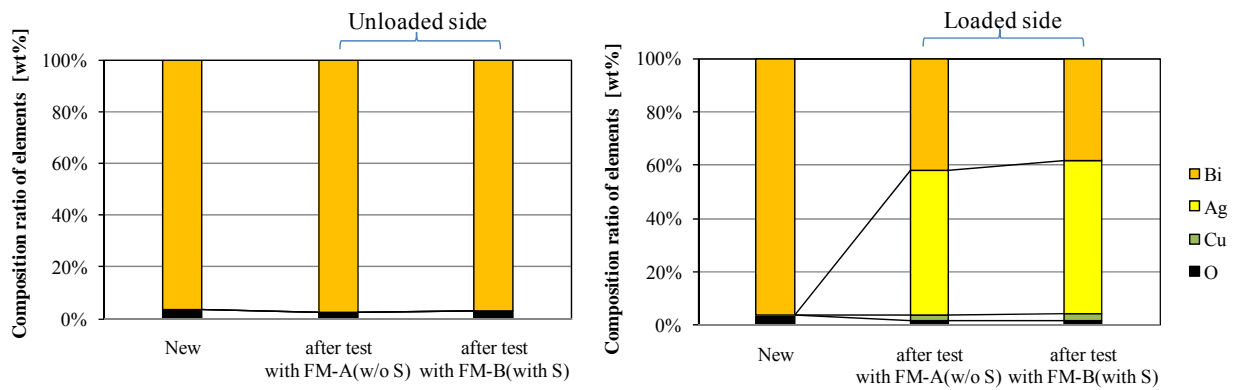
Figure 5-28 Relative shaft displacement in vertical direction and CR ratio vs. relative shaft displacement in horizontal direction with PB-D (Bi/Ag-Al)

In case of the base oil, the CR ratios tend to immediately decrease for most of the tests when a load is increased. This can be because the lubricating condition is shifting from hydrodynamic to mixed lubrication, subsequently to boundary lubrication even at a small load. If the oils containing the friction modifiers were used, the limitation of the load was increased compared with the base oil for all of the cases. In case of FM-A (w/o S), the CR ratios were decreased at a small load but basically maintained at higher positions than the base oil especially with PB-A (Bi/Ag-Cu) and PB-B (Bi-Cu) bearing as shown in Figures 5-27 and Figure 28. It is therefore considered that FM-A (w/o S) affected to avoid serious damage of the bearing in mixed lubrication. On the other hand, in case of FM-B (with S) the CR ratios are decreasing with a very small slope and maintain at high values until approximately 5 kN with PB-C (Bi/Ag-Al) and PB-D (Bi/Ag-Al). This also implies that FM-B (with S) worked effectively in the vicinity to mixed lubrication.

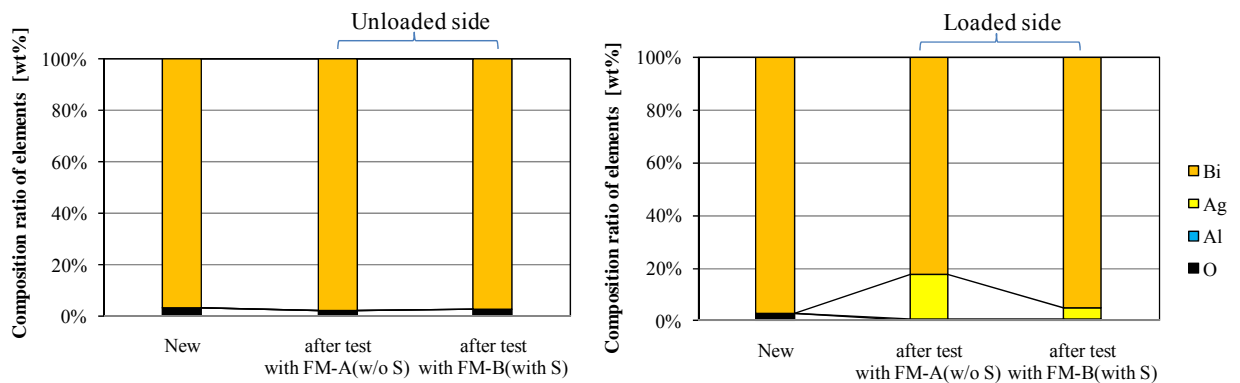
In order to confirm the reasoning, the surface of the plain bearing was analyzed. Table 5-3 and Figure 5-29 show the results of the ingredients on the plain bearings (PB-A (Bi/Ag-Cu), PB-D (Bi/Ag-Al)) of the loaded side and unloaded side tested with FM-A (w/o S) and FM-B (with S) as well as the plain bearings before testing. The analysis was conducted by using a scanning electron microscopy-energy dispersive spectrometer (SEM-EDS). The ingredients of the tested plain bearings (PB-A (Bi/Ag-Cu), PB-D (Bi/Ag-Al)) are almost same as the new plain bearings for the unloaded side. However, the change of the ingredients for the loaded side of the plain bearings is large. For example, in case of PB-A (Bi/Ag-Cu) of the Cu alloy bearing, the amount of Bi on the surface of the plain bearings with FM-A (w/o S) is larger than with FM-B (with S) for the loaded side of the bearing, although the CR ratio reduction is small and the test was carried out until the higher load condition with FM-B (with S). The amount of Ag and Cu of the lining layer with FM-A (w/o S) is less than with FM-B (with S).

Table 5-3 Composition ratio of elements on PB-A (Bi/Ag-Cu) and PB-D (Bi/Ag-Al)

| | New | | FM-A (w/o S) | | | | FM-B (with S) | | | |
|--------------------|-------|------|-------------------|------|---------------------|------|-------------------|------|---------------------|------|
| | (wt%) | | Loaded side (wt%) | | Unloaded side (wt%) | | Loaded side (wt%) | | Unloaded side (wt%) | |
| PB-A (Bi/Ag-Cu) | Bi | 96.2 | Bi | 42.0 | Bi | 97.3 | Bi | 38.5 | Bi | 96.9 |
| | O | 3.8 | Ag | 54.1 | O | 2.7 | Ag | 56.9 | O | 3.1 |
| | | | Cu | 2.2 | | | Cu | 2.9 | | |
| | | | O | 1.6 | | | O | 1.7 | | |
| PB-D (Bi/Ag-Al) | Bi | 97.0 | Bi | 82.6 | Bi | 97.9 | Bi | 94.9 | Bi | 97.4 |
| | O | 3.0 | Ag | 16.9 | O | 2.1 | Ag | 4.2 | O | 2.6 |
| | | | Al | 0.6 | | | Al | 0.9 | | |



(a) PB-A (Bi/Ag-Cu) using Cu alloy



(b) PB-D (Bi/Ag-Al) using Al alloy

Figure 5-29 Composition ratio of elements on PB-A (Bi/Ag-Cu) and PB-D (Bi/Ag-Al)

On the other hand, in case of PB-D (Bi/Ag-Al) Al alloy bearing, the composition ratio of Bi is decreased but it was found that larger amount of Bi was remained with FM-B (with S). Although the bearing test was conducted with FM-B (with S) until higher load because of small reduction of the CR ratio, it is clear that the surface of the plain bearing was protected due to the effect of FM-B (with S) with the Bi surface.

From these results, it is apparent that the friction modifiers prevent the reduction of the CR ratio and protect the overlay. It was therefore considered that increasing the CR ratio with the

friction modifiers in the same Hersey number is the mechanism to decrease friction coefficient in small Hersey number region.

5-10 Conclusions

The influence of friction modifiers in lubricants on bearing performance was examined with the bearing test apparatus using lead-free plain bearings developed in response to environmental regulations. The conclusions are the following:

- (1) Since the friction coefficients of the bearing and the metal contact status between the shaft and the bearing depended on different lead-free bearing materials, the reliability (load carrying capacity) also greatly varied according to the bearing materials in mixed lubrication.
- (2) The influence of the friction modifiers varied with the lead-free bearing materials. The bearing alloy was closely related to the expression of the performance of the friction modifiers. The ester type friction modifiers without and with sulfur reduced the friction coefficients and increased the CR ratios respectively for the Cu alloy bearings and the Al alloy bearings in mixed lubrication region.
- (3) The addition of the friction modifiers that adapt to the plain bearings effectively functions to reduce the friction coefficients and the metal contact between the shaft and the plain bearing in mixed lubrication. Therefore, the load carrying capacity greatly varied with the combination of the friction modifiers and the plain bearing materials. Although the viscosity of the oils with friction modifiers was almost the same as the base oil, the load carrying capacity became double.

Chapter 6

Effect of polymers on plain bearing performance

From the viewpoint of energy saving, polymers have been widely used for decreasing apparent viscosity at a low temperature keeping a high temperature viscosity at a certain limit for most of engine oil. It is known that viscosity of polymer-containing oils is decreased at a high shear rate. Also, while such a viscosity reduction contributes to decrease friction loss, it causes metal contact and deteriorates the reliability of plain bearings. However, it was confirmed in our previous study that polymer-containing oils showed the effect of metal contact prevention between a shaft and a plain bearing in addition to low friction loss [70].

In order to investigate the effect of polymers on plain bearing performance in hydrodynamic lubrication, we proceeded to further study using polymers with different molecular weight. The present chapter describes their effect in the friction reduction for the Cu-Pb bearing and the Al-Si bearing.

6-1 Plain bearings used

The same plain bearings (Cu-Pb bearing and Al-Si bearing) as used for the experiments in the chapter 4 were used. Plain bearings of which outside diameter, width and thickness are respectively 56 mm, 26 mm and 1.5 mm are used. A Cu-Pb alloy bearing with an overlay and an Al-Si alloy bearing with no overlay, as representatives of the Cu alloy and Al alloy plain bearings of automobiles were evaluated for comparison. The bearing clearances of the Cu-Pb bearing and the Al-Si bearing were 40 and 37 μm , respectively. Tables 6-1 and 6-2 respectively show the ingredients of the Cu-Pb plain bearing and the Al-Si plain bearing.

Table 6-1 Ingredients of the Cu-Pb plain bearing (The same as Table 4-1)

| Ingredients of inner layer (%) | | | Ingredients of overlay (%) | | |
|--------------------------------|----|-----|----------------------------|----|----|
| Cu | Pb | Sn | Pb | Sn | In |
| Rem | 23 | 3.5 | Rem | 9 | 9 |

Table 6-2 Ingredients of the Al-Si plain bearing (The same as Table 4-2)

| Ingredients of bearing metal (%) | | | | |
|----------------------------------|----|-----|-----|-----|
| Al | Sn | Si | Cu | Pb |
| Rem | 12 | 2.5 | 0.7 | 1.7 |

6-2 Lubricant samples tested

Table 6-3 shows the kinematic viscosity, the density and the HTHS viscosity (high temperature high shear viscosity) of lubricants used. The kinematic viscosity at 40 and 100 °C was measured and that at 60 and 80 °C was calculated with the Mac Coull and Walther formula. In order to confirm the behavior of temporary viscosity loss as Newtonian fluids, the HTHS viscosity at 100 °C was measured using the TBS (Tapered Bearing Simulator) viscometer which was produced by Tannas Co. and enables to measure viscosity at a shear rate of $1 \cdot 10^6 \text{ s}^{-1}$. The TBS viscometer was designated for standard operation in ASTM 4683 and widely used for testing passenger car engine oils.

Bearing tests were carried out with a base oil and two kinds of oils containing polymers which molecular weight (Mw) were 25,000 and 370,000. The base oil used is polyalphalefin (PAO, Group IV base oil) of approximately $7 \text{ mm}^2 \cdot \text{s}^{-1}$ at 100 °C. The polymers used were polymethacrylate types of which monomers were the same. To make the polymer-containing oils, the polymers were mixed with a low viscosity base oil of PAO (approx. $4 \text{ mm}^2 \cdot \text{s}^{-1}$ at 100 °C) and their viscosity was initially adjusted to approximately $10 \text{ mm}^2 \cdot \text{s}^{-1}$ at 100 °C. After each bearing test, samples of the lubricants were taken from the oil tank and their kinematic viscosity, the density and the HTHS viscosity were measured. The measured kinematic viscosity and the density after the bearing test were used to calculate dynamic viscosity and subsequently a Hersey number.

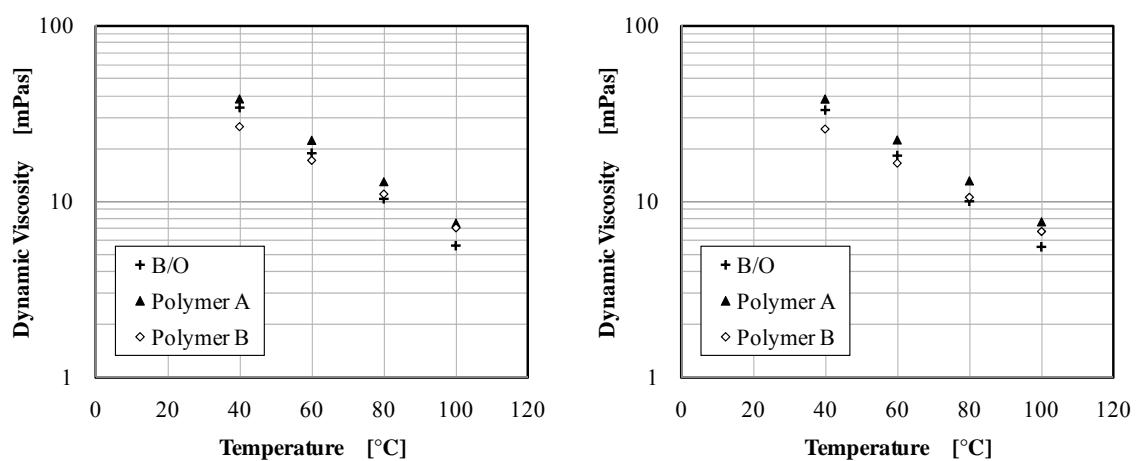
As seen in Table 6-3, the calculated dynamic viscosity for the base oil at 100 °C was almost equal to the HTHS viscosity measured with the TBS viscometer. On the other hand, the HTHS viscosity for polymer A and polymer B was lower than the calculated dynamic viscosity (the magnitude of the viscosity reduction at a high shear rate of $1 \cdot 10^6 \text{ s}^{-1}$ for polymer B was larger than that for polymer A). It was therefore confirmed that the polymer-containing oils

(polymer A and polymer B) used in this study showed the behavior of the temporary viscosity loss although the shear rate at which the HTHS viscosity was measured was only $1 \cdot 10^6 \text{ s}^{-1}$ at one temperature (100 °C).

Table 6-3 Typical properties of the lubricants tested

| Sample Name | | | B/O | | Polymer A | | Polymer B | |
|-------------------------|--------|-----------------------------------|----------------------|---------------------|-----------------------------|---------------------|------------------------------|---------------------|
| Remarks | | | base oil | | oil with polymer of Mw25000 | | oil with polymer of Mw370000 | |
| | | | after Cu- Pb bearing | after Al-Si bearing | after Cu- Pb bearing | after Al-Si bearing | after Cu- Pb bearing | after Al-Si bearing |
| Kinematic Viscosity | 40 °C | $\text{mm}^2 \cdot \text{s}^{-1}$ | 41.85 | 40.85 | 46.61 | 46.00 | 32.98 | 31.92 |
| | 60 °C | $\text{mm}^2 \cdot \text{s}^{-1}$ | 20.22 | 19.84 | 24.43 | 24.54 | 19.88 | 19.00 |
| | 80 °C | $\text{mm}^2 \cdot \text{s}^{-1}$ | 11.43 | 11.26 | 14.53 | 14.78 | 13.08 | 12.40 |
| | 100 °C | $\text{mm}^2 \cdot \text{s}^{-1}$ | 7.230 | 7.143 | 9.498 | 9.741 | 9.211 | 8.681 |
| Density | 15 °C | g/cm^3 | 0.832 | 0.832 | 0.842 | 0.842 | 0.829 | 0.829 |
| Calculated Dynamic Vis. | 100 °C | mPa·s | 5.64 | 5.56 | 7.50 | 7.67 | 7.13 | 6.72 |
| HTHS Vis. | 100 °C | mPa·s | 5.62 | 5.53 | 7.33 | 7.31 | 5.34 | 5.21 |

The dynamic viscosity calculated from the kinematic viscosity and the density is also shown in Figures 6-1 (a) and 6-1(b) for the Cu-Pb bearing and the Al-Si bearing tests, respectively. The dynamic viscosity of polymer A is the highest among the tested oil samples at the tested temperatures from 60 to 100 °C. Polymer B shows higher dynamic viscosity than the base oil at 100 °C as well as polymer A, but its dynamic viscosity becomes lower than the base oil at low temperatures (40 and 60 °C).



(a) Samples after the Cu-Pb bearing tests (b) Samples after the Al-Si bearing tests

Figure 6-1 Dynamic viscosity versus temperature of the lubricants tested

6-3 Test results with the Cu-Pb plain bearings under static load condition

Figures 6-2 to 6-4 show the friction coefficients and the contact resistance (CR) ratios between the shaft and the plain bearing for the Cu-Pb bearing at a feeding temperature of 100 °C under loads from 1 to 10 kN and shaft speeds of 500, 1,000, 2,000 and 3,000 rpm with the base oil and the polymer-containing oils (polymer A and polymer B), respectively (the Hersey number was calculated by using the back face temperature of the uppermost part of the bearing as the representative value). Although the bearing tests were also carried out at 60 and 80 °C, only the data at 100 °C, which is the most severe test condition were plotted in the figures.

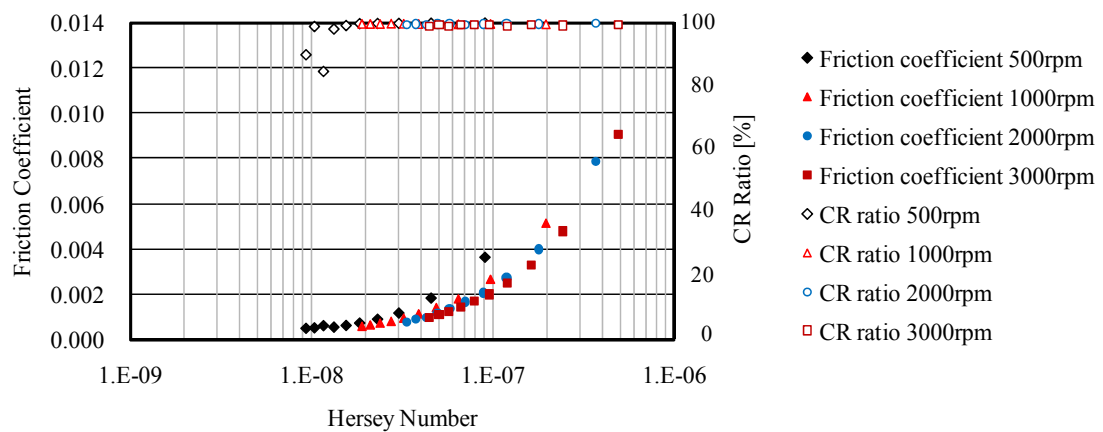


Figure 6-2 Friction coefficient and CR ratio vs. Hersey number at 100 °C for the base oil with the Cu-Pb bearing

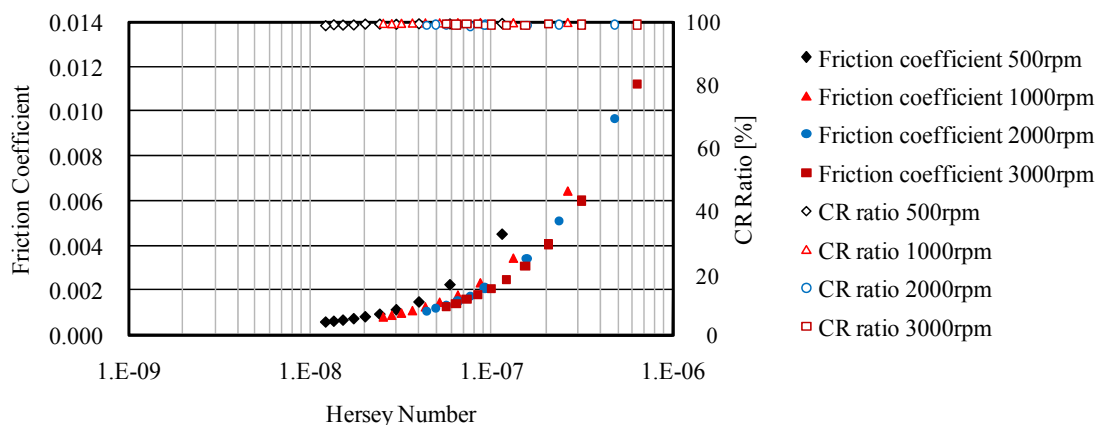


Figure 6-3 Friction coefficient and CR ratio vs. Hersey number at 100 °C for polymer A with the Cu-Pb bearing

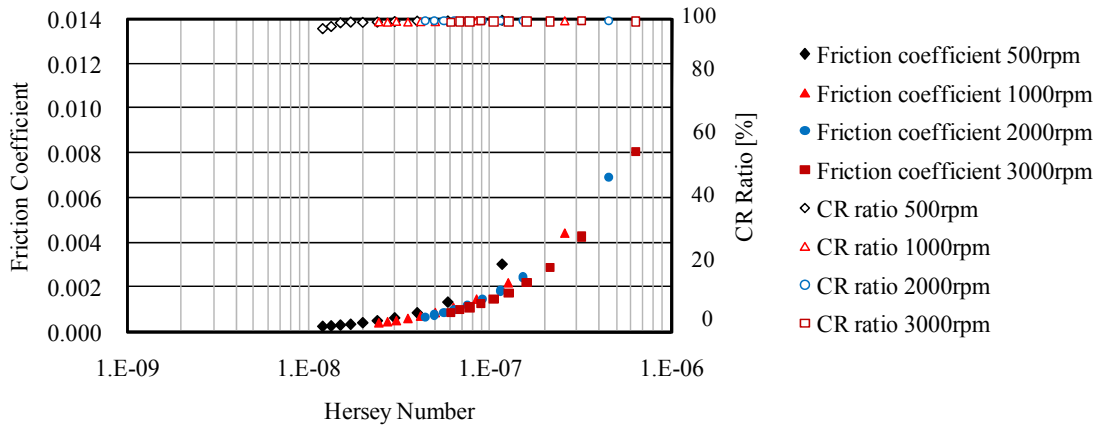


Figure 6-4 Friction coefficient and CR ratio vs. Hersey number at 100 °C for polymer B with the Cu-Pb bearing

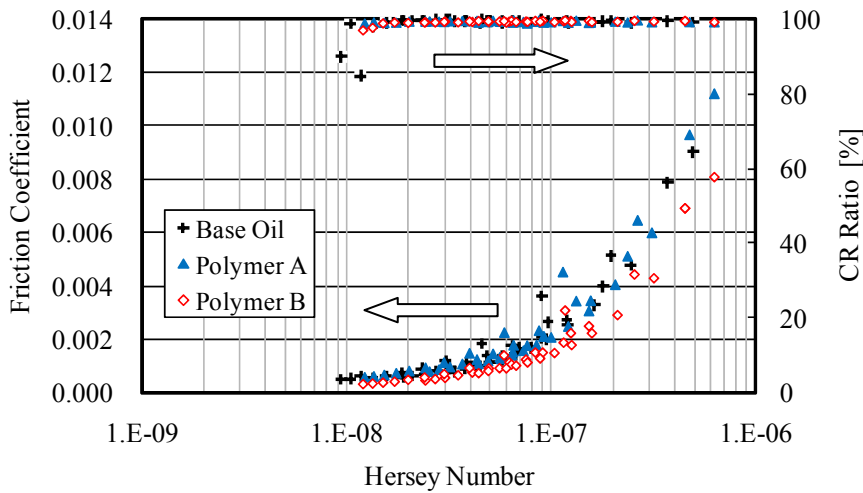


Figure 6-5 Comparison of friction coefficient and CR ratio vs. Hersey number at 100 °C with the Cu-Pb bearing

In order to readily compare the data, the friction coefficients and the CR ratios for all of the oil samples were also arranged in Figure 6-5. All of the bearing tests were successfully completed without any serious damage of the plain bearings. The CR ratios for the base oil in Figure 6-2 are likely to decrease in the vicinity of $1 \cdot 10^{-8}$ of a Hersey number. This was because its viscosity was lower than the polymer-containing oils and the bearing tests were carried out until a smaller Hersey number. In Figure 6-5, it was observed that the friction coefficients for polymer B were lower than those for the base oil and polymer A under an equal Hersey number. Normally, lower friction coefficients can be expected for polymer-containing oils due to a temporary viscosity loss by shear and it could affect the friction reduction for polymer B. On the other hand, the friction coefficients for polymer A were almost the same as those for the base oil even if polymer A contains polymer. It is conceivable that the temporary viscosity loss

for polymer A could be much smaller than that for polymer B in the actual bearing test as the results in the HTHS viscosity measurements.

6-4 Test results with the Al-Si plain bearings under static load condition

Figures 6-6 to 6-8 show the friction coefficients and the contact resistance (CR) ratios between the shaft and the plain bearing for the Al-Si bearing at a feeding temperature of 100 °C under loads from 1 to 10 kN and shaft speeds of 500, 1,000, 2,000 and 3,000 rpm with the base oil, polymer A and polymer B, respectively. The friction coefficients and the CR ratios were also arranged to compare each oil in Figure 6-9. All of the bearing tests were successfully completed without any serious damage of the plain bearings as well as the Cu-Pb plain bearing tests.

A significant difference in the friction coefficients between the base oil and the polymer-containing oils was hardly observed as shown in Figure 6-9. As mentioned above, viscosity for polymer-containing oils is normally reduced at a high shear rate but such effect did not greatly contribute the friction reduction in the Al-Si plain bearing. This is a different tendency from the results with the Cu-Pb plain bearing and suggests that the bearing materials may have affected the plain bearing performance.

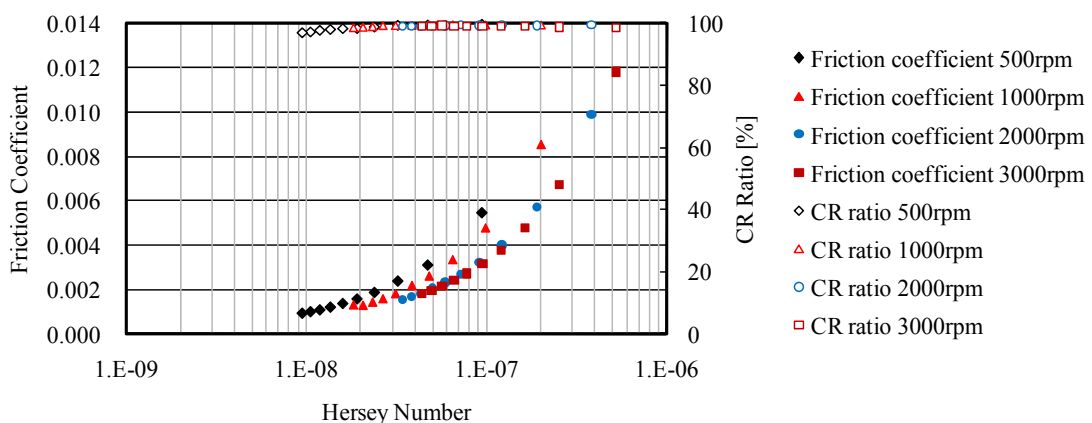


Figure 6-6 Friction coefficient and CR ratio vs. Hersey number at 100 °C for the base oil with the Al-Si bearing

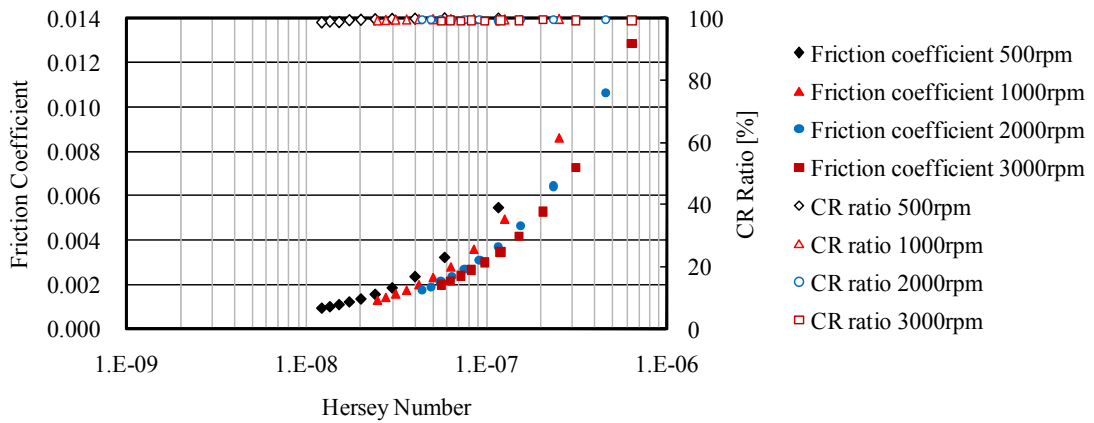


Figure 6-7 Friction coefficient and CR ratio vs. Hersey number at 100 °C for polymer A with the Al-Si bearing

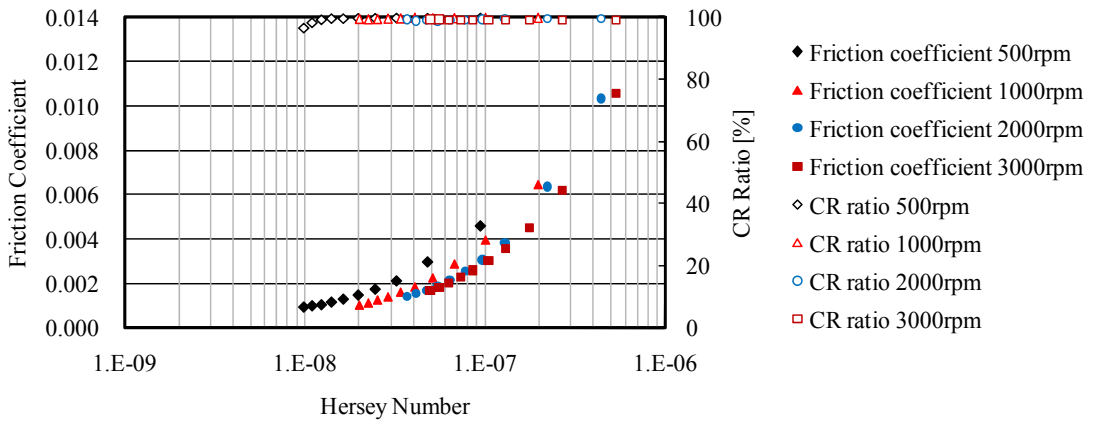


Figure 6-8 Friction coefficient and CR ratio vs. Hersey number at 100 °C for polymer B with the Al-Si bearing

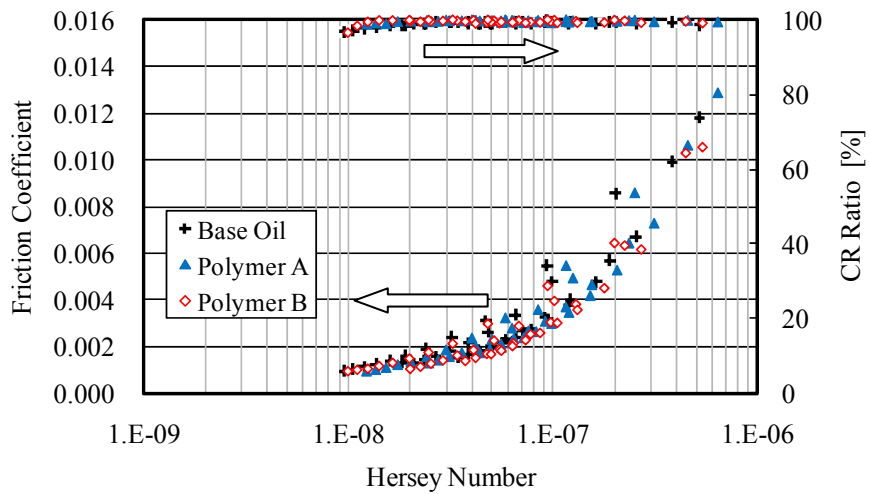


Figure 6-9 Comparison of friction coefficient with the Al-Si bearing

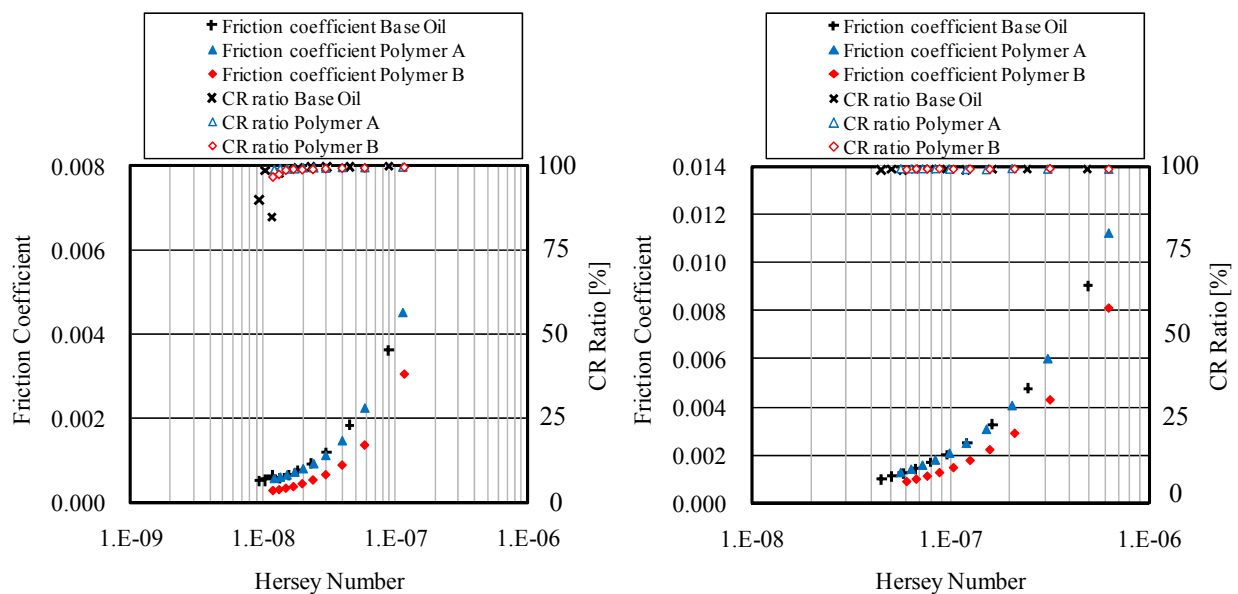
6-5 Discussion of the effect of polymer-containing oils under static load condition

In order to further discuss the effect of the polymers, the data of the friction coefficients and the CR ratios only for shaft speeds of 500 and 3,000 rpm and a feeding oil temperature of 100 °C were arranged for both of the Cu-Pb plain bearing and the Al-Si plain bearing in Figures 6-10 and 6-11. The relative shaft displacement at 100 °C for shaft speeds of 500 and 3,000 rpm was additionally shown in Figures 6-12 and 6-13 to discuss the behavior of the polymer-containing oils.

As shown in Figures 6-10(a) and 6-10(b), the friction coefficients for polymer B with the Cu-Pb plain bearing was apparently lower than those for the base oil and polymer A at shaft speeds of 500 and 3,000 rpm under an equal Hersey number. The order of the friction coefficients can be summarized as follows:

(High) Base oil, Polymer A > Polymer B (Low)

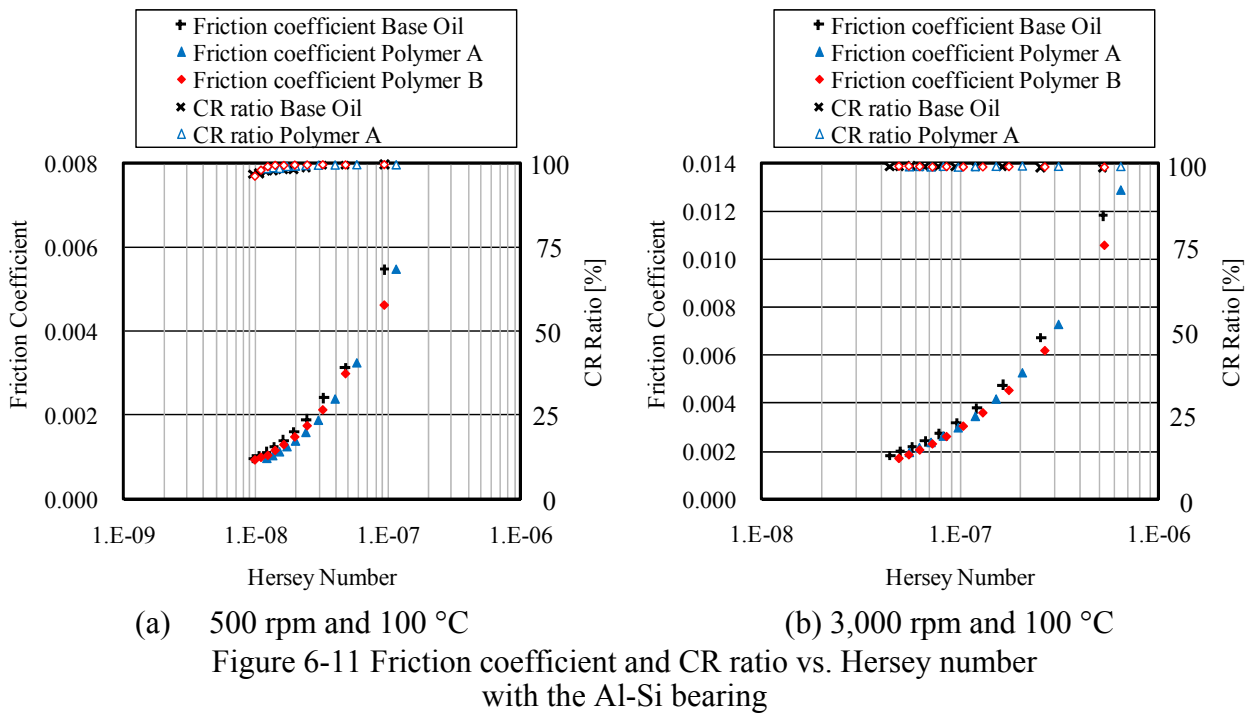
On the other hand, in Figure 6-11(b) for the Al-Si bearing the friction coefficients with the base and polymer A at 3,000 rpm were almost equal, and those with polymer B were placed slightly at a lower position than with the other oils in the small Hersey number range. However, the friction coefficients with polymer A became lower at a shaft speed of 500 rpm (Figure 6-11(a)) than with the base oil and polymer B. In fact, the ability to reduce the friction varies



(a) 500 rpm and 100 °C

(b) 3,000 rpm and 100 °C

Figure 6-10 Friction coefficient and CR ratio vs. Hersey number with the Cu-Pb bearing



at different shaft speeds. The order of the friction coefficients for the Al-Si bearing is the following:

(High) Base oil, Polymer B > Polymer A (Low) at 500 rpm
 (High) Base oil > Polymer A > Polymer B (Low) at 3,000 rpm

As the test results for the two bearing materials were discussed in the chapter 4, the difference in the friction coefficients was considered to be significant compared with the uncertainty of the measurements. The clearance difference between the two bearings should hardly affect the friction coefficients. The measurement of the bearing back-face temperature is appropriate to calculate the Hersey number. Therefore, it is conceivable that the effectiveness of the polymers depended on the bearing materials and the friction coefficients varied.

Figure 6-12(a) and 6-12(b) show the relative shaft displacement for the Cu-Pb bearing at a feeding oil temperature of 100 °C and shaft speeds of 500 rpm and 3,000 rpm, respectively. As shown in Figures 6-12(a), the relative shaft displacement in the horizontal axis is basically changing from negative values to positive values when the load is increased from 1 to 10 kN for all of the oils. The relative shaft displacement with the base oil in the horizontal axis is decreased under the high load conditions while a reduction of the CR ratios was observed in the small Hersey number as shown in Figure 6-10. In Figure 6-12(b), the relative shaft displacement at 3,000 rpm decreases downward with increase of a load.

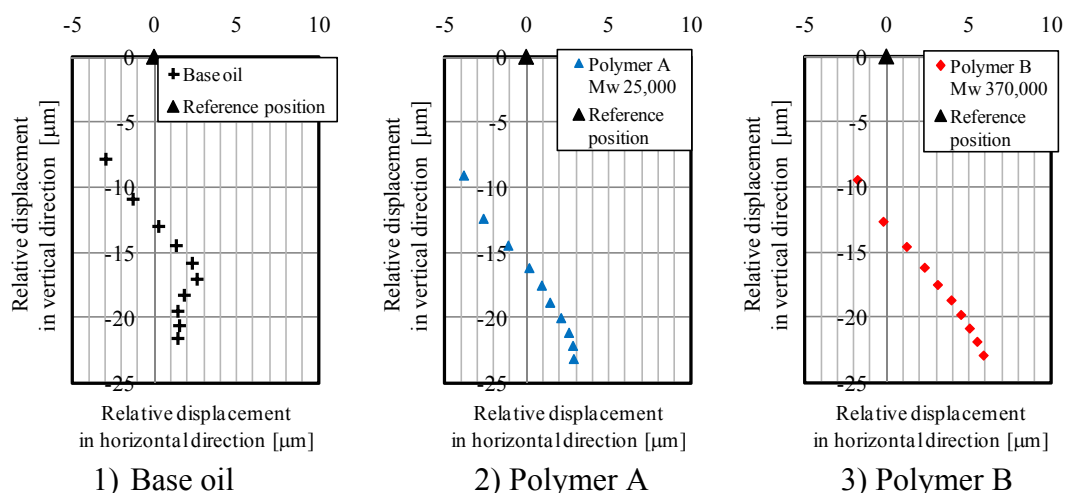


Figure 6-12(a) Relative shaft displacement with Cu-Pb bearing for 500 rpm and 100 °C

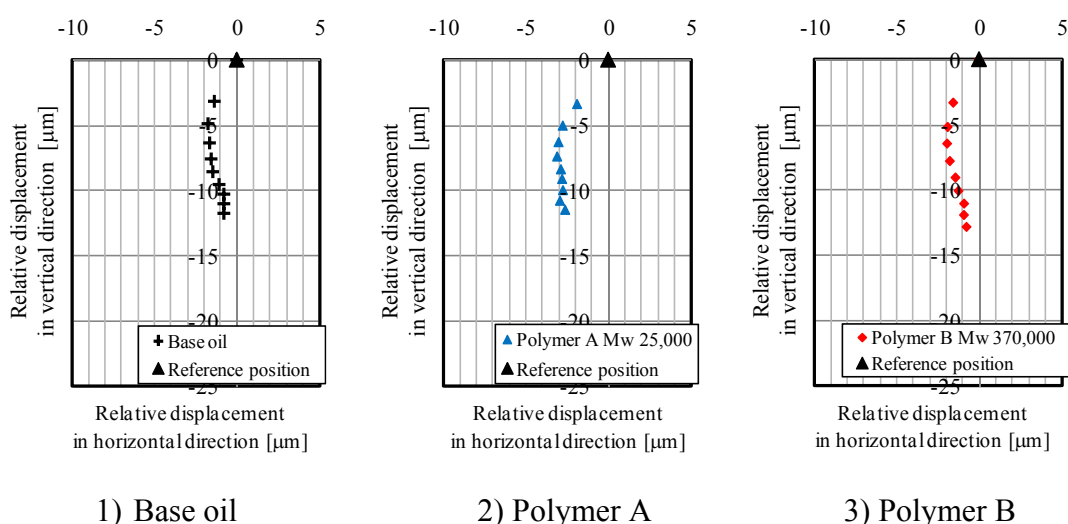


Figure 6-12(b) Relative shaft displacement with Cu-Pb bearing for 3,000 rpm and 100 °C

On the other hand, in case of the Al-Si bearing, the relative shaft displacement in the horizontal direction is negative for both 500 rpm and 3,000 rpm as shown in Figures 6-13(a) and 6-13(b). This is a different tendency from the results with the Cu-Pb bearing even if the same lubricants were used. It suggests that the difference of the bearing materials may have affected the effect of the polymers on the oil film formation.

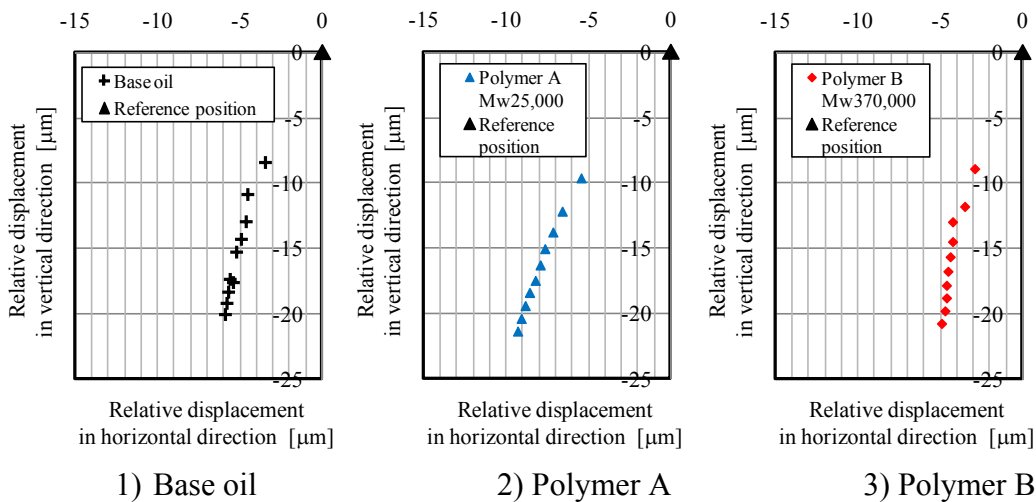


Figure 6-13(a) Relative shaft displacement with Ai-Si bearing for 500 rpm and 100 °C

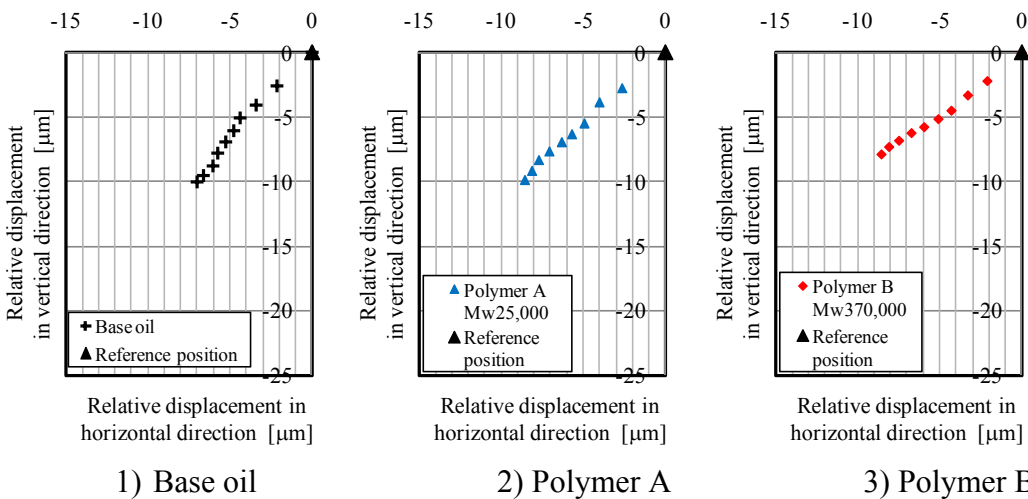


Figure 6-13(b) Relative shaft displacement with Ai-Si bearing for 3,000 rpm and 100 °C

Overall, a different behavior in the friction coefficients and the relative shaft displacement for the polymer-containing oils appeared between the two bearings. The viscosity loss was considered to affect the friction reduction for the Cu-Pb bearing but not for the Al-Si bearing in hydrodynamic lubrication region. Since the relative shaft displacement differed between the two bearings, the effectiveness of the polymers could depend on the bearing materials. However, the relative shaft displacement does not represent the actual oil film thickness. It was very difficult to discuss the behavior of the polymer-containing oils with the relationship between the viscosity loss and the oil film thickness.

Further investigation with the evaluation of rheological properties of oils will be therefore needed. It will be described in the chapter 7.

6-6 Test results with the Cu-Pb plain bearing and the Al-Si plain bearing under dynamic load condition

Figures 6-14 and 6-15 show the bearing torques and the CR ratios with the base oil and the polymer-containing oils for the Cu-Pb plain bearing at a shaft speed of 1,000 rpm in comparison with the results for the Al-Si plain bearing. While the results at 80 °C were plotted for the base oil, those at 100 °C were plotted for the polymer-containing oils because the dynamic viscosity of the base oil at 100 °C was lower than that of the polymer-containing oils.

In Figure 6-14 for the Cu-Pb bearing, no reduction of the CR ratios for the base oil and the polymer-containing oils was observed. The friction coefficients for polymer B were lower than those for the base oil and polymer A. The same tendency was observed under the dynamic load condition with the Cu-Pb bearing as the static load condition.

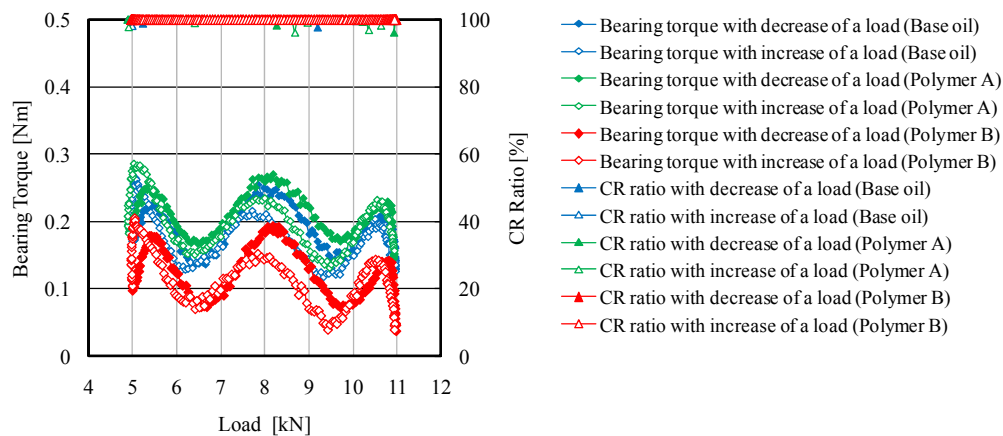


Figure 6-14 Bearing torque and CR ratio for the base oil (80°C) and the polymer-containing oils (100 °C) at 1,000 rpm with the Cu-Pb bearing under dynamic load condition

In Figure 6-15, for the Al-Si bearing, a slight reduction of the CR ratios was observed with the base oils although its magnitude was 20 % which was considered to be relatively small. This suggests that the ability to form the oil film can be worse for the base oil than the other polymer-containing oils under the dynamic load condition. Polymer B showed much lower bearing torques than the base oil and polymer A unlike the results under the static load condition. In addition to the fact that the dynamic viscosity of polymer A at 100 °C is slightly lower than that of the base oil at 80 °C and polymer B at 100 °C, it is also conceivable that the temporary viscosity loss could occur with polymer B under the dynamic load conditions.

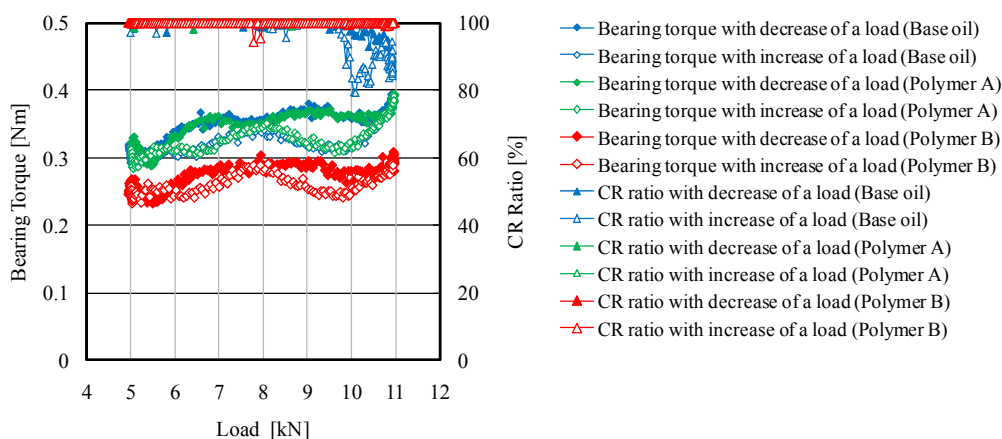


Figure 6-15 Bearing torque and CR ratio for the base oil (80°C) and the polymer-containing oils (100 °C) at 1,000 rpm with the Al-Si bearing under dynamic load condition

6-7 Conclusions

The investigation of the effect of the polymer-containing oils was examined using the two polymers of which molecular weight was 25,000 and 370,000 compared with the base oil. The conclusions are the following:

- (1) The oil containing polymer of high molecular weight (polymer B) showed lower friction coefficients than the base oil and the oil with low molecular weight polymer for the Cu-Pb plain bearing under an equal Hersey number in hydrodynamic lubrication region but did not for the Al-Si plain bearing. The effect of the polymer-containing oils on the bearing performance was different between the two bearings. However, further study is required to ensure the theory of the effect of the bearing material.
- (2) The finding in this chapter suggests the necessity of polymer selection taking into account the bearing materials as well as the other lubricants components such as base oils and friction modifiers.

In order to investigate the behavior of the polymer-containing oils, the analysis was not sufficient because of the limited results only from the plain bearing tests. It is therefore necessary that further investigation will be made comparing the plain bearing performance with

other rheological properties of polymers. The analysis of the behavior of polymer-containing oils is described further in the chapter 7.

Chapter 7

Experiments and numerical analysis of bearing lubrication with polymer-containing oils, investigation of the mechanism of their action

It was suggested in the study of the chapter 6 that the oil film formation of non-Newtonian fluids (polymer-containing oils) could differ from that of Newtonian fluids, and it could affect the friction characteristics and the reliability of plain bearings.

In order to further investigate more deeply the effect of polymer-containing oils in plain bearing performance, additional experiments were carried out using a plain bearing test apparatus owned by the Poitiers University as collaboration among the Poitiers University, CNRS and Idemitsu Kosan Co., Ltd. Although the plain bearings used were different from automotive bearings, the test apparatus enabled to measure the bearing pressure distribution and the fluid film temperature distribution in addition to the frictional bearing torque and the shaft displacement. In the automotive plain bearing apparatus used in the previous chapters, it was not possible to measure the bearing pressure distribution and the fluid film temperature because of the difficulty of sensor installation. If the behavior of polymer-containing oils as non-Newtonian fluids is different from that of Newtonian fluids, a difference should appear even in the bearing pressure. Also, the fluid film temperature should provide a better estimate for the viscosity calculation. It was necessary to select another bearing test apparatus in order to observe the behavior of polymer-containing oils.

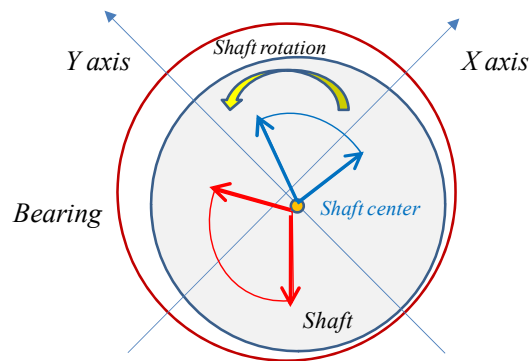
The oil film formation was discussed only with the relative shaft displacement obtained from the bearing tests in the chapter 6. However, it was not sufficient to justify the actual influence of polymer-containing oils on the oil film thickness even if the friction reduction was confirmed. Therefore, in this chapter the behavior of polymer-containing oils (non-Newtonian fluids) was analyzed comparing the experiments and simulation (numerical analysis) of plain bearing performance.

In addition, the evaluation of the rheological properties such as viscosity and normal stress at high shear rates was not sufficiently performed even if they are considered to affect the bearing performance. Only the viscosity at 150 °C and a shear rate of $6 \cdot 10^6 \text{ s}^{-1}$ was measured in the chapter 6. However, in order to discuss the relationship between the rheological properties and the bearing performance, the viscosity and the normal stress at various share rates and temperatures are measured using a rheometer manufactured in the laboratory in this chapter.

It is well known that the temporary viscosity loss of oils at a high shear rate contributes to improve the frictional property of plain bearings. Also, there are publications concerning the investigation of the effect of normal stress [18, 25, 43, 45, 46]. However, all of such research activities mostly state the correlation between the normal stress and the bearing load-carrying capacity, which means the reliability in bearing lubrication. Therefore, we decided to investigate the effect of polymer in the bearing performance in relation to the temporary viscosity loss and the normal stress.

Figure 7-1 shows an illustration which indicates the estimated shaft displacement due to the temporary viscosity loss and normal stress (first normal stress) generation in non-Newtonian fluids. First normal stress is defined as the component of stress at right angle to the applied shear stress (the direction to the shaft center in case of journal bearing lubrication). In fact, in the area of small gap between a shaft and a bearing, especially in the active zone of a bearing, the value of the first normal stress is considered to be large because of a high shear rate. Therefore, the first normal stress can contribute to move the shaft towards the positive direction in the X axis. On the other hand, if the viscosity is reduced at a high shear rate, the shaft can mostly move towards the negative direction in the X axis.

If the normal stress increases oil film thickness, the frictional property for polymer-containing oils should also vary because the increase of the oil film thickness can cause a reduction of shear rate and consequently affect the temporary viscosity loss. If the viscosity is decreased at a high shear rate, it can cause a further increase of shear rate and subsequently affect the normal stress. It is then conceivable that the friction reduction and the reliability in the bearing lubrication can depend on the balance of the temporary viscosity loss and the normal stress.



- Displacement direction due to oil viscosity reduction
- Displacement direction due to first normal stress generation

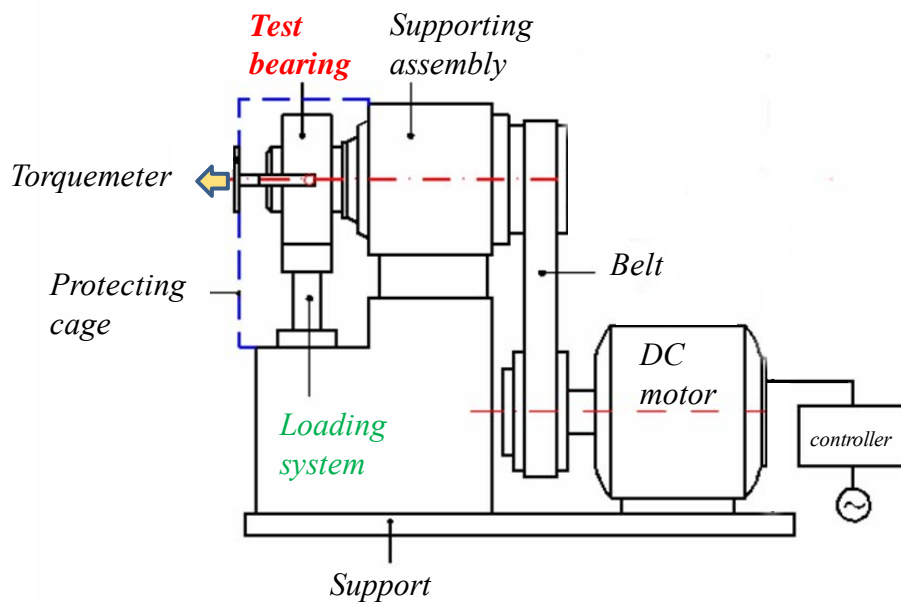
Figure 7-1 Estimated shaft displacement due to temporary viscosity loss and first normal stress generation

In this chapter, the measurement of the viscosity and the first normal stress at high shear rates and the analysis of the plain bearing performance compared to rheological properties of the lubricant are described in addition to the analysis using the simulation.

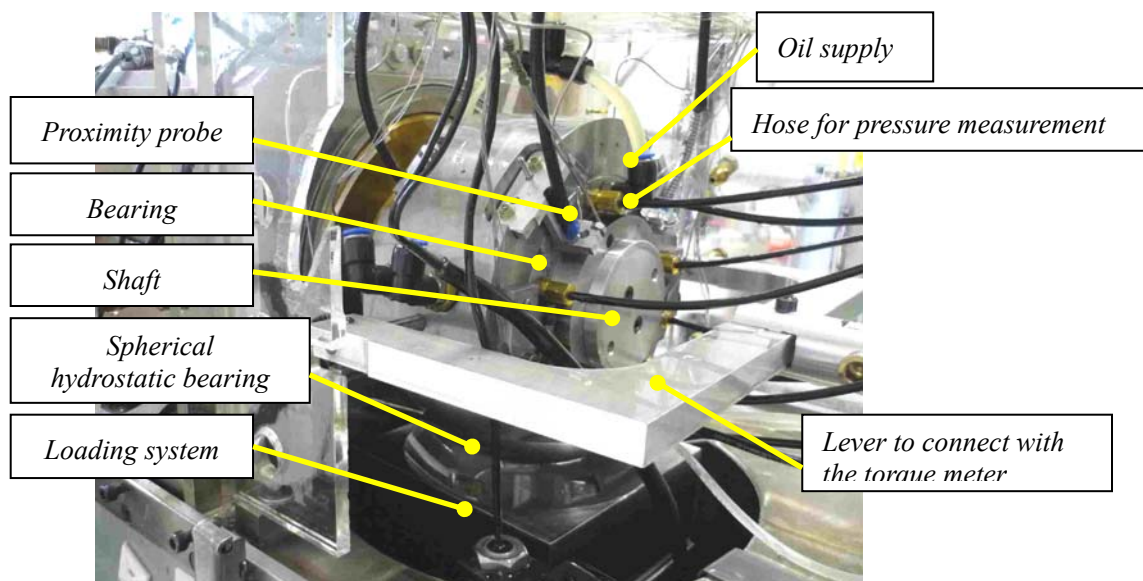
7-1 Plain bearing test

7-1-1 Plain bearing test apparatus

A schematic representation of the plain bearing test apparatus used is shown in Figure 7-2(a). It was originally designed in 1980 by Ferron et al. in the Laboratory of Solid Mechanics of the Poitiers University [62]. Figure 7-2(b) shows a picture of the main portion of the device.



(a) Schematic representation of the bearing test apparatus



(b) Main portion of bearing test apparatus

Figure 7-2 Bearing test apparatus at the Poitiers University

The shaft made of steel is driven by an electric motor of 21 kW connected to an electronic controller. The shaft speed was controlled with an accuracy of ± 10 rpm. The loading system is a pneumatic cylinder connected to a pressure gauge. The load is applied to the bearing housing along the vertical direction without friction by using a static hydraulic pressure with the same fluid as the tested oil. The feeding oil pressure is maintained at 0.13 MPa. The feeding oil temperature is also controlled with a type K thermocouple located upstream of the oil supply groove and maintained at a tested temperature. Friction torque of the plain bearing is measured using a torquemeter through the lever that was set on the bearing housing with a variation of ± 0.01 Nm. The relative shaft position inside the bearing is determined by sensors located at ± 45 degrees in reference to the load direction.

Plain bearings used are shown in Figures 7-3 and 7-4. They are not automotive plain bearings but bearings with several materials were used in order to evaluate the plain bearing performance with different lubricants in detail. Those bearing materials are also different from the ones used in the previous chapters. The results obtained in this chapter are therefore compared with those in the chapter 6 in the later paragraph to confirm if they are applied to automotive bearing lubrication. Figure 7-3 and 7-4 respectively show the Babbitted bearing and the bronze bearing used.

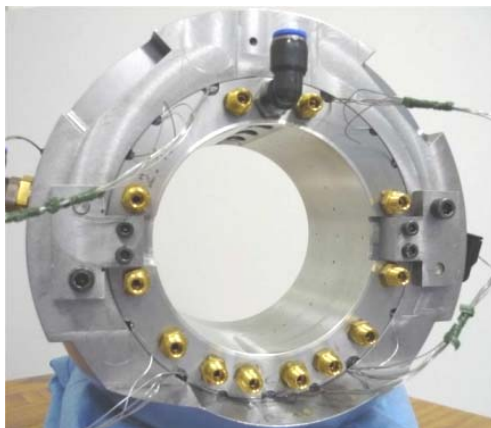


Figure 7-3 Babbitted bearing



Figure 7-4 Bronze bearing

Table 7-1 shows the plain bearings dimensions, which were measured at room temperature. The radial bearing clearances slightly varied because of a difference in the bearing diameter although they were within the manufacturing specification of 85 to 95 μm .

Table 7-1 Characteristics of the plain bearings

| | | Babbitted | Bronze | Bronze with an lead-based overlay |
|----------------------------------|---------------|-----------|---------|-----------------------------------|
| Bearing diameter (D) | mm | 100.016 | 100.034 | 100.016 |
| Bearing length (B) | mm | 80 | | |
| Shaft diameter (D _s) | mm | 99.844 | | |
| Radial clearance at 20 °C | μm | 86 | 95 | 86 |

7-1-2 Measurement items of plain bearing performance and test conditions

Figure 7-5 shows positions where temperatures, pressures and gaps between the shaft and the bearing were measured. Temperatures were measured at twenty nine positions. Installed thermocouples of type K gave the internal bearing surface temperatures (they are in contact with the fluid film). Fifteen thermocouples were mounted in the mid plane of the bearing and the other fourteen thermocouples were mounted in seven different axial directions. The feeding oil temperature was measured with a thermocouple of type K, and was controlled with a variation of ± 0.5 °C of the setting temperature. Hydrodynamic pressure was measured with pressure transducers connected to a set of eleven holes (diameter of 1 mm) drilled in the mid-plane of the plain bearing. The uncertainty of the pressure measurements were ± 2 percent.

Four proximity probes were installed at the positions of X and Y axis on both sides of the bearing with aluminum supports to measure the displacement of the bushing relatively to the shaft. As mentioned above, they are located at ± 45 degrees in reference to the load direction. Two of them were placed in the front section of the plain bearing whereas the two others sit in the back section. An average value calculated from the data of the front and back gap sensors was used in order to determine a relative shaft displacement. In fact, the bearing diameter, the shaft diameter and the length of the aluminum supports are increased due to the thermal expansion in the bearing test operation. Therefore, the relative shaft displacement between the bearing and the shaft was compensated by calculating the deformation of each part. In order to calculate the deformation of the bearing and the aluminum supports, their temperatures which were actually measured with thermocouples were used. The thermal expansion coefficients used for the Babbitted bearing, the bronze bearings and the aluminum supports were $12 \cdot 10^{-6}$, $18 \cdot 10^{-6}$ and $23 \cdot 10^{-6} \text{ K}^{-1}$, respectively.

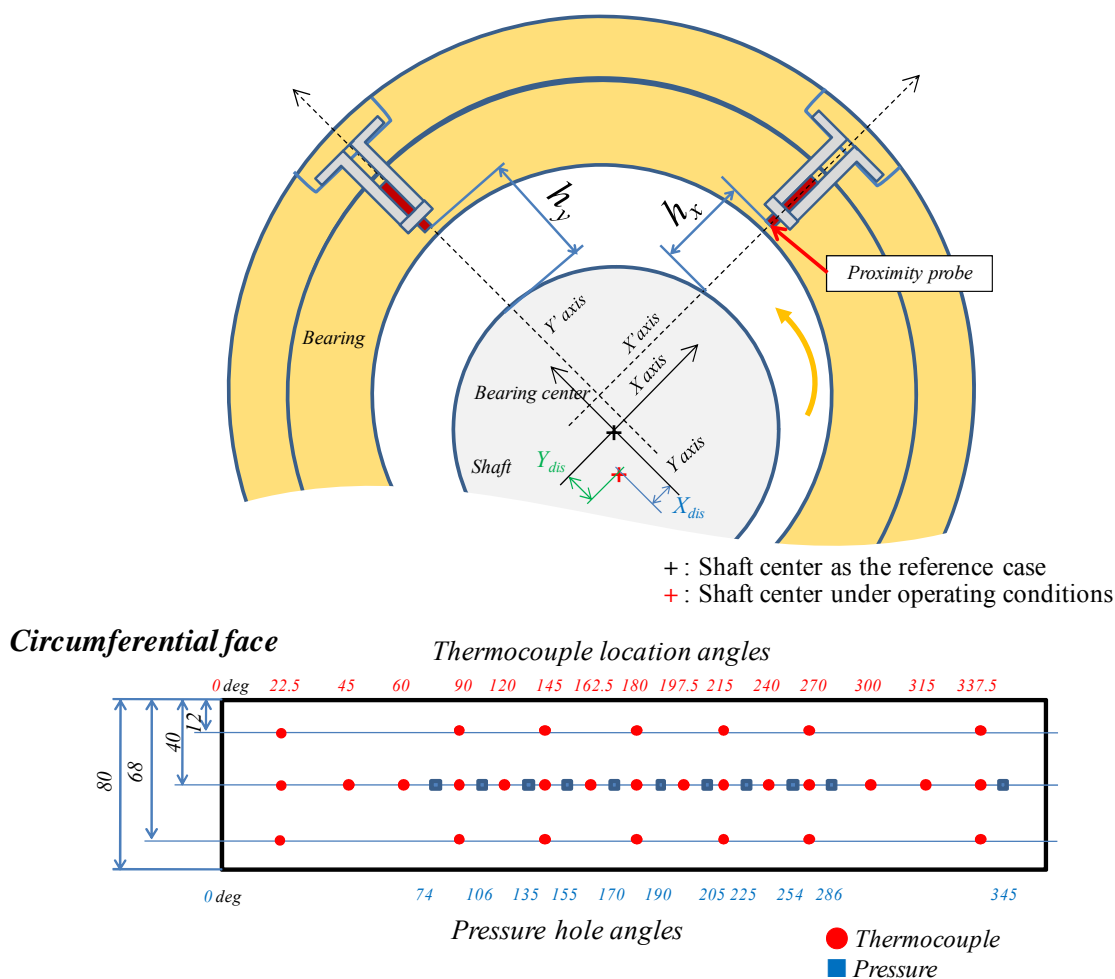


Figure 7-5 Location of thermocouples, pressure holes and gap sensors

The relative shaft displacement (X_{dis} , Y_{dis}) in the X and Y axes were calculated with the following formulas:

$$X_{dis} = h_{x\ ref} - h_x - (d_{x\ alm} - d_{x\ brg})$$

$$Y_{dis} = h_{y\ ref} - h_y - (d_{y\ alm} - d_{y\ brg})$$

where the terms $h_{x\ ref}$ and $h_{y\ ref}$ are the gaps between the shaft and the bearing in the X and Y axes as the reference case under the condition of 2,000 rpm and 0.8 kN. This case has been chosen because the shaft is placed at a relatively “centered” position. The terms h_x and h_y are those under operating conditions. The terms $d_{x\ alm}$ and $d_{y\ alm}$ are the deformation of the aluminum supports, and the terms $d_{x\ brg}$ and $d_{y\ brg}$ are of the plain bearing inside diameter in the X and Y axes.

Table 7-2 shows test conditions of the plain bearing test. Bearing tests were performed at 1,000 and 500 rpm under loads of 0.8 to 9.0 kN and three feeding oil temperatures of 40, 60

and 80 °C. In fact, low shaft speed, high load and high temperature conditions were needed so that the tests could be carried out under very severe operating conditions and the oil film thickness was likely to be very thin because the evaluation of the reliability in addition to the friction was very important (a bearing test for 2,000 rpm and 0.8 kN was also carried out at each feeding oil temperature as a reference case in order to calculate the relative shaft displacement).

Table 7-2 Plain bearing test conditions

| Feeding oil temp. °C | Shaft speed rpm | Load N |
|-------------------------|--------------------|-----------|
| 40 & 80 | 2000 | 800 |
| | 500 & 1000 | 7200 |
| | | 9000 |
| 60 | 2000 | 800 |
| | 500 & 1000 | 800 |
| | | 1720 |
| | | 3600 |
| | | 7200 |
| | | 9000 |

7-1-3 Plain bearing test procedure

Figure 7-6 shows the bearing test pattern. Oil circulation is started and oil temperature is increased until sufficient fluidity was obtained without the shaft rotation. A low static load of 0.8 kN is applied by the loading system with a pneumatic cylinder. Rotation of the shaft is started and maintained at 2,000 rpm under a load of 0.8 kN for more than two hours in order to increase the feeding oil temperature to a tested temperature and homogenize the test apparatus. After the shaft rotation is stopped and the zero position of the torque meter is adjusted, the rotation is resumed at 2,000 rpm.

Measurements of the friction torque, the temperature distribution, the pressure distribution and the shaft displacement are taken at a shaft speed of 2,000 rpm under a load of 0.8 kN as a reference case. In case of a feeding oil temperature of 60 °C, the shaft speed is changed to 1,000 rpm and maintained until the data is homogenized. After measurement is taken again, the static load is increased to 1.72, 3.6, 7.2 and 9.0 kN measuring the homogenized data at each loading condition (in case of 40 and 80 °C, measurements are taken only for 7.2 and 9.0 kN). After completion of all the measurements, the load is decreased to 0.8kN and the shaft rotation is changed to 2,000 rpm in order to reconfirm the reference data.

The bearing test apparatus was basically operated under hydrodynamic lubrication even for

a very severe operating condition to avoid serious damage of the bearings.

Labview system was used for the data acquisition. All of the converted data with an A/D converter are transferred to a personal computer every 100 ms for 2 minutes, and are then averaged.

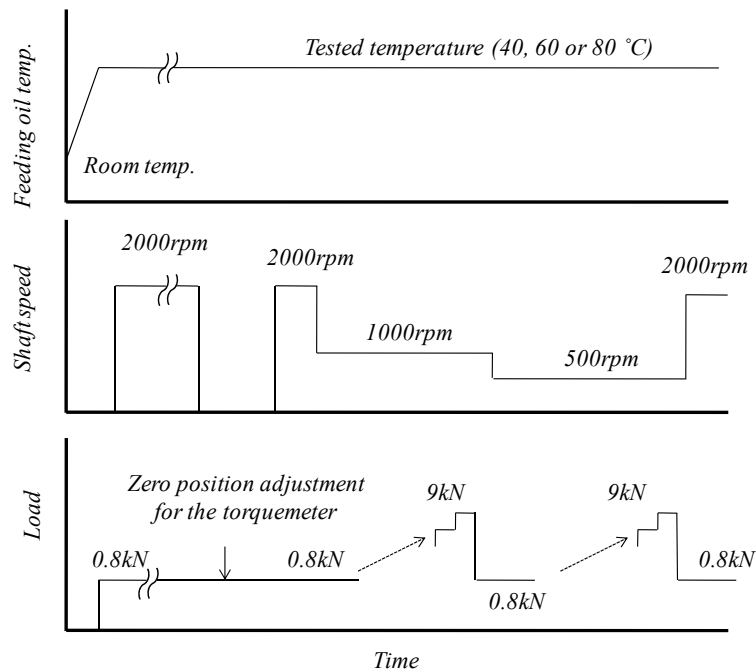


Figure 7-6 Bearing test pattern

7-1-4 Typical property of lubricants used in the bearing tests

Table 7-3 shows the typical properties of lubricants tested. The kinematic viscosity at 40 and 80 °C was measured and that at 60 °C was calculated with the Mac Coull and Walther formula.

Bearing tests were carried out with a base oil and three kinds of polymer (polymethacrylate)-containing oils. The polymers used consist of the same monomer but their molecular weight (Mw) was different (Mw=25,000, 190,000 and 370,000). The polymers of which Mw is 25,000 and 370,000 were the same as used for the plain bearing tests presented in the chapter 6. The base oil used was polyalphaplefin (PAO) with kinematic viscosity of $6 \text{ mm}^2 \cdot \text{s}^{-1}$ at 100 °C. To make the polymer-containing oils, the polymers were mixed with lower viscosity base oils (PAOs of 2 and $4 \text{ mm}^2 \cdot \text{s}^{-1}$ at 100 °C with the same mixture ratio) and their viscosity was initially adjusted to approximately $9 \text{ mm}^2 \cdot \text{s}^{-1}$ at 80 °C. After each bearing test, a sample of the lubricant was taken from the oil tank and its kinematic viscosity and density were measured as shown in Table 7-3. The viscosity of PMA3 became less than $8 \text{ mm}^2 \cdot \text{s}^{-1}$ at 80 °C. Then, a reduction of the viscosity for PMA3 which contains the highest

molecular weight polymer was observed after the bearing test. This may be because a part of the long polymer chains was broken during the plain bearing tests. Dynamic viscosity calculated from the kinematic viscosity and the density is also shown in Figure 7-7 for the bronze bearing tests as an example to present the viscometric properties of each oils. The viscosity difference in each lubricant becomes larger at low temperatures than at 80 °C.

Table 7-3 Typical property of the lubricants for the bearing tests

| Sample Name | | | B/O | | PMA1 | |
|---------------------|-------|----------------------------------|-------------------|----------------|-----------------------------|----------------|
| Remarks | | | base oil | | oil with polymer of Mw25000 | |
| | | | Babbitted bearing | bronze bearing | Babbitted bearing | bronze bearing |
| Kinematic Viscosity | 40 °C | mm ² ·s ⁻¹ | 27.72 | 29.19 | 22.32 | 22.25 |
| | 60 °C | mm ² ·s ⁻¹ | 14.48 | 15.16 | 13.30 | 13.24 |
| | 80 °C | mm ² ·s ⁻¹ | 8.669 | 9.028 | 8.721 | 8.670 |
| Density | 40°C | g/cm ³ | 0.809 | 0.810 | 0.814 | 0.814 |

| Sample Name | | | PMA2 | | PMA3 | |
|---------------------|-------|----------------------------------|------------------------------|----------------|------------------------------|----------------|
| Remarks | | | oil with polymer of Mw190000 | | oil with polymer of Mw370000 | |
| | | | Babbitted bearing | bronze bearing | Babbitted bearing | bronze bearing |
| Kinematic Viscosity | 40 °C | mm ² ·s ⁻¹ | 20.67 | 20.90 | 17.05 | 16.71 |
| | 60 °C | mm ² ·s ⁻¹ | 13.36 | 13.52 | 11.06 | 10.80 |
| | 80 °C | mm ² ·s ⁻¹ | 9.286 | 9.404 | 7.728 | 7.520 |
| Density | 40°C | g/cm ³ | 0.803 | 0.803 | 0.800 | 0.800 |

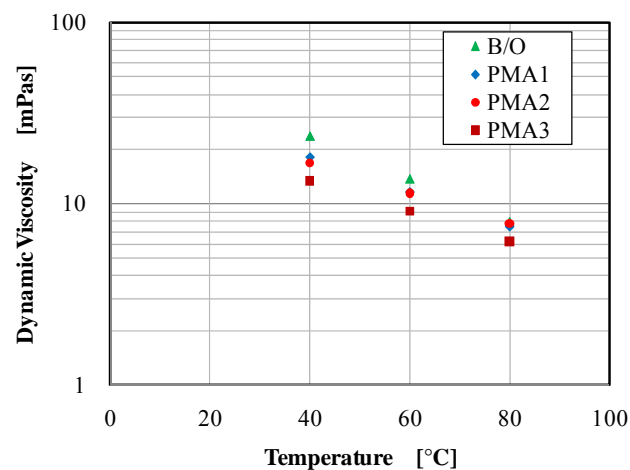


Figure 7-7 Dynamic viscosity of the lubricants used for the bronze bearing test

7-2 Measurement of rheological property for the polymer-containing oils

In order to discuss the effect of the polymer-containing oils in the plain bearing performance compared with the oil rheology, viscosity and normal stress were measured at various shear rates.

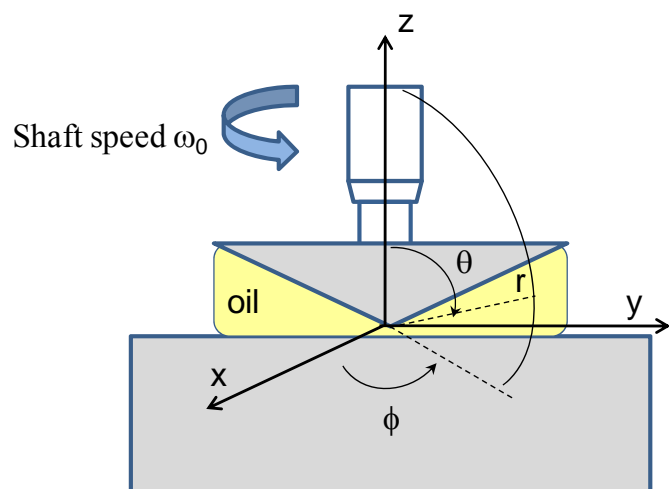
Rotational type rheometers are commonly used for the measurement of rheological properties but are not suitable at high shear rates because oils are likely to disperse due to centrifugal force of a rotor in a high shear rate range. Therefore, the measurements were made with a commercially available rotational type rheometer in a low shear rate range. In addition, manufacture of a slit die type rheometer was also examined to measure high-shear viscosity and normal stress in a high shear rate range. Research activities on the successful measurement of rheological properties with slit die rheometers can be found in the literatures [71-75]. Therefore, the measurement with a slit die type rheometer was determined. In this paragraph, the measurement methods and the results are described.

7-2-1 Rheometer for measurement in a low shear rate range

Figure 7-8(a) shows the rotational type rheometer (Gemini 150 made by Marvern), which is owned by the laboratory at LEA (Laboratoire d'Etudes Aérodynamiques) of the Poitiers University. A diagram to define co-ordinates of the cone geometry is indicated in Figure 7-8(b). The diameter and angle of the cone geometry used were 40 mm and 4 degrees, respectively.



(a) Photograph of the rheometer



(b) Diagram of co-ordinates

Figure 7-8 Rotational (Cone and plate) type rheometer

A small amount of oil is applied between the cone and the plate. Temperature of the oil is controlled using the Peltier system equipped under the plate, and the flow of a mixture of glycol and water is provided to dissipate the heat generated from the Peltier system.

Measurements were made at shear rates up to 200, 500, and 1,000 s⁻¹ for 80, 60 and 40 °C, respectively. For the measurements of viscosity, rotational torque is detected with a sensor which is attached in the upper part of the cone geometry; the values of the viscosity are then calculated with the following formulas:

$$\text{Shear stress factor } C1 = 3/(2 \pi r^3)$$

$$\text{Shear rate factor } C2 = 1/\text{cone angle}$$

$$\text{Shear stress } \sigma = C1 \times T \text{ (Torque)}$$

$$\text{Shear rate } \dot{\gamma} = C2 \times \omega_0 \text{ (Angular velocity)}$$

$$\text{Viscosity} = \sigma / \dot{\gamma}$$

The first normal stress difference N1, which is considered to affect the bearing performance, is defined as the following:

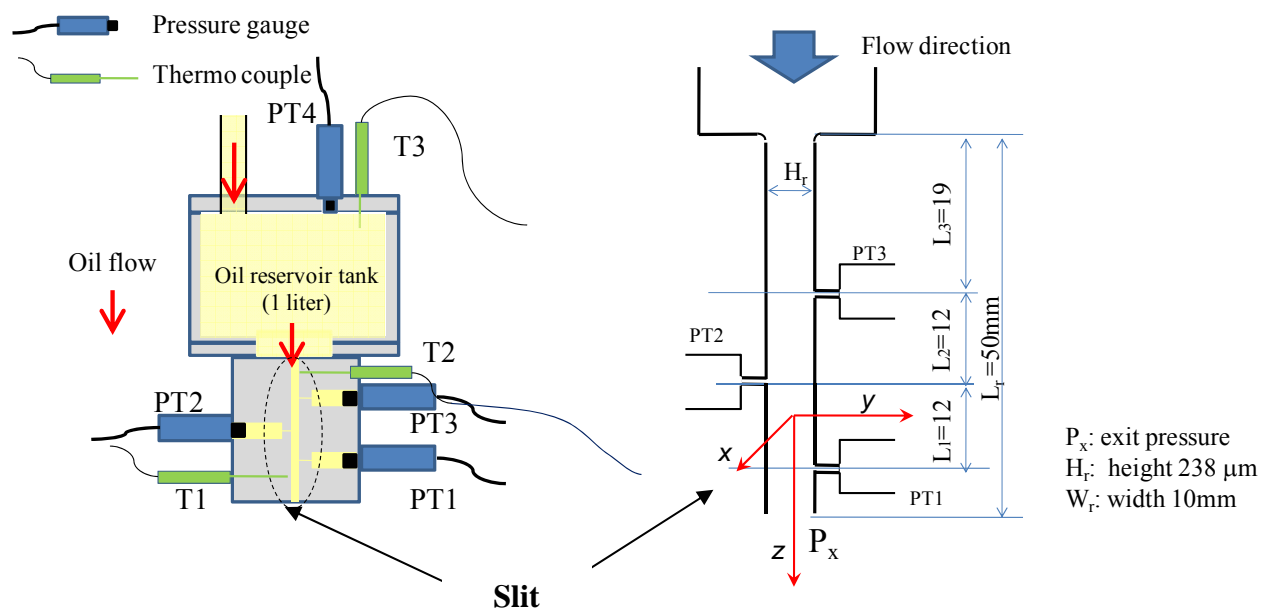
$$N1 = \sigma_{zz} - \sigma_{\varphi\varphi}$$

$\sigma_{\varphi\varphi}$ and σ_{zz} are the stresses along the flow direction and the flow gradient direction, respectively. In fact, $\sigma_{\varphi\varphi}$ is considered to be very small compared with σ_{zz} and almost negligible. The force along the vertical direction is detected with a sensor in the rheometer and is converted to the first normal stress.

7-2-2 Rheometer for measurement in a high shear rate range

Figure 7-9 shows a schematic of the slit die designed for this study. The die was made from two rectangular blocks of steel bolted together. The slit height (H_r), length (L_r) and width (W_r) were 238 μm , 50 mm and 10 mm, respectively. The existing hydraulic system with which the test fluids were supplied to the slit die rheometer was used. The capacity of the oil tank is 80 liters and a test fluid of 60 liters was prepared for each lubricant. The oil was supplied by a hydraulic pump in a pressure range between 0.5 and 1.7 MPa so that sufficient shear rates can be given to the oils. The supply oil pressure was controlled with a relief valve mounted in the hydraulic system (the existing hydraulic system at the Poitiers University was used and the upper limit of the pressure was 1.7 MPa).

When the pressure varies from 0.5 to 1.7 MPa, the shear rate becomes approximately $6 \cdot 10^4$ to $6 \cdot 10^5 \text{ s}^{-1}$ for the oils used. In fact, if the height of the designed slit was larger than the original design, the oil flow would be faster and even a higher shear rate could be applied to the oils. However, in order to maintain the laminar flow in the slit, a height of $250 \mu\text{m}$ was finally determined, and the slit die was actually manufactured with a slit height of $238 \mu\text{m}$. The Reynolds number being approximately 1,000 at 1.7 MPa for the oil of the lowest viscosity, the laminar condition for the flow has been ensured.



(a) Structure of the rheometer (b) Dimension of the slit and diagram of co-ordinates
Figure 7-9 Schematic of the slit die rheometer

Three pressure transducers (PT1, PT2, PT3) were mounted with the slit die wall through holes of 0.5 mm diameter. The fourth pressure transducer (PT4) was mounted at the top of the reservoir tank attached on the slit die. Transducers of which pressure range of 0 to 0.3 and 0.7 MPa were used for PT1 and PT2, respectively. Transducers of 0.7 and 3.5 MPa were used in PT3 for the supply pressure of less than 1.1 MPa and over 1.4, respectively. The pressure range of 3.5 MPa was used for PT4. In order to remove air bubbles in the ducts which were connected to the pressure transducers, open valves were attached to each duct. The uncertainties for the low pressure transducer of 0.3 MPa was $\pm 0.3 \%$, and the transducers were calibrated using another manometer. The transducers of 0.7 MPa and 3.5 MPa have the uncertainties of $\pm 2\%$, and were calibrated using other manometers. Figure 7-10 shows the pressures measured using the base oil at $60 \text{ }^\circ\text{C}$ for supply pressures of 0.5, 0.8, 1.1 and 1.7 MPa.

The pressure gradient being basically constant from the entrance of the slit, a fully developed flow is attained even from the slit entrance. Also, the exit pressures calculated with the extrapolation using the pressures of PT1, PT2 and PT3 were negative values. This is the normal tendency for base oils (Newtonian fluids).

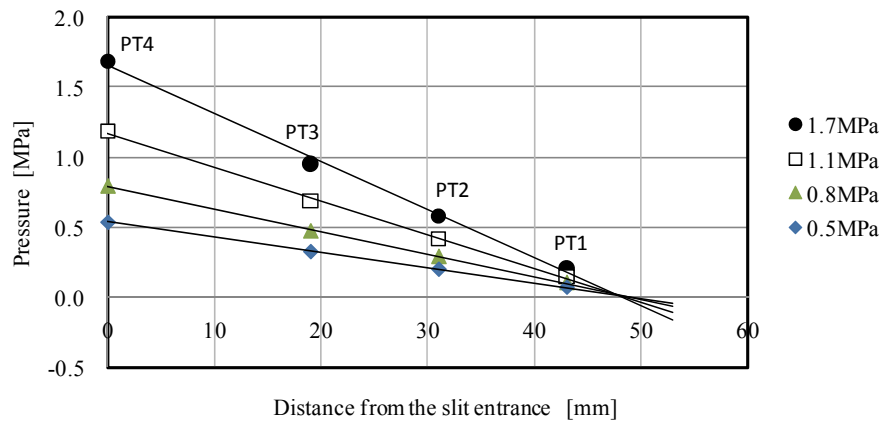


Figure 7-10 Pressure profiles in the rheometer with the base oil at 60 °C (Pressure vs. distance from the slit entrance)

The precise temperature control is necessary for the accurate measurement as well as the oil supply pressure. The supply oil temperature was controlled with two electric heaters in the tank and a heat exchanger using a type K thermocouple (T2) located at a distance of 8 mm from the slit entrance. The temperature with the thermocouple (T2) was maintained at a tested temperature in a variation of 0 to -0.5 °C. The other two thermocouples of type K were attached to the top of the reservoir tank and at a distance of 5 mm from the slit exit.

The oil flow rates were also measured using a flow meter mounted in the system for 60 and 80 °C of oil supply temperatures. They were manually measured for 40 °C by measuring the amount of the oil which was flowing out of the slit die rheometer because the sensitivity of the flow meter did not allow us to measure such a low flow rate.

<Viscosity measurement>

The viscosity was actually calculated using the values measured with the rheometer. The apparent shear rate is given by

$$\dot{\gamma}_a = 6Q/H_r^2 W_r$$

where Q is the volumetric flow rate. The true wall shear rate is given by

$$\dot{\gamma}_w = \dot{\gamma}_a \left[\frac{2}{3} + \frac{d \ln \dot{\gamma}_a}{3d \ln \sigma_w} \right]$$

σ_w is the wall shear stress and then the viscosity is obtained from the following formula:

$$\text{Viscosity} = \sigma_w / \dot{\gamma}_w$$

<Exit pressure method to determine normal stress>

The first normal stress difference $N1$ is defined as the following:

$$N1 = \sigma_{yy} - \sigma_{zz}$$

σ_{yy} and σ_{zz} are the stresses along the flow gradient direction and the flow direction, respectively. (σ_{zz} is considered to be very small compared with σ_{yy} and almost negligible.) In order to determine the first normal stress difference, the following equation using the exit pressure of the slit was used:

$$N1 = P_x + \sigma_w \frac{d \ln P_x}{d \ln \sigma_w}$$

where P_x and σ_w are the exit pressure and the wall shear stress, respectively. The analysis of the exit pressure was originally reported by Han [81-83].

The wall shear stress (σ_w) is calculated with the following formula:

$$\sigma_w = \frac{H_r (p_{PT2} - p_{PT1})}{2L_1}$$

where p_{PT1} and p_{PT2} are the pressures measured with the pressure transducers of PT1 and PT2.

<Test conditions>

Measurements were taken at three supply oil temperatures (40, 60 and 80 °C) under five supply pressures from 0.5 MPa to 1.7 MPa. The range of the apparent shear rate applied to the lubricants should become approximately between $6 \cdot 10^4$ and $6 \cdot 10^5 \text{ s}^{-1}$. The test conditions are the following:

- (1) Supply oil temperature : 40, 60 and 80 °C
- (2) Supply pressure : 0.5, 0.8, 1.1, 1.4 and 1.7 MPa
(0.5, 0.8, 1.1 and 1.7 MPa for the base oil)

7-2-3 Lubricants tested

Three polymer-containing oils (PMA1a, PMA2a and PMA3a) were blended again using polymethacrylates of Mw25,000, Mw190,000 and Mw370,000 with the same formulation (the same dosage of the polymers) as the oils used for the plain bearing tests while the same base oil was tested. Table 7-4 shows the kinematic viscosity and the density of the oil samples. Even if the samples of the polymer-containing oils for the measurements of rheological properties were made with the same formulation, the kinematic viscosity was slightly different from that of the oils for the bearing tests. It is because the oil samples for the measurements of rheological properties were blended with base oils of different manufacturing lots, and the kinematic viscosity of the bearing test oil samples was measured for the samples taken from the tank after the tests were completed.

In order to investigate the effect of the polymer concentration, an oil sample (PMA2a+) was also made with a high dosage of the Mw190,000 polymer. (The dosage of the polymer was increased by 20 wt% for PMA2a+ compared with PMA2a.) A letter of “a” was added at the end of the sample names for the polymer-containing oils in the rheological property measurements to discriminate from the bearing test oil samples.

Table 7-4 Typical property of the oil samples tested with the rheometers

| Sample Name | | | Base Oil | PMA1a | PMA2a | PMA2a+ | PMA3a |
|------------------------|-------|---------------------------------|----------|--|---|---|---|
| | | | | Oil containing polymer Polymer: Mw 25,000 | Oil containing polymer Polymer: Mw 190,000 | Oil containing polymer Polymer: Mw 190,000 | Oil containing polymer Polymer: Mw 370,000 |
| Kinematic Viscosity | 40 °C | mm ² s ⁻¹ | 27.65 | 25.74 | 21.47 | 25.64 | 18.91 |
| | 60 °C | mm ² s ⁻¹ | 14.44 | 15.20 | 14.20 | 16.85 | 12.73 |
| | 80 °C | mm ² s ⁻¹ | 8.639 | 9.887 | 10.03 | 11.83 | 9.133 |
| Density | 40°C | g/cm ³ | 0.809 | 0.816 | 0.803 | 0.805 | 0.802 |

7-2-4 Rheological property of the lubricants tested

Figure 7-11 shows the results of the viscosity measurements against the shear rates for 40, 60 and 80 °C of supply oil temperatures. For the viscosity obtained with the cone plate rheometer, only limited data were plotted in Figure 7-11 because oil samples were dispersed at a high shear rate. The viscosity measured for low shear rates with the cone plate rheometer was basically the same as that measured at the lowest supply pressure (0.5 MPa) with the slit die rheometer (at the smallest shear rate in each oil sample).

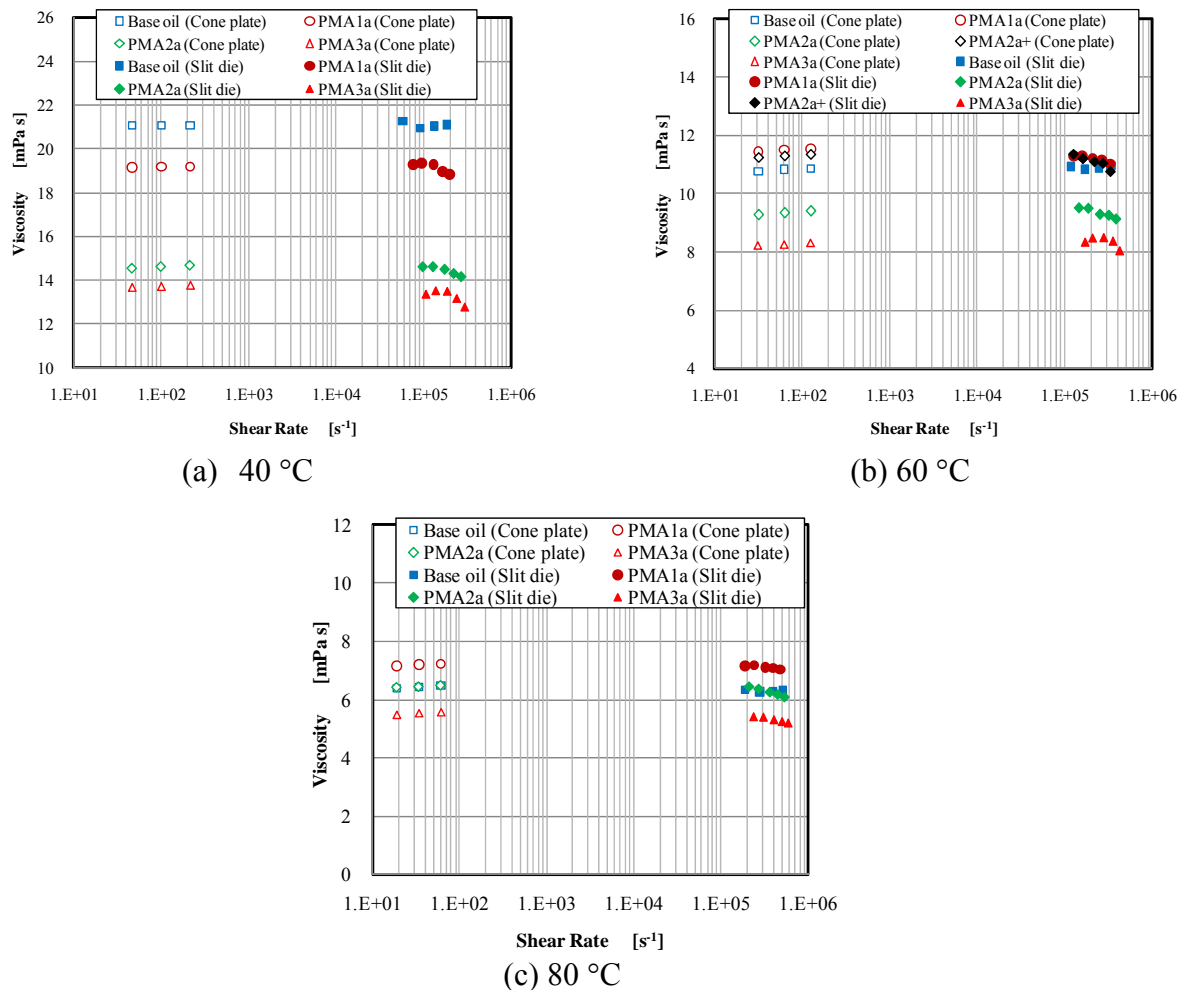


Figure 7-11 Viscosity vs. shear rate for the base oil and the polymer-containing oils at 40, 60 and 80 °C

In the results with the slit die rheometer, the viscosity of the polymer-containing oils is likely to decrease with increase of a shear rate for all of the oil supply temperatures while that of the base oil is not. It can be said that the behavior as non-Newtonian fluids appeared for the polymer-containing oils in the high shear rate range.

A reduction of 4 to 5 % in the viscosity was observed with PMA2a and PMA3a at the highest shear rate for all of the oil supply temperatures (the magnitude of the viscosity reduction is small at 80 °C, but its reduction ratio was close to that at 40 and 60 °C). A viscosity reduction of 2 % was also observed with PMA1a at the highest shear rate for all of the temperatures. The controlled oil temperature greatly affects the viscosity. However, since it was maintained with a variation of 0.5 °C, the viscosity change due to the unevenness of the temperature should be less than 1 % and the viscosity loss of 2 to 5 % is considered to be

significant. In case of PMA2a+, the reduction of viscosity was 5 % at 60 °C, while it was 4 % in PMA2a. The viscosity reduction ratio can be influenced by increasing the polymer content.

Overall, it is likely that the higher the molecular weight of polymer, the greater the viscosity reduction at high shear rates. Also, it was observed that the viscosity with PMA1a and PMA2a began to decrease at a lower shear rate than the other oil (PMA3a) containing higher molecular weight polymer. This may be due to higher concentration of polymer in PMA1a and PMA2a than in PMA3a and the behavior as a non-Newtonian fluid could appear from a lower shear rate.

The results of the first normal stress difference measurement using the slit die rheometer is shown in Figure 7-12. The measurement of the first normal stress difference was also attempted with the cone plate rheometer but it was not detected in the low shear rate range.

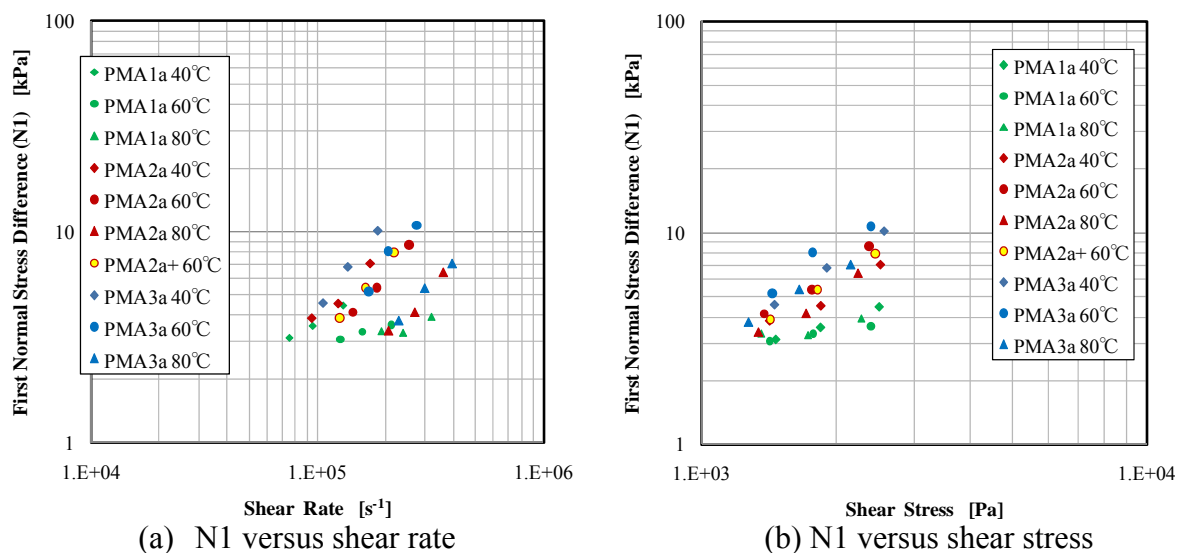


Figure 7-12 First normal stress difference (N1) vs. wall shear rate and wall shear stress for the polymer-containing oils at 40, 60 and 80 °C

Figure 7-12(a) shows the relationship between the first normal stress difference (N1) and the shear rate for the polymer-containing oils. Since the pressure transducer of 0.7 MPa for PT3 was needed to be changed to one of 3.5 MPa when the rheological properties were measured at 1.4 and 1.7 MPa of feeding oil pressures, the first normal stress difference was measured only at 0.5, 0.8 and 1.1 MPa of feeding oil pressures because of the uncertainty of the high pressure transducer.

Basically, it is likely that the higher the molecular weight, the higher the normal stress difference. The first normal stress difference increases with increase of a shear rate. The lower

the temperature, the higher the normal stress difference.

The data were also arranged in relation to the wall shear stress as shown in Figure 7-12(b). The normal stress difference increases with increase of the wall shear stress. In fact, there was relatively a good relationship between the first normal stress difference and the wall shear stress. It is likely that the higher the shear stress, the higher the normal stress difference. Also, it was confirmed that the normal stress difference with PMA2a+ was almost on the same line as PMA2a. As a result of the rheological property measurement, the existence of the temporary viscosity loss and the first normal stress difference for the polymer-containing oils used in this study were definitely confirmed. Thus, it is possible that the bearing performance is discussed compared with the rheological properties.

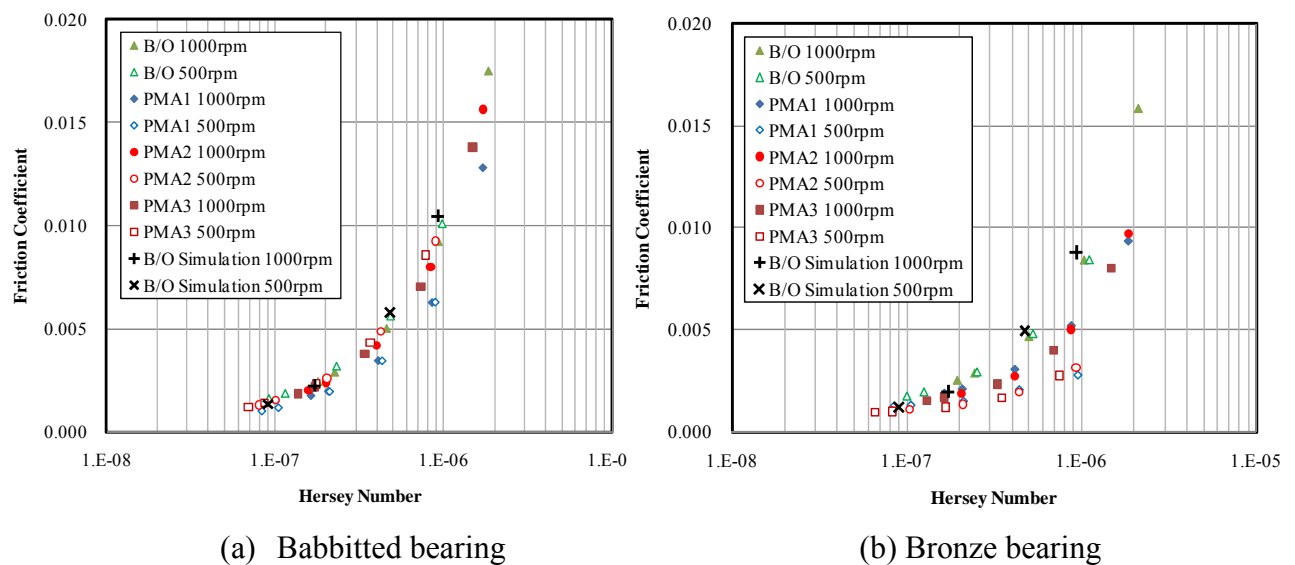
7-3 Plain bearing performance of the Babbitted bearing in comparison with the bronze bearing

In this paragraph, the experimental results of the friction coefficient, the relative shaft displacement, the bearing pressure distribution and the bearing temperature distribution are presented for the polymer-containing oils in comparison with the base oil. In addition, the calculated results with the THD analysis (simulation) developed at the Poitiers University are also indicated and compared with the experimental results as well as the comparison between the polymer-containing oils and the base oil. It was considered to be a sufficient method in order to discuss and qualitatively analyze the behavior of the polymer-containing oils. In fact, lubricants are treated as Newtonian fluids in the simulation of the current THD analysis. If the effect of the polymer-containing oils as non-Newtonian fluids appears, a difference between the experimental results and the simulation should be observed.

7-3-1 Friction coefficient

In order to ignore the factor of the viscosity difference in the lubricants tested, the friction coefficients of the bearings were arranged compared with the Hersey number for both of the Babbitted bearing and the bronze bearing tests. Figures 7-13(a) and 7-13(b) show the relationship between the Hersey Number and the friction coefficients for the bearing tests, which were carried out at a feeding oil temperature of 60 °C, for shaft speeds of 1,000 and 500 rpm and under loads from 0.8 to 9 kN. The Hersey number was calculated with the formula of

$\mu N/P_{\text{spec}}$ (μ : dynamic oil viscosity at average bearing temperature, N: revolutions per second of the shaft, P_{spec} : specific bearing load). μ was calculated with the average temperature measured at twenty nine locations on the bearing circumferential face. Also, the friction coefficients which were calculated under the condition of 1.72 and 9 kN, and 1,000 and 500 rpm using the THD analysis, were plotted for the base oil in the same figures (Figures 7-13(a), 7-13(b)) for reference. The detail of the THD analysis is indicated in Appendix I.



(a) Babbitted bearing (b) Bronze bearing
 Figure 7-13 Friction coefficient vs. Hersey number at 60 °C for the Babbitted bearing and the bronze bearing

The friction coefficients calculated in the THD analysis were very close to those in the experiments with the base oil for both of the Babbitted bearing and the Bronze bearing. This supports the accuracy of the bearing torque measurement. In fact, when the friction coefficients for the base oil were compared between the Babbitted bearing and the bronze bearing, those for the Babbitted bearing are placed at higher positions than for the bronze bearing. As mentioned above, the initial bearing clearance of the Babbitted bearing was 86 μm , which was smaller than that (95 μm) of the bronze bearing. The bearing clearance varies with thermal expansion of the shaft and the bearing during the operation of the apparatus. Figure 7-14 shows the calculated bearing clearance change versus the feeding oil temperatures for the two bearings under the condition of 500 rpm and 9 kN. While the bearing clearance of the Babbitted bearing basically keeps constant even at high temperatures, that of the bronze bearing is increased and the difference between the two becomes larger. Therefore, this could affect the friction coefficients. Since the calculated friction coefficients were almost the same as the

experimental results, the effect of the bearing material is considered to be small for the base oil but the polymer-containing oils actually showed a different behavior between the two bearings.

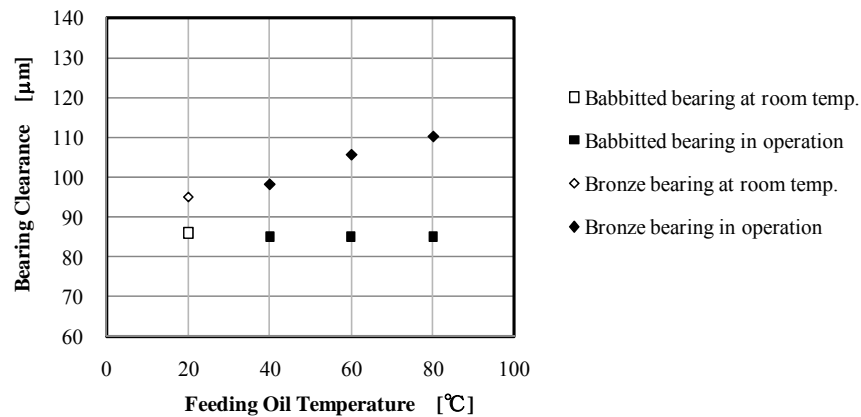


Figure 7-14 Bearing clearance vs. feeding oil temperature for the base oil in the Babbitted bearing and the bronze bearing

As seen in Figure 7-13(a), the friction coefficients in the Babbitted bearing are almost on the same line for most of the tested oils except for PMA1, which contains low molecular weight polymer ($M_w=25,000$). Only PMA1 showed slightly lower friction coefficients than the others.

On the other hand, in case of the bronze bearing the friction coefficients for the polymer-containing oils were significantly lower than those for the base oil under an equal Hersey number. Although a difference in the friction coefficients between 1,000 rpm and 500 rpm was hardly observed for the base oil, the friction coefficients for the polymer-containing oils were greatly decreased when the shaft speed was changed from 1,000 rpm to 500 rpm. This can suggest that the viscosity was decreased with an increase of shear rates for the polymer-containing oils because the oil film thickness could be decreased at a low shaft speed.

In order to confirm the influence of temperature, the friction coefficients for 60 and 80 °C at a shaft speed of 500 rpm and loads of 7.2 and 9 kN are arranged in Figure 7-15. In case of the Babbitted bearing, the friction coefficients at 80 °C for PMA3 became lower than those for the base oil although they were almost the same at 60 °C. It is considered that the increase of the feeding oil temperature decreased the viscosity and the oil film thickness. Then, an increase of the shear rate caused the temporary viscosity loss for PMA3, in which the largest molecular polymer is included and the magnitude of the temporary viscosity loss is large.

In case of the bronze bearing, the friction coefficients at 80 °C for the polymer-containing

oils became almost the same as those for the base oil. Also, the friction coefficients at 80 °C under 9 kN with which the Hersey number was the smallest, were placed at slightly higher positions than at 7.2 kN for all the test oils. This suggests that the lubricating condition could be shifting from hydrodynamic lubrication to mixed lubrication at a feeding oil temperature of 80 °C. It can be because the larger bearing clearance in the bronze bearing caused smaller minimum oil film thickness than in the Babbitted bearing and the friction coefficients were increased although serious damage on the bronze bearing was not observed after the tests.

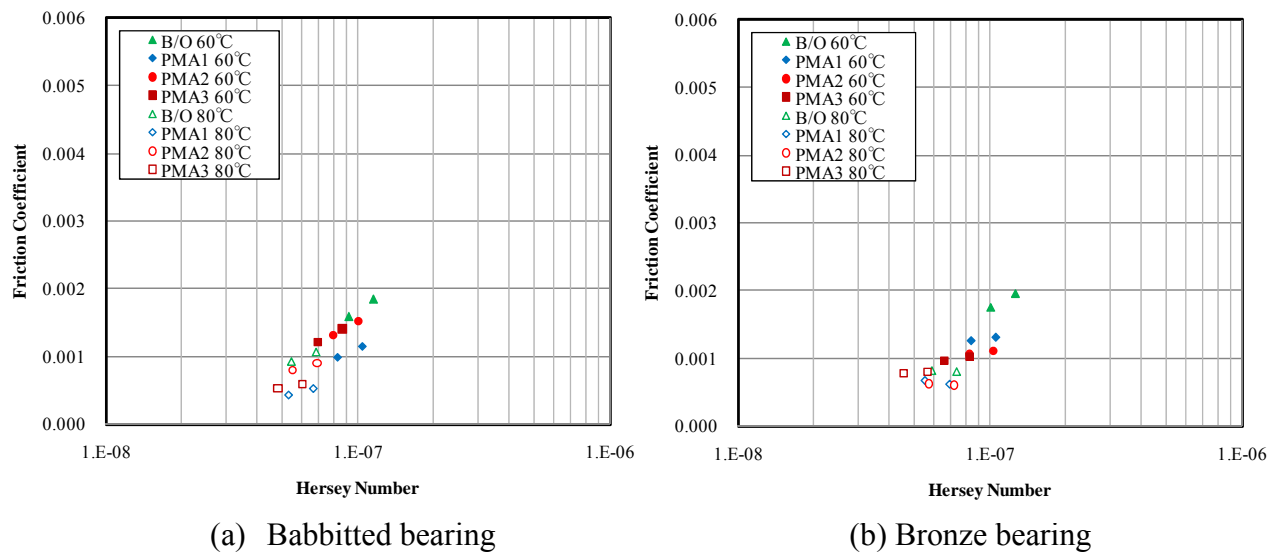


Figure 7-15 Friction coefficient vs. Hersey number at 60 and 80 °C, and 500 rpm under 7.2 and 9.0 kN for the Babbitted bearing and the bronze bearing

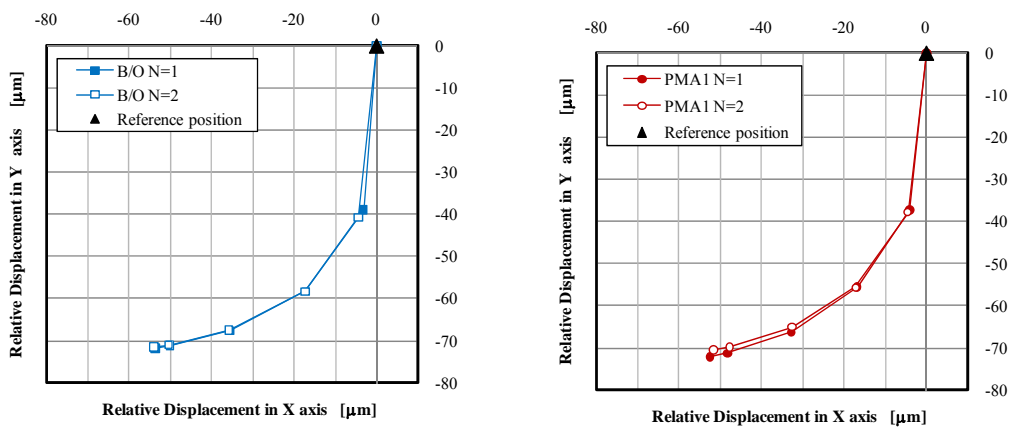
Overall, the friction coefficients were decreased for all of the polymer-containing oils at 60 °C with the bronze bearing and for PMA1 and PMA3 with the Babbitted bearing at 80 °C. The ability to reduce the friction coefficients with the different plain bearings varies among the polymer-containing oils, and it is very difficult to explain these phenomena only with the temporary viscosity loss at high shear rates. It is therefore necessary to discuss the effect of the polymer-containing oils in the friction coefficient compared with the oil film formation which can be affected by the temporary viscosity loss and the normal stress and can be estimated with the relative shaft displacement.

7-3-2 Relative shaft displacement

Figures 7-16(a), 7-16(b), 7-16(c) and 7-16(d) show the relative shaft displacement obtained

from the experiments at 0.8, 1.72, 3.6, 7.2 and 9.0 kN under the condition of 500 rpm and 60 °C for the Babbitted bearing and the bronze bearing. The relative shaft displacement was calculated at a reference point under a load of 0.8 kN and a shaft speed of 2,000rpm. The reference position was indicated at the coordinate of (0, 0) with a triangle symbol. The results obtained with the two tests for each oil sample were plotted in the same figures. Good repeatability was confirmed (the variation of the relative displacement was 1 to 2 μm at most).

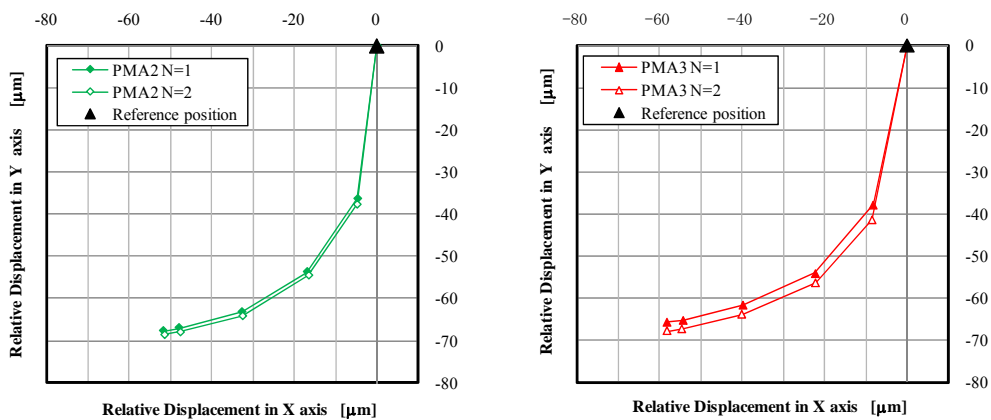
Comparing Figure 7-16(a) and 7-16(b) with 7-16(c) and 7-16(d), the magnitude of the relative shaft displacement for the Babbitted bearing in the X and Y axes is globally smaller than that for the bronze bearing. This is due to the smaller bearing clearance in the Babbitted bearing than in the bronze bearing. Since the relative shaft displacement for PMA2 and PMA3 with the bronze bearing is likely to increase at a load of 9 kN in Figure 7-16(d), it is conceivable that the eccentricity ratio is larger than with the Babbitted bearing.



1) Base oil

2) PMA1

Figure 7-16(a) Relative shaft displacement in the experiment at 500 rpm and 60 °C for the Babbitted bearing

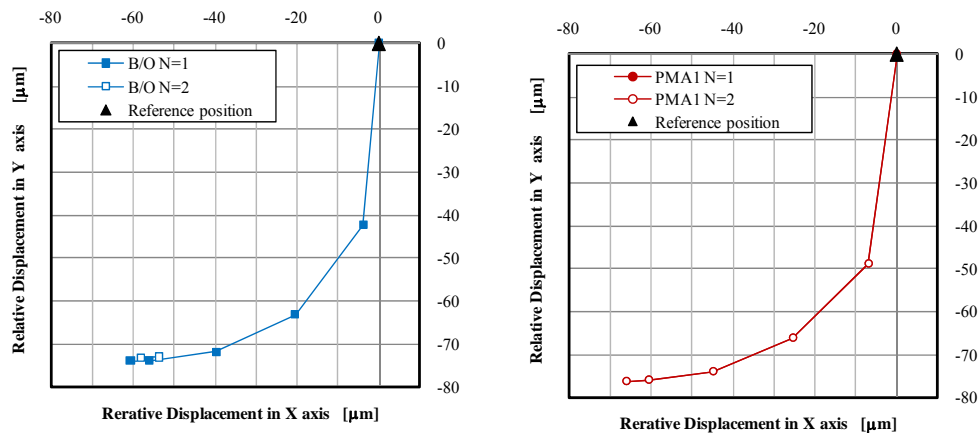


3) PMA2

4) PMA3

Figure 7-16(b) Relative shaft displacement in the experiment at 500 rpm and 60 °C for the Babbitted bearing

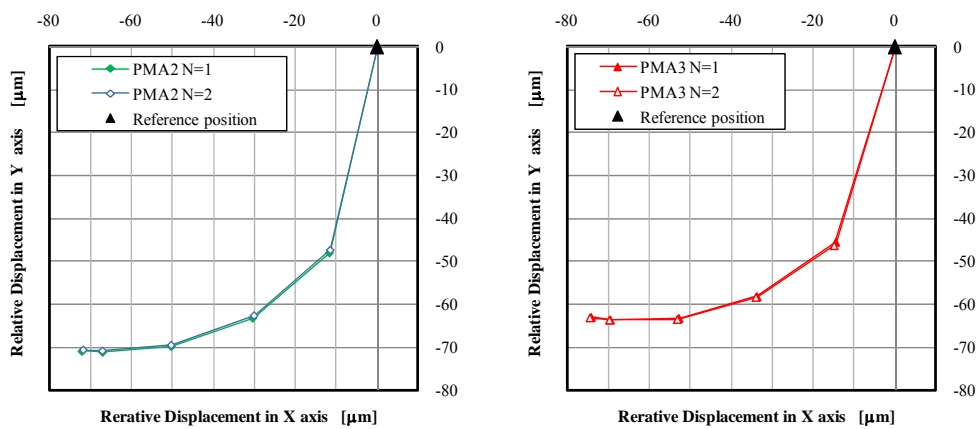
Also, it can explain the reason why a reduction of the friction coefficient was observed for the bronze bearing but not for the Babbitted bearing. The thinner oil film thickness for the bronze bearing is considered to increase the shear rate and cause the temporary viscosity loss for the polymer-containing oils. A shear rate which is given to the polymer-containing oil may have not reach the minimum shear rate to decrease the viscosity for the Babbitted bearing.



1) Base oil

2) PMA1

Figure 7-16(c) Relative shaft displacement in the experiment at 500 rpm and 60 °C for the bronze bearing



3) PMA2

4) PMA3

Figure 7-16(d) Relative shaft displacement in the experiment at 500 rpm and 60 °C for the bronze bearing

It was observed in the experimental results that the relative shaft displacement of the polymer-containing oils was higher in the Y axis than that of the base oil for both of the bearings. There is a tendency that the larger the molecular weight of polymers, the higher the relative shaft displacement in the Y axis. In fact, this should include the effects due to the difference of the viscosity at a low shear rate and as the non-Newtonian fluids for the polymer-containing oils.

Since the significant friction reduction was observed for the bronze bearing when the shaft speed was changed from 1,000 to 500 rpm but not for the Babbitted bearing, the relative shaft displacement in both the experiment and the simulation at 1,000 and 500 rpm under a load of 9 kN was also arranged in Figures 7-17 and 7-18 in order to confirm a relationship between the friction coefficient and the ability of the oil film formation. The relative shaft displacement measured with the first experiment for each oil sample was plotted in those figures. In the simulation, all of the tested oils were treated as Newtonian fluids even for the polymer-containing oils as mentioned above.

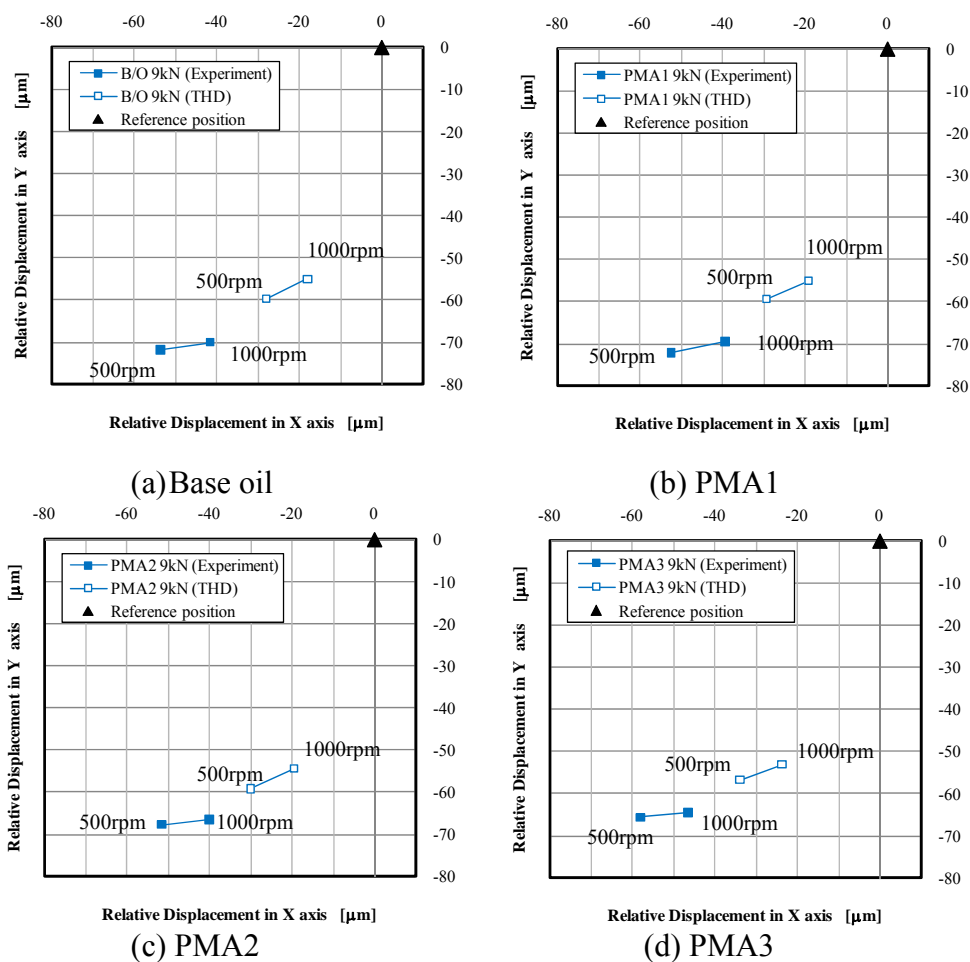


Figure 7-17 Relative shaft displacement under 60 °C, 1,000 & 500 rpm, and 9 kN for the Babbitted bearing

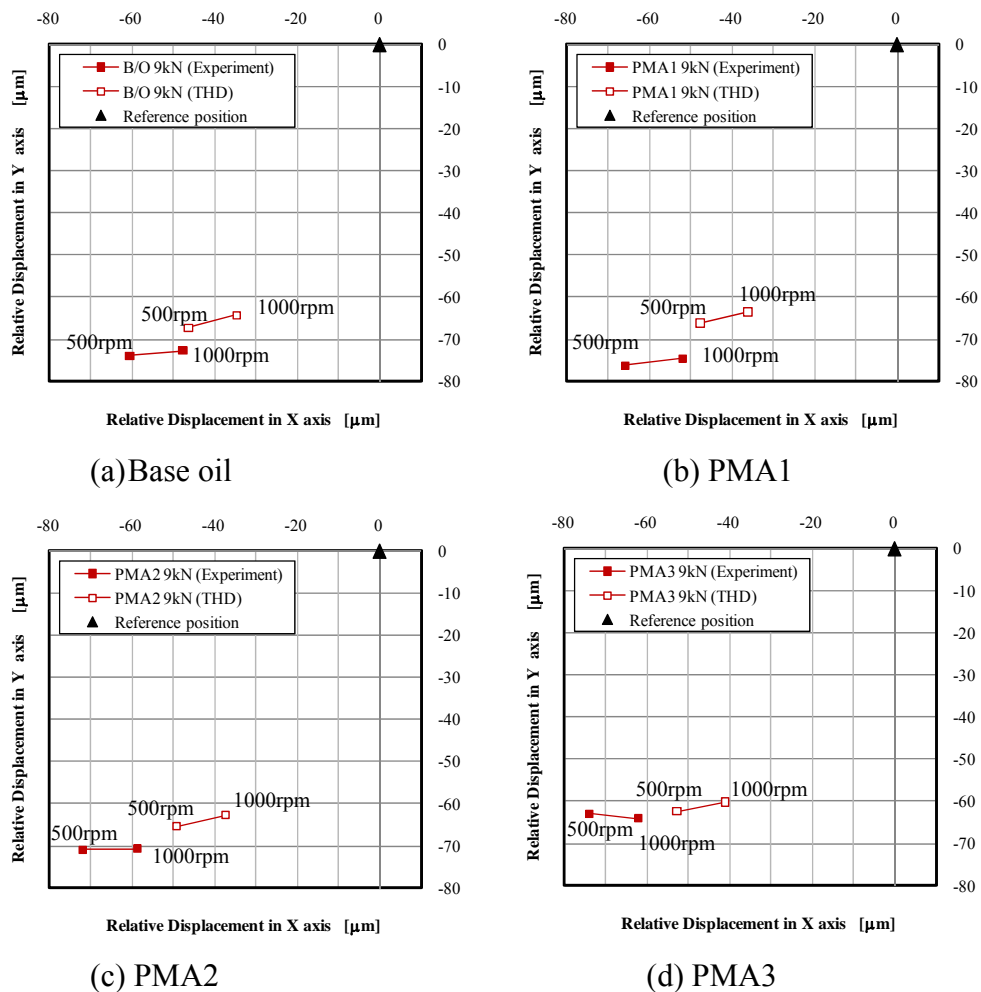


Figure 7-18 Relative shaft displacement under 60 °C, 1,000 & 500 rpm, and 9 kN for the bronze bearing

The absolute values of the relative shaft displacement in the experiment in the X axis greatly reduced for the two bearings when the shaft speed was decreased as well as in the simulation.

However, it is very difficult to clearly distinguish the effect of the polymer-containing oils of non-Newtonian fluids from the base oil of a Newtonian fluid, because the lubricants tested had different viscometric properties as shown in Table 7-3 and Figure 7-7. Therefore, in order to compensate the influence of the viscosity difference as well as for the friction coefficient, the relative shaft displacement in the X axis and the Y axis at 60 °C under the condition of shaft speeds of 1,000 and 500 rpm and a load of 9 kN versus the Hersey number was arranged for the Babbitted bearing and the bronze bearing in Figures 7-19 and 7-20. The Hersey number was calculated with the formula of $\mu N/P_{spec}$.

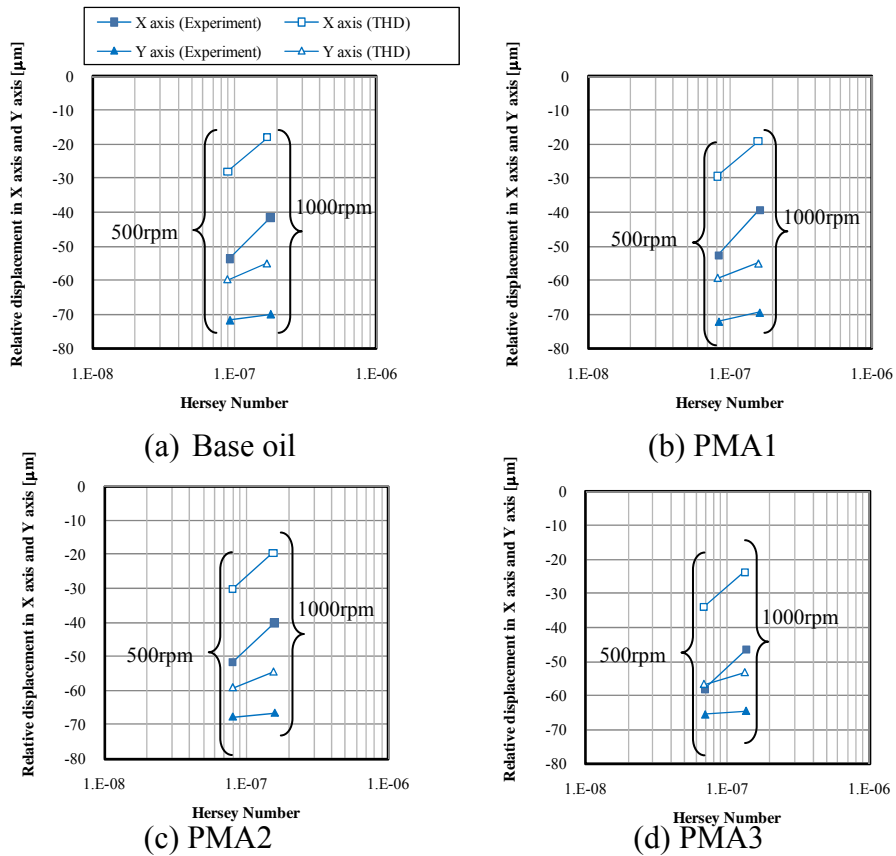


Figure 7-19 Relative shaft displacement vs. Hersey number under 60 °C, 1,000 & 500 rpm, and 9 kN for the Babbitted bearing

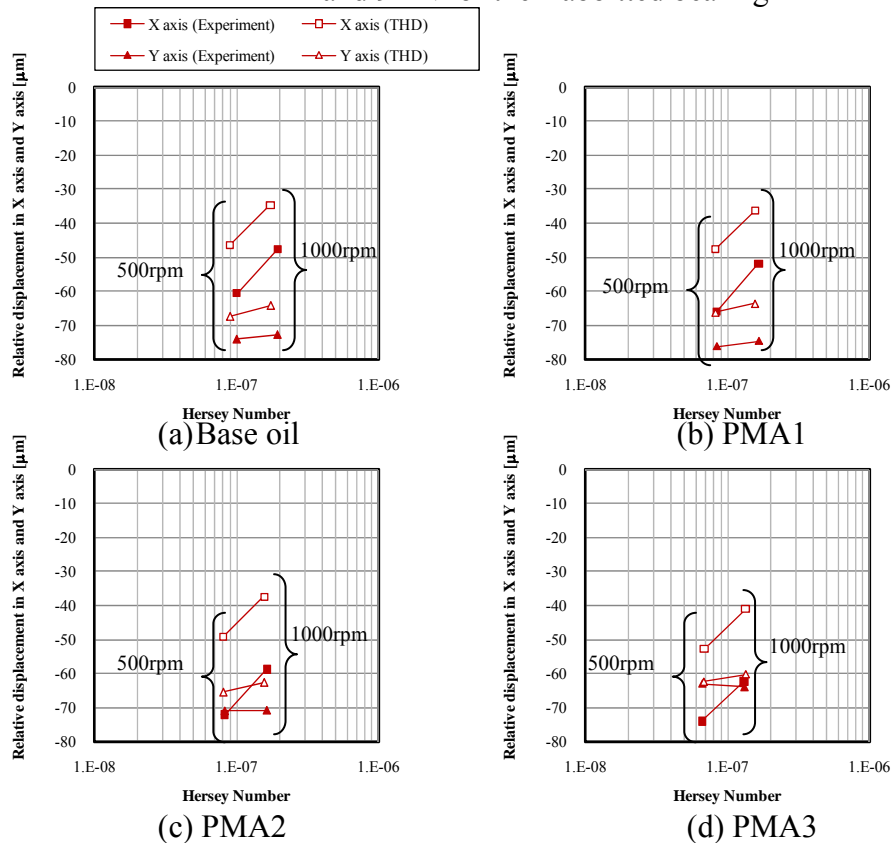


Figure 7-20 Relative shaft displacement vs. Hersey number under 60 °C, 1,000 & 500 rpm, and 9 kN for the bronze bearing

In the simulation, the relative shaft displacement in the X axis for all of the lubricants was almost placed on the same line for both of the two bearings as shown in Figure 7-19 and 7-20. There were however differences between the base oil and the polymer-containing oils in the experimental results. In Figure 7-19, the lines of the relative shaft displacement in the X axis with the polymer-containing-oils were placed at equal or higher positions than with the base oil in case of the Babbitted bearing. The magnitude of the relative shaft displacement for the polymer-containing oils could be smaller than that expected as Newtonian fluids. This suggests that the appearance of the normal stress effect from the polymer-containing oil is anticipated with the Babbitted bearing tests.

For the bronze bearing in Figure 7-20, the lines of the relative shaft displacement in the X axis for the polymer-containing oils were placed at lower positions than with the base oil. The magnitude of the relative shaft displacement could be larger than that expected as Newtonian fluids. Basically, the oils containing large molecular weight polymers (PMA2 and PMA3) are likely to show lower relative shaft displacement than the base oil. It was the opposite tendency compared with the Babbitted bearing. Therefore, the effect of the temporary viscosity loss is considered to be greater than that of the normal stress.

These results suggest that the relative shaft displacement (namely oil film formation in the bearings) obtained from the experiments with the Babbitted bearing and the bronze bearing relate with the friction coefficients. Since relatively the same tendency as the experimental results for the Al-Si bearing and the Cu-Pb bearing performance (presented in the chapter 6) was observed, the friction coefficients for those bearings are indicated again in Figure 7-21 and 7-22 for 500 rpm in order to readily compare with the results for the Babbitted bearing and the bronze bearing.

The friction coefficients for PMA1 and Polymer A in which the low-molecular weight polymer is included, were lower than those for the base oil and the other polymer-containing oils with the Babbitted bearing and the Al-Si bearing. Since the magnitude of the relative shaft displacement with the Babbitted bearing was smaller than the bronze bearing, the eccentricity ratio should be small. In case of the bronze bearing, all of the polymer-containing oils showed lower friction coefficients than the base oil although only Polymer B containing the high molecular weight polymer presented low friction with the Cu-Pb bearing.

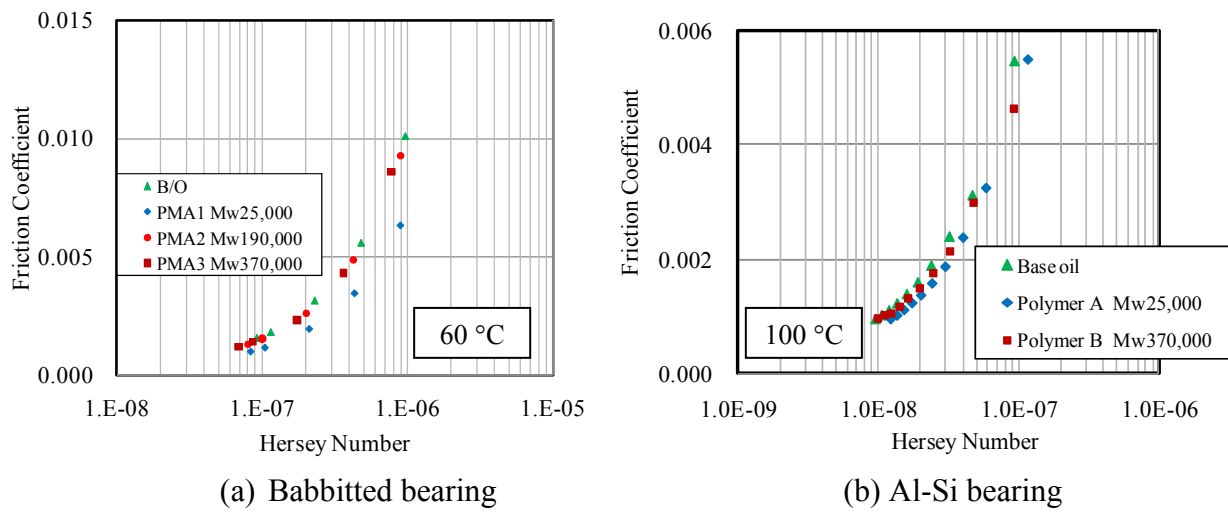


Figure 7-21 Comparison of the friction coefficient at 500 rpm in the Babbitted bearing and the Al-Si bearing

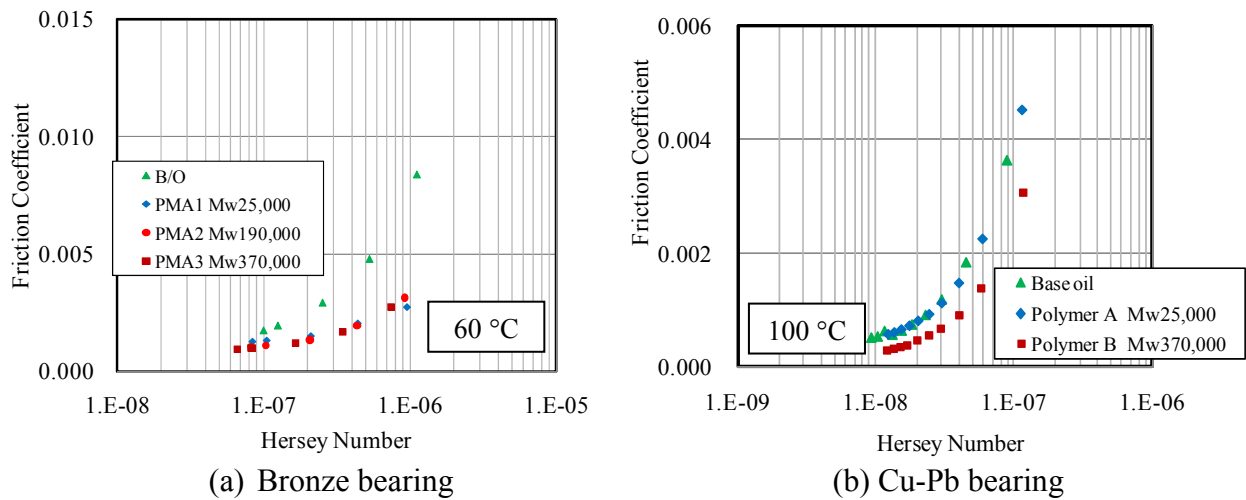


Figure 7-22 Comparison of the friction coefficient at 500 rpm in the bronze bearing and Cu-Pb bearing

From these results, overall it can be said that the large magnitude of the relative shaft displacement (which means thin oil film thickness) could cause the friction reduction basically for the oils containing high molecular weight polymers. In contrast, the oils with low molecular weight polymers could show the friction reduction when the relative shaft displacement is small. One reason to explain this phenomenon can be due to the influence of the normal stress.

On the other hand, it is conceivable that the influence of the bearing clearance difference

was greater than that of the bearing materials in case of the Babbitted bearing and the bronze bearing compared with the cases of the Al-Si bearing and the Cu-Pb bearing (there may have been the effect of the bearing materials in the bearing performance with the Babbitted bearing and the bronze bearing as well as the Al-Si bearing and the Cu-Pb bearing). However, the magnitude of the effect of the polymer-containing oils is considered to be very small with the Babbitted bearing and the bronze bearing. In other words, it can be said that the geometry of the bearing could affect the bearing performance with the polymer-containing oils. This implies that in case of automotive plain bearings, the bearing deformation during the engine operation can affect the effect of the polymer-containing oils, and the development of engine oils taking into account the stiffness of the bearing materials can be required. In fact, the maximum specific load for the tests carried out with the Babbitted and bronze bearings was 1.1 MPa, but it reaches 50 MPa at most in case of the bearings in actual operation of the latest gasoline engines.

7-3-3 Bearing pressure distribution

Figures 7-23 and 7-24 show the influence of the polymer-containing oils versus the base oil on the bearing pressure distribution under the condition of 60 °C, 500 rpm and 9,000 N for the bearing angles from 90 to 270 degrees with the Babbitted bearing and the bronze bearing. Those figures are arranged with the simulated results in addition to the bearing pressure distribution obtained from the experiments.

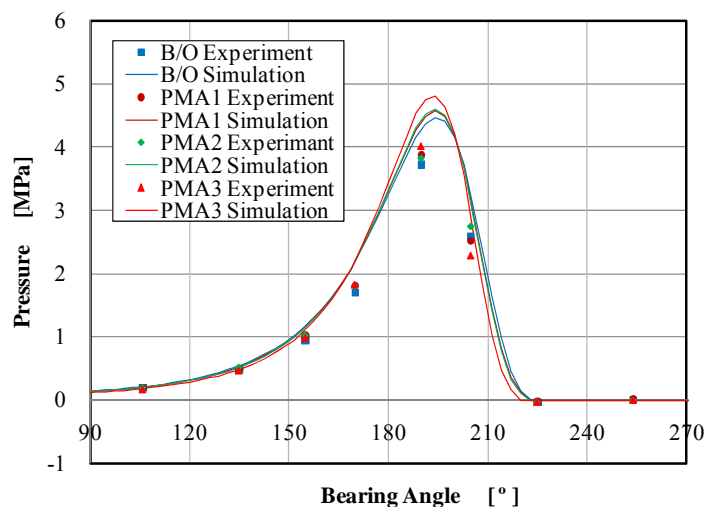


Figure 7-23 Pressure distribution vs. bearing angle in the mid-plane of the Babbitted bearing (60 °C, 500 rpm and 9,000 N)

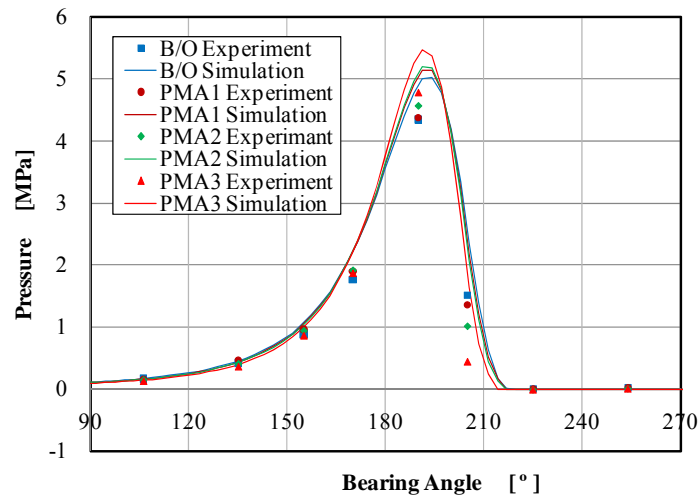


Figure 7-24 Pressure distribution vs. bearing angle in the mid-plane of the bronze bearing (60 °C, 500 rpm and 9,000 N)

If the pressure distribution with the Babbitted bearing in Figure 7-23 is globally compared with the bronze bearing in Figure 7-24 for the experiment and the simulation, they are broader and the maximum pressures with the Babbitted bearing placed at lower positions than with the bronze bearing. This is because the bearing clearance of the Babbitted bearing was smaller than that of the bronze bearing.

A slight difference in the pressure between the experiment and the simulation was observed in the middle range of the bearing angle even for the base oil in Figures 7-23 and 7-24. The pressure distribution in the simulation even for the base oil was placed at a slight higher position than in the experiment, while they basically showed the same tendency as the experimental pressure. The pressures in the experiments were obtained only at eleven locations on the bearing circumferential surface, and it is difficult to determine the bearing angle of the actual maximum pressure although it can be readily expected to be placed between 190 and 205 degrees bearing angle. Also, if a slight misalignment existed in the bearing, it could affect the bearing pressure distribution. Therefore, it was concluded that the experimental results can be discussed in comparison with the simulation for the base oil and the polymer-containing oils.

The pressures for the polymer-containing oils were higher than those for the base oil with both of the bearings in the middle bearing angles (170 and 190 degrees). The higher the high molecular weight polymer, the higher the pressure. However, since there is a viscosity difference among the oils used at 60 °C and 500 rpm under 9 kN, it is needed to compensate them. Thus, the pressure data were therefore arranged by comparing with the Hersey number for bearing angles of 155, 170 and 190 degrees which were in the active pressure zone of the

bearings. The pressures versus the Hersey number are shown in Figures 7-25 and 7-26 for the Babbitted bearing and the bronze bearing, respectively.

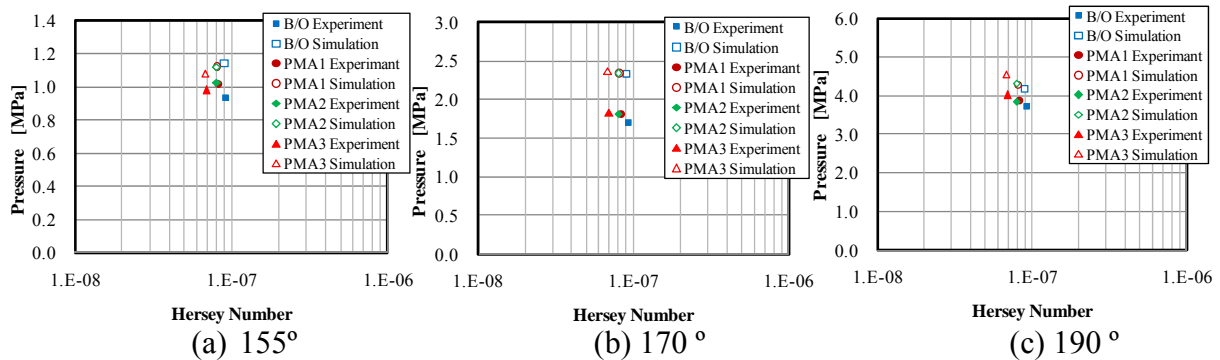


Figure 7-25 Pressure vs. Hersey number at bearing angles of 155, 170 and 190 degrees for the Babbitted bearing (60 °C, 500 rpm and 9,000 N)

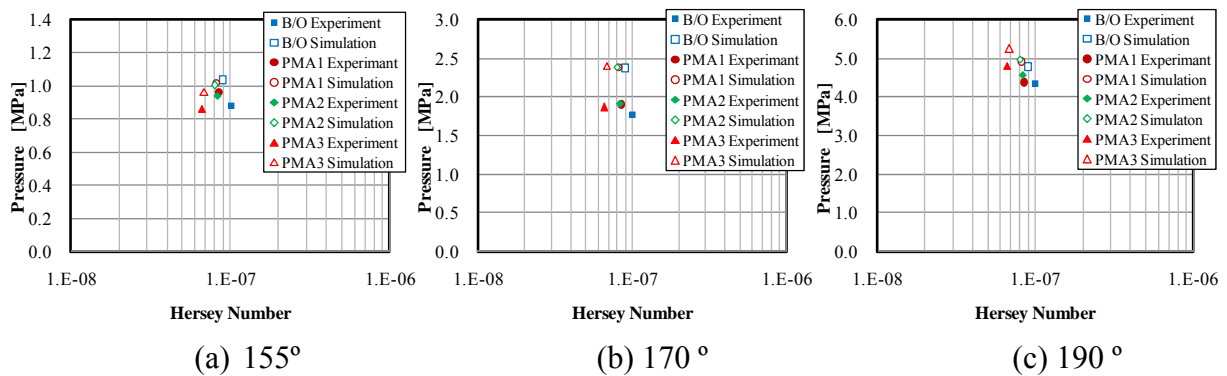


Figure 7-26 Pressure vs. Hersey number at bearing angles of 155, 170 and 190 degrees for the bronze bearing (60 °C, 500 rpm and 9,000 N)

In case of the Babbitted bearing in Figure 7-25, the pressures in the experiment for the polymer-containing oils (PMA1, PMA2 and PMA3) were placed at a higher position than those for the base oil at bearing angles of 155 and 170 degrees if they were compared with the relationship between the base oil and the polymer-containing oils in the simulation. Basically, pressure increases with either a reduction of the oil film thickness due to the viscosity reduction or the normal force appearance. In fact, the magnitude of the relative shaft displacement with the Babbitted bearing for the polymer-containing oils was smaller as previously shown and their oil film thickness could be thicker than that expected for Newtonian fluids. Therefore, it suggests that one of the reasons why the pressures with the polymer-containing oils were higher could be the sufficient normal stress appearance for the Babbitted bearing. There could be the influence of the polymer-containing oils in the pressure distribution for the two bearings, but the normal stress measured with the slit die rheometer was only 20 kPa at $5 \cdot 10^5 \text{ s}^{-1}$ of a shear

rate even for the oils containing the high molecular weight polymers. The effect of the polymer-containing oils will be further discussed with the calculation using the rheological properties obtained with the rheometer in the later paragraph.

In case of the bronze bearing in Figure 7-26, the pressures in the experiment for the polymer-containing oils (PMA1, PMA2 and PMA3) were placed at a higher position than those for the base oil at bearing angles of 155 and 170 degrees as well as the Babbitted bearing. The magnitude of the relative shaft displacement for the polymer-containing oils was larger and their oil film thickness could be considered to be thinner than that expected for Newtonian fluids. Therefore, in this case, such an oil film thickness reduction could be considered to cause the pressure increase.

7-3-4 Bearing temperature distribution

Figures 7-27 and 7-28 show the experimental temperature distribution in the mid-plane of both the Babbitted bearing and the bronze bearing compared with the simulation under the condition of 60 °C, 500 rpm and 9 kN. If the bearing friction with the polymer-containing oils is lower than that with the base oil, the bearing temperature in the experiment can be also lower than in the simulation for the polymer-containing oils. In fact, if the experiment was repeated more than twice, the bearing surface temperatures measured in the experiments varied with a variation of $\pm 0.5^{\circ}\text{C}$, and the change of the feeding oil temperature greatly affected the bearing temperature distribution. Therefore, the apparent different tendency in the temperature distribution for the polymer-containing oils was not observed even if the comparison between the experimental results and the simulation was attempted.

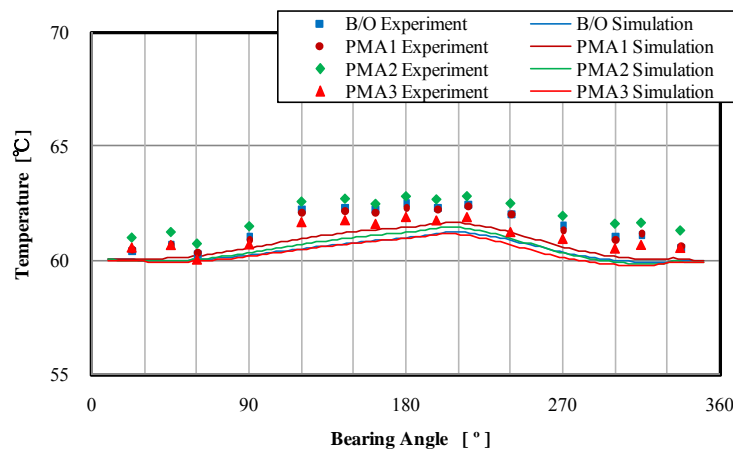


Figure 7-27 Temperature distribution vs. bearing angles for the Babbitted bearing (60 °C, 500 rpm and 9,000 N)

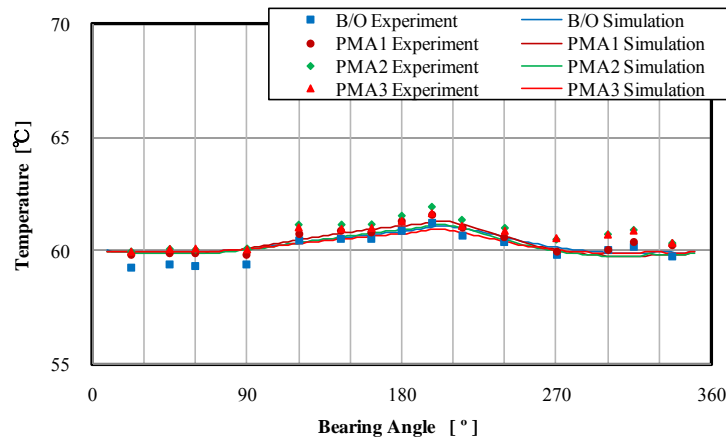


Figure 7-28 Temperature distribution vs. bearing angles for the bronze bearing (60 °C, 500 rpm and 9,000 N)

Overall, the polymer-containing oils presented a different behavior for the friction coefficients, the relative shaft displacement and the pressure distribution. However, since the extent of their effect compared with the rheological properties has not been clarified, the further analysis will be presented in the later paragraph (7-5).

7-4 Analysis of the effect of the temporary viscosity loss and the normal stress at high shear rates on the bearing performance with the Babbitted bearing and the bronze bearing

The existence of the temporary viscosity loss and the normal stress in the polymer-containing oils was confirmed from the results of the rheological properties measurements at high shear rates up to $6 \cdot 10^{-5} \text{ s}^{-1}$. In fact, their magnitude depends on the polymers used. Basically, the larger the polymer molecular weight, the larger the temporary viscosity loss and the normal stress. It also depends on the magnitude of the shear rate in the bearings.

On the other hand, it was confirmed that the friction coefficients were significantly decreased for the polymer-containing oils with the bronze bearing but not with the Babbitted bearing. Indeed, the different phenomena were observed between the two bearings. Since a difference in the relative shaft displacement between the Babbitted bearing and the bronze bearing was observed, it is considered that the distribution of the shear rates in the bearing also differs between the two bearings, and it may have affected the difference of the behavior of the polymer-containing oils. In fact, the phenomena of the polymer-containing oils could be

considered as a balance of the temporary viscosity loss and the normal stress.

The THD analysis shown in Appendix I was attempted by taking into account the temporary viscosity loss and/or the normal stress for the Babbitted bearing and the bronze bearing in order to determine their effectiveness.

7-4-1 Approximation equations for the temporary viscosity loss and the first normal stress difference

In order to make the simulation with the rheological properties possible, it is needed to induce approximation equations for the dynamic viscosity and the first normal stress difference with respect to a shear rate or a shear stress. The equation used for dynamic viscosity in the polymer- containing oils is the following:

$$\eta = \eta_c \left(\frac{\dot{\gamma}}{\dot{\gamma}_c} \right)^{n-1}$$

where n and $\dot{\gamma}$ are respectively a constant and a shear rate. η_c is the same as the zero shear viscosity, and $\dot{\gamma}_c$ is the shear rate at which the dynamic viscosity begins to decrease. The viscosity is η_c up to a shear rate of $\dot{\gamma}_c$. Figure 7-29 shows the viscosity obtained with the slit die rheometer and the approximation equations induced from the experimental results for 60 °C. In fact, only the simulation of the bearing performance with PMA1a (with polymer of Mw25,000) and PMA3a (with polymer of 370,000) for a feeding oil temperature of 60 °C was attempted to confirm the effect of the molecular weight of the polymer on the Babbitted bearing and the bronze bearing performances.

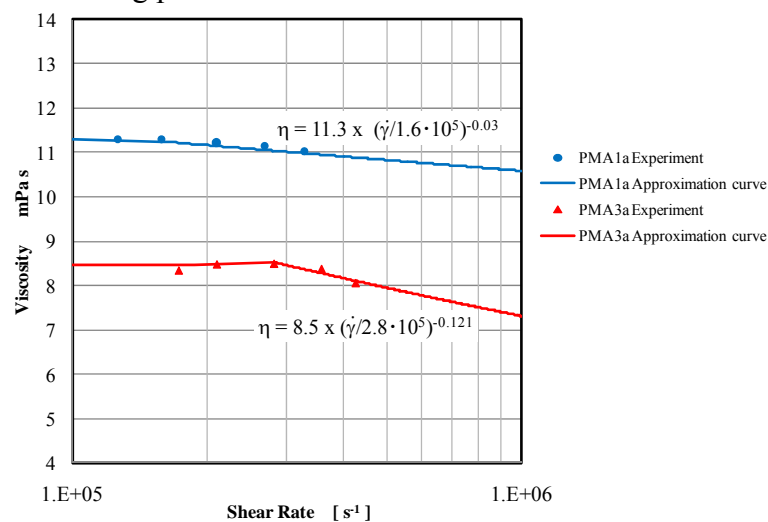


Figure 7-29 Viscosity measured with the slit die rheometer and the induced approximation equations for 60 °C

In Figure 7-29, the constant values of η_c are 11.3 and 8.5 mPa·s for PMA1a and PMA3a at a feeding oil temperature of 60 °C. However, since the temperature along the circumferential bearing surface varies, the value of η_c was adjusted using the Mac Coull and Walther formula while the same values in Figure 7-29 were used for $\dot{\gamma}_c$ and n.

Approximate equations for the first normal stress difference were also deduced from the experimental data obtained with the slit die rheometer. As mentioned above, a good correlation was observed between the first normal stress difference and the shear stress with our experiments. Also, it has been known that the first normal stress difference (N1) is well represented by a power law of the following:

$$N1 = A\sigma^\alpha$$

where A and α are respectively a constant and σ is the shear stress. Figure 7-30 shows the first normal stress difference with the approximate equations.

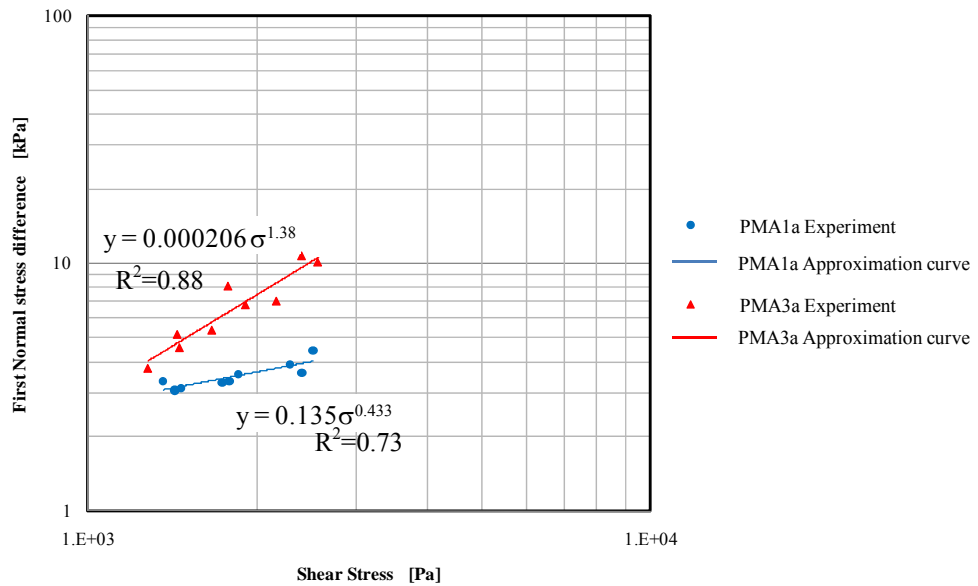


Figure 7-30 First normal stress difference measured with the slit die rheometer and the induced approximation equations for 60 °C

Since the values of the first normal stress difference measured were very low compared with the Reynolds pressure generated in the bearing, the pressure distribution was calculated by adding the first normal stress difference to the calculated Reynolds pressure at each bearing angle. Subsequently, the friction coefficient, the oil film thickness and the temperature distribution were calculated using the pressure distribution.

7-4-2 Simulation condition

The simulation was attempted under the conditions indicated in Table 7-5. In addition to the conditions of the bearing tests at 500 rpm under 1.72 and 9 kN, the bearing performance with a higher load (27 kN) and/or a higher shaft speed (2,000 rpm) conditions was calculated to increase the shear rates and investigate their influence.

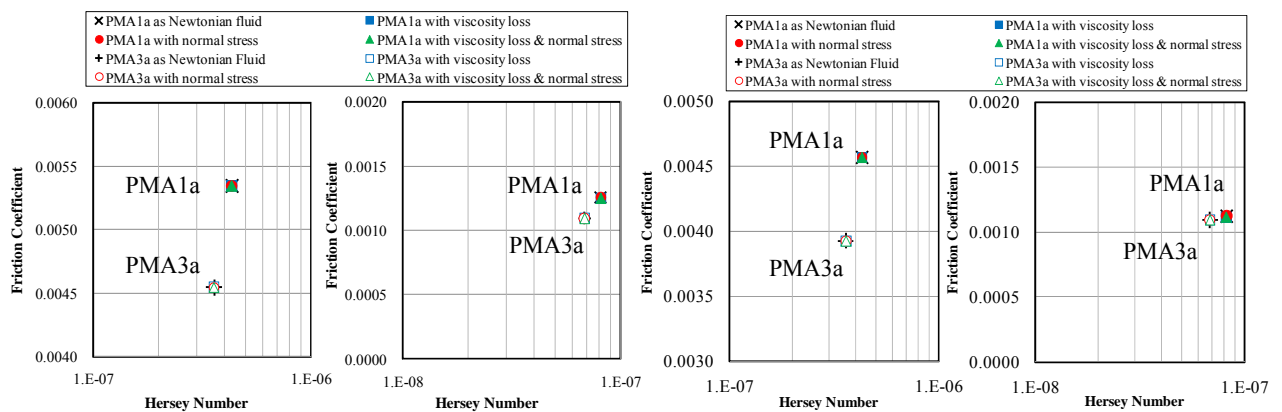
Table 7-5 Simulation conditions

| Feeding oil temp. °C | Shaft speed rpm | Load kN |
|----------------------|-----------------|---------|
| 60 | 500 | 1.72 |
| | | 9 |
| | | 27 |
| | 2000 | 27 |

7-4-3 Effect of the temporary viscosity loss and the first normal stress difference in the bearing performance

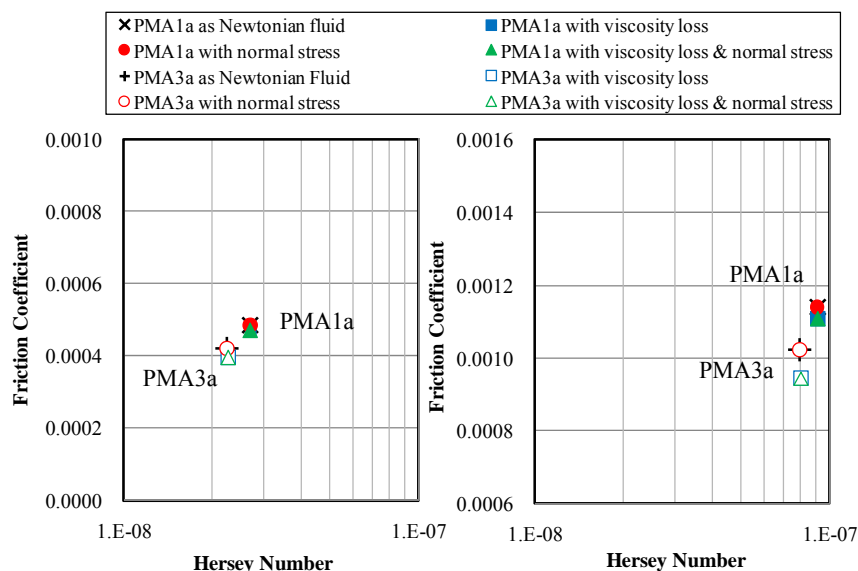
In order to estimate the influence of the temporary viscosity loss and/or the first normal stress difference, the plain bearing performance (friction coefficient, oil film thickness, and temperature distribution) for a feeding temperature of 60 °C was calculated using the approximation equations of the rheological properties for PMA1a and PMA3a of lubricant samples in which low (Mw25,000) and high (Mw370,000) molecular weight polymers were included, respectively. In addition, the simulation with the viscosity which was treated as a Newtonian fluid ($\eta=\eta_c$) was also attempted for comparison.

The friction coefficients versus the Hersey number which were calculated with PMA1a and PMA3a under the condition of 1.72 kN and 9.0 kN of loads and a shaft speed of 500 rpm are shown for the Babbitted bearing and the bronze bearing in Figure 7-31. Even if the temporary viscosity loss and the normal stress were taken into account in the simulation, a significant difference in the friction coefficients was not observed compared with the result calculated as a Newtonian fluid. The calculated shear rates reached approximately $2.5 \cdot 10^5$ to $3 \cdot 10^5 \text{ s}^{-1}$ at most under a load of 9.0 kN in the bearing angle where the film thickness becomes minimum. They are not considered to be high enough to reduce the viscosity and the temporary viscosity loss is only 1 % in case of PMA1a. Also, the maximum first normal stress difference for PMA1a and PMA3a in the simulation was approximately 5 kPa which is a smaller value than the Reynolds pressure generated in the bearings.



(a) Babbitted, 1.72 kN (b) Babbitted, 9.0 kN (c) Bronze, 1.72 kN (d) Bronze, 9.0 kN
 Figure 7-31 Influence of the temporary viscosity loss and the normal stress (Friction coefficient versus Hersey number for the Babbitted and bronze bearings under 1.72 & 9.0 kN, 500 rpm and 60 °C)

In the experimental results for the Babbitted bearing, as previously shown in Figure 7-13, there was no difference in the friction coefficient between the base oil and PMA3 which contains the same polymer as PMA3a. This is the same result as the simulation. It can be therefore said that the reason why the effect of the viscosity loss did not appear was the low shear rate generated in the bearing. On the other hand, it is very difficult to explain why PMA1 slightly reduced the friction in the experiment for the Babbitted bearing and all the polymer containing oils did for the bronze bearing.



(a) 27kN and 500 rpm (b) 27 kN and 2,000 rpm
 Figure 7-32 Influence of the temporary viscosity loss and the normal stress (Friction coefficient versus Hersey number for the bronze bearings under 27 kN at 2,000 rpm and 60 °C)

In order to clearly observe the effect of the viscosity loss and the normal stress, the additional calculations for the bronze bearing were attempted using a higher load of 27 kN and a higher shaft speed of 2,000 rpm at 60 °C which can generate a higher shear rate in the bearing.

The friction coefficients versus the Hersey number are presented for 27 kN at 500 rpm and 27 kN at 2,000 rpm compared with the results for 9 kN at 500 rpm in Figure 7-32. Since the load applied for the simulation was 27 kN which is a much larger value than 9 kN, the calculated friction coefficients become small because of the large denominator to calculate them. Therefore, the data in Figure 7-32 was arranged with the enlarged scale for the vertical axis compared with Figure 7-31.

As seen in Figure 7-32, the friction coefficients were decreased for PMA1a and PMA3a especially under the condition of 27 kN and 2,000 rpm. The magnitude of the friction coefficient reduction with PMA1a was very small and the reduction ratio was approximately 3 % for both of the conditions of 27 kN at 500 rpm and 27 kN at 2,000 rpm. In case of PMA3a, the reduction ratio in the friction coefficient was 6 % and 8 % for 27 kN at 500 rpm and 27 kN at 2,000 rpm, respectively. The maximum shear rate in the bearing reached a range of $7 \cdot 10^5$ to $1 \cdot 10^6$ s⁻¹. It can be said that the increase of the shear rate affected the reduction of the viscosity and the friction coefficient. The first normal stress difference did not affect the friction coefficient. It is considered that the first normal stress difference was still small to enhance the bearing pressure distribution and the oil film thickness. The maximum value of the first normal stress difference with PMA3a was actually 90 kPa even for 27 kN at 2,000 rpm.

Figures 7-33 and 7-34 show the oil film thickness in the middle range of the bearing angle and the temperature distribution for the bronze bearing under the condition of 27 kN and 2,000 rpm. As well as the effect in the friction coefficient, the first normal stress difference is not likely to affect the oil film thickness because its magnitude was very small.

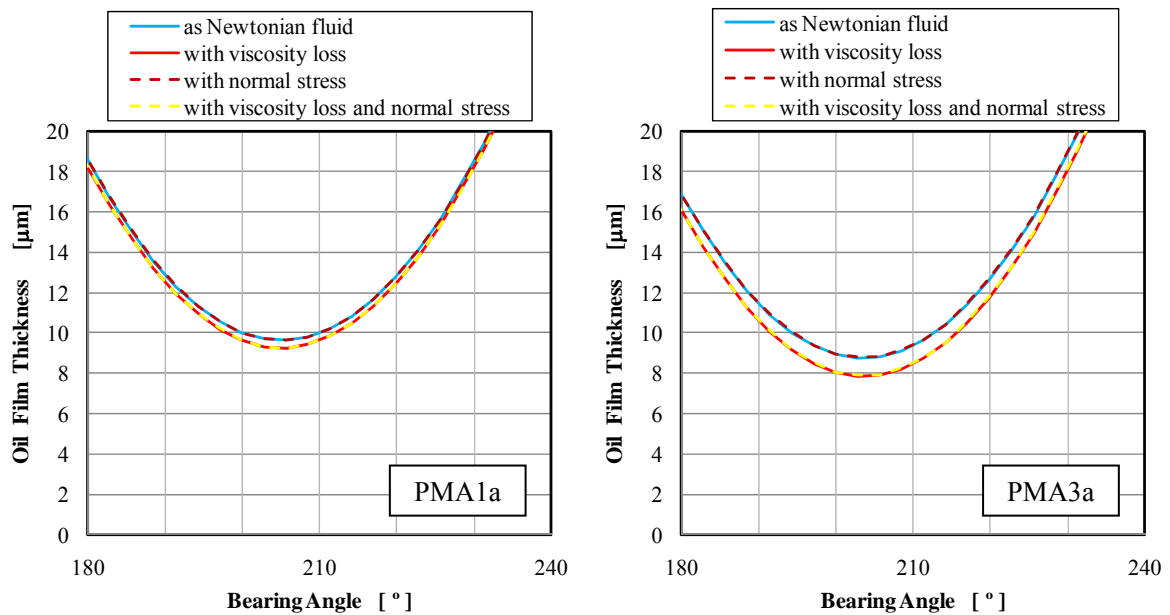


Figure 7-33 Influence of the temporary viscosity loss and the normal stress (Oil film thickness versus bearing angle for the bronze bearings under 27 kN at 2,000 rpm and 60 °C)

The temperature was slightly decreased if the temporary viscosity loss was taken into account for PMA1a and PMA3a in the simulation while the first normal stress difference did not affect the temperature distribution.

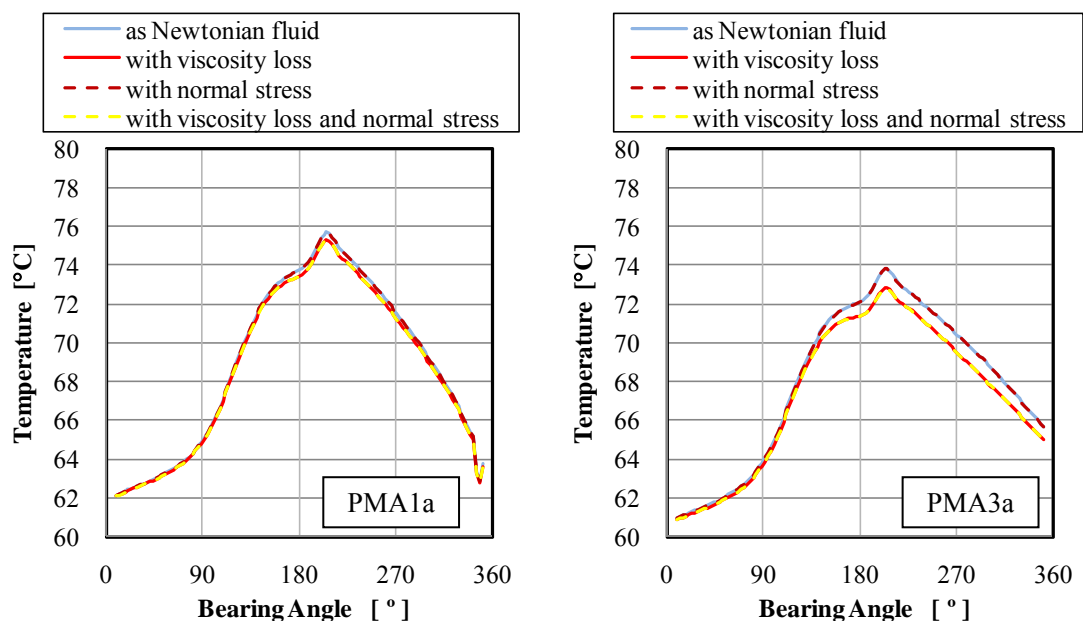


Figure 7-34 Influence of the temporary viscosity loss and the normal stress (Temperature versus bearing angle for the bronze bearings under 27 kN at 2,000 rpm and 60 °C)

Overall, the temporary viscosity loss affected the friction reduction, the oil film thickness and the temperature distribution. The larger the viscosity reduction ratio, the larger the influence in the bearing performance. The effect appeared only with the case that a higher load and a higher rotational speed than the actual bearing test condition were applied in the simulation. However, it is a fact that the polymer-containing oils showed the behavior of the friction reduction especially for the bronze bearing tests. In addition, it is a fact that the bearing performance (friction coefficient, relative shaft displacement and pressure distribution) was affected by kinds of base oil, additives and bearing materials as shown in the previous chapters.

The polymer-containing oils were blended with a polymer and lower viscosity base oils (PAOs of 2 and 4 mm²·s⁻¹ at 100 °C) than the base oil (PAO of 6 mm²·s⁻¹ at 100 °C) which was tested for the bearing tests, because it is a normal method to make multi-grade engine oils. There is then a possibility that such a combination influenced the oil film formation. It is supposed that the oil film thickness could be much thinner than that expected in the simulation for the bronze bearing and the shear rate in the bearing could be very high. In fact, the magnitude of the relative shaft displacement could be larger for the polymer-containing oils with the bronze bearing tests than that expected as Newtonian-fluids. It can explain a thinner oil film thickness in the actual bearing lubrication, and the high shear rate could cause the sufficient temporary viscosity loss.

The first normal stress difference hardly affected the bearing performance even under 27 kN and 2,000 rpm in the simulation. Bair measured the first normal stress difference for polymer-containing oils under high pressures up to 240 MPa, and the effect of the pressure was indicated [54]. He reported that the effect of pressure is to increase the normal stress for a fixed shear rate. Therefore, it is conceivable that the actual normal stress in the bearing could be larger than that in the simulation because of the influence of the generated Reynolds pressure. Since the thicker oil film thickness for the polymer-containing oils than expected as Newtonian fluids was anticipated with the relative shaft displacement for the Babbitted bearing tests, the effect of the first normal stress is considered to be appeared in the actual bearing lubrication.

There are still some facts that the phenomena appeared in the bearing tests cannot be explained as follows:

- A) PMA1 which includes a low molecular weight (Mw25,000) polymer reduced the friction in both of the Babbitted bearing and the bronze bearing tests.
- B) While the reduction in the friction coefficients was 8 % even under 27 kN of a

high load at 2,000 rpm of a high shaft speed in the simulation with the bronze bearing, that in the experiment was over 40 % under 9 kN at 500 rpm.

It is very difficult to explain the above phenomena only with the simulation using the temporary viscosity loss and the normal stress. From the results in the bearing tests and the simulation, they raised a necessity of further analyses to investigate the behavior of polymers in more detail. Some works to be currently suggested are the investigations of the polymer effect in the oil flow (velocity distribution) between a bearing surface and a shaft surface, and the interaction between polymers and bearing materials.

7-6 Conclusions

The effect of the polymer-containing oils in the bearing performance was examined using the three polymers of which molecular weight were 25,000, 190,000 and 370,000 compared with the base oil. The conclusions are the following:

- (1) The friction coefficients with the polymer-containing oils in the experiments were greatly reduced for the bronze bearing compared to the base oil but not for the Babbitted bearing. It was confirmed that the effect of the polymer-containing oils depended on the bearings used. However, since differences in the bearing clearances were observed, it was considered that the geometry of the bearings can influence the bearing performance (this should be an additional guideline for the development of fuel saving oils with polymers). This also suggests that the deformation of bearings in actual engine operations can affect the effectiveness of polymer-containing oils.
- (2) The relative shaft displacement was measured in the experiments and simulated with the THD analysis. Comparing the experimental results with the simulation, it was considered that the oil film thickness for the polymer-containing oils was thinner with the bronze bearing and thicker with the Babbitted bearing than that expected for Newtonian fluid. It was conceivable that the viscosity loss and the normal stress for the polymer-containing oils affected the frictional property in hydrodynamic lubrication.

Chapter 8

Conclusions

<Summary of the research activity>

From the viewpoint of the prevention from global warming (reduction of CO₂), it has been necessary to improve fuel economy in automotive engines. The improvement of the fuel economy with engine has been also required. It is well known that lowering oil viscosity is effective to reduce the friction in the lubrication of engine parts, but this raises the importance of securing the reliability of the plain bearings. Indeed, it is very important to cope with both of the performance. Also, there is the trend that lead-free materials have been required for automotive plain bearings because of the regulation. From such a background, this study aimed at the following:

- (1) To investigate the effect of base oils on the friction reduction in hydrodynamic lubrication and the reliability improvement in mixed lubrication,
- (2) To investigate the influence of bearing materials on the friction reduction in hydrodynamic lubrication and the reliability improvement in mixed lubrication,
- (3) To investigate the effect of friction modifiers on the reliability improvement in mixed lubrication,
- (4) To investigate the effect of polymers on the friction reduction in hydrodynamic lubrication,
- (5) To experimentally and numerically analyze the bearing lubrication with polymer-containing oils and investigate the mechanism of their action

The plain bearing performance was investigated basically using the bearing test apparatus with different plain bearings for several lubricant components such as base oils, friction

modifiers and polymers. In order to find the effect of the lubricants in the friction reduction and the reliability, the discussion focused in the friction coefficients, the CR ratios and the relative shaft displacement which represents the oil film formation in the bearings. The additional evaluation of the effect of polymers was carried out in the collaboration among the Poitiers University-CNRS-Idemitsu Kosan Co., Ltd. Also, the THD analysis program developed by the Poitiers University was applied to further analyze and confirm the behavior of the lubricant components, especially for the polymers.

As a result of the above mentioned research activities, the conclusions are summarized as follows:

<Conclusions>

Although the summary of the results of the bearing performance evaluation with various lubricant components and bearings is indicated below, overall, it was found that the lubricant components such as base oil, friction modifiers and polymers as well as the bearing materials, affected the frictional property and the reliability in the plain bearing lubrication. It was then confirmed that optimizing the combination of lubricant components enables the improvement of the fuel economy maintaining the reliability of bearing lubrication. These findings lead to a method to enhance the frictional property in plain bearing lubrication-by not only lowering oil viscosity (improving viscosity index) but also carefully selecting lubricant components to be used.

- (1) To investigate the effect of base oils on the friction reduction in hydrodynamic lubrication and the reliability improvement in mixed lubrication
 - a) The contact between the shaft and the plain bearing occurs more readily when low-viscosity base oils were used in comparison with high-viscosity base oils under an equal Hersey number in mixed lubrication region. Thus, even if the viscosity was the same in the test operating conditions, the high-viscosity base oils presented superior reliability in bearing lubrication.
 - b) In addition, frictional losses in the high-viscosity base oils were less than in the low-viscosity base oils under an equal Hersey number in hydrodynamic lubrication.
 - c) The contact between the shaft and the bearing was more likely to occur with highly refined base oils than with low refined base oil (group I base oil)

among base oils with the same low viscosity in mixed lubrication region. Higher friction coefficients were also observed with the group I base oil of low-viscosity in mixed lubrication.

- (2) To investigate the influence of bearing materials on the friction reduction in hydrodynamic lubrication and the reliability improvement in mixed lubrication
 - a) The contact between the shaft and the bearing with the Cu-Pb bearing was likely to occur in a larger Hersey number than with the Al-Si bearing. Thus, the lubricating mode with the Cu-Pb bearing shifted from hydrodynamic to mixed lubrication under a smaller applied load than with the Al-Si bearing.
 - b) The Cu-Pb plain bearing showed a higher friction coefficient than the Al-Si plain bearing in hydrodynamic lubrication and in the region that the lubrication condition with the Cu-Pb was considered to be mixed lubrication.

- (3) To investigate the effect of friction modifiers on the reliability improvement in mixed lubrication
 - a) It was confirmed that the influence of the friction modifiers varied with the lead-free bearing materials. The bearing alloy was closely related to the expression of the performance of the friction modifiers. The ester type friction modifiers without and with sulfur reduced the friction coefficients and increased the CR ratios respectively for the Cu alloy bearings and the Al alloy bearings in mixed lubrication region.

- (4) To investigate the effect of polymers on the friction reduction in hydrodynamic lubrication
 - a) The oil containing polymer of high molecular weight showed lower friction coefficients than the base oil and the oil with low molecular weight polymer for the Cu-Pb plain bearing under an equal Hersey number in hydrodynamic lubrication region but did not for the Al-Si plain bearing. The effect of the polymer-containing oils on the bearing performance was different between the two bearings.

(5) To experimentally and numerically analyze the bearing lubrication with polymer-containing oils and investigate the mechanism of their action

- a) The friction coefficients with the polymer-containing oils in the experiments were greatly reduced for the bronze bearing compared to the base oil but not for the Babbitted bearing. It was confirmed that the effect of the polymer-containing oils depended on the bearings used. However, since differences in the bearing clearances were observed, it was considered that the geometry of the bearings could influence the bearing performance.
- b) The relative shaft displacement was measured in the experiments and simulated with the THD analysis. Comparing the experimental results with the simulation, it was considered that the oil film thickness for the polymer-containing oils was thinner with the bronze bearing and thicker with the Babbitted bearing than that expected for Newtonian fluid. It was conceivable that the viscosity loss and the normal stress for the polymer-containing oils affected the frictional property and the reliability in hydrodynamic lubrication.

<Necessary future work>

In this study, the effect of the bearing performance was globally evaluated with the experiments using the plain bearing test apparatuses and with the simulation (THD analysis). Also, the chemical reaction between the lubricant and the bearing materials was analyzed using the surface analysis device (SEM-EDS) for some cases, in order to confirm the phenomena which occurred in the bearing lubrication.

However, there were some phenomena that cannot be exactly explained only with the results obtained in this study. It was found that the friction coefficient depended on kinds of the lubricant components and the bearing materials even in hydrodynamic lubrication region. Although the differences of each result were considered to be more than the uncertainty of the various measurements, further study should be required in order to ensure it because it has not been the established theory in hydrodynamic lubrication.

In order to confirm the correlation between the frictional property and the oil film formation, measurement of the actual oil film thickness and temperature should be needed using various bearing materials. Another idea is the analysis of the effect of lubricant components and

bearing materials on the oil flow especially for polymer-containing oils because the friction coefficients were significantly reduced using polymers.

In addition, further investigation should be needed under more severe dynamic load conditions because this study mainly focused on the experiments and the analysis under static load conditions.

< A new approach to develop fuel economy engine oils for the future >

Figure 8-1 shows a new approach to develop engine oils which cope with both of the friction reduction and the reliability for plain bearings. Of course, lowering oil viscosity greatly affects the friction reduction. However, it is also important to optimize the rheological properties of lubricants mainly with base oils and polymers. The temporary viscosity loss and the normal stress can affect the oil film formation in the bearing, and subsequently the friction reduction and the reliability in the bearing lubrication. The balance of the viscosity loss and the normal stress could be important.

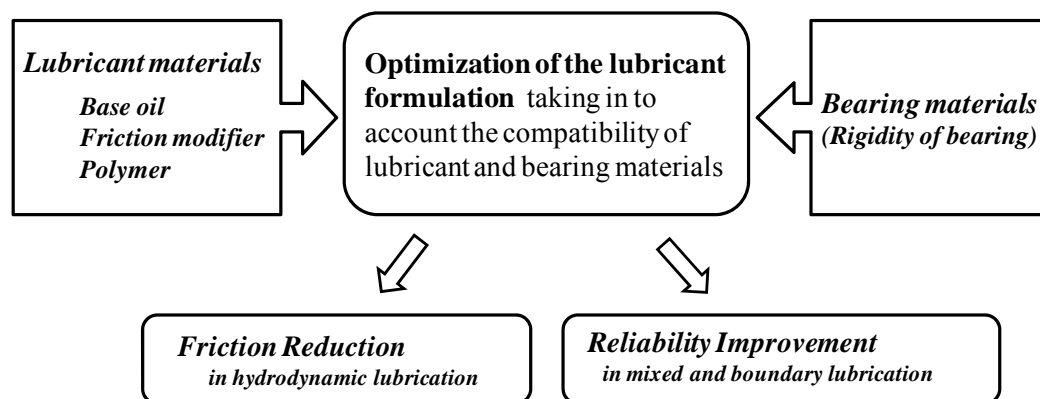


Figure 8-1 A new approach to reduce friction and improve reliability with lubricants

In addition, friction modifiers were confirmed to be effective for improving the plain bearing performance. Materials such as base oils, polymers and friction modifiers therefore need to be carefully selected because the plain bearing performance depends on plain bearing materials (the stiffness of the bearing materials is also needed to be considered for the lubrication with polymer-containing oils although it can be a new subject to be investigated).

As mentioned in the introduction, the standard of the SAE (Society of Automotive

Engineers) gives viscosity grades for engine oils. The lowest viscosity grade is currently 0W-20, which is mainly for gasoline engine oils. The findings in the study enable to enhance the fuel economy and the reliability for engine oils of such an existing viscosity-grade in addition to the contribution due to the viscosity index improvement.

Some of car manufactures and lubricant manufactures have started the examination of lower viscosity engine oils than 0W-20. Also, the standardization of 0W-10 grade was under consideration at the SAE, but it was decided that it would not be standardized because of the concern about damage of plain bearings. However, if the engine oil of such a low-viscosity grade was formulated with carefully selected lubricant materials taking into account bearing materials used, it would enable a great enhancement of the reliability and accelerate the trend of lowering engine oil viscosity which leads to the fuel economy improvement.

APPENDIX I - THD Analysis of plain bearing performance

In order to analyze the effects of the polymer-containing oils on the plain bearing performance, friction coefficient, relative shaft displacement, pressure distribution, temperature distribution and minimum oil film thickness were calculated with the THD analysis program developed at the Poitiers University [66-70]. The most detailed information on the THD analysis was presented by Pierre and Fillon in 2004 [66].

<Theoretical model>

The numerical analysis used was a three-dimensional THD study of a plain journal bearing with an axial groove. The geometry and the coordinate system of the journal bearing are defined in Figure A1. The oil is supplied from opposite side of the loading direction from the bottom.

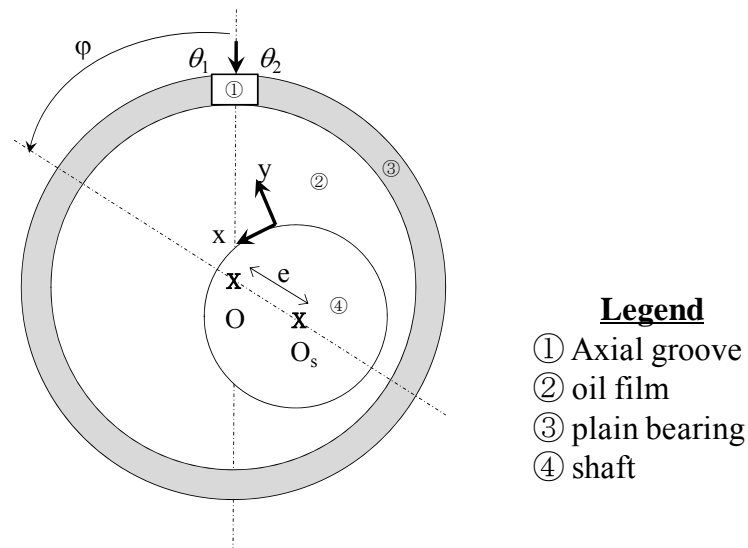


Figure A1 Plain bearing geometry

Generalized Reynolds equation

The generalized Reynolds equation in laminar conditions is expressed as follows.

$$\frac{\partial}{\partial x} \left(g\gamma G \frac{\partial \Theta}{\partial x} \right) + \frac{\partial}{\partial z} \left(g\gamma G \frac{\partial \Theta}{\partial z} \right) = R\omega \frac{\partial}{\partial x} \left(\Theta \frac{I_2}{J_2} \right)$$

with

$$G = \int_0^h \frac{y}{\mu} \left(y - \frac{I_2}{J_2} \right) dy \quad I_2 = \int_0^h \frac{y}{\mu} dy \quad J_2 = \int_0^h \frac{dy}{\mu}$$

In this expression, γ varies with the lubricant compressibility in the full-film region and the pressure p is given by

$$p = g \gamma \ln \Theta + p_c \quad \Theta = \frac{\rho}{\rho_c}$$

p_c is the pressure at cavitation. In the full-film zone, Θ is the ratio of the local fluid density ρ to the oil cavitated density ρ_c . In the rupture zone, Θ represents the local fraction of the bearing gap occupied by lubricant. The cavitation index g is equal to 0 in the cavitation zone ($\Theta < 1$) or equal to 1 in the full-film zone ($\Theta \geq 1$).

The Reynolds equation is solved numerically by finite difference techniques and requires the following boundary conditions:

$$p = \begin{cases} p_{\text{sup}} & \text{in the supply groove} \\ 0 & \text{at } z=0 \text{ and } z=B \end{cases}$$

Temperature field

The temperature field in the lubricant film is determined by solving the energy equation:

$$\rho C_p \left(\frac{u}{R^2} \frac{\partial T}{\partial \theta} + v \frac{\partial T}{\partial y} + w \frac{\partial T}{\partial z} \right) = K \frac{\partial^2 T}{\partial y^2} + \mu \left[\left(\frac{\partial u}{\partial y} \right)^2 + \left(\frac{\partial w}{\partial y} \right)^2 \right]$$

In addition, the THD analysis involves the treatment of the heat transfer into the bush by using the Laplace equation:

$$\frac{\partial^2 T_b}{\partial r_b^2} + \frac{1}{r_b} \frac{\partial T_b}{\partial r_b} + \frac{1}{r_b^2} \frac{\partial^2 T_b}{\partial \theta_b^2} + \frac{\partial^2 T_b}{\partial z_b^2} = 0$$

In order to determine the temperature field, the following thermal boundary conditions are applied:

- The continuity of heat flux at the film/bush interface is imposed.
- The average temperature at the leading edge is obtained by using a balance of thermal flux in the groove.
- A nil energy balance determines the temperature at the film/shaft interface.

Local oil film thickness

The local oil film thickness h is determined with the following equation:

$$h(\theta, z) = C + e_0 \cos(\theta - \varphi)$$

<Lubricant characteristics>

For the lubricants, the dynamic viscosity μ_L depends on the temperature field; the Mac Coull and Walther relationship can be used:

$$\log_{10} \log_{10} \left(\frac{\mu_L(\theta, y, z)}{\rho_L} + a \right) = -m \log_{10} [T(\theta, y, z)] + n$$

where the coefficients m and n depend on the lubricant type and are determined by two values of viscosity obtained for different temperatures. For the coefficient a , a value of $0.6 \text{ mm}^2 \cdot \text{s}^{-1}$ is applied, as commonly used in numerical simulations.

The thermal characteristics of the base oils and the polymer-containing oils for $60 \text{ }^\circ\text{C}$ are shown in table1 A1 and A2.

Table A1 Thermal characteristics of the base oils

| | | Sample A | Sample AA |
|----------------------|---------|------------------|------------------|
| | | Group I base oil | Group I base oil |
| | | 150N | 500N |
| Specific heat | J/kg °C | 1865 | 1851 |
| Thermal conductivity | W/m °C | 0.129 | 0.128 |

Table A2 Thermal characteristics of the base oil and the polymer-containing oils

| | | B/O | PMA1 | PMA2 | PMA3 |
|----------------------|---------|----------|---------------------|----------------------|----------------------|
| | | Base oil | Polymer of Mw25,000 | Polymer of Mw190,000 | Polymer of Mw370,000 |
| Specific heat | J/kg °C | 1916 | 1911 | 1924 | 1929 |
| Thermal conductivity | W/m °C | 0.138 | 0.138 | 0.138 | 0.138 |

<Thermal characteristics of the bearings>

The thermal characteristics used for the Cu-Pb bearing, the Al-Si bearing, the Babbitted bearing and the bronze bearing are shown in Tables A3.

Table A3 Thermal characteristics for the bearings used

| | | Cu-Pb | Al-Si | Babbitt | Bronze |
|---|--------------------|---------|---------|---------|---------|
| Thermal conductivity | W/m K | 71 | 155 | 45 | 65 |
| Heat exchange coefficient between the bearing housing and the external bearing surface | W/m ² K | 1,000 | 1,000 | - | |
| Heat exchange coefficient between the ambient air and the external bearing surface | W/m ² K | - | - | 40 | |
| Heat exchange coefficient between the supply oil and the bearing groove surface | W/m ² K | 750 | | | |
| Thermal expansion coefficient | K ⁻¹ | 18.0E-6 | 24.0E-6 | 12.0E-6 | 18.0E-6 |

References

- [1] Tamoto Y., Kido M. and Murata H., 2004, “Possibilities of Ultra-Low-Viscosity Fuel-Saving Gasoline Engine Oil”, SAE Paper 2004-01-1936, 6 pages
- [2] Ogita Y., Niwa K and Tanaka T., 1988, “Measurement of Bearing Friction Loss under Dynamic Load”, SAE Paper 880547, 10 pages
- [3] Sagawa T., Ueno T., Nakamura K., Ishikawa T., Ando T. and Ishikawa M., 2002, “Development of 0W-20 ILSAC GF-3 Gasoline Engine Oil”, SAE Paper 2002-01-1636, 9 pages
- [4] Kawai H., Hoshino K. and Akiyama K., 1998, “Fuel Efficiency of SAE 5W-20 Friction Modified Gasoline Engine Oil”, SAE Paper 982506, 6 pages
- [5] Tanaka H., Nagashima T., Sato T. and Kawauchi S., 1999, “The Effect of 0w-20 Low Viscosity Engine Oil on Fuel Economy”, SAE Paper 1999-01-3468, 5 pages
- [6] Bennett J. and Chudasama D., 2000, “The Use of Low Viscosity Oils to Improve Fuel Economy in Light-Duty Diesel Engines”, SAE Paper 2000-01-2054, 6 pages
- [7] Jeon S.I., Kim H.G., Yoo S.E. and Oh M.H., 2007, “The Effect on Friction of Engine Oil Seal Using Low Viscosity Engine Oil for Fuel Economy Improvement”, SAE Paper 2007-01-3539, 6 pages
- [8] Fontaras G., Samaras Z. and Vouitsis E., 2009, “Experimental Evaluation of Low Viscosity Lubricant Fuel Consumption and CO2 Emissions Reduction Potential”, SAE Paper 2009-01-1803, 9 pages
- [9] Daido Metal Co., Ltd., 2002, Data Book of Plain Bearing Technology for Automobile Engines (in Japanese)
- [10] Ono A., Kurimoto S., Kawachi T., Arai K. and Kuribayashi T., 1998, “Properties of Engine Bearing Lubricated with Low HTHS Viscosity Oil”, SAE Paper 980702, 9 pages
- [11] Katafuchi T., and Kasai M., 2009, “Effect of Base Stocks on the Automotive Engine Bearing”, Tribology International, Vol. 42, pp. 548-553
- [12] Council Decision of 20 September 2006 Amending Annex II of Directive 2000/53/EC of the European Parliament and of the Council on End-of-Life Vehicles (2005/673/EC)
- [13] Sakai K., Zushi K., Sugita M. and Ishikawa H., 2004, “Development of Lead-Free-Copper-Based Alloy for Three Layers Bearings under Higher Load Engines”, SAE Paper 2004-01-1600, 7 pages

- [14] Kawachi T., Takayanagi S., Asakura H., and Ishikawa H., 2005, "Development of Lead Free Overlay for Three Layer Bearings of Highly Loaded Engines", SAE Paper 2005-01-1863, 8 pages
- [15] Okrent E. H., 1961, "The Effect of Lubricant Viscosity and Composition on Engine Friction and Bearing Wear", ASLE Trans., Vol. 4, pp. 97-106
- [16] Okrent E. H., 1961, "The Effect of Lubricant Viscosity and Composition on Engine Friction and Bearing Wear II", ASLE Trans., Vol. 4, pp. 257-262
- [17] Okrent E. H., 1964, "Engine Friction and Bearing Wear. III. The Role of Elasticity in Bearing Performance", ASLE Trans., Vol. 7, pp. 147-152
- [18] Tao F. F. and Philippoff W., 1967, "Hydrodynamic Behavior of Viscoelastic Liquids in a Simulated Journal Bearing", ASLE Trans., Vol. 10, pp. 302-315
- [19] Waddey W.E. and Pearce A.F., 1969, "Effects of Crankcase Oil Composition on Engine Wear", SAE Paper 690774, 8 pages
- [20] U. Schardel, 1970, "Polymethacrylates for Tomorrow's Multigrade Oils", SAE Paper 700054, 7 pages
- [21] Wada S. and Hayashi H., 1970, "Hydrodynamic Lubrication of Journal Bearings by Pseudo-Plastic Lubricants: Part 1, Theoretical Studies", Transactions of the Japan Society of Mechanical Engineers, Vol. 36, pp. 1183-1193
- [22] Wada S. and Hayashi H., 1970, "Hydrodynamic Lubrication of Journal Bearings by Pseudo-Plastic Lubricants: Part 2, Experimental Studies", Transactions of the Japan Society of Mechanical Engineers, Vol. 36, pp. 1194-1201
- [23] Rosenberg R.C., 1973, "A Method for Determining the Influence of Multigrade Oils on Journal Bearing Performance", SAE Paper 730483, 11 pages
- [24] Rosenberg R.C., 1975, "The influence of Polymer Additives on Journal Bearing Performance", SAE Paper 750692, 13 pages
- [25] Harnoy A., 1977, "Three Dimensional Analysis of the Elastico-viscous Lubrication in Short Journal Bearings", Rheologica Acta, Vol. 16, pp. 51-60
- [26] Bell J.C. and Voisey M.A., 1977, "Some Relationships between the Viscometric Properties of Motor Oils and Performance in European Engines", SAE Paper 770378, 12 pages
- [27] McMillan M.L., Rosenberg R.C. and Murphy C.K., 1978, "Viscosity Effects on Engine Wear Under High Temperature, High-Speed Conditions", SAE Paper 780982, 18 pages

- [28] Dancy J.H., Marshall H.T. and Oliver C.R., 1980, "Determining Frictional Characteristics of Engine Oils by Engine Friction and Viscosity Measurements", SAE Paper 800364, 8 pages
- [29] Dancy J.H., Marshall H.T. and Oliver C.R., "A Test to Relate The Loss of Hydrodynamic Lubrication in an Automotive Journal Bearing to Lubricant Viscosity", SAE Paper 810798, 10 pages
- [30] DeHart A.O., Rosenberg R.C., Hill R.F. and Schneider E.W., 1980, "Determining Frictional Characteristics of Engine Oils by Engine Friction and Viscosity Measurements", SAE Paper 800361, 8 pages
- [31] Phan-Thien N. and Tanner R.I., 1981, "Journal Lubrication and Normal Stress Measurement", *J. Non-Newtonian Fluid Mech.*, Vol. 9, pp. 107-117
- [32] Van Os N., Rhodes R. B. and Covey D. F., 1981, "A Study of Lubricating Oil Performance in a Journal Bearing Rig, II", SAE Paper 810801, 6 pages
- [33] Van Os N., Garcia-Franco C.A., Gottenberg W.G. and Tripp H.A., 1983, "The Effect of Lubricant Elasticity on Journal Bearing Performance under Static Load", SAE Paper 831690, 14 pages
- [34] Rhodes R.B. and Henderson B.M., 1981, "The Effects of Engine Oil Viscosity and Composition on Bearing Wear", SAE Paper 811224, 14 pages
- [35] Filowitz M.S., King W.H. and Appeldoorn J.K., 1982, "Oil-Film Thickness in a Bearing of a Fired Engine", SAE Paper 820511, 8 pages
- [36] Craig R.C., King Jr. W.H., and Appeldoorn L.K., 1982, "Oil Film Thickness in a Bearing of a Fired Engine Part II: The Bearing as a Capacitor", SAE Paper 821250, 8 pages
- [37] Schneider E. W. and Rosenberg R. C., 1982, "The Effect of Fuel-Saving Engine Oils on Journal Bearing Load Capacity - A Radiometric Evaluation", SAE Paper 821205, 10 pages
- [38] Hutton J.F., Jones B. and Bates T.W., 1983, "Effects of Isotropic Pressure on the High Temperature High Shear Viscosity of Motor oils", SAE Paper 830030, 12 pages
- [39] Bates T.W., Williamson B. P., Spearot J. A. and Murphy C. K., 1986, "Rheology and Oil Film Thickness in Engine Journal Bearings", SAE paper 860376, 18 pages
- [40] Bates T. W. and Toft G. B., 1989, "Effect of Oil Rheology on Journal Bearing Performance: Part 4 - Bearing Durability and Oil Film Thickness, SAE Paper 892154, 14 pages
- [41] Olson D.H., 1987, "Relationship of Engine Bearing Wear and Oil Rheology", SAE Paper 872128, 10 pages

- [42] Rastogi A. and Gupta R.K., 1990, "Lubricant Elasticity and the Performance of Dynamically Loaded Short journal Bearings", *J. of Rheology*, Vol. 34, 8, pp. 1337-1356
- [43] Davies A.R. and Li X.K., 1994, "Numerical Modeling of Pressure and Temperature Effects in Viscoelastic Flow between Eccentrically Rotating Cylinder, *J. of non-Newtonian Fluid Mechanics*, Vol. 54, pp. 331-350
- [44] Berker A., Bouldin M.G., Kleis S.J. and VanArsdale W.E., 1995, "Effect of Polymer on Flow in Journal Bearings", *J. of Non-Newtonian Fluid Mechanics*, Vol. 56, pp. 333-347
- [45] Williamson B.P. and Milton A., 1995, "Characterisation of the Viscoelasticity of Engine Lubricants at Elevated Temperatures and Shear Rates", SAE Paper 951032, 18 pages
- [46] Williamson B. P., Walters K., Bates T. W., Coy R.C. and Milton A. L., 1997, "The Viscoelastic Properties of Multigrade Oils and their Effect on Journal-Bearing Characteristics", *J. Non-Newtonian Fluid Mech.*, Vol. 73, pp. 115-126
- [47] Williamson B. P., 1997, "Enhancement of Journal Load Bearing Capacity by Polymer Containing Oils", SAE Paper 971697, 20 pages
- [48] Li X.K., Phillips T.N., Williamson B.P., Scales L.E. Davies A.R. and Gwynllyw D.Rh., 1997, "The Effect of Lubricant Rheology on the Performance of Dynamically Loaded Journal Bearings", SAE Paper 973002, 9 pages
- [49] Bair S., 1996, "Normal stress difference in liquid lubricants sheared under high pressure", *Rheologica Acta.*, Vol. 35, pp. 13-23
- [50] Bair S., Lockwood F. E., Anderson W. B., Zhang Z. and Dotson D., 2007, "Measurements of Elasticity in Multigrade Motor Oil at Elevated Pressure", *Tribology Transactions*, Vol. 50, pp. 407-414
- [51] Sorab J., Korcek S., Brower C.L. and Hammer W.G., 1996, "Friction Reducing Potential of Low Viscosity Engine Oils in Bearings", SAE Paper 962033, 8 pages
- [52] Ono A., Kurimoto S., Kawachi T., Arai K. and Kuribayashi T., 1998, "Properties of Engine Bearings Lubricated with Low HTHS Viscosity Oil", SAE Paper 980702, 9 pages
- [53] Kawagoe K., Kanayama H., Desaki T. and Fuwa Y., 2003, "New Conceptual Lead Free Overlays Consisted of Solid Lubricant for Internal Combustion Engine Bearings", SAE Paper 2003-01-0244, 7 pages
- [54] Hunter J. C. and Whitney Jr. W. J., 2005, "A New Family of Lead-Free Aluminum-Base Engine Bearing Alloys", SAE Paper 2005-01-1866, 9 pages
- [55] Asakura H., Tsuji H., Kagohara Y., Sonobe H. and Fujita M., 2008, "A Study of Lead-Free Aluminum Alloy Bearings with Overlay for Recent Automotive Engines", SAE Paper 2008-01-0091, 8 pages

- [56] Wang J.L., Stohr T., Eisenberg B., Muller M. and Bartels T., 2009, "Defined Comb-Shaped Viscosity Modifiers and Their Impact on Fuel Economy in Modern Driveline Lubricants and Engine Oils", Proceedings of World Tribology Congress 2009, pp. 71(C2-142)
- [57] Tokunaga H., Nishida M., Koike M. and Nakanishi H., 2009, "Viscosity Index Improvers for Low Viscosity Lubricants", Proceedings of World Tribology Congress 2009, pp. 325(C2-232)
- [58] Yoshida S., Maruyama M. and Naito Y., 2009, "Fuel Efficiency of Super High Viscosity Index 0W-20 Engine Oil", Proceedings of World Tribology Congress 2009, pp. 574(C2-342)
- [59] Wang Y. and Jane W.Q, 2006, "Development of a Set of Stribeck Curves for Conformal Contacts of Rough Surfaces" STLE Tribology Transactions, Vol. 49, pp. 526-535
- [60] Base Oil Interchangeability Guidelines: API Publication 1509, API, 13th Ed., Washington D.C., 1995
- [61] Pierre I., Bouyer J. and Fillon M., 2004, "Thermohydrodynamic Behavior of Misaligned Plain Journal Bearings: Theoretical and Experimental Approaches", STLE Tribology Transaction, Vol. 47, pp. 594-604
- [62] Ferron J., Frene J. and Boncompain R., 1983, "A Study of the Thermohydrodynamic Performance of a Plain Journal Bearing-Comparison Between Theory and Experiments", ASME J. Lubr. Technol., Vol. 105, pp. 422-428
- [63] Bouyer J. and Fillon M., 2002, "An Experimental Analysis of Misalignment Effects on Hydrodynamic Plain Journal Bearing Performances", ASME Journal of Tribology, Vol. 124, pp. 313-319
- [64] Pierre I. and Fillon M., 2000, "Influence of Geometric Parameters and Operating Conditions on The Thermohydrodynamic Behaviour of Plain Journal Bearings", Proc. Instn Mech. Engrs, Part J: J. Engineering Tribology, Vol. 214, pp. 445-457
- [65] Boncompain R., Fillon M. and Frene J., 1986, "Analysis of Thermal Effects in Hydrodynamic Bearings", ASME Journal of Tribology, Vol.108, pp. 219-224
- [66] Boedo S. and Booker J.F., 1997, "Surface Roughness and Structure Inertia in a Mode-Based Mass-Conserving Elastohydrodynamic Lubrication Model", ASME Journal of Tribology, Vol. 119, pp. 449-455
- [67] Ozasa T., 2008, "Surface Roughness and Pressure Effect on Viscosity in Elastohydrodynamic Lubrication Model of Engine Bearings", The Japan Society of Mechanical Engineers, Vol. 74, 740, pp. 1034-1041 (in Japanese)

- [68] Tala-Ighil N., Maspeyrot P., Fillon M. and Bounif A., 2007, "Effects of Surface Texture on Journal-bearing Characteristics Under Steady-state Operating Conditions", Proc. Instn Mech. Engrs, Part J: J. Engineering Tribology, Vol. 221, pp. 623-633
- [69] Katafuchi T. and Shimizu N., 2007, "Evaluation of the Antiwear and Friction Reduction Characteristics of Mercaptocarboxylate Derivatives as Novel Phosphorous-Free Additives", Tribology International, Vol. 40, pp. 1017-1024
- [70] Choo J.H., Spikes H.A., Ratoi M., Glovnea R.P. and Forrest A.K., 2007, "Friction Reduction in Low-load Hydrodynamic Lubrication with a Hydrophobic Surface", Tribology International, Vol. 40, pp. 154-159
- [71] Choo J.H., Glovnea R.P., Forrest A.K. and Spikes H.A., 2007, "A Low Friction Bearing Based on Liquid Slip at The Wall", ASME Transaction Journal of Tribology, Vol. 129, pp. 611-620
- [72] Choo J.H., Forrest A.K. and Spikes H.A., 2007, "Influence of Organic Friction Modifier on Liquid Slip: A New Mechanism of Organic Friction Modifier Action", Tribology Letter, Vol. 27, pp. 239-244
- [73] Katafuchi T. and Kasai M., 2007, "Effects of Polymer-Additives on Plain Bearing Performance", Tribology Conference Proceedings in Saga Japan, pp. 293-294 (in Japanese)
- [74] Loadge A.S., 1989, "An Attempt to Measure the First Normal-Stress Difference N_1 in Shear Flow for a Polyisobutylene/Decalin Solution "D2b" at Shear Rates up to 10^6 s^{-1} ", Journal of Rheology, Vol.33, pp. 821-841
- [75] Boger D.V. and Denn M.M., 1980, "Capillary and Slit Methods of Normal Stress Measurements", Journal of Non-Newtonian Fluid Mechanics, Vol.6, pp. 163-185
- [76] Han C.D, Charles M. and Philippoff W., 1970, "Rheological Implication of the Exit Pressure and Die Swell in Steady Capillary Flow of Polymer Melts. I. The Primary Normal Stress Difference and the Effect of L/D Ratio on Elastic Properties", Transaction of the Society of Rheology, Vol. 14.3, pp. 393-408
- [77] Han C.D. and Kim K.U., 1972, "Viscoelastic Properties of Polymer Solutions. II. Measurements of the Wall Normal Stress in Slit Flow", Rheologica Acta, Vol. 11, pp. 323-329
- [78] Han C.D., 1974, "On Slit- and Capillary-Die Rheometry", Transaction of the Society of Rheology, Vol. 18.1, pp. 163-190

List of figures

Figure 1 Effect of oil viscosity in engine motoring torque (fuel economy)

Figure 1-1 General formulation of engine oil

Figure 1-2 Viscometric property for base oil with and without polymer

Figure 1-3 Common approach to reduce friction and improve reliability in plain bearing lubrication with lubricants

Figure 2-1 Main portion of the developed apparatus

Figure 2-2 Disassembled apparatus

Figure 2-3 Schematic representation of the bearing test apparatus

Figure 2-4 Location of proximity probes

Figure 2-5 Circuit diagram to measure the CR (contact resistance) ratio

Figure 2-6 Positions for measuring the gap between the shaft and the plain bearing and the definition of the displacement direction

Figure 2-7 Bearing test patterns

Figure 2-8 Friction coefficient and CR ratio vs. applied load for base oil of API Group III 150N at an oil temperature of 60 °C and a shaft speed of 500 rpm (Cu-Pb plain bearing)

Figure 2-9 Friction coefficient and CR ratio vs. Hersey number for API Group IV 500N at 100 °C with Cu-Pb bearing (η was calculated with the feeding oil temp.)

Figure 2-10 Friction coefficient and CR ratio vs. Hersey number for API Group IV 500N at 100 °C with Cu-Pb bearing (η was calculated with temperature at the bearing back-face)

Figure 2-11 Repeatability for friction coefficient and CR ratio vs. Hersey number for API Group IV 500N at 100 °C with Cu-Pb bearing (η was calculated with the temperature of the bearing back-face)

Figure 2-12 Relative shaft displacement for Group III 500N at 100 °C with Cu-Pb bearing

Figure 2-13 Relationship between applied dynamic load and rotation phase of the shaft

Figure 2-14 Bearing torque, CR ratio and relative shaft displacement vs. load under dynamic load for Group IV 500N at 100 °C with Cu-Pb bearing

Figure 3-1 Dynamic viscosity vs. temperature for the base oil samples

Figure 3-2 Friction coefficient and CR ratio vs. Hersey number for sample A at 60 °C

Figure 3-3 Friction coefficient and CR ratio vs. Hersey number for sample B at 60 °C

- Figure 3-4 Friction coefficient and CR ratio vs. Hersey number for sample C at 60 °C
- Figure 3-5 Friction coefficient and CR ratio vs. Hersey number for sample D at 60 °C
- Figure 3-6 Friction coefficient and CR ratio vs. Hersey number for sample AA at 100 °C
- Figure 3-7 Friction coefficient and CR ratio vs. Hersey number for sample BB at 100 °C
- Figure 3-8 Friction coefficient and CR ratio vs. Hersey number for sample CC at 100 °C
- Figure 3-9 Friction coefficient vs. Hersey number for the low-viscosity base oils at 500 rpm and 60 °C
- Figure 3-10 CR ratio vs. Hersey number for the low-viscosity base oils at 500 rpm and 60 °C
- Figure 3-11 Relative shaft displacement for the low-viscosity base oils at 500 rpm and 60 °C
- Figure 3-12 Photograph of the Cu-Pb bearing surface
- Figure 3-13 Friction coefficient vs. Hersey number for the high-viscosity base oils at 500 rpm and 100 °C
- Figure 3-14 CR ratio vs. Hersey number for the high-viscosity base oils at 500 rpm and 100 °C
- Figure 3-15 Relative shaft displacement for the high-viscosity base oils at 500 rpm and 100 °C
- Figure 3-16 Friction coefficient vs. Hersey number in the experiment and simulation (60 °C, 500 rpm)
- Figure 3-17 Bearing pressure distribution vs. bearing angle in the simulation for sample AA (60 °C, 500 rpm and 10 kN, Angle 0°: The opposite side of the loading.)
- Figure 3-18 Bearing torque, CR ratio and relative shaft displacement vs. load for sample A at 60 °C and 1,000 rpm
- Figure 3-19 Bearing torque, CR ratio and relative shaft displacement vs. load for sample C at 60 °C and 1,000 rpm
- Figure 3-20 Bearing torque, CR ratio and relative shaft displacement vs. load for sample AA at 80 °C and 1,000 rpm
- Figure 3-21 Bearing torque, CR ratio and relative shaft displacement vs. load for sample CC at 80 °C and 1,000 rpm
- Figure 4-1 Three-dimensional images and surface roughness of the new plain bearings
- Figure 4-2 Friction coefficient and CR ratio vs. Hersey number for 60 °C and shaft speeds of 500, 1,000, 2,000 and 3,000 rpm with sample A
- Figure 4-3 Friction coefficient and CR ratio vs. Hersey number for 60 °C and shaft speeds of 500, 1,000, 2,000 and 3,000 rpm with sample B
- Figure 4-4 Friction coefficient and CR ratio vs. Hersey number for 60 °C and shaft speeds of 500, 1,000, 2,000 and 3,000 rpm with sample C

- Figure 4-5 Friction coefficient and CR ratio vs. Hersey number for 60 °C and shaft speeds of 500, 1,000, 2,000 and 3,000 rpm with sample D
- Figure 4-6 Friction coefficient vs. Hersey number at 500 rpm and 60 °C
- Figure 4-7 CR ratio vs. Hersey number at 500 rpm and 60 °C
- Figure 4-8 Bearing back-face temperature vs. load for sample A at a feeding oil temperature of 60 °C
- Figure 4-9 Friction coefficients vs. Hersey number calculated using the back-face temperature of the Cu-Pb bearing for the Al-Si bearing test with sample A
- Figure 4-10 Relative shaft displacement at 500 rpm and 60 °C
- Figure 4-11 Estimated shaft displacement for sample A
- Figure 4-12 Friction coefficient vs. Hersey number in the experiment and simulation (60 °C, 500 rpm)
- Figure 4-13 Friction coefficient and CR ratio vs. Hersey number at 60 °C and 3,000 rpm
- Figure 4-14 Relative shaft displacement at 60 °C and 3,000 rpm
- Figure 4-15 Bearing torque, CR ratio and relative shaft displacement vs. load for sample A at 60 °C under dynamic load condition
- Figure 4-16 Bearing torque, CR ratio and relative shaft displacement vs. load for sample C at 60 °C under dynamic load condition
- Figure 5-1 Structure of cross-section of the plain bearings
- Figure 5-2 Dynamic vis. of the oils tested
- Figure 5-3 Friction coefficient and CR ratio vs. Hersey number with the base oil in PB-A (Bi/Ag-Cu)
- Figure 5-4 Friction coefficient and CR ratio vs. Hersey number with the base oil in PB-B (Bi-Cu)
- Figure 5-5 Friction coefficient and CR ratio vs. Hersey number with the base oil in PB-C (Bi/Ag-Al)
- Figure 5-6 Friction coefficient and CR ratio vs. Hersey number with the base oil in PB-D (Bi/Ag-Al)
- Figure 5-7 Friction coefficient and CR ratio vs. Hersey number with FM-A (w/o S) in PB-A (Bi/Ag-Cu)
- Figure 5-8 Friction coefficient and CR ratio vs. Hersey number with FM-A (w/o S) in PB-B (Bi-Cu)
- Figure 5-9 Friction coefficient and CR ratio vs. Hersey number with FM-A (w/o S) in PB-C (Bi/Ag-Al)

- Figure 5-10 Friction coefficient and CR ratio vs. Hersey number with FM-A (w/o S) in PB-D (Bi/Ag-Al)
- Figure 5-11 Friction coefficient and CR ratio vs. Hersey number with FM-B (with S) in PB-A (Bi/Ag-Cu)
- Figure 5-12 Friction coefficient and CR ratio vs. Hersey number with FM-B (with S) in PB-B (Bi-Cu)
- Figure 5-13 Friction coefficient and CR ratio vs. Hersey number with FM-B (with S) in PB-C (Bi/Ag-Al)
- Figure 5-14 Friction coefficient and CR ratio vs. Hersey number with FM-B (with S) in PB-D (Bi/Ag-Al)
- Figure 5-15 Friction coefficient with PB-A (Bi/Ag-Cu)
- Figure 5-16 Friction coefficient with PB-B (Bi-Cu)
- Figure 5-17 Friction coefficient with PB-C (Bi/Ag-Al)
- Figure 5-18 Friction coefficient with PB-D (Bi/Ag-Al)
- Figure 5-19 CR ratio with PB-A (Bi/Ag-Cu)
- Figure 5-20 CR ratio with PB-B (Bi-Cu)
- Figure 5-21 CR ratio with PB-C (Bi/Ag-Al)
- Figure 5-22 CR ratio with PB-D (Bi/Ag-Al)
- Figure 5-23 Reciprocating type friction tester
- Figure 5-24 Friction coefficients vs. reciprocating number with the reciprocating friction tester
- Figure 5-25 Relative shaft displacement in vertical direction and CR ratio vs. relative shaft displacement in horizontal direction with PB-A (Bi/Ag-Cu)
- Figure 5-26 Relative shaft displacement in vertical direction and CR ratio vs. relative shaft displacement in horizontal direction with PB-B (Bi-Cu)
- Figure 5-27 Relative shaft displacement in vertical direction and CR ratio vs. relative shaft displacement in horizontal direction with PB-C (Bi/Ag-Al)
- Figure 5-28 Relative shaft displacement in vertical direction and CR ratio vs. relative shaft displacement in horizontal direction with PB-D (Bi/Ag-Al)
- Figure 5-28 Composition ratio of elements on PB-A (Bi/Ag-Cu) and PB-D (Bi/Ag-Al)
- Figure 6-1 Dynamic viscosity versus temperature of the lubricants tested
- Figure 6-2 Friction coefficient and CR ratio vs. Hersey number at 100 °C for the base oil with the Cu-Pb bearing
- Figure 6-3 Friction coefficient and CR ratio vs. Hersey number at 100 °C for polymer A with the Cu-Pb bearing

- Figure 6-4 Friction coefficient and CR ratio vs. Hersey number at 100 °C for polymer B with the Cu-Pb bearing
- Figure 6-5 Comparison of friction coefficient and CR ratio vs. Hersey number at 100 °C with the Cu-Pb bearing
- Figure 6-6 Friction coefficient and CR ratio vs. Hersey number at 100 °C for the base oil with the Al-Si bearing
- Figure 6-7 Friction coefficient and CR ratio vs. Hersey number at 100 °C for polymer A with the Al-Si bearing
- Figure 6-8 Friction coefficient and CR ratio vs. Hersey number at 100 °C for polymer B with the Al-Si bearing
- Figure 6-9 Comparison of friction coefficient with the Al-Si bearing
- Figure 6-10 Friction coefficient and CR ratio vs. Hersey number for 500 rpm and 100 °C with the Cu-Pb bearing
- Figure 6-11 Friction coefficient and CR ratio vs. Hersey number for 500 rpm and 100 °C with the Al-Si bearing
- Figure 6-12(a) Relative shaft displacement with Cu-Pb bearing for 500 rpm and 100 °C
- Figure 6-12(b) Relative shaft displacement with Cu-Pb bearing for 3,000 rpm and 100 °C
- Figure 6-13(a) Relative shaft displacement with Ai-Si bearing for 500 rpm and 100 °C
- Figure 6-13(b) Relative shaft displacement with Ai-Si bearing for 3,000 rpm and 100 °C
- Figure 6-14 Bearing torque and CR ratio for the base oil (80°C) and the polymer-containing oils (100 °C) at 1,000 rpm with the Cu-Pb bearing under dynamic load condition
- Figure 6-15 Bearing torque and CR ratio for the base oil (80°C) and the polymer-containing oils (100 °C) at 1,000 rpm with the Al-Si bearing under dynamic load condition
- Figure 7-1 Estimated shaft displacement due to temporary viscosity loss and first normal stress generation
- Figure 7-2 Bearing test apparatus at the Poitiers University
- Figure 7-3 Babbitted bearing
- Figure 7-4 Bronze bearing
- Figure 7-5 Location of thermocouples, pressure holes and gap sensors
- Figure 7-6 Bearing test pattern
- Figure 7-7 Dynamic viscosity of the lubricants used for the bronze bearing test
- Figure 7-8 Rotational (Cone and plate) type rheometer
- Figure 7-9 Schematic of the slit die rheometer
- Figure 7-10 Pressure profiles in the rheometer with the base oil at 60 °C

Figure 7-11 Viscosity vs. shear rate for the base oil and the polymer-containing oils at 40, 60 and 80 °C

Figure 7-12 First normal stress difference (N1) vs. wall shear rate and wall shear stress for the polymer-containing oils at 40, 60 and 80 °C

Figure 7-13 Friction coefficient vs. Hersey number at 60 °C for the Babbitted bearing and the bronze bearing

Figure 7-14 Bearing clearance vs. feeding oil temperature for the base oil in the Babbitted bearing and the bronze bearing

Figure 7-15 Friction coefficient vs. Hersey number at 60 and 80 °C, and 500 rpm under 7.2 and 9.0 kN for the Babbitted bearing and the bronze bearing

Figure 7-16(a) Relative shaft displacement in the experiment at 500 rpm and 60 °C for the Babbitted bearing

Figure 7-16(b) Relative shaft displacement in the experiment at 500 rpm and 60 °C for the Babbitted bearing

Figure 7-16(c) Relative shaft displacement in the experiment at 500 rpm and 60 °C for the bronze bearing

Figure 7-16(d) Relative shaft displacement in the experiment at 500 rpm and 60 °C for the bronze bearing

Figure 7-17 Relative shaft displacement under 60 °C, 1,000 & 500 rpm, and 9 kN for the Babbitted bearing

Figure 7-18 Relative shaft displacement under 60 °C, 1,000 & 500 rpm, and 9 kN for the bronze bearing

Figure 7-19 Relative shaft displacement vs. Hersey number under 60 °C, 1,000 & 500 rpm, and 9 kN for the Babbitted bearing

Figure 7-20 Relative shaft displacement vs. Hersey number under 60 °C, 1,000 & 500 rpm, and 9 kN for the bronze bearing

Figure 7-21 Comparison of the friction coefficient and the expected shaft locus at 500 rpm in the Babbitted bearing and the Al-Si bearing

Figure 7-22 Comparison of the friction coefficient and the expected shaft locus at 500 rpm in the bronze bearing and Cu-Pb bearing

Figure 7-23 Pressure distribution vs. bearing angle in the mid-plane of the Babbitted bearing (60 °C, 500 rpm and 9,000 N)

Figure 7-24 Pressure distribution vs. bearing angle in the mid-plane of the bronze bearing (60 °C, 500 rpm and 9,000 N)

Figure 7-25 Pressure vs. Hersey number at bearing angles of 155, 170 and 190 degrees for the Babbitted bearing (60 °C, 500 rpm and 9,000 N)

Figure 7-26 Pressure vs. Hersey number at bearing angles of 155, 170 and 190 degrees for the bronze bearing (60 °C, 500 rpm and 9,000 N)

Figure 7-27 Temperature distribution vs. bearing angles for the Babbitted bearing (60 °C, 500 rpm and 9,000 N)

Figure 7-28 Temperature distribution vs. bearing angles for the bronze bearing (60 °C, 500 rpm and 9,000 N)

Figure 7-29 Viscosity measured with the slit die rheometer and the induced approximation equations for 60 °C

Figure 7-30 First normal stress difference measured with the slit die rheometer and the induced approximation equations for 60 °C

Figure 7-31 Influence of the temporary viscosity loss and the normal stress (Friction coefficient versus Hersey number for the Babbitted and bronze bearings under 1.72 & 9.0 kN, 500 rpm and 60 °C)

Figure 7-32 Influence of the temporary viscosity loss and the normal stress (Friction coefficient versus Hersey number for the bronze bearings under 27 kN at 2,000 rpm and 60 °C)

Figure 7-33 Influence of the temporary viscosity loss and the normal stress (Oil film thickness versus bearing angle for the bronze bearings under 27 kN at 2,000 rpm and 60 °C)

Figure 7-34 Influence of the temporary viscosity loss and the normal stress (Temperature versus bearing angle for the bronze bearings under 27 kN at 2,000 rpm and 60 °C)

Figure 8-1 A new approach to reduce friction and improve reliability with lubricants

Figure A1 Plain bearing geometry

List of tables

Table 3-1 API base oil category

Table 3-2 Typical properties of the base oils tested

Table 4-1 Ingredients of the Cu-Pb plain bearing

Table 4-2 Ingredients of the Al-Si plain bearing

Table 4-3 Typical properties of the base oils tested

Table 5-1 Ingredients of lead-free plain bearings

Table 5-2 Typical properties of the oils tested

Table 5-3 Composition ratio of elements on PB-A (Bi/Ag-Cu) and PB-D (Bi/Ag-Al)

Table 6-1 Ingredients of the Cu-Pb plain bearing (The same as Table 4-1)

Table 6-2 Ingredients of the Al-Si plain bearing (The same as Table 4-2)

Table 6-3 Typical properties of oils tested

Table 7-1 Characteristics of the plain bearings

Table 7-2 Plain bearing test conditions

Table 7-3 Typical property of the lubricants for the bearing tests

Table 7-4 Typical property of the oil samples tested with the rheometers

Table 7-5 Simulation conditions

Table A1 Thermal characteristics of the base oils

Table A2 Thermal characteristics of the base oil and the polymer-containing oils

Table A3 Thermal characteristics for the bearings used

Acknowledgement

My heartfelt appreciation goes to my supervisor of Prof. Michel Fillon who provided me fruitful advice, comments and suggestions during the years at the Poitiers University. I am most grateful to Dr. Jean Bouyer and Dr. Sébastien Jarny for their supports and advice mainly in the experimental works for the collaboration research activity. I also would like to express my gratitude to Daido Metal Co., Ltd. which offered valuable advice during the development of the automotive bearing test apparatus and supplied plain bearings. I am deeply grateful to Dr. Tadashi Katafuchi who worked together in the study at Idemitsu R&D and supported me even during the years at the Poitiers University. Finally, I would like to express my gratitude to my family for their moral support and warm encouragement.

Réduction du frottement et amélioration de la fiabilité de la lubrification des paliers avec des huiles de moteurs automobiles

Du point de vue de la prévention du réchauffement global, il a été nécessaire d'améliorer le rendement des moteurs thermiques en agissant sur la nature des huiles de moteur. D'une part, le règlement sur l'utilisation du plomb dans les matériaux de paliers a été mis en place dans le but d'empêcher la pollution par les métaux lourds. Le développement de matériaux de paliers sans plomb fut donc nécessaire. Bien que l'efficacité d'abaisser la viscosité de l'huile soit très grande, trop peu de recherches ont été réalisées dans ce domaine en raison des incidences sur la lubrification des paliers de moteur.

Un dispositif d'essais pour les paliers de moteurs automobiles a été développé afin d'évaluer l'efficacité en termes de frottement et la fiabilité des huiles de moteur. Les performances de composants de lubrifiants tels que les huiles de base, les modificateurs de frottement et les polymères ont été évaluées à l'aide de la machine d'essais développée sur divers paliers. En outre, l'effet du polymère a été analysé expérimentalement et numériquement en régime thermo-hydrodynamique, en collaboration avec l'université de Poitiers. Les résultats ont confirmé que l'efficacité en termes de frottement et la fiabilité de la lubrification des paliers dépendent du type de composants du lubrifiant et varient avec la nature des matériaux des paliers. Ainsi, il est montré que le choix judicieux des composants du lubrifiant, en considérant le type de matériaux de palier employés, améliore les performances des paliers.

Mots-clés : Matériaux, Lubrification hydrodynamique, Lubrification limite
Palier et coussinets, Polymère-Rhéologie, Huiles lubrifiantes-Additifs

Friction Reduction and Reliability Improvement of Plain Bearing Lubrication with Lubricating Automotive Engine Oil

From the viewpoint of the prevention from global warming, it has been necessary even for engine oil to improve fuel economy in automotive engines. On the other hand, the regulation of lead in bearing materials has begun with the goal of preventing heavy metal pollution, necessitating the development of lead-free bearing materials. Although the effectiveness of lowering oil viscosity is greater, sufficient amounts of research have not been carried out in this area because of concerns about the influence in engine plain-bearing lubrication.

A test apparatus for automotive plain bearings has been developed in order to evaluate the frictional property and the reliability for engine oil. Lubricant components such as base oils, friction modifiers and polymers were evaluated using the developed apparatus with various bearings. In addition, the polymer effect was analyzed with experiment and THD analysis in collaboration with the Poitiers University. As a result, it was confirmed that the frictional property and the reliability of plain bearing lubrication depended on the kinds of lubricant components and varied with bearing materials. Thus, it was found that carefully selected lubricant components considering bearing materials to be used would enhance the plain bearing performance.

Keywords: Materials, Hydrodynamic lubrication, Boundary lubrication,
Journal bearing, Polymer-Rheology, Lubricating oils-Additives